# PenteFoiling

## Final Report - Version 2.0

## AE3200: Design Synthesis Exercise

Group 11

Delft University of Technology


| | | | |
|---|---|---|---|
| Jakub Barciński | 5531594 | Bram Luiks | 5563011 |
| Dimitrios Bosch | 5076153 | David Mol | 5578841 |
| Vito Elsman | 5585155 | Panagiotis Sachinis | 5526957 |
| Robert Galaska | 5523931 | Szymon Szeliga | 5488303 |
| Thomas van Holten | 5290147 | Koen Veldman | 4870220 |



Date: June 25, 2024
Faculty: Faculty of Aerospace Engineering, Delft
Tutor: Ronald van Gent

This page is intentionally left blank.

# Executive Overview

The executive overview provides a concise overview of this report, aiming to provide key issues, findings and recommendations. Each section will describe a separate part of the report, including methodology, results and supporting figures and tables where necessary.

## Project Description

*PenteFoiling* is an aerial sport where the user's glide is assisted by an inflatable wing directly attached to their body. The system is designed for inherent stability and effective, reliable control mechanisms are incorporated, all of which enhance safety. Thanks to the inflatable structure, the PenteFoil is easily foldable and transportable. This system can be deployed in a wide range of areas and is designed to cover large altitude differences, e.g. by taking off from mountainous terrain. The mission need and project objective statements are presented below.

**Mission Need Statement:** Create an aerial sport which provides a level of excitement on par with wingsuit flying, without the fatal risks involved, and with the ease to attain comparable to "parapente".

**Project Objective Statement:** To upgrade the present "Parapente" experience by using an inflatable aerofoil attached to the pilot instead of the pilot hanging underneath the aerofoil using paracords, by 10 students in 10 weeks.

## Market Analysis

Market analysis is an essential part of development of any new product. It has been conducted to determine the market potential of the PenteFoil, analyse its sources of revenue and growth, and provide an overview of different aspects of SWOT analysis.

First, the market analysis has identified key stakeholders that include:

- **End Users** that are the most critical stakeholder
- **TU Delft** which is the primary facility organisation for the project
- **Regulatory Agencies** which are responsible for safety and regulatory certificates for the product
- **DSE Group 11** as the motivated creators behind the PenteFoil
- **Manufacturers** that play a significant role in the production of the PenteFoil
- **Environmental Agencies** that provide guidelines for the environmental sustainability of the product
- **Investors and Sponsors** that provide the funding needed for the development

Furthermore, the non-key stakeholders who have less influence of the product development are **Distributors, Research Facilities, and Test Pilots.** The stakeholders have been divided into groups based on their interest and influence on the product and play a significant role in establishing the user requirements.

The market need analysis showed a lack of product on the market that would be safe and provide extreme adrenaline experience at the same time. The range of the yearly revenues for the PenteFoil has been established at 13.6 - 37.1 Million USD and the growth rate of around 8.5% with a possible deviation of up to 3%. The project shows large potential for generating revenue from other sources such as sponsorships and marketing.

SWOT analysis uncovered the project's strengths, weaknesses, opportunities and threats which are summarised in Figure 2.3.


**Figure 1:** SWOT analysis.

# Aerodynamic Design

The Aerodynamic Design part provides a detailed analysis of the aerodynamic design of the wing and control mechanisms.

### Subsystem Requirements

First, the detailed subsystem requirements relevant for the aerodynamic design and control mechanisms are defined. These include requirements for trim speed, turn rates and stability. This is followed by a description of aerodynamic target values to design for, flowing from the subsystem requirements. These can be seen in Table 2.

### Airfoil Selection

To select an airfoil for the wing, multiple airfoils were considered and analysed using XFLR5. As a flying wing, without a tail was chosen, mostly reflexed airfoils were considered to provide longitudinal stability. To compare the airfoils, the lift, drag and pitching moment characteristics following from the XFLR5 analysis were evaluated to choose the best airfoil. The MH 81 with a 5° upwards flap was chosen due to its optimal combination of lift and pitching moment performance. For structural reasons the rear of the airfoil had to be replaced by a sail. The effect of this change has been analysed by a higher fidelity CFD analysis using Ansys. Upon iteration with structural considerations, the sail was placed at 70% of the chord maintaining adequate aerodynamic performance and stability performance similar to the original airfoil.

### Wing Design

The wing was designed and analysed in XFLR5 using the viscous VLM2 method. The selection of the wing followed from an iterative process where parameters such as sweep, dihedral and chord length were varied in a structured manner. By varying these parameters and comparing the simulation results to the target parameters in Table 2, the design was optimised such that all target values were met while also taking structural and operational practicality into account. The final wing can be seen in Figure 2, with the dimensions in Table 1.

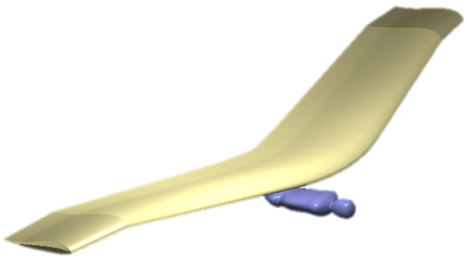

**Figure 2:** Isometric view of the Final Wing Design.

**Table 1:** Final Wing Dimensions.

| Parameter | Value |
|---|---|
| Wing Span | 10 [m] |
| Wing Area | 12.41 [$m^2$] |
| Taper Ratio | 0.73 [-] |
| Quarter-Chord Sweep | 11.99 [°] |
| Maximum Dihedral | 5 [°] |
| Pilot $X_{C.G.}$ w.r.t. LE | 0.81 [m] |

To account for the shortcomings of XFLR5, two corrections were applied. The first correction is to account for

the discrepancies between the airfoil analysis in XFLR5 and the CFD analyses. The second correction takes the drag from the pilot into account since this is not something XFLR5 is capable of doing. The results of the performance of the system can be seen in Table 2. The large correction to the value of $L/D$ at trim can be explained by a correction to both the lift and drag at the trim condition. Especially the addition of pilot drag has a big influence on the $L/D$.

**Table 2:** Performance on Target Parameters.

| Parameter | Target Value | XFLR5 Value | Corrected Value |
|---|---|---|---|
| $C_{m_\alpha}$ at Trim | -0.013 [-] | -0.013 [-] | -0.013 [-] |
| $C_L S$ at Trim | 3.50 - 4.72 [m$^2$] | 6.29 [m$^2$] | 4.36 [m$^2$] |
| $C_L S$ at Stall | $\geq$ 11.50 [m$^2$] | 20.17 [m$^2$] | 20.17 [m$^2$] |
| $L/D$ at Trim | $\geq$ 7 [-] | 29.06 [-] | 12.17 [-] |

**Sensitivity Analysis**
A sensitivity analysis was performed on the wing design. It was found that C.G. shifts influenced the performance of the wing significantly, however, as these are used as a control method this can be used to the pilot's advantage.

**Stability Analysis**
A detailed stability analysis of the system provided the team with stabilty derivatives and a visualisation of the dynamic eigen motions. A linear, time-invariant (LTI) state-space model was used to solve the decoupled longitudinal and lateral equations of motion. The longitudinal stability analysis yielded the stability coefficients displayed in Table 3. The eigenvalues corresponding to the phugoid and short period motions, as well as the period and time to half-amplitude values are shown in Table 4. Their negative values indicate a damped motion.

**Table 3:** PenteFoil Longitudinal Stability Derivatives.

| Coefficient | Value | Coefficient | Value |
|---|---|---|---|
| $C_{x_u}$ | -0.0333 | $C_{m_0}$ | 0.0555 |
| $C_{x_\alpha}$ | 0.2992 | $C_{m_u}$ | 0.0068 |
| $C_{z_u}$ | -0.0034 | $C_{m_\alpha}$ | -0.7312 |
| $C_{z_\alpha}$ | -4.6058 | $C_{m_q}$ | -3.2384 |

**Table 4:** Eigenvalues of symmetric motion.

| Motion | Eigenvalue | Period $P$ [s] | Half Time $T_{\frac{1}{2}}$ [s] | Time Constant $\tau$ [-] |
|---|---|---|---|---|
| *Phugoid* | $-0.02251 \pm 0.10021j$ | 62.70 | 30.79 | 44.42 |
| *Short Period* | $-9.75784$ | - | 0.07104 | 0.10248 |

Similarly, the stability coefficients for lateral motion are given in Table 5. The eigenvalues of the lateral stability state-space system which characterize the behaviour of these modes are shown in Table 6. The PenteFoil displays a stable spiral motion, assisted by its low center of gravity generating a stabilizing pendulum effect. The negative eigenvalues for the dutch roll and aperiodic roll indicate that these eigenmotions are stable as well.

**Table 5:** PenteFoil Lateral Stability Derivatives.

| Coefficient | Value | Coefficient | Value | Coefficient | Value |
|---|---|---|---|---|---|
| $C_{Y_b}$ | -0.01523 | $C_{l_\beta}$ | -0.06472 | $C_{n_\beta}$ | 0.00143 |
| $C_{Y_p}$ | -0.02073 | $C_{l_p}$ | -0.50757 | $C_{n_p}$ | -0.07172 |
| $C_{Y_r}$ | 0.01390 | $C_{l_r}$ | 0.12576 | $C_{n_r}$ | -0.21970 |

‘

**Table 6:** Eigenvalues of asymmetric motion.

| Motion | Eigenvalue | Period $P$ [s] | Half Time $T_{\frac{1}{2}}$ [s] | Time Constant $\tau$ [-] |
|---|---|---|---|---|
| *Dutch Roll* | $-0.10058 \pm 0.47007j$ | 13.36636 | 6.89141 | 9.94221 |
| *Aperiodic Roll* | $-26.17581$ | - | 0.02648 | 0.03820 |
| *Spiral* | $-47.39596$ | - | 0.01462 | 0.02110 |

**Control Analysis**
An analysis into the control characteristics was performed. The control system, CG shift for primary pitch and roll control, and folding wing tips for supplementary roll control, was quantified using aerodynamic data, allowed for the determination of the relevant control derivatives. The control derivatives were thus used in the aforementioned stability state-space system to calculate the control response of the PenteFoil. Calculations were also performed on the required control forces, showing their feasibility. Lastly, an effectiveness calculation was performed on the effect of the folding tips on aerodynamic performance.

The control performance of the Pentefoil is thus shown in Table 7.

**Table 7:** PenteFoil Control Performance Characteristics

| Parameter | Symbol | Value | Unit |
|---|---|---|---|
| Maximum Pitch Rate (CG) | - | 23.20 | °/s |
| Maximum Roll Rate (CG) | - | 93.20 | °/s |
| Maximum Roll Rate (Folding Tips) | - | 92.60 | °/s |
| Maximum Control Force (Folding Tips) | - | 75.7 | N |
| Typical Control Force @ Trim (Folding Tips) | - | 170.6 | N |

**Recommendations**
Several recommendations can be applied to improve the aerodynamic design and process, including:

- Apply an optimizer to the airfoil and wing iteration phase.
- Increase scope of aerodynamic simulations, including 3D and transient.
- Apply a two-body dynamic system for stability and force calculations.
- Minimize design likeness to a hang glider, implement vertical tail, adopt other non-conventional control concepts.

# Structural Design

The Structural Design provides a detailed analysis of the engineering considerations for creating a safe, lightweight, and cost-effective structure.

**Requirements and Methodology**
The design process begins with the definition of subsystem requirements. These, focus on ensuring the structure has adequate strength and stiffness at the ultimate loads (n=7.95, n=-3) and through the 30000 Pa inflation pressure range. The structural design methodology considers stresses and deflections from shear and bending loads, spar and rib buckling resistance, stresses from inflation pressure, and concentrated loads from user attachment and the wingtip deflection mechanism.

**Final Design**
The wing's aerodynamic shape is formed by 10 inflatable cells of varying sizes, covering the first 70% of the wing. The trailing edge consists of two straight fabric pieces connected to a cable. Each cell shares a straight Dyneema fabric web, with the top and bottom parts made from ripstop nylon. Inside each cell, an airtight TPU bladder retains air after inflation.

The core structural elements are two web Tensairity beams: the first between the 2nd and 3rd cells, and the second between the 5th and 6th cells. These beams use modular 6x4 mm CFRP tubes for compression and 2 mm Dyneema cables for tension. The front beam has two compression and two tension elements symmetrical to the chordline to handle negative loads. The Tensairity beams are truncated 1 meter from each tip for the wingtip deflection mechanism. Tubular ribs, with diameters decreasing from 10 cm to 5 cm, are spaced every meter to support the airfoil shape. A cover skin, made from ripstop nylon enhances aerodynamics and can be opened for assembling and disassembling the Tensairity compression elements. An aluminium steering frame is integrated for control. The wing structure weighs 8.40 kg, with material costs totalling €1009. The internal structure is visualised in Figure 3.

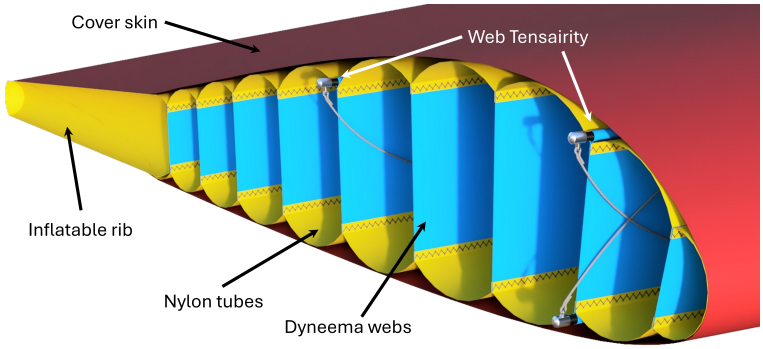


**Figure 3:** Visualisation of the internal structure.

### Recommendations

Several recommendations are proposed for improving the structural design, including:

- Evaluating the weakening of the structure due to discontinuities in compression elements and fabrics
- Analysing the impact of deflections on aerodynamics
- Considering UV radiation effects
- Performing FEM simulations

## Flight Operations

The Flight Operations provide an overview of the equipment, all the flight operations, and detailed descriptions of the take-off and landing procedures.

### Equipment

For each piece of equipment a commercially available option suitable for application in PenteFoiling is suggested, however the user is free to select the equipment themselves. Three different harness options are feasbile based on the user's experience: a training harness, and a PenteFoil Skypod or capsule harness for more experienced users or pilots engaged in freestyle flight maneuvers.

Following the harness options, the emergency parachute is discussed. The parachute should be usable with speeds of up to 49 m/s, support a weight of 105 kg, and conform to the EN12491 standard. The suggested parachute is *Supair* emergency parachute[1].

The equipment also includes a hook knife to release the attachment in emergency and a helmet. It is common to observe aerial sport pilots opting for downhill mountain bike helmets (ASTM F1952 certified) or e-bike helmets (NTA-8776 certified) due to their higher safety ratings and thus these helmets are recommended in the report[2].

Lastly, a *Decathlon* hand pump is recommended as it allows for easy inflation of the structure within 10 minutes and is cheap and widely available[3].

### Flight Procedure

The in-flight procedures begin with outlining the control of the PenteFoil. The pitch of the system can be controlled by the pilot pushing or pulling the control bar, thereby moving their center of gravity backward or forward to pitch up or down, respectively. The Roll of the PenteFoil can be controlled by the user moving their center of gravity to the left or right to roll to that respective side.

To make a turn both pitch and roll control will be used as the user will first need to roll to the side in which they want to turn and then pitch up to make the turn.

Wingtip folding is achieved by moving the control handles in or out to fold or unfold the tips respectively. The folding mechanism is uncoupled for both tips to act as an extra control method for more experienced users. Experienced users can also utilise thermal winds, diving or spiralling to increase the thrilling experience.

### Take-Off

An analysis of take-off locations was performed. From this analysis, it is apparent that for the take-off location, the wind direction is important for safe take-off, as the winds on the leeward side of the mountain are weaker and more turbulent.

[1] https://supair.com/en/produit/parachute-supair-shine/, Accessed on 04/06/2024.
[2] https://www.hangglidingflightschool.com/equipment.php, Accessed on 04/06/2024.
[3] https://www.decathlon.nl/p/handpomp-voor-kamperen-ultim-comfort-10-psi-aanbevolen-voor-opblaasbare-tent/_/R-p-327638?channable=02893b736b756964003431303839366337a&mc=8601387&utm_source=google, Accessed on 14/06/2024.

The take-off incorporates, similarly to hang gliders, a running take-off towards the mountain ridge with utilisation of headwind or ridge lift. A detailed take-off procedure is provided in the report.

**Landing**
The landing is conducted on foot, without the use of the parachute. The landing procedure greatly resembles the procedure used in hang gliders, with a stall and a flare before touchdown to minimise landing speed. Emergency landing procedure is conducted using the emergency parachute provided in the equipment.

# Ground Operations

After the flight operations, the ground operations are discussed. This deals with the folding and transportation of the system. Also, the training of users is discussed and a sensitivity analysis is performed.

**Folding**
The main advantage of an inflatable structure is the fact that it is foldable and therefore easily transportable. However, the stiff carbon are not inflatable, thus thy are separated into tubes of 1 metre length to comply with folding requirements. The folded tubes resemble a tent-like structure with sleeves on the ends of the tubes and a line going through the middle.

The volume estimation of the folded up structure results in a volume of the PenteFoil at 50.8 litres.

Also, an estimation for the time it takes to initialise and terminate the system was conducted and resulted in 27 and 17 minutes for assembly and disassembly of the system respectively.

**Transportation**
With a volume of 50.8 litres a backpack of 60 l volume is considered sufficient with margin for non-perfect folding of the structure and positioning in the backpack and thus recommended for the user. In later stages of design a custom harness can be considered, which may also serve as a backpack to reduce cost, volume and mass. The total weight of all the equipment is approximately 15 kg, depending on the backpack chosen by the user.

**Training**
A comprehensive training plan was designed to ensure all users can safely operate the PenteFoil. This training includes safety training, VR training, and Parafoiling as practice.

The safety training instructs users on the proper use, procedure and timing of the emergency parachute as well as flight recovery attempt. The safety training also consists of practical training in an indoor facility, allowing users to familiarise themselves with the flight equipment, practice deploying the parachute and emergency landings using the parachute landing fall method.

The VR training is a crucial part of the procedure, as it allows for practice without the risk of injuries or fatal accidents. The VR setup includes the QUEST 2 VR glasses from META, running MYRTUS XR software, and a rig that represents the steering frame. Additionally, a fan is incorporated to simulate wind, enhancing the realism of the experience.

The Parafoiling training is a recreational activity where the user is towed behind a boat [4]. Since the user is towed above the water, they can safely learn to control the PenteFoil. The consequences of a crash are significantly mitigated by the water, making it a safer environment for training.

**Sensitivity Analysis**
A sensitivity analysis was performed to evaluate the impact of various factors on the design. This analysis discusses how the take-off procedure impacted the attachment, how the landing procedure impacted the requirement on the stall speed of 11.5, how the transportability influenced the weight and volume to be 55 L and 15 kg and how the system's safety influenced the systems control and agility.

# Design and Performance Summary

The PenteFoil features a sporty wing design, with a higher aspect ratio than a typical hang glider, resulting in a surface area of 12.41 $m^2$ and a span of 10 m. The ribs and majority of the platform is inflated, which is well visible in the visualisations. The system operates similarly to a hang glider in terms of take-off, flight and landing operations. The PenteFoil's primary advantage over hang gliders lies in its inflatable wing design, minimising the need for stiff elements. This feature allows the wing to be folded down to a compact size, fitting neatly into a regular-sized backpack. Figure 4 provides an isometric view of the designed PenteFoil. Table 8 provides a shortened overview of the PenteFoil's key parameters.

[4] `https://parasailingnederland.nl/`, Accessed on 25/06/2024.

The specified inflation pressure ranges can be converted into altitude ranges, although the exact span of this interval depends on factors such as altitude, atmospheric pressure, and temperature. For example, referencing the International Standard Atmosphere (ISA), if the landing is planned at sea level, the PenteFoil can take off from an altitude of up to 3000 meters. However, if the flight starts from a higher altitude, like 4500 meters, the PenteFoil can safely descend to 1000 meters.

**Figure 4:** Isometric view of the PenteFoil.

**Table 8:** PenteFoil Performance Parameters.

| Parameter | Value | Unit |
|---|---|---|
| Trim speed | 20.83 | m/s |
| Never exceed speed | 49 | m/s |
| Trim sink rate | 1.71 | m/s |
| Trim L/D | 12.17 | - |
| Operational inflation pressure range | 0.2-0.5 | MPa |
| Folded Volume | 50.8 | litres |
| Total system mass | 15 | kg |
| Nominal user mass | 80 | kg |
| Maximum user mass | 90 | kg |

## Manufacturing

The manufacturing of the PenteFoil was separated into 2 parts: prototype manufacturing and full-scale production. The goal of the prototype is to obtain an aerodynamically accurate wing, used as proof of concept, for testing and design iteration. For the first prototype, cheap and accessible materials can be used. As the production process doesn't have to be scalable, it will be done by hand, using cheap tools. Creating the first prototype is estimated to cost under €2500, and take 8-12 weeks. This cost includes generous margins for additional material to allow for mistakes throughout the process.

For full-scale production, scalability is key. Because of that, it will be done by external suppliers and manufacturers. Once these are selected detailed production plans and technical drawings will be created and provided to them.

## Verification & Validation

The V&V process of the PenteFoil is designed to ensure compliance with all requirements and the capability to fulfill its intended mission. This process begins with detailed pre-flight tests, including literature studies, inspection tests, computer model simulations, wind tunnel testing, structural assessments, environmental evaluations, and potential user feedback to thoroughly validate the subsystems. Following successful pre-flight tests, flight tests are conducted, starting with parafoiling methods to gather real-time data on aerodynamic performance and stability. Subsequently, take-off and landing procedures are tested in controlled environments to ensure safety and functionality. Upon successful completion of these tests, certification is pursued to meet all regulatory standards, enabling the PenteFoil's market entry. Additionally, participation in events like the Red Bull Flugtag offers practical performance insights and extensive publicity, showcasing the PenteFoil's innovative design and rapid deployment capabilities. The V&V process establishes the PenteFoil's reliability, safety, and market readiness.

## Requirements Compliance & Feasibility

To check whether the design complies with all requirements, a compliance matrix was made. The requirement compliance matrix lists the requirements, including the verification method for each and their current status, which can be 'verified', 'not verified', or 'pending'.

Certain requirements are marked as 'pending' for future verification during later design stages or testing, and 'shown by analysis' indicates that while testing is pending, current analyses support the feasibility of these requirements. The yaw requirement (REQ-MIS-01-2-2) is not met due to the inherent coupling of roll and pitch in the system, making a separate yaw control mechanism unnecessary; similarly, REQ-SYS-01-2-1 is affected by this coupling. Requirements REQ-MIS-02-4 (including REQ-MIS-02-4-1 and REQ-MIS-02-4-2) and REQ-SYS-01-4-3-1, which specify direct attachment of the user to the wing, are not met due to the infeasibility of landing with a direct attached PenteFoil and the limiting center of gravity shift for control. This negatively impacts the degree of connection to the wing that the pilots experience, but could not be solved timely due to the constrains imposed by the landing procedure. Investigating possible landing methods without the need of a suspension by wires below the wing is left as a recommendation for further research.

# Technical Risk Management

To prevent any failures of the system, a list of possible risks was analysed. All the risks were assigned a weight in likelihood and impact on a scale from 1 to 5, the quantification of this scale can be found in Table 9. The risks were placed in a risk map, where the risk is quantified by the likelihood multiplied by the impact. From the risk map, the most severe risks were identified and a risk mitigation plan was made and implemented in the design to reduce its severity. Risk mitigation varies from applying safety factors in the structural calculations to defining training procedures. The mitigation actions reduce the likelihood or impact of the risks, from this a post-mitigation risk map was made as can be seen in Table 9. Initially most of the risks were in the orange or red parts of the table, but after the mitigation the risks reached an acceptable level for the system development to be continued.

**Table 9:** Post-mitigation risk map showing the impact and likelihood of all risks after mitigation actions.

| | | | | | |
|---|---|---|---|---|---|
| **5 (Catastrophic)** | TR-OPS-2, TR-ENV-3, TR-STR-9, TR-STR-10 | | | | |
| **4 (Significant)** | TR-STR-2, TR-ENV-1, TR-ENV-2, TR-OPS-3, TR-OPS-4, TR-OPS-5, TR-OPS-7, TR-STR-3, TR-STR-7, TR-STR-8 | | | | |
| **3 (Moderate)** | TR-ENV-4, TR-STR-11, TR-OPS-6, TR-STR-5, TR-STR-6 | TR-STR-1 | | | |
| **2 (Low)** | | | | | |
| **1 (Negligible)** | TR-OPS-1 | TR-STR-4 | | | |
| Impact / Likelihood | **1 (<1%)** | **2 (>1%, <30%)** | **3 (>30%, <50%)** | **4 (>50%, <70%)** | **5 (>70%)** |

# RAMS Analysis

The Reliability, Availability, Maintainability, and Safety (RAMS) analysis for the PenteFoil focuses on ensuring the system's performance, safety, and dependability. The reliability of the PenteFoil is critical, requiring that the wing structure and skin remain intact 100% of the time during flight. Availability analysis highlights the need for minimal downtime, with an overall availability of 94.86%. Maintainability is ensured through rigorous pre-flight, post-flight, regular maintenance, and annual overhauls. Safety analysis addresses potential risks and how they are mitigated.The PenteFoil is designed with several safety measures to mitigate various flight hazards. Its robust wing structure can withstand significant load factors, preventing wing collapses and enabling stability even in turbulent air. In case of control system failures, pilots can adjust their center of gravity to maintain control, and an emergency parachute is available for critical situations. Pilot training emphasises adherence to safety protocols and correct maneuver execution to prevent errors and collisions. Additionally, the wing's design minimises the risk of stalls by automatically adjusting pitch and velocity under high angles of attack. Regular structural inspections and thorough pre-flight weather checks further ensure the aircraft's safety and reliability under diverse flying conditions. Also, an analysis of accidents in paragliding and hang gliding was performed. For this analysis fatality reports from the United States Hang Gliding and Paragliding Association were analysed. The main causes identified were wing collapses, collisions, pilot errors and gusts. For the PenteFoil's safety, these causes must be contained and therefore also these causes were addressed in order to mitigate the risk.

# Cost Breakdown Structure

The CBS covers labor, material, and overhead costs, providing a comprehensive financial overview for producing 380 PenteFoils annually. Material costs amount to €307,000.00 for a batch of 380 units, benefiting from bulk purchasing and negligible freight costs to Sri Lanka. Production costs in Sri Lanka, chosen for its expertise in kite manufacturing, are €1,733.74 per unit. This needs to be done sustainably, as discussed in Chapter 17. For a one batch production costs add up to €659,000. Additionally, 5 employees assure the quality of the PenteFoil right after manufacturing, they receive a gross salary of €4,200 a month, resulting in a yearly expense of €252,000. Overhead costs include a €38,000 annual lease for a 150 m² plot in Delft, €32,000 for warehouse construction, and €10,000 for office supplies. A 15% contingency is applied for unexpected expenses, resulting in total first-year expenses of €1,740,000. Overview of costs is shown in Table 10. Scaling up production as demand grows will reduce overhead costs and improve profitability, allowing for growth and further development of the PenteFoil.

**Table 10:** Cost Breakdown of the PenteFoil Company.

| Cost | Price |
|---|---|
| Materials Costs | €307,000 |
| Production & Quality Assurance Costs | €911,000 |
| Salary Employees | €214,000 |
| Overhead Costs | €79,300 |
| Subtotal | €1,510,000 |
| **Total** | €1,740,000 |

# Return On Investment (ROI) & Operational Profit Overview

The ROI & Operational Profit analysis provides a comprehensive overview of the cost and ROI calculation of the project. Additionally, it presents a detailed analysis of the monthly and yearly operational profits for the first three years. The purpose of examining the financial aspects of the project is to provide stakeholders, potential investors, and project team members with valuable insights into the economic viability and sustainability of the project.

The first activity is a pre-seed crowdfunding campaign, followed by a first seed round. Next, an involvement in additional funding options like the Graduate Entrepreneur program and a second seed round is considered. Additionally, subsequent funding rounds, such as Series A, Series B, and beyond, will be pursued to scale the business, expand into new markets, and achieve profitability.

Following this, the research and development (R&D) costs are estimated, which include the construction of three prototypes in the first year. Then the operational costs for the subsequent year are detailed, along with the production costs for the first batch of 380 units. The final results of these costs are shown in Table 11.

**Table 11:** Estimated R&D and setup costs plus a cost estimation of producing a single batch of 380 PenteFoil units.

| Category | Description | Estimated Cost |
|---|---|---|
| R&D + Setup Costs | Conceptual Design, Prototyping, Testing, Research Personnel, Manufacturing/warehouse Setup | €309,084.97 |
| Batch (380 Units) Cost | Raw Materials, Manufacturing Processes, Logistics, certification | €777,553.34 |
| Operational Cost (per month) | Leasing, Salary: (Warehouse Worker, Co-founders, Quality Assurance Team) | €35,910.45 |
| Contingency | Unexpected Expenses Per Batch (15%) | €116,633.00 |
| Batch Cost + 15% Contingency Margin | | €894,186.34 |

The total R&D + Setup costs of first three years of €617,000 is the sum of:

- Total personnel cost for the conceptual design = €0.
- Cost of materials for three prototypes = €6,000.
- Windtunnel testing costs = €106,812.
- Flight testing costs = €12,048.
- Structural testing costs = €24,000.
- Certification costs = €888.
- Environmental test machine = €3,640.
- Total personnel cost for three years of R&D = €297,979.2.
- Warehouse setup cost (building) = €31,248.
- Nine months of marketing = €142,000

The total cost per PenteFoil unit is €2,046.193 which is the sum of:

- Total cost of the compressive elements and the control frame = €230.08.
- Manufacturing cost per unit = €1,503.66.
- Logistics cost per unit = €16.453.
- Certification costs per unit = €296.

The total operational cost per month after the first year is €35,910.45 which is the sum of the monthly expenses of:

- Cost of the warehouse worker = €3,810.75.

- Total cost of the five quality assurance team members which act as support staff and sales representatives for the month there is no active production = €20,655.83.
- Total cost of the four co-founders = €8,277.20.
- Total cost for leasing the land where the warehouse will be built on = 3,166.67.

The costs are followed by the revenue projections, starting with determining the price point of the PenteFoil at €10,000. The potential revenue streams for the PenteFoil include direct-to-consumer (B2C) sales, business-to-business (B2B) wholesale transactions, leasing arrangements, and licensing agreements with established distributors serving the hang glider and aerial sport sectors. The primary focus is on establishing the PenteFoil and the overarching company as an exciting new brand that captivates consumers' interest and entices them to experience it firsthand.

Marketing expenses are set at 5% of total revenue for both B2B and B2C. The PenteFoil company will be producing 380 units in the second year and doubling that production in the third year. This results in marketing budgets of €15,833.33 per month in the fourth year and €31,666.66 per month in the fifth year.

The analysis is concluded with a five-year financial forecast, ROI calculation, and a five-year profit and loss statement. The final, most relevant values are shown in Table 15.3.

**Table 12:** Annual financial projections for the PenteFoil project.

| Year | Expected Costs (€) | Expected Revenue (€) | ROI (%) | Net Profit (€) |
|---|---|---|---|---|
| 1-3 | 617,000 | 0 | -100 | -617,000 |
| 4 | 1,515,111.70 | 3,420,000 | 125.58 | 1,903,898 |
| 5 | 2,599,298.04 | 6,840,000 | 163.15 | 4,240,702 |

## Further Development

After the completion of the DSE, several crucial steps need to be taken to turn the PenteFoil from a concept to a commercially viable product. Initially, building a functional prototype is essential to validate the design and attract potential investors. This prototype phase will address the limitations of the theoretical design by providing real-world data. Additionally, tests and research will be conducted to improve the safety of the sport.

Subsequent steps include establishing partnerships with manufacturers for full-scale production and launching targeted marketing campaigns to generate interest and secure market position.

## Sustainable Development Strategy

To contribute to a greener future, sustainability was taken into account during the design phase. The sustainable development strategies implemented in the design are, among others, a circular and a minimalistic design approach, sustainable manufacturing processes and modular design for repair. Some of these strategies have already been implemented in the design and some strategies are mentioned for future development. Furthermore, the sustainable strategies implemented by the team are assigning a sustainability officer and incorporating sustainability into decision-making process

## Recommendations

Several recommendations are proposed which go beyond the work done in this report, and the planned future development. The recommendations include:

1. Ergonomics Testing
2. Stakeholder Involvement
3. Material Exploration
4. Initialisation and Folding Mechanisms
5. Aerodynamic Improvements
6. Training Program Development
7. Model Variations
8. Partnerships
9. Durability Testing
10. Safety Research

# Contents

# Nomenclature

## Symbols

| | | |
|---|---|---|
| $\alpha$ | *Angle of Attack* | ° |
| $\alpha_{trim}$ | *Trim Angle of Attack* | ° |
| $\alpha_s$ | *Stall Angle of Attack* | ° |
| $\beta$ | *Yaw (Sideslip) Angle* | ° |
| $\gamma$ | *Glide Angle* | ° |
| $\delta$ | *Deflection* | m |
| $\delta_w$ | *Wing Tip Control Displacement* | ° |
| $\epsilon$ | *Strain* | - |
| $\theta$ | *Pitch Angle* | ° |
| $\theta_g$ | *Longitudinal CG Control Displacement* | ° |
| $\mu$ | *Dynamic Viscosity* | Pa s |
| $\mu_b$ | *Lateral Mass Inertia Constant* | 1/(kg $m^5$) |
| $\mu_c$ | *Longitudinal Mass Inertia Constant* | 1/(kg $m^5$) |
| $\mu_g$ | *Aeroplane Mass Ratio* | - |
| $\xi$ | *Lateral CG Control Displacement* | ° |
| $\rho$ | *Density* | kg/$m^3$ |
| $\sigma$ | *Stress* | MPa |
| $\sigma_b$ | *Bending Stress* | MPa |
| $\sigma_h$ | *Hoop Stress* | MPa |
| $\sigma_l$ | *Longitudinal Stress* | MPa |
| $\phi$ | *Roll Angle* | ° |
| | | |
| $A$ | *Cross-sectional Area* | $m^2$ |
| $b$ | *Wing span* | m |
| $c$ | *Chord Length* | m |
| $\overline{c}$ | *Mean Aerodynamic Chord* | m |
| $C_D$ | *Drag Coefficient* | - |
| $C_{D_{stall}}$ | *Stall Drag Coefficient* | - |
| $C_d$ | *Airfoil Drag Coefficient* | - |
| $C_f$ | *Skin Friction Coefficient* | - |
| $C_L$ | *Wing Lift Coefficient* | - |
| $C_{L_{max}}$ | *Maximum Wing Lift Coefficient* | - |
| $C_{L_0}$ | *Airfoil Lift Coefficient* | - |
| $C_l$ | *Airfoil Lift Coefficient* | - |
| $C_l$ | *Rolling Moment Coefficient* | - |
| $C_m$ | *Airfoil Pitching Moment Coefficient* | - |
| $C_{m_\alpha}$ | *Gradient of Pitching Moment vs Angle of Attack* | - |
| $C_{m_{ac}}$ | *Pitching Moment Coefficient at the Aerodynamic Center* | - |
| $C_M$ | Wing Pitching Moment Coefficient | - |
| $C_n$ | *Yawing Moment Coefficient* | - |
| $D_b$ | *Lateral Stability System Time Derivative* | - |
| $D_c$ | *Longitudinal Stability System Time Derivative* | - |
| $d_t$ | *Distance of Hinge Point from Wing Tip* | - |
| $e$ | *Oswald Efficiency Factor* | - |
| $F_z$ | *Veritcal Force on the Wing* | N |
| $E$ | *Young's Modulus* | GPa |
| $g$ | *Gravitational Constant on Earth* | $m/s^2$ |
| $h_{web}$ | Web Height | m |
| $I$ | *2nd Moment of Inertia* | $m^4$ |
| $I_{in}$ | *Turbulent Intensity (Inlet)* | % |
| $I_{out}$ | *Turbulent Intensity (Oulet/Backflow)* | % |
| $K_g$ | *Gust Alleviation Factor* | - |
| $L$ | *Lift Force* | N |

| | | |
|---|---|---|
| $L$ | *Rolling Moment* | N m |
| $L$ | *Characteristic Length* | m |
| $L/D$ | *Lift To Drag Ratio* | - |
| $(L/D)_{stall}$ | *Stall Lift To Drag Ratio* | - |
| $M$ | *Pitching Moment* | N m |
| $n$ | *Wing Loading* | - |
| $N$ | *Yawing Moment* | N m |
| $p$ | *Inflation Pressure* | Pa |
| $p$ | *Roll Rate* | °/s |
| $P$ | *Force in Compressive Elements* | N |
| $q$ | *Pitch Rate* | °/s |
| $R$ | *Inflatable Cell Radius* | m |
| $Re$ | *Reynolds Number* | - |
| $r$ | *Yaw Rate* | °/s |
| $S$ | *Wing Surface Area* | $m^2$ |
| $t$ | *Wall/Fabric Thickness* | m |
| $T_{1/2}$ | *Time to half amplitude* | s $\hat{u}$ |
| *Velocity Disturbance* | - | |
| $V$ | *Velocity* | m/s |
| $V_D$ | *Dive Speed* | m/s |
| $V_m$ | *Maneuvering Speed* | m/s |
| $V_{ne}$ | *Never Exceed Velocity* | m/s |
| $V_{trim}$ | *(Target) Trim Velocity* | m/s |
| $V_s$ | *Stall Velocity* | m/s |
| $V_0$ | *Initial Velocity* | m/s |
| $W$ | *Weight* | N |
| $x$ | *Position Along the Wing Chord* | m |
| $X$ | *Axial Force (X-Axis)* | N |
| $X_{C.G.}$ | *X-Position of the Center of Gravity* | m |
| $y$ | Position Along the Wing Span | m |
| $Y$ | *Axial Force (Y-Axis)* | N |
| $Y_h$ | *Mesh Wall Spacing* | μm |
| $Y_+$ | *Y+ Value* | - |
| $Z$ | *Axial Force (Z-Axis)* | N |
| $\infty$ | *Free-Stream Indicator* | - |

**Standard Format for Stability and Control Derivative Notation**

| | | |
|---|---|---|
| $X$ | *Steady aerodynamic axial force or moment* | - |
| $Y$ | *Aerodynamic parameter (e.g.* $\alpha$*)* | - |
| $C_X$ | *Dimensionless coefficient of force or moment* | - |
| $C_{X_Y}$ | *Derivative of axial force or moment with respect to aerodynamic parameter* | - |
| | | |
| $I_{XX}$ | *Moment of inertia about axis X* | kg $m^2$ |
| $K_{X2}$ | *Normalised moment of inertia about axis X* | - |
| $K_{XZ}$ | *Normalised moment of inertia around axes X and Z* | - |

*Note: The X and Y variables presented here do not necessarily represent their existing counterparts, and are used for demonstration purposes only.*

# Abbreviations

| | |
|---|---|
| AC | *Aerodynamic Center* |
| AR | *Aspect Ratio* |
| B2B | *Business-to-Business* |
| B2C | *Business-to-Customer* |
| BASE | *Buildings, Antennas, Spans, and Earth* |
| BHPA | *British Hang Gliding and Paragliding Association* |

| | |
|---|---|
| CAD | *Computer Aided Design* |
| CAGR | *Compounded Annual Growth Rate* |
| CBS | *Cost Breakdown Structure* |
| CFD | *Computational Fluid Dynamics* |
| CFRP | *Carbon Fibre Reinforced Polymer* |
| C.G. | *Center of Gravity* |
| DES | *Detached Eddy Simulation* |
| DSE | *Design Synthesis Exercise* |
| EASA | *European Union Aviation Safety Agency* |
| EU | *European Union* |
| FAA | *Federal Aviation Administration* |
| FAI | *Fédération Aéronautique Internationale* |
| FBD | *Free Body Diagram* |
| FEM | *Finite Element Method* |
| GRP | *Glass Reinforced polymer* |
| ISA | *International Standard Atmosphere* |
| KNVvL | *Koninklijke Nederlandse Vereniging Voor Luchtvaart* |
| LDPE | *Low-Density Polyethylene* |
| LE | *Leading Edge* |
| MAC | *Mean Aerodynamic Chord* |
| MTBF | *Mean Time Between Failures* |
| MTTR | *Mean Time To Repair* |
| NACA | *National Advisory Committee for Aeronautics* |
| PLF | *Parachute Landing Fail* |
| R&D | *Research and Development* |
| RAMS | *Reliability, Availability, Maintainability and Safety* |
| ROI | *Return on Investment* |
| SAM | *Serviceable Available Market* |
| SOM | *Serviceable Obtainable Market* |
| SE | *Seam Efficiency* |
| SF | *Safety Factor* |
| SM | *Safety Margin* |
| SWOT | *Strengths, Weaknesses, Opportunities, Threats* |
| TAM | *Total Addressable Market* |
| TE | *Trailing Edge* |
| TU | *Technical University* |
| TPU | *Thermopolyurethane* |
| UAV | *Unmanned Aerial Vehicle* |
| USD | *United States Dollar* |
| UV | *Ultraviolet Light* |
| UWV | *Uitvoeringsinstituut Werknemersverzekeringen (Institute for Employee Insurance)* |
| V&V | *Verification and Validation* |
| VLM | *Vortex Lattice Method* |
| VR | *Virtual Reality* |
| WBS | *Work Breakdown Structure* |
| WFD | *Work Flow Diagram* |

# Acknowledgements

We would like to express our sincere gratitude to Ir. R.N.H.W. van Gent for his invaluable support and guidance throughout this project. We also extend our thanks to the TU Delft Faculty of Aerospace Engineering for providing the necessary resources and facilities.

Special thanks to Dimitris Apostolidis and Luccas Kavabata for their continuous encouragement and insightful feedback, which greatly enhanced the quality of our project. Additionally, we acknowledge the assistance of Alfarouk Khalil, whose guidance was instrumental in the completion of this work. We also extend our gratitude to Joep Breuer, Dr. Otto Bergsma, and Dr. Carmine Varriale for providing their expertise and advice.

We are grateful to each individual member of our group for creating a collaborative environment, creating a positive atmosphere, and encouraging each other to excel in our work over the past 10 weeks.

We also wish to thank Dimitris, Maria and Konstantinos from Maria's Homemade, and Maurizio, Jenny, Giacomo, Marta, and Andrea from Sapori di Casa, for fueling the team members with delicious food and ensuring that our brains worked at their highest capacity.

Finally, we are thankful to our families and friends for their continuous support throughout this Design Synthesis Exercise.

# Part I - Problem Definition

# 1 | Introduction

The idea of achieving flight using only the (slightly modified) human body, mimicking flying animals, has excited humankind for millennia. Notable examples include the tale of Icarus, originating from Ancient Greece[1], and the work of Leonardo da Vinci in the 15$^{th}$ century [1]. In the present day, methods to achieve this age-old dream of autonomous flight include aerial sports such as paragliding, hang gliding, skydiving and wingsuit flying.

Wingsuit flying unifies flying sports enthusiasts all over the world. Aesthetically resembling a flying squirrel, it offers an intense and thrilling experience at high speeds, pushing the human limit. Unfortunately, these thrilling wingsuits are the cause of death of many experienced fliers. High-speed flight near terrain, trees, cliffs, or buildings, combined with the lack of control methods other than physically demanding subtle body movements, means that even a slight trajectory miscalculation or an impulsive body movement can lead to catastrophic consequences. These are not the only reasons for wingsuit-related accidents: any unexpected weather conditions, such as strong winds or fog limited visibility can cause accidents. Furthermore, human error is often the culprit through, for example, overconfidence or delayed reaction speeds caused by mental fatigue. It is estimated that around 1 in every 500 wingsuit jumps results in death[2]. More specifically, BASE jumping has a 1.7% mortality rate per year, with a staggering 61% of all fatal accidents in the most recent years being wingsuit-related [2] [3].

Seeking to improve the safety of wingsuit flying, inspiration can be drawn from paragliding, with a mortality rate of around 0.05% per year [4]. According to a 2015 study of the American National Institutes of Health [5], between the years 2004-2011, the mortality rate of paragliding jumps was 7/100,000. Paragliding owes its safe reputation mainly to the fact that it contains a large, inflatable wing, that is designed to be inherently stable. The wing is connected to the pilot via suspension lines, which distribute the load evenly and help maintain the canopy's shape and stability. The low C.G. induced by the pilot hanging beneath the canopy creates a pendulum-like effect, providing dynamic stability. The presence of the wing as a lifting surface decreases the sink rate, giving the user more time to react to unexpected events.

Compared to wingsuit flying, paragliding is relatively slow. The physical engagement in the sport is limited: paragliding involves a lot of passive flying, where the pilot mainly enjoys the view and the sensation of flight. The perception of it being 'safe' might make it seem less daring and thus less exciting for thrill-seekers. Finally, some people may not enjoy paragliding because the experience of flying while hanging from long suspension lines does not closely resemble the flight of any flying animal, diminishing the sense of natural freedom and connection with nature they might seek.

Such reasoning has led to the birth of an idea that will bridge the gap between the two sports, merging the excitement of wingsuit flying with a paraglider's safety and attainability, while resembling the flight mechanics of a bird and providing a level of extremity on par with wingsuit flying. *PenteFoiling* is an aerial sport where the user's glide is assisted by an inflatable wing directly attached to their body. The inclusion of the lifting surface, - the PenteFoil - reduces the sink rate and enables designing for inherent stability and the incorporation of effective, reliable control mechanisms, all of which enhance safety. This system can be deployed in a wide range of areas, allows for take-off and landing using legs only and is designed to cover large altitude differences, e.g. by taking off from mountainous terrain. This idea served as the inspiration for this DSE project and was formalised into mission needs and project objectives that became a starting point for the project. This system was named *the PenteFoil*, and the operations accompanying the system are collectively referred to as *PenteFoiling*.

**Mission Need Statement:** Create an aerial sport which provides a level of excitement on par with wingsuit flying, without the fatal risks involved, and with the ease to attain comparable to "parapente".

**Project Objective Statement:** To upgrade the present "Paragliding" experience by using an inflatable aerofoil attached to the pilot instead of the pilot hanging underneath the aerofoil using paracords, by 10 students in 10 weeks.

This report marks the end of the detailed design phase. It is the last in a series of four, documenting the work performed by a group of 10 students during the Design Synthesis Exercise in Spring 2024 at Delft University of Technology. The previous reports covered the project planning phase, baseline phase and conceptual design phase. The first two phases yielded a group organisation and project planning, literature review of relevant concepts, functional analysis and requirement definition and a subsystem breakdown. Some of these documents complement the contents of this report and are included in Chapter 10 and Appendix A, such as the functional

[1] https://www.commonlit.org/en/texts/the-myth-of-daedalus-and-icarus, Accessed on 28/05/2024.
[2] https://www.skydiveorange.com/2023/12/21/what-is-wingsuit-flying/, Accessed on 28/05/2024.

diagrams and the requirements. The conceptual design phase was concluded with the selection of a design concept, after conducting a thorough trade-off of concepts.

This phase of design kicks off with a market analysis in Chapter 2, to determine the demand for this product and to gain an overview of the market landscape. This is an essential step in the development of any new product, to ensure that the final design meets the needs and expectations of users and to identify opportunities and challenges within the market.

The main aim of this report, however, is to document the activities performed in the detailed design phase, where the chosen concept flowing from the trade-off is worked out and designed in detail. This design is a combination of aerodynamics, flight performance, structures & materials and operations. Therefore, three departments were established: the wing department, structural department and operations department. The wing department's main output was the final shape of the wing and a worked out concept for the control system, along with the relevant control forces and control and stability coefficients. The design process is documented in Chapter 3. The structural department aims to design a structure strong and stiff enough to withstand the aerodynamic and structural loads without compromising on performance. The structural design is described in detail in Chapter 4. Both aerodynamic design and structural design include a sensitivity analysis, which demonstrates the feasibility of the final design in case it is subject to a change of conditions or parameters. The design is concluded with a design and performance summary, in which the design is summarised and an overview is given of all relevant performance parameters.

Subsequently, the operations department is responsible for developing and defining all operational aspects of the system. These include the landing and take-off procedure, flight envelope, safety aspects and operational guidelines. Initially the flight operations are described in Chapter 5, after which the ground operations are explained in Chapter 6. The design along with operational aspects is then summarised in Chapter 7, along with a performance overview. Manufacturing and a verification & validation are also considered to be part of operations, hence a manufacturing plan and verification & validation plan were set up in Chapter 8 and Chapter 9, respectively. This concludes all technical and operational parameters of the PenteFoil design so far. With this part finalised, compliance with the requirements can be checked, which were developed in the baseline phase. Therefore, an extensive requirement compliance matrix was created, and a feasibility analysis was performed to elaborate upon the requirements that were not met. This is presented in Chapter 10. The operations part of the report is concluded with a breakdown of mass and time budgets in Chapter 11.

With a clear overview of what the design will look like, and all operational aspects defined, precise and well-founded risk evaluation (Chapter 12) and financial analyses can be performed. They can also be performed in more detail than previously in the midterm phase. Combining these sections gives a good overview of the entire project's feasibility, in which both finances and risk management play a major role. Part of the financial analyses are the cost breakdown structure, which can be found in Chapter 14, and the return on investment & operational profit overview in Chapter 15.

This is followed by a description of the project planning and description of future development in Chapter 16. This is supported by the Project Design and Development Logic diagram and the Project Gantt Chart, which visualise the future of the PenteFoil concept. The conclusion and recommendations are presented in Chapter 18. Appendix A contains the functional diagrams, which were set up in the baseline phase and used to identify the main functions of the system.

It is important to keep in mind that there are limitations to the scope of the research. As the project is performed in the short time of 10 weeks, not every part of the design has been worked out in sufficient detail. While the general performance is described and quantified with preliminary analyses, the wing's stall behaviour, which is essential to analyse for the landing procedure, has not been analysed with advanced methods. The same is true for the structures department; finite element methods are recommended to analyse the transfer of loads within the system, but are not in the scope of this phase of design. Furthermore, due to time constraints, financial constraints and resource limitations, no testing or prototyping can take place in these 10 weeks. As a lot of the requirements that were set up should be verified by means of testing or demonstration, they remain unverified by the end of this design phase.

# 2 | Market Analysis

Market analysis is an essential aspect in development of any new product. Firstly, stakeholder analysis is conducted in section 2.1, followed by defining the market need in section 2.2, and market share analysis in section 2.3. Lastly, a SWOT analysis is conducted for product's market in section 2.4.

## 2.1. Stakeholder Analysis

To analyse the relevant requirements for the PenteFoil project, a comprehensive list of stakeholders was assembled and divided into key and non-key stakeholders. The key stakeholders are listed below. The parentheses at the end of each bullet point contain relevant requirements for the given stakeholder.

- **End Users:** The end users are perhaps the most critical stakeholder not directly involved in the development of the PenteFoil. As the ultimate market success of the product depends on them, feedback of potential users must be considered throughout the design process, while the requirements of the end users must be carefully examined through an in-depth market need analysis. End users include instructors, wingsuit pilots and extreme sports enthusiasts (**REQ-STK-02-2**, **REQ-STK-02-4**).
- **Delft University of Technology:** As the primary organization which facilitated the development of this project, the TU Delft and its staff play a critical role in the progression of this project by providing guidance, academic resources and facilities for the development of the project (**REQ-STK-03**).
- **Regulatory Agencies:** Regulatory agencies are critical as they allow for the procurement of safety and regulatory certificates critical for the success of the PenteFoil in the market. As such, the relevant regulations and restrictions must be closely monitored throughout development. The agencies relevant to the PenteFoil project are the Fédération Aéronautique Internationale World Air Sports Federation (FAI), and the Koninklijke Nederlandse Vereniging Voor Luchtvaart (KNVvL, Dutch Aerospace Engineering Association). Due to a novel design, the development of the PenteFoil poses a challenge of creating new certification requirements, or adjusting the current ones for making the PenteFoil a feasible piece of equipment (**REQ-STK-05**).
- **DSE Group 11:** The primary developers of this project, hence the most interested and most influential on its success (**REQ-STK-01, REQ-STK-03**).
- **Manufacturers:** The design of the PenteFoil must not only be theoretically feasible, but must also be manufactured within both certain time and cost constraints. As such, potential manufacturers must be kept informed and collaboration must occur in order to ensure the final product can be manufactured (**REQ-STK-04**).
- **Environmental Agencies:** A critical focus of this project is sustainability. As such, national and international sustainability regulations particularly pertaining to materials, recycling, and circular use, must be monitored and adhered to. Furthermore, as defined previously, sustainable working and management practices must be employed to ensure adherence to regulations agreed on (**REQ-STK-03**).
- **Investors and Sponsors:** The investors and sponsors play a vital role in the development of the project due to the funding needed for the project launch and possible marketing opportunities. These can play a critical role in the overall success of the PenteFoil, and its consequential market share and revenue potential (**REQ-STK-02-3**).

Besides these, non-key stakeholders also have relevant roles in the project. These include the following:

- **Distributors:** Distributors have an indirect stake in the successful development of the PenteFoil. It is assumed that the current retailers of extreme sporting equipment, such as kitesurf boards, parapentes, paraglides, wingsuits and similar, might be interested in the opportunity of including a PenteFoil into their offer.
- **Research Facilities:** PenteFoil provides research/thesis opportunities for people interested in the subject matter. Because of the early stage of development of the PenteFoil, there is a large area for research and development of the product, which includes advanced modelling techniques, structural and aerodynamic experiments or materials research.
- **Test Pilots:** The test pilots are involved in the development of the PenteFoil as the first users of the PenteFoil. Their feedback will be crucial for the development of the PenteFoil.

Figure 2.1 presents the relation between each of the stakeholder's interest and influence on the PenteFoil development.

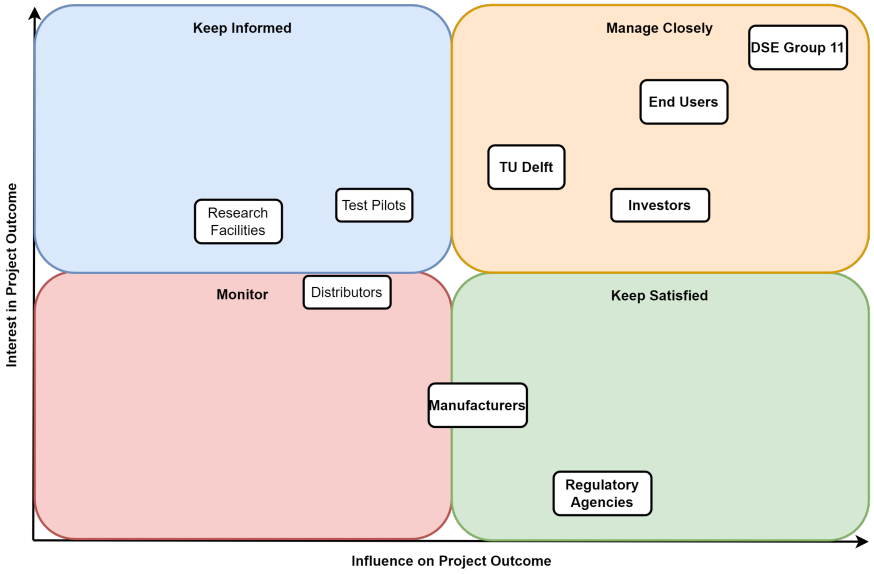


**Figure 2.1:** Stakeholder map.

Based on the stakeholder map from figure 2.1, the stakeholders can be divided into 4 groups, based on their main takeaway from the PenteFoil Development. The division is presented as follows.

- **Keep informed:** These are the stakeholders that have little influence on the project outcome due to their indirect influence of the development, however have a high interest in a project success. Investors choose to become a part of the stakeholder's by their belief in the project's success.
- **Monitor:** These stakeholders have little influence on the project outcome and interest in a project success. They mainly consist of the operations or manufacturing regulatory agencies, whose level of influence on the project is dependent on the strictness of the laws concerned with the development of a new structure.
- **Manage closely:** These stakeholders have the highest levels of influence and interest in the project. They consist of the project developers, TU Delft and the future users of the PenteFoil.
- **Keep Satisfied:** These stakeholders have a lot of influence on the development of the PenteFoil due to their valuable feedback or possibilities and opportunities that they provide for the development, however they have limited interest in the project's success.

## 2.2. Market Need

In the realm of extreme aerial sports, a unique market demand arises from contrasting experiences of parapenting and wingsuit flying. Wingsuit flying provides a distinct thrill of adrenaline. However, with a high cost and a high death rate of wingsuit flyers, while parapenting can be considered inherently safe in comparison to wingsuits, some users may perceive a lack of adrenaline due to its low speed and indirect connection between the body and the wing.

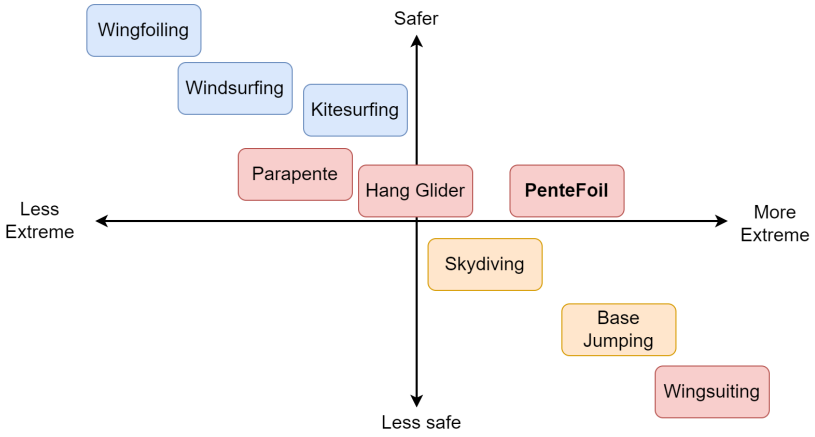


**Figure 2.2:** Market map of 'extreme' sports ranked by safety and 'extremeness'. - Blue = Water sports, Yellow = Skydiving related sports, Red = Gliding sports

This disparity shows a clear market gap, which is a desire for a sport that blends the excitement of wingsuit flying with the safety assurances of paragliding. The PenteFoil is positioned to meet this demand by delivering a thrilling experience while maintaining a high level of safety.

Figure 2.2 provides an overview of selected extreme sports related to wind/air, categorised by safety level and intensity. Water sports are represented in blue, flying sports in red, and air jumping sports in yellow.

A clear trend emerges from the graph regarding the relationship between the safety and excitement that comes from each sport. The correlation underscores the essential dynamics of extreme sports: the more exciting a sport is, the lower its safety, often due to factors such as increased speeds, increased risk of human error or equipment malfunction. Thus we are aiming to recreate the excitement that PenteFoil will evoke, without compromising on the safety.

## 2.3. Market Share Analysis

This section will provide an overview of the conducted market share estimation/analysis of the PenteFoil based on analysis and interpolation of available sources on similar extreme sports. Market share analysis is a fundamental step in every project development. It will outline how big the market for a PenteFoil actually is. Unfortunately, due to the niche market, little data on similar products is readily available or verifiable. Thus, the market share analysis can only provide a rough estimate on the market size for PenteFoil.

### 2.3.1. Potential Customers

The market share analysis is started with defining the potential customers who are likely to be interested in PenteFoiling. This identification process relies on intuition and understanding the source of potential customers, which are mostly assumed to come from similar sports. Additionally, the assessment of potential customers will play a crucial role in determining the market size for PenteFoil.

- **Paraglider flyers** wanting to transition into a sport that provides higher levels of adrenaline but are concerned about the safety of sports such as wingsuiting.
- **Hang glider flyers** looking for a more accessible, easily transportable piece of equipment.
- **Skydivers** wanting to transition into wingsuiting, however they do not possess enough experience. Wingsuit flying often requires 1000+ skydiving jumps before one can be certified to use a wingsuit, making it a considerably demanding sport to enter.
- **Current wingsuiters** seeking a safer alternative to their full of adrenaline, but risky sport.
- **Other users** that are inexperienced in extreme aerial sports but might be interested in undertaking such activities.

Each of the groups can obtain different benefits from the successful development of the project.

The paraglider flyers are deemed to be the largest potential user group, due to their inherent interest in flying sports rather than skydiving. Furthermore, current wingsuit community remains relatively small due to its highly positioned entry point and a high death toll, and thus can be considered a user base of low significancy. However, the high positioned entry point for wingsuiting might provide a lot of new PenteFoil users from the skydiving group. Other, inexperienced users might be inclined to join extreme aerial sports community based on the popularity and success of PenteFoil.

### 2.3.2. Market Size Estimation: Conservative

Estimating the market size for a novel product like a PenteFoil requires a balanced approach due to the inherent uncertainties. The market size analysis will include a two estimation methods, providing a feasible range of the market size, instead of providing a single number.

For Method 1, an interpolation of the market share data from the Wingfoiling market will be used. The aim of the Wingfoil was to introduce a new sport that combines the ”fun” elements of windsurfing and kitesurfing - a direct connection between the sail and the user for high-speed maneuverability similar to windsurfing, along with the freedom to perform jumps and tricks characteristic of kitesurfing.

Wingfoiling is a relatively new concept and is still in the phase of rapid growth. Wingfoiling emerges as a closely related market to the PenteFoil, serving as a valid base for comparison between the two. The relation stems from similar user base interested in extreme water sports that combines kite- and windsurfing.

Unfortunately, it should be noted that wingfoiling has not been widely embraced within the kite- and windsurfing community in the beginning, primarily due to the community dynamics of kite- and windsurfers. Due to this reason, wingfoiling currently has a relatively low market share within these watersports. Wingfoiling emerges as the closely related to PenteFoiling market, which is why such comparison is valid.

Assuming that at the end of the dynamic growth phase PenteFoiling is able to overtake a similar market share of extreme flying sports, as wingfoiling did for water sports, can be considered conservative. This approach suggests potential challenges in penetrating established markets and acquiring a share of the existing or expanding the current customer base.

Table 2.1 provides market data estimation of wingsurfing, kitesurfing, and wingfoiling which will be used for market comparison.

**Table 2.1:** Market size of windsurfing, kitesurfing, and wingfoiling[3,4].

| Sport | Market size [M $] | Total market share [%] |
|---|---|---|
| Windsurfing | 4812.7 | 80.3 |
| Kitesurfing | 918.1 | 15.3 |
| Wingfoiling | 265.0 | 4.4 |
| Total | 5995.8 | 100.0 |

Assuming a normal market share distribution, it can be suggested that a hybrid sport conceptually similar to wingfoiling will have a market share between 4% and 5%, based on the 4.4% figure in Table 2.1 with the conservative assumption. Thus, to calculate the relevant potential market size for the PenteFoil, a reverse correlation will be derived from market size data for paragliding, hang gliding, and wingsuiting. These are shown below in Table 2.2.

**Table 2.2:** Market size of wingsuiting, paragliding, hang gliding, and PenteFoiling [5,6,7].

| Sport | Market size [M $] | Total market share [%] |
|---|---|---|
| Wingsuit | 125.0 | 40.3 |
| Paragliding | 114.6 | 37.0 |
| Hang gliding | 56.8 | 18.3 |
| PenteFoil | ***13.6*** | 4.4 |
| Total | 310 | 100.0 |

The estimation of the wingsuit market was made as an extrapolation of the global market value of the skydiving industry, which has a worth of 1.25 Billion USD, of which roughly 10% of users are associated with some wingsuiting related activity. As such, an estimated potential market price of 13.6 Million USD can be extracted from the data.

### 2.3.3. Market Size Estimation: Optimistic

Method 2 involves determining how many potential customers there are and what amount of money they are willing and able to spend on the product per year. To obtain a rough estimation for the number of potential customers and the potential market size, the skydiving, paragliding, and BASE jumping markets must be examined. This method can be considered more optimistic than the first method.

The difficulty in estimating the number of potential customers, or the customer reach, of the PenteFoil lies in the lack of information regarding the number of users in each of the relevant sports (to calculate the Total Addressable Market (TAM)). For example, skydiving is a sport which few in the world posses licenses for, while over half a million try it for the first time in the United States alone yearly. As such, predicting the size of the user base is not trivial. This becomes increasingly difficult when considering BASE jumping, the foundation of wingsuiting and other related 'extreme' sports, as its underground nature does not allow for sufficient documentation of the active user base. Table 2.3 shows estimations for the global number of **active** users in each of the aforementioned sports. The numbers were roughly estimated from a variety of online sources.

As such, the TAM can be calculated to be roughly 138,500 users globally. To calculate the Serviceable Available Market (SAM), a market interest of 5% will be used. This both aligns with the value of the market share defined in the previous section, while also providing a realistic initial target for the market price. Hence, also assuming

[3] https://www.vantagemarketresearch.com/industry-report/windsurf-boards-market-0435, Accessed on 30/05/2024.
[4] https://www.linkedin.com/pulse/kiteboarding-equipment-market-size/, Accessed on 30/05/2024.
[5] https://www.marketresearchintellect.com/product/global-skydivingmarket-size-forecast/, Accessed on 30/05/2024.
[6] https://www.mordorintelligence.com/industry-reports/hang-glider-market, Accessed on 30/05/2024.
[7] https://www.linkedin.com/pulse/paragliders-market-size-share-industry-9l2ke, Accessed on 30/05/2024.

**Table 2.3:** Estimated global number of active users in wingsuiting, BASE jumping, and paragliding [6].

| Sport | Number of Users [-] |
|---|---|
| BASE Jumping | $\sim 3,000$ |
| Wingsuiting | $\sim 8,000$ |
| BASE Wingsuiting | $\sim 500$ |
| Paragliding and Handgliding | $\sim 127,000$ |
| Total | $\sim 138,500$ |

global production and distribution capabilities (no geopolitical restrictions), the Serviceable Obtainable Market (SOM) results to 6,925.

While seemingly quite small, it is not out of reasonable bounds of estimation for such a sport, particularly considering the current values for hang gliding and wingsuiting present globally. Lastly, to compute the potential market price, a yearly average spending per user must be defined. Assuming each user purchases at least one PenteFoil at the target price of €10,000 (**REQ-STK-02-3** in Chapter 10), which is not replaced within two years, an average yearly spending of €5,000 can be set per customer (conservative, as this assumes no extra gear and equipment is included in the market value). The two year life estimation is set assuming a nominal use during the year, with the replacement being made due to advancements in technology and/or safety considerations, rather than product failure. Finally, an estimation of the market value can be made, resulting in a value of 34.6 Million EUR, which currently converts to 37.1 Million USD.

As such, the two market size estimation methods have presented a range for the potential market size between 13.6 and 37.1 Million USD.

### 2.3.4. Additional Sources of Revenue

Due to its 'extreme' nature, PenteFoiling might be an attractive sport for marketing companies and sponsors. The extreme sports market is an ideal platform for brands seeking to advertise to a diverse audience. PenteFoiling can provide exposure by enabling sponsors to advertise on the equipment or by creating opportunities for extreme sporting events. The revenue from this kind of source is difficult to estimate, as no clear figure of popularity of PenteFoiling across the general public can be derived. Moreover, the popularity of PenteFoil is very dependent on its exposure strategy. Thus, maximizing visibility through strategic partnerships, social media, and participation in events becomes paramount for attracting sponsors effectively.

In conclusion, to maintain a conservative approach, the potential additional revenue (which increases the market value of PenteFoiling sport) should not be added into account for 2 reasons: its estimation is highly challenging, and it represents a potential rather than a guaranteed source of revenue.

### 2.3.5. Customer Research

Market analysis involves customer research - any product ideas have to be validated by asking potential customers if they are interested in the product at all. A brief analysis was conducted by interviewing various individuals involved in extreme sports whether the PenteFoil concept would interest them. This demographic included wingsuiters, windsurfers, kitesurfers, para- and hang- gliding enthusiasts, and general students which have previously been involved in other such sports. From this demographic, a majority voted that they would be interested in the PenteFoil concept, due to its increased safety potential, while also providing a similar experience to the thrill of wingsuiting.

### 2.3.6. Growth Estimate

Growth potential of the PenteFoil can be considered very high, but it's difficult to provide a specific figure due to its early stages of development. However, once PenteFoil surpasses its initial rapid growth phase and becomes an established part of the market, its growth rate can be estimated for subsequent periods. Several elements of the deployment and organization of the PenteFoil will affect its market share, as well as it's growth rate. Primarily, these depend on social factors such as reception by the customer base, safety record, and marketability. As such, deploying and marketing the PenteFoil to the correct customer base is critical for its success, ensuring correct promotion, marketing, and customer satisfaction.

To provide a general estimate for the potential growth rate of the PenteFoil, the Compound Annual Growth Rate (CAGR) of other aforementioned markets are shown in Table 2.4.

As shown, an average CAGR of 8.55% is seen for related aerial extreme sports over a 10 year forecast period. Allowing for some margin due to potential delays and difficulties that may be faced during the deployment of

**Table 2.4:** CAGR of various extreme sports [6,7,8].

| Market | CAGR - 10 Year Forecast Period [%] |
|---|---|
| Skydiving | 8.15 |
| Paragliding | 14.47 |
| Hangliding | 3.02 |
| *Average* | 8.55 |

the PenteFoil, and strong growth potential, a potential CAGR of 8.5% $\pm$ 3% can be assumed (the average deviation from other markets).

## 2.4. SWOT Analysis

The SWOT analysis evaluates PenteFoil's market landscape, providing strategic insights for stakeholders in the extreme sports industry. It is conducted in order to distinguish position of the product in market and assess the competitiveness of the product.

### Strengths

1. **Uniqueness of the product**
   PenteFoil is a unique product that addresses a market gap identified in Figure 2.2. Initial customer research has uncovered that the product is desired as it forms a novel niche market that has not been filled yet.
2. **Focus on safety**
   The project's main goal is to create a safe piece of equipment which will greatly decrease the accident risk in the extreme flying sports industry.
3. **Motivated team**
   Behind the project stands a highly motivated team of students with innovative ideas and determination. This positively affects the chances of the project's success.
4. **Academic Resources Availability**
   Since the project is conducted within the TU Delft's Faculty of Aerospace Engineering, it provides the team with external expertise from specialists in the field of structures, materials and aerodynamics, which are beneficial for the project development.

### Weaknesses

1. **Regulatory Compliance**
   Extreme sports equipment regulations are very strict, which ensures safyety of the equipment on one hand, however also slows down the development process. Furthermore compliance with the regulations cannot be estimated accurately timewise.
2. **Uncertainty of acceptance by the market**
   Similarly to every novel product, there is a high uncertainty whether the product will be as successful as estimated.
3. **Excess User Caution**
   Due to the novelty of the sport and lack of statistics regarding safety, convincing potential users that PenteFoil is safe, might pose a challenge.
4. **High cost**
   PenteFoil, being a niche and a complex product has a high unit cost due to possible use of specialized materials, limited production runs, and complex manufacturing processes.

### Opportunities

1. **Growth potential**
   Extreme sports market is rapidly growing with positive forecasts for the next years[4].
2. **Marketing opportunities**
   A new, rapidly growing extreme sport might provide a lot of sponsorship and marketing opportunities aimed towards both the general audience, as well as extreme sports enthusiasts.
3. **Partnerships**
   Possibility of collaboration with established brands in the extreme sports industry might positively influence further development by providing expertise, resources, and distribution channels, market reach and credibility.

4. **Technological advancement**
   Such new structure might provide research and development reasons and opportunities in the materials and structures industry, by creating a new market need in this sector.

Threats

1. **Competition**
   There is a well established competition for extreme aerial sports providing different experiences to the PenteFoil. Usually, in well established markets, it is challenging for a new product to penetrate the market effectively.
2. **Accidents**
   Any potential safety incidents will provide a negative publicity for a product such as the PenteFoil. It may decrease the attractiveness of the product, which is supposed to be a safe alternative, thus utmost focus must be directed towards safety.
3. **Economic instability**
   An inessential product like the PenteFoil is highly affected by market downturns caused by economic events.
4. **Supply chain disruptions**
   Due to a lack of an independent supply chain, the development and production of the PenteFoil is highly affected by delays, order cancellations, or other disruptions in the supply chain, which may lead to more delays in the development.

The SWOT analysis has been summarized and presented graphically in Figure 2.3.


**Figure 2.3:** SWOT analysis of PenteFoil's market landscape.

# Part II - Design

# 3 | Aerodynamic Design

In order to get the best performance out of the system, several geometrical parameters need to be determined. These include the type of airfoil used and the general shape of the wing, including parameters such as sweep, dihedral, taper and twist. The choices made to converge to the final design are explained and justified in this chapter, starting with the requirements in Section 3.1 and the assumptions made for this in Section 3.2. From the requirements also flow the design targets, which can be found in Section 3.3. Section 3.4 presents the reasoning behind the choice of airfoil. This is done in more detail in Section 3.5, after which the wing design is discussed in Section 3.6. Once satisfactory aerodynamic performance is achieved through wing design, the control method needs to be designed in detail for the specific wing design. This design starts off by listing the relevant requirements and design targets for the subsystem, and includes the sizing of possible control surfaces, their deflections and the control forces necessary to realise these deflections. Finally, recommendations for further research and other possible control methods are presented.

## 3.1. Subsystem Requirements

The subsystem requirements in Table 3.1 for the wing design follow from the requirements set up during the baseline phase.

**Table 3.1:** Wing Subsystem Requirements.

| ID | Requirement |
|---|---|
| **REQ-AERO-01-1** | The system shall have a $L/D$ of 7 or higher at trim. |
| **REQ-AERO-01-2** | The system shall have a trim speed of 75 km/h. |
| **REQ-AERO-01-3** | The lift provided by the system shall be equal to or higher than the weight of the system at trim. |
| **REQ-AERO-02** | The system shall have a top speed of at least 120 km/h. |
| **REQ-AERO-03-1** | The sink rate during landing shall be at most 5 m/s. |
| **REQ-AERO-03-2** | The horizontal speed during landing shall be at most 8.5 m/s. |
| **REQ-AERO-03-3** | The airspeed during landing shall be at most 11.5 m/s. |
| **REQ-AERO-04** | The stall speed of the system shall be 13 m/s or lower. |
| **REQ-AERO-05** | The $C_{m_\alpha}$ of the system shall be between -0.011 and -0.015. |
| **REQ-AERO-06** | The system shall remain stable while experiencing gust speeds of up to 7.5 m/s at trim speed. |
| **REQ-AERO-07** | The length of the wing shall be smaller than 2.5 m in the longitudinal direction. |
| **REQ-AERO-08** | The system shall provide a turn rate of 20 seconds to complete a 360-degree turn. |
| **REQ-AERO-09** | The control mechanism shall provide a pitch rate of 20°/s at trim speed. |
| **REQ-AERO-10** | The control mechanism shall provide a roll rate of 40°/s at trim speed. |

## 3.2. Assumptions

Below is a summary of the assumptions and simplifications made during the wing design process, each accompanied by a justification. These measures were implemented mainly due to resource constraints and to maintain the project scope.

**ASM-WING-01** *The flow is incompressible.* This is a valid assumption for Mach numbers below 0.3. The PenteFoil's top speed is well below this limit, justifying this assumption. This is an assumption inherent to the VLM analysis of XFLR5, ensuring accurate aerodynamic predictions for subsonic speeds.

**ASM-WING-02** *The flow interference between the pilot and the wing is neglected.* Analysing the influence of the pilot on the aerodynamic performance of the system is left as a recommendation, and will be done in a later stage as part of windtunnel testing or later CFD analyses.

**ASM-WING-03** *The wing structure is assumed to be rigid, neglecting any significant elastic deformations or structural vibrations.* According to the requirements, the structural deformation must not exceed 3% of the span. This is considered sufficiently small as to not have a significant effect on the aerodynamic performance of the wing.

**ASM-WING-04** *The control surface deflections are assumed to reach their final positions instantly, allowing for the calculation of forces and moments based on these steady-state deflections. Transient effects during the deflection motion are neglected.* This assumption simplifies the analysis by focusing on the steady-state aerodynamic forces and moments, which are most relevant for evaluating the overall performance and stability of the control surfaces.

## 3.3. Design Targets

To design a wing meeting the requirements, some target values for the design were set. From the trim requirements listed in Section 3.1, the system requires a $L/D$ of 7 or higher, a trim speed of 75 km/h, and a lift equal to the weight. This combination results in a sink rate of around 3 m/s, ensuring an enjoyable flight time for the pilot. Two target values are considered in the design iteration to ensure these requirements are met. First of all, the $L/D$ of 7, and following from the lift equation a $C_L S$ between 3.5 and 4.7 m$^2$. This was calculated using a total system mass of 95 kg, assuming a pilot mass of 80 kg and a PenteFoil mass of 15 kg based on iterations up until the final wing design. A density range of 1.225 until 0.9093 kg/m$^3$ was used corresponding to an altitude of 0 to 3000 m, so that the trim speed will be reached within the flight envelope. Furthermore, from REQ-AERO-09 the $C_{m_\alpha}$ at trim conditions has to be between -0.011 and -0.015 to ensure longitudinal stability while keeping the system controllable. This range was chosen because traditional hang gliders have similar values for $C_{m_\alpha}$ [7][8][9]. The design target for $C_{m_\alpha}$ was set to -0.013 to be in the middle of this range.

From the landing requirements, the system requires an airspeed of at most 11.5 m/s and a maximum sink rate of 5 m/s. A headwind of at least 3 m/s is assumed, so that the speed relative to the ground is 8.5 m/s or lower, allowing for a safe landing. For the landing procedure, with the help of the steering frame the angle of attack is increased until stall and beyond. The operational aspects of this procedure are elaborated on in Section 5.5. The pilot will land beyond stall, but the performance after stall has not been analysed due to time limitations. Instead, a conservative maximum target value of 11.5 m/s for the stall speed was chosen, as the assumption was made that the airspeed will decrease further when increasing the angle of attack beyond stall. Following from the lift equation, the minimum required value of $C_L S$ to get below this stall speed is 11.50 m$^2$. Beyond stall the flow will fully separate, causing the lift to decrease drastically and thereby increasing the sink rate. As the performance after stall will not be analysed, the sink rate will be verified by comparing to hang gliders with the same landing method and similar wing parameters and performance up to stall. The design targets are summarised in Table 3.2.

**Table 3.2:** Design Targets.

| Target Parameter | Target Value |
|---|---|
| $C_{m_\alpha}$ at Trim | -0.013 [-] |
| $C_L S$ at Trim | 3.50 - 4.72 [m$^2$] |
| $C_L S$ at Stall | $\geq$ 11.50 [m$^2$] |
| $L/D$ at Trim | $\geq$ 7 [-] |

## 3.4. Airfoil Selection

After an extensive literature review of airfoils for aerial sports and tailless wings, over 20 airfoils were selected and imported into the aerodynamic analysis software XFLR5, aided by a database search[8]. The airfoils considered for this analysis are displayed in the list below.

- E180
- E193
- E387
- EPPLER 326
- EPPLER 328
- EPPLER 331
- EPPLER 335
- EPPLER 340
- EPPLER 343
- FAUVEL 14
- FX63-137
- MH 32
- MH 60
- MH 81
- MH 82
- MH 84
- NACA 4412
- NACA 23012
- NACA 24112
- PW51
- RONCZ

[8] `http://airfoiltools.com/search/index`, Accessed on 04/06/2024.

To perform the analysis, a Reynolds number has to be defined. Equation 3.1 was used to find a Reynolds number of $1.9 \cdot 10^6$. This value was obtained using sea level density ($\rho$), the dynamic viscosity of air ($\mu$), the trim speed ($V$) and the current estimate for the MAC ($L$).

$$Re = \frac{\rho V L}{\mu} \tag{3.1}$$

The most important airfoil parameters to check for in this design are lift, drag and pitching moment. Therefore, the airfoils were compared by means of their drag polars ($C_L$ - $C_D$), lift curves ($C_L$ - $\alpha$) and static longitudinal stability graphs ($C_m$ - $\alpha$). High lift and low drag is desired, and the airfoil should have a positive (pitch-up) $C_m$. The latter helps in achieving static longitudinal stability, as the C.G. is located in front of the center of pressure generating a nose-down moment. To achieve this positive $C_m$, mostly **reflexed** airfoils are considered for the analysis. The reflex at the TE slightly deflects the flow upwards such that a small amount of downforce at the trailing edge is able to generate a positive moment.

Other parameters of importance are stall behaviour and compatibility with other wing parameters. The stall behaviour (i.e. how ”smoothly” stall occurs) requires an extensive aerodynamic analysis using CFD software and is done only for the selected airfoil. If undesirable stall behaviour is detected in the CFD analysis, additional measures such as wing twist or stall strips may be deemed necessary. For the airfoil specifically, the stall angle can be checked in XFLR5. If this angle is too low, the airfoil will be eliminated from the selection. The airfoil's compatibility with the selected wing parameters is analysed in Section 3.6, as it is impossible to determine this by merely analysing the airfoil.

After comparing all airfoils, some were discarded due to major deviation from the target values. Some, for example, generated a large negative moment, which would make it difficult to design a longitudinally stable wing. Other airfoils were discarded due to mediocre performance in all metrics. The comparison resulted in the five airfoils presented in Figure 3.1: EPPLER 331, EPPLER 335, MH 81, MH 82 and MH 84.

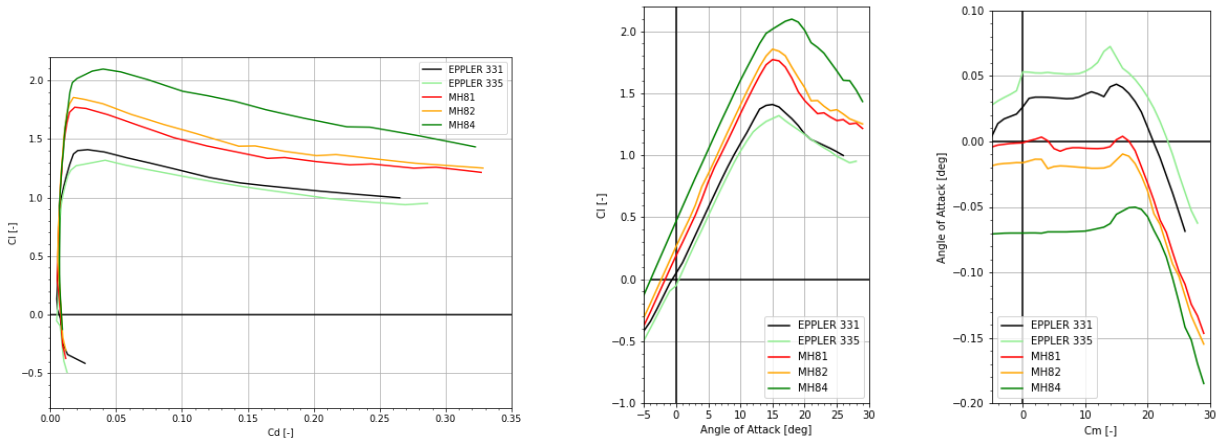


**(a)** Airfoil drag polar **(b)** Airfoil lift curve **(c)** Airfoil longitudinal stability curve

**Figure 3.1:** Airfoil curves

As can be seen in Figure 3.1, the airfoils that perform well in terms of longitudinal stability generally perform worse in terms of lift performance and vice versa. Moreover, from preliminary structural calculation, the thickness of the wing cannot be too low. For these reasons, the airfoils have been modified for the final comparison. The thickness-to-chord ratio has been set to 0.15 for all airfoils considered to achieve a sufficient structural thickness. Moreover, the MH 81, MH 82, and MH 84 airfoils exhibit lower stability. To address this, artificial reflex values were applied to them, implemented as upward flaps in XFLR5. These changes yielded the graphs displayed in Figure 3.2.

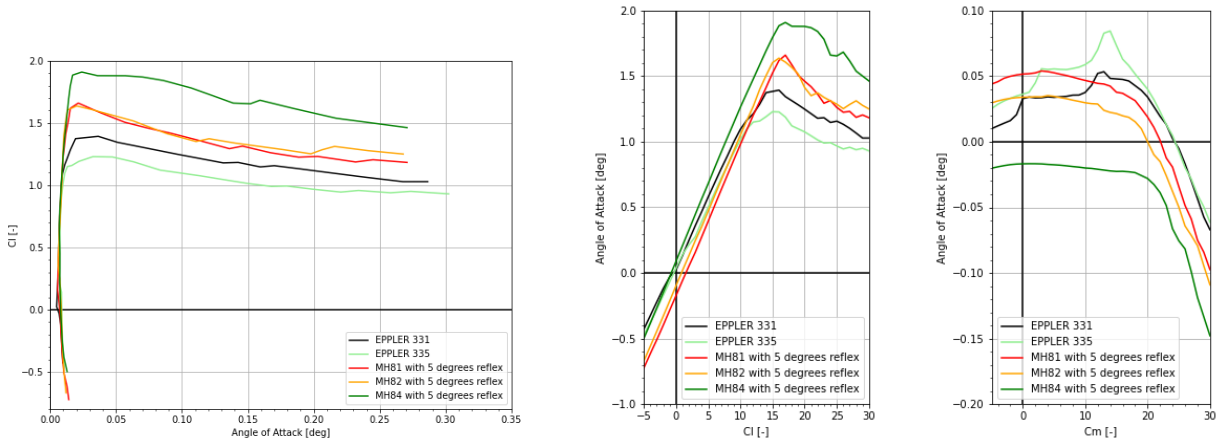


**(a)** Airfoil drag polar **(b)** Airfoil lift curve **(c)** Airfoil longitudinal stability curve

**Figure 3.2:** Airfoil curves

Figure 3.2 illustrates that while the MH 84 airfoil still lacks sufficient stability, while both the MH 81 and MH 82 airfoils demonstrate good stability characteristics. The lift performance of MH 81 and MH 82 is quite similar; however, MH 81 exhibits superior stability compared to MH 82. Additionally, when compared to the EPPLER 331, the MH 81 airfoil offers both better lift and enhanced stability at angles of attack below 10 degrees. MH 81 also surpasses EPPLER 335 in lift performance and exhibits a more gradual and predictable stability behavior. This contrast is evident from the sharp increases in the moment curve observed with EPPLER 335. For the aforementioned reasons, the MH 81 airfoil with a thickness-to-chord ratio of 15% and a 5° upward flap has been selected.

## 3.5. Higher-Fidelity Airfoil Analysis

As a result of structural limitations imposed on the aerodynamic design by the nature of flexible and non-rigid aerodynamic structures and surfaces (such as fabric lifting surfaces), certain adjustments must be made to the airfoil shape. Particularly, the reflexed shape at the trailing edge presented a significant challenge in maintaining the overall aerodynamic shape. As such, a decision was made to alter the shape of the airfoil between some percentage of the chord and the trailing edge by directly connecting these two points. Consequently, the upper and lower airfoil surfaces would not have any curved sections which would aid in maintaining their desired aerodynamic shape.

For the analysis, a set of six airfoil shapes were investigated, including the original MH81 airfoil and five altered airfoils, with the cutoff point varying between 40% and 80% of the chord. Adjusting the airfoil geometry with the aforementioned method past 80% did not alter the geometry significantly to be included in the analysis. An overview of the altered shapes is shown in Figure 3.3.

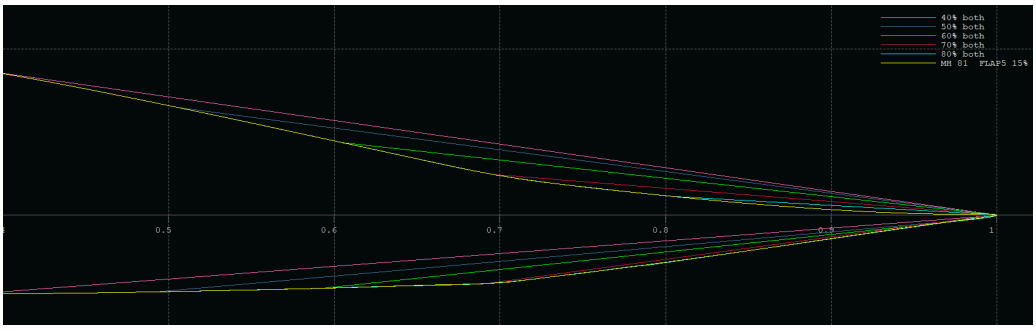


**Figure 3.3:** Trailing Edges of Altered MH81 Airfoil Shapes.

The generated shapes only alter the trailing edge and subsequent section of the airfoil. Care was taken to ensure that the leading edge, as well as the overall airfoil geometry at critical locations was preserved to minimise the effect to aerodynamic performance.

Hence, to correctly quantify the effect of the altered airfoil geometry on the aerodynamic performance, a higher fidelity aerodynamic simulation was deemed necessary. As such, a Computational Fluid Dynamics (CFD) method was implemented to perform higher-fidelity aerodynamic analysis, compared to the lattice methods

of XFLR5. Such a simulation was chosen to both increase the accuracy of the aerodynamic performance values, as well as to ensure that the analysis was coherent to the shape changes made to the airfoil. XFLR5's use of XFOIL as a framework for its calculations disguises limitations in the analysis of foil designs with a higher geometric complexity and can often diverge from experimental data, leading to the decision to implement a CFD analysis.

### 3.5.1. CFD Model Implementation and Validation

The ANSYS Fluent solver was used to simulate the aerodynamic flow around the airfoils. A 2D analysis was implemented to reduce computational time while remaining within the scope of the overall design goals. The airfoils were analysed throughout an $\alpha$ range between $0° - 15°$, with linear spacing of the design points throughout the range. The lift, drag, and pitching moment coefficients were set as the output metrics (pitching moment determined around quarter-chord 0.25c to facilitate comparison with XFLR5 results).

A steady-state solver was implemented, using the Transition SST turbulence model [10] which uses a combination of the k-epsilon and k-omega models to resolve the viscous flow. After initial testing, this model was chosen due to its balance between computational time and result accuracy. Other models, such as Spalart-Allmaras, k-omega, k-epsilon, and Detached Eddy Simulation (DES) were considered, however were not implemented due to time and resource restrictions within the project. A number of assumptions were made in the implementation of the model, detailed below:

- **CFD-ASS-1: Steady Flow -** Constant flow velocity ensures no fluctuations/perturbations at inlet.
- **CFD-ASS-2: Constant Atmospheric Parameters -** Atmospheric constants and parameters (density, pressure) remain constant.
- **CFD-ASS-3: Far-Field Flow -** Airfoil isolated in the flow, perturbations from other components not considered.
- **CFD-ASS-4: No-Slip Wall Condition -** As per boundary layer theory, a no slip condition is implemented on the foil wall.
- **CFD-ASS-5: Turbulent Flow -** Flow is assumed to be fully turbulent (high Reynolds number).
- **CFD-ASS-6: Steady-State Analysis -** Steady-state analysis neglects transient effects. As such, results at $\alpha$ approaching stall will tend to diverge from experimental results due to the increased prevalence of transient flow fluctuations.

For the simulation boundary conditions, the trim speed $V_{trim} = 20.83$ m/s at standard sea-level conditions ($\rho = 1.225$ kg/m$^3$) was used. This velocity was deemed the most relevant for this analysis due to its importance in the flight envelope. Standard sea level atmospheric density was used as the subsequent effect of the change in Reynolds number as a result of decreasing the density was deemed negligible for the scope of this analysis. The overall parameters and conditions of the model are shown in Table 3.3.

**Table 3.3:** 2D Airfoil Analysis CFD Model Parameters.

| Property | | Value | Unit |
|---|---|---|---|
| Free-Flow Velocity | $V_\infty$ | $20.83$ | m/s |
| Air Density | $\rho_\infty$ | $1.225$ | kg/m$^3$ |
| Dynamic Viscosity | $\mu$ | $1.789 \cdot 10^{-5}$ | N s/m$^2$ |
| Reference Length (Chord) | $c$ | 1 | m |
| Reynolds Number | $Re$ | $1,425,995$ | - |
| Turbulent Intensity (Inlet) | $I_{in}$ | $1\%$ | - |
| Turbulent Intensity (Outlet/Backflow) | $I_{out}$ | $5\%$ | - |
| Turbulent Viscosity Ratio | - | $10$ | - |
| Outlet Gauge Pressure | - | $0$ | Pa |
| Y+ Value | $Y_+$ | $0.355$ | - |
| Wall Spacing | $Y_h$ | $6$ | μm |

Meshing of the airfoil geometries was implemented in ANSYS Meshing. A structured, C-Type quadrilateral-dominant mesh was used due to its flexibility and short generation time. Such a mesh also allows for increased orientation of the mesh elements with the flow in the desired $\alpha$ range, increasing the overall mesh quality [11]. An inflation layer was implemented near the airfoil wall to ensure the boundary layer was resolved correctly.

The required wall spacing $Y_h$ was calculated by using the flow conditions and the $Y_+ < 1$ requirement as presented in [12]. As such, a wall spacing of roughly $6$ $\mu$m was used, with a subsequent $Y_+$ value of $0.355$. Following a preliminary mesh convergence study, the generated mesh consisted of $155,682$ nodes and $154,829$ quadrilateral elements. Vertically, $440$ divisions were used for the height of the fluid volume, with an inflation rate of $1.2$ near the airfoil and a bias factor of $50,000$. $220$ divisions were used for the chord-wise discretization of the airfoil. Figure 3.4 and Figure 3.5 show the far and near-field meshing respectively for the reference MH81 airfoil.

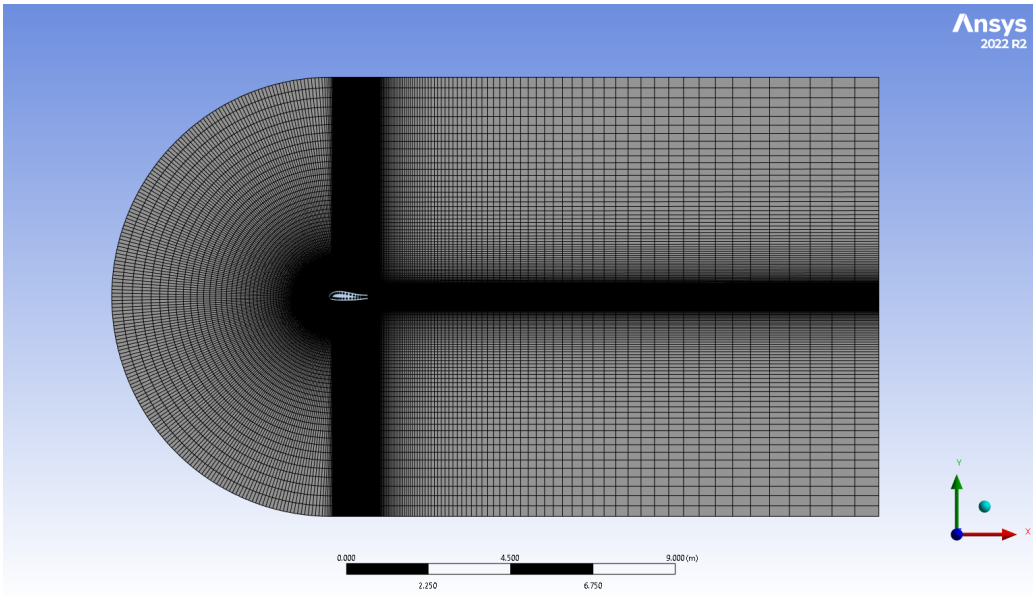


**Figure 3.4:** Far-Field Meshing of MH81 Airfoil.

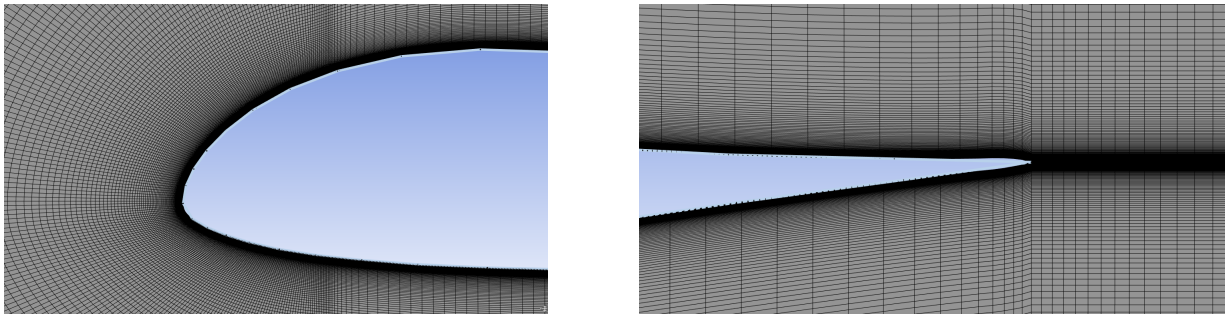

**(a)** Near-Field Leading Edge Meshing of MH81 Airfoil.

**(b)** Near-Field Trailing Edge Meshing of MH81 Airfoil

**Figure 3.5:** Near-Field Meshing of MH81 Airfoil in ANSYS.

From preliminary tests of the model at the given conditions, the $Y_+$ value was calculated at each point of the chord to ensure compliance. These results are shown in Figure 3.6, showing the values below one at all points.

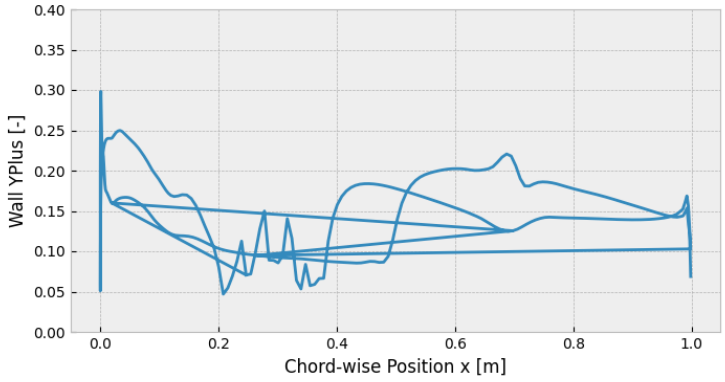


**Figure 3.6:** Chord-wise $y+$ value on MH81 airfoil.

To prevent regeneration of the mesh at each subsequent design point, inlets were placed in both the circular boundary and the two horizontal boundaries. This allowed for the flow to be rotated instead of the geometry, significantly reducing the computational complexity. Computing time was roughly two hours per parametric study, totalling roughly 12 hours of computing time for all the design points.

Validation of the model was performed briefly to ensure the coherence of the results. The methods presented by NASA's Langley Research Center were used, with a simulated flow around a reference NACA 0012 airfoil at a Reynolds Number $Re = 6,000,000$. Mesh size was further refined for this simulation around the airfoil to ensure the adequate $y+$ value as a result of the higher Reynolds number. The results of the model validation are shown in Figure 3.7.

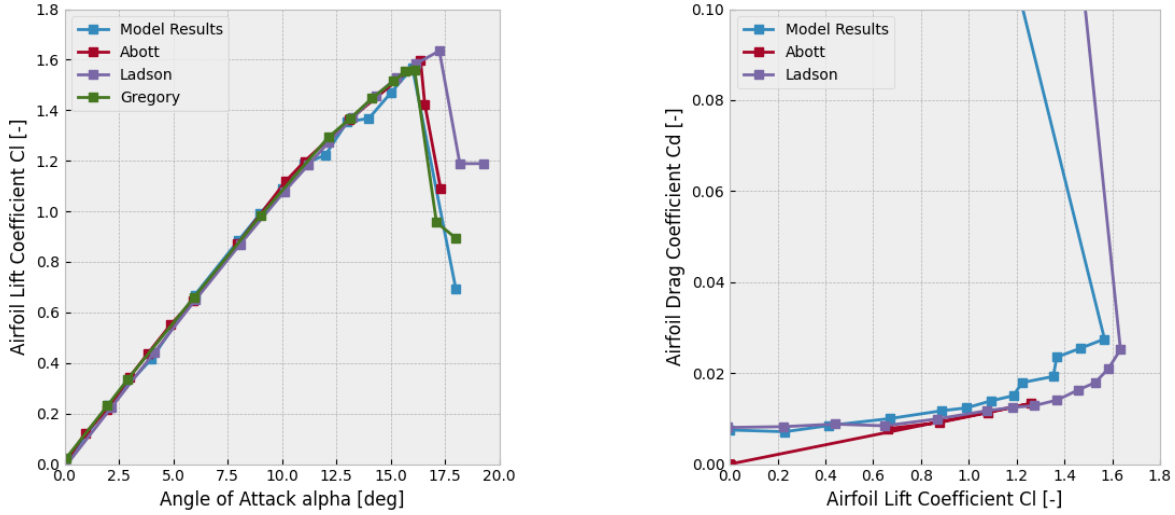


**(a)** NACA 0012 Lift Curve for SA Model Validation.

**(b)** NACA 0012 CL-CD Curve for SA Model Validation.

**Figure 3.7:** NACA 0012 Model Validation Results.

As shown, the SST model slightly overestimates the drag coefficient. With this in consideration, the degree of error is acceptable for the scope of this study.

### 3.5.2. Airfoil Analysis Results

The alterations made to the airfoil geometry, as expected, will have a significant impact on the performance of the airfoils. When the transition occurs closer to the leading edge, the overall effect of the additional reflex added to the airfoils will be decreased. As such, an increase in lift but a significant decrease in positive pitching moment is expected. Figure 3.8a and Figure 3.8b show the lift curve $C_l - \alpha$ and drag polar $C_l - C_d$ respectively.

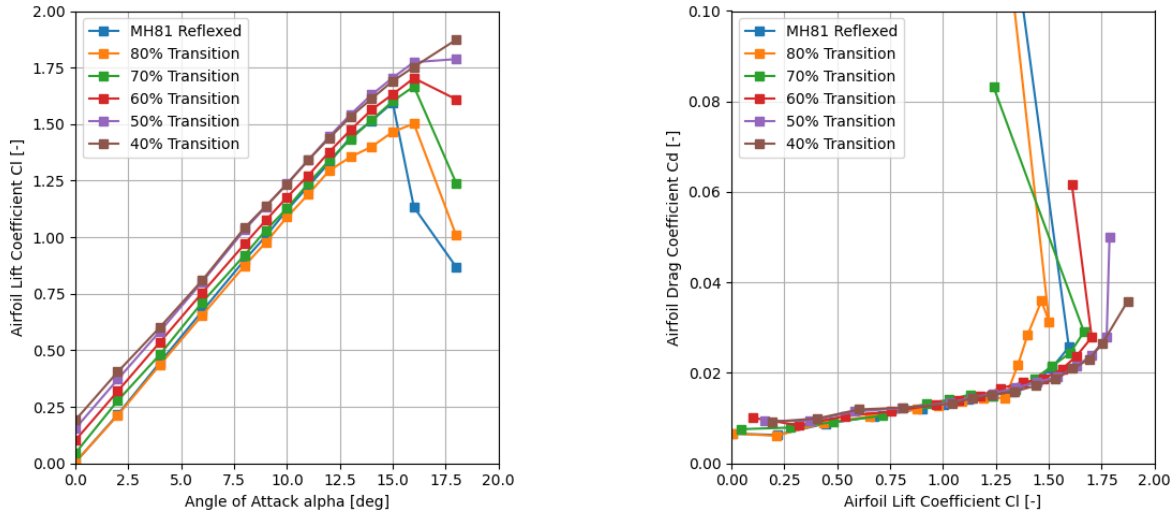


**(a)** Airfoil CFD $C_l - \alpha$ Results.

**(b)** Airfoil CFD $C_l - C_d$ Results.

**Figure 3.8:** Results of altered airfoils.

As expected, there is an inverse relation between the chord-wise position of the transition and the lift generated. This is expected as previously mentioned due to the decrease in the effective reflex of the airfoil. Furthermore, the airfoils with the transition closer to the leading edge also show a decrease in drag and an increase in the stall angle of attack. The increased stall $\alpha$ is a result of the reduction of the total camber of the airfoil, as well as the introduction of a higher slope on the lower surface which helps re-orient the flow at the trailing edge. As such, the airfoils with an earlier transition are more aerodynamically efficient than the MH81 airfoil. However, due to the stability requirements in the design of a flying wing, the pitching moment must also be analysed, shown in Figure 3.9.

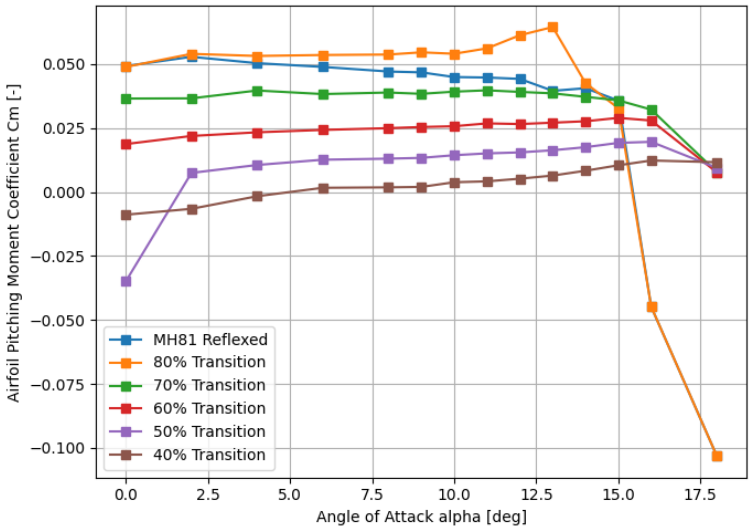


**Figure 3.9:** Airfoil CFD $C_m - \alpha$ Results (Moment Around 0.25c).

The pitching moment was calculated around the quarter-chord point 0.25c, an assumption for the location of the aerodynamic center. The airfoils with the highest lift and efficiency performance also show the lowest performance in terms of pitching moment. Hence, a compromise must be made between lift performance and stability. In the scope of the overall design process, this decision was a combination of aerodynamic, stability, and structural considerations. Ultimately, the transition point was selected at **70%** of the chord, maintaining adequate aerodynamic performance with stability performance similar to the original airfoil.

## 3.6. Wing Design

In order to converge to a final wing design, analyses were executed using XFLR5. All analyses mentioned in this section were performed using the viscous ring vortex lattice method (VLM2). This method used a varying angle of attack analysis, with $V = 20.83$ m/s (trim speed) and standard sea-level atmospheric conditions. Alpha was varied at 0.1° increments. To preliminarily assess the lateral stability of the wing the stability analysis of XFLR5 was used, which computes the eigenvalues of the eigenmotions and the stability derivatives. Meshing was performed on each wing after a preliminary convergence analysis, with focus on boundary refinement. The coordinate system used in the wing design is shown in Figure 3.10. The origin is located at the LE of the root of the wing.

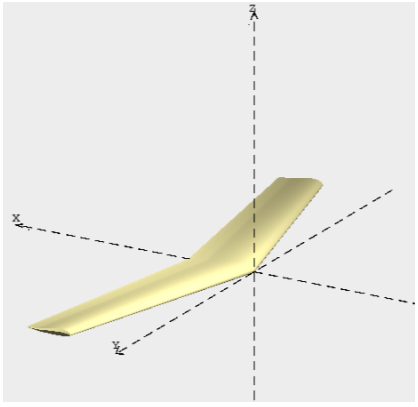

**Figure 3.10:** Coordinate System.

### 3.6.1. Limitations of XFLR5

As XFLR5 is used to design the wing, some corrections had to be made for aspects the model does not account for. One correction that needs to be accounted for is that the program only computes the aerodynamic performance of the wing and is not able to estimate the effects of the pilot, the attachment and the control system. To calculate the total drag area of the system, the drag area of all these elements should be added together. From literature study an estimate drag area for everything apart from the wing of 0.3 $m^2$ in trim configuration and a drag area of 0.53 $m^2$ in landing configuration was found [13]. Adding this to the wing drag area from XFLR5 leads to a more realistic $L/D$ for the whole system for both trim and landing conditions.

Another correction that needs to be accounted for is the fact that the results of the airfoil analyses in XFLR5 do not precisely line up with the higher-fidelity airfoil analyses performed in Section 3.5. To account for this error, the values of $C_L$ as derived from XFLR5 need to be corrected to obtain more realistic values. To perform this correction, an assumption is made that the airfoil-based parameters ($C_l$, $C_d$, $C_m$) can be linearly translated to the wing parameters ($C_L$, $C_D$, $C_M$) through translation factors, calculated by dividing the obtained wing value at a designated angle of attack by the value for the airfoil at the same angle of attack. While in reality changes in the airfoil shape may not lead to totally linear translations, different factors were applied for each wing design (as the translation factors themselves changed), and as such, the error was minimised.

To calculate the desired angle of attack for required calculations, such as performance calculations at trim condition, the following methodology may be applied (assuming a fixed C.G. position):

1. Analyse the wing geometry with and without the pilot mass in XFLR5 (decoupling the pitching moments).
2. Plot the difference between the two $C_m - \alpha$ curves, which now represents the (effective) moment generated by the pilot's mass around the system C.G.
3. Use the CFD airfoil analysis results to find the new target $C_m$ value, applying the relevant translation factor.
4. Find the relevant angle of attack from the pilot's graph. This value of $\alpha$ represents the new design point angle of attack, and the relevant translation factors may now be used to calculate the new $C_L$ and $C_D$ values from the CFD airfoil data. The plot related to this methodology is shown in Figure 3.11.

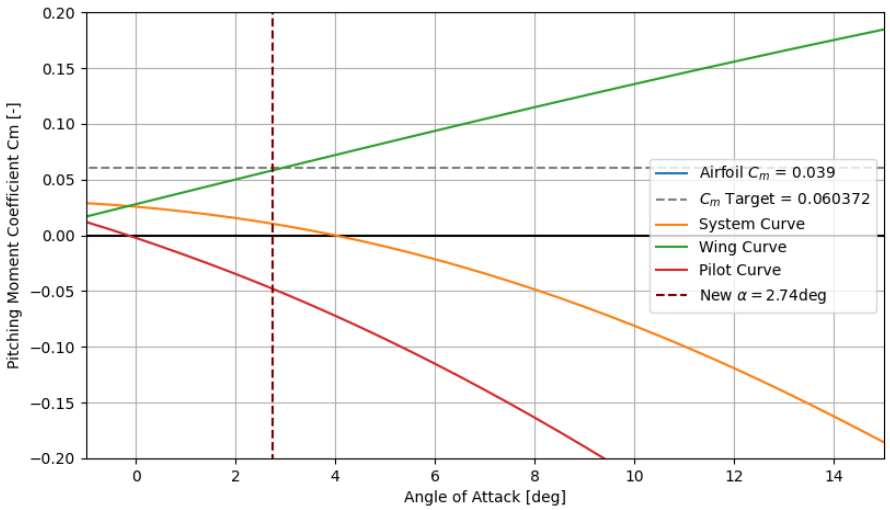


**Figure 3.11:** Transformation between Airfoil Data Sets using Linear Transformation Airfoil-Wing Factors.

These lift and drag corrections were applied to all results that were derived from analyses performed in XFLR5.

### 3.6.2. Iteration Process

To optimise the wing, the design targets mentioned in Section 3.3 were assessed. To summarise, the $C_{m_\alpha}$, $C_L S$ and $L/D$ at trim together with the $C_L S$ at stall had to be optimised. It was previously decided to proceed with the design configuration of a stable flying wing without a tail [14]. For the detailed design of the wing planform, a number of parameters needed to be chosen and/or optimised. A few of these parameters could be preliminarily taken from previous calculations and choices. This includes the airfoil chosen in Section 3.4, a preliminary wing area of 13.5 $m^2$ [14], a pilot mass of 80 kg, a pilot $Z_{C.G.}$ of -0.55 m and a preliminary wing mass of 15 kg. A span of 10 m was taken, since this was determined as the maximum achievable span from preliminary structural calculations, taking into account the chosen wing area and airfoil thickness.

Setting these parameters as constants left the sweep, dihedral, twist, taper ratio and pilot $X_{C.G.}$ as variables. In order to be able to independently examine the effect of each of these variables on the aerodynamic performance of the wing, a base wing was created as reference. This base wing had zero degrees of sweep, dihedral and twist and no taper. A pilot $X_{C.G.}$ of 0.8 m was chosen as a baseline because this allows for alignment of the top of the head with the LE of the wing.

This base wing was then altered with respect to each of the mentioned variables to examine their effects. It was found that sweep and pilot $X_{C.G.}$ had by far the biggest effect on $C_{m_\alpha}$ as well as on lift at the trim condition. Their effect was overall very similar, while more sweep also seemed to increase the stall angle of attack. Changing dihedral and taper did not seem to have a big influence on the target parameters. Adding twist when no sweep was present also had a negligible impact, but adding negative twist in a swept wing was found to increase lift at trim and stall conditions without noticeably affecting $C_{m_\alpha}$.

The findings on the effect of changing these variables were used in the wing design process going forwards. Since the effect of the taper ratio on aerodynamic performance was negligible, a taper ratio of $\frac{2}{3}$ was chosen for aesthetic reasons. The span of 10 m and wing area of 13.5 $m^2$ remained unchanged. Dihedral also had a negligible impact on aerodynamics and longitudinal stability, meaning it can be added later on to allow for lateral stability but was not included for now. Since the amount of sweep and the pilot $X_{C.G.}$ have a similar effect and the biggest overall impact on performance, these parameters were the most important. The range of possible values for the pilot $X_{C.G.}$ is limited, since the design needs to allow for attachment of the pilot at a reasonable position under the wing. For this reason, the range of pilot $X_{C.G.}$'s analysed was from 0.2 to 1 m from the LE of the wing. Multiple wing designs were made, where $X_{C.G.}$ was altered by increments of 0.1 m within its feasible range. Subsequently, the sweep was increased to find the minimum required sweep to get a $C_{m_\alpha}$ of -0.013. All of these wings, with their respective pilot $X_{C.G.}$ and sweep, were analysed for the design targets. It was found that most of the wings had a very similar performance because of their identical $C_{m_\alpha}$ and that all of them could meet the requirements. This meant that no twist had to be implemented and even allowed for the chord and thus wing area to be scaled down, which is preferable since it reduces wing weight. For structural reasons, a wing with this span, taper and thickness needed a root chord of at least 1.5 m. Implementing this new chord for all pilot $X_{C.G.}$ possibilities resulted in a new wing area of 12.5 m. As a result of updated structural calculations the wing mass was also iterated from 15 to 8 kg. Even with this chord reduction, the wings still met the requirements and still showed very small differences in aerodynamic performance. This meant that any of these wing configurations could be chosen, as long as it was structurally and operationally viable. It was chosen to go with a pilot $X_{C.G.}$ of 0.8 m, since this allows for alignment of the top of the head with the LE of the wing. Furthermore, this design did not need excessive sweep, looked aesthetically pleasing and was structurally and operationally viable.

Dihedral was added to this preliminary design since it aids the use of folding wing tips, looks aesthetically pleasing and introduces no major downsides. As an additional benefit, dihedral also increases stability of the spiral motion. To quantify the amount of dihedral to add, the minimum amount of dihedral which was necessary to make the spiral motion stable was implemented. The implemented dihedral was gradual, meaning no sharp corners were introduced into the structure. Foldable wing tips were also implemented into the design at this stage. The mentioned alterations in dihedral slightly changed the $C_{m_\alpha}$. To counteract this, the sweep was adjusted to once again get a $C_{m_\alpha}$ of -0.013. Since sharp corners are not preferred structurally, this sweep was also made gradual afterwards. The small effect this had on $C_{m_\alpha}$ was accounted for by adjusting the pilot $X_{C.G.}$.

## 3.7. Final Wing Results

A render of the final wing design can be seen in Figure 3.12. Its relevant parameters are summarised in Table 3.4. As mentioned, the final design assumed a pilot mass of 80 kg, a wing mass of 8 kg and a pilot $Z_{C.G.}$ of -0.55 m.

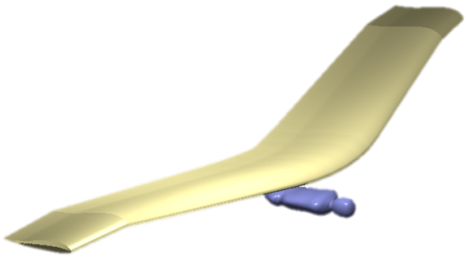

**Figure 3.12:** Isometric View of the Final Wing Design.

**Table 3.4:** Final Wing Dimensions.

| Parameter | Value |
|---|---|
| Wing Span | 10 [m] |
| Wing Area | 12.41 [$m^2$] |
| Taper Ratio | 0.73 [-] |
| Quarter-Chord Sweep | 11.99 [°] |
| Maximum Dihedral | 5 [°] |
| Pilot $X_{C.G.}$ w.r.t. LE | 0.81 [m] |

The lift behaviour and longitudinal stability of the final wing prior to implementing the corrections for XFLR5 are illustrated in Figure 3.13. The performance on the target parameters is summarised in Table 3.5.

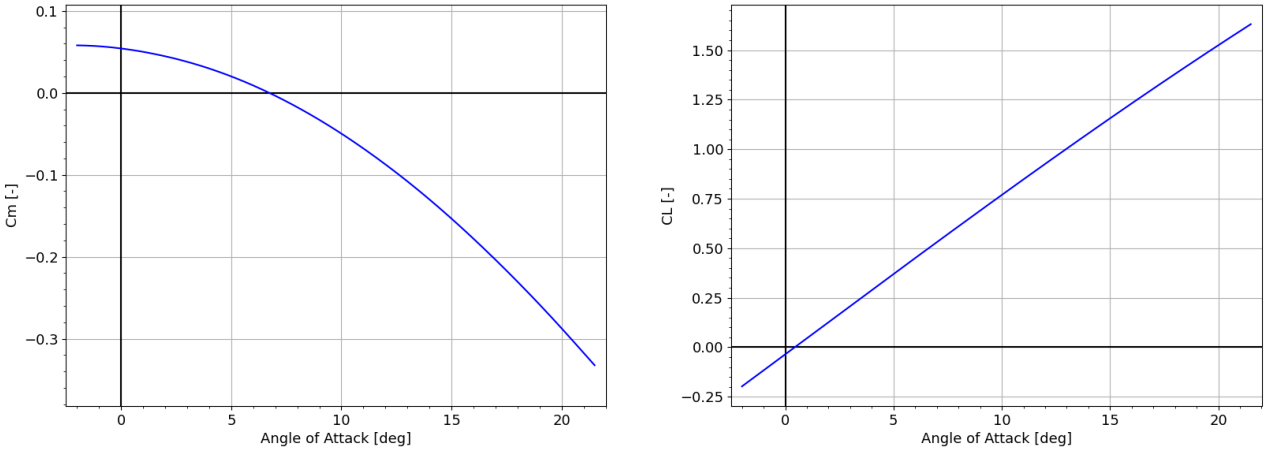


**(a)** $C_m - \alpha$ curve. **(b)** $C_L - \alpha$ curve.

**Figure 3.13:** Results of aerodynamic analysis of the final wing design using XFLR5.

**Table 3.5:** Performance on Target Parameters.

| Parameter | Target Value | XFLR5 Value | Corrected Value |
|---|---|---|---|
| $C_{m_\alpha}$ at Trim | -0.013 [-] | -0.013 [-] | -0.013 [-] |
| $C_L S$ at Trim | 3.50 - 4.72 [m$^2$] | 6.29 [m$^2$] | 4.36 [m$^2$] |
| $C_L S$ at Stall | $\geq$ 11.50 [m$^2$] | 20.17 [m$^2$] | 20.17 [m$^2$] |
| $L/D$ at Trim | $\geq$ 7 [-] | 29.06 [-] | 12.17 [-] |

As can be seen in Table 3.5, the final design meets all target values after the corrections for XFLR5 are taken into account. In addition to meeting the target values, the final wing design is also stable for all dynamic eigenmotions - the short period, phugoid, aperiodic roll, dutch roll and spiral - based on a lateral stability analysis in XFLR5.

To come full circle with the requirements, the obtained corrected values for $C_L S$ can be translated back into trim and stall speed. Since the trim speed is dependent on air density, the trim speed of the wing is function of altitude. For the obtained value of $C_L S$ at trim, the target trim speed of 20.83 m/s is met at an altitude of approximately 2250 m. Stall speed is mostly relevant for the landing, which is assumed to be done at low altitude and consequently at approximately sea-level density. From the obtained value of $C_L S$ at stall, the stall speed comes out to be 8.68 m/s. This means that the requirements for stall and landing speed are comfortably met.

As mentioned earlier in Section 3.3, the design has been evaluated at stall to compare to hang gliders with the same landing procedure. As comparison the Wills Wing Talon 2 hang glider was chosen, as its wing area of 13.38 m$^2$ is similar to that of the final wing. Furthermore, the stall speed of the Talon 2 is 9.16 m/s at a pilot mass of 80 kg, which is very similar to the stall speed of 8.68 m/s of the final wing and identical pilot mass of 80 kg. Comparing the sink rate at stall of 0.96 m/s of the Talon 2 to a sink rate of 0.81 m/s of the final wing, it can be concluded that the aerodynamic performance at stall is similar or even better in terms of a safe landing [15]. The sink rate of the final wing has been calculated using the stall speed and $L/D$ at stall. To calculate the $L/D$ at stall a drag area correction of 0.4 m$^2$ of the pilot has been used as estimation between trim configuration and landing configuration of the pilot [13]. As the performance up to stall and the wing area are similar, it is assumed the behaviour beyond stall is comparable as well and the pilot is able to land safely. For further development the landing procedure should be verified by means of a CFD analysis or a wind tunnel test.

## 3.8. Sensitivity Analysis

Two sensitivity analyses have been performed on the final wing design. The first sensitivity analysis was performed to examine the impact of several in-flight uncertainties on the lift generation and longitudinal stability of

the final wing design. The second sensitivity analysis focused on the influence of pilot mass on the trim and stall speed.

### 3.8.1. In-Flight Uncertainties

The examined uncertain variables were pilot mass, pilot C.G. position, velocity and density. The results of this sensitivity analysis are shown in Figure 3.14. Changes in trim angle of attack and the $C_{m_\alpha}$ at trim can seen in Figure 3.14a. $C_L$ at the trim condition (where $C_m = 0$) can be read from Figure 3.14b by looking at where the graphs intersect the y-axis.

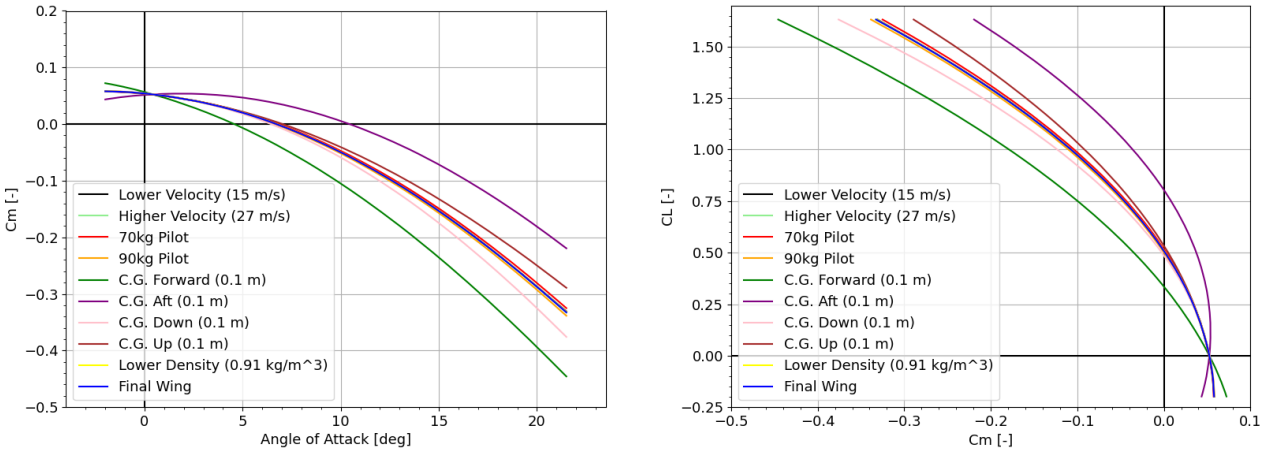


**(a)** $C_m - \alpha$ curves.

**(b)** $C_L - C_m$ curves.

**Figure 3.14:** Results of sensitivity analysis of the final wing design using XFLR5.

The sensitivity analysis shows that from the in-flight uncertainties, the pilot $X_{C.G.}$ has by far the biggest influence on the lift generation and longitudinal stability of the final wing design. A more forward pilot C.G. increases stability but decreases lift at the trim condition, while a more aft C.G. has the opposite effect. Even a 0.1 m shift in pilot $X_{C.G.}$ has quite a big effect, but it should be taken into account that this is desired since shifting the C.G. will be used for velocity and pitch control. All other in-flight uncertainties have an insignificant impact on the lift generation and longitudinal stability of the final wing design. That being said, the pilot $Z_{C.G.}$ has the second biggest influence, followed by the pilot weight. Velocity and density have the smallest impact on the $C_m - \alpha$ and $C_L - C_m$ curves. It should, however, be noted that while the dimensionless coefficients are not significantly impacted, the actual lift and drag produced by the wing will change for different velocities and densities.

### 3.8.2. Influence of Pilot Mass

Previously, the obtained corrected values for $C_L S$ were translated back into trim and stall speed. Since both of these are dependent on pilot mass however, the influence of pilot mass also needs to be analysed. Both the trim and stall speed will thus be evaluated for a lower and a higher pilot mass next to the assumed pilot mass of 80 kg.

Since the trim speed is a function of density, the trim speed of the wing will be plotted with respect to altitude for different pilot masses. The results of the trim speed calculations are presented in Figure 3.15. The final stall speed, including the influence of pilot mass, is presented in Table 3.6.

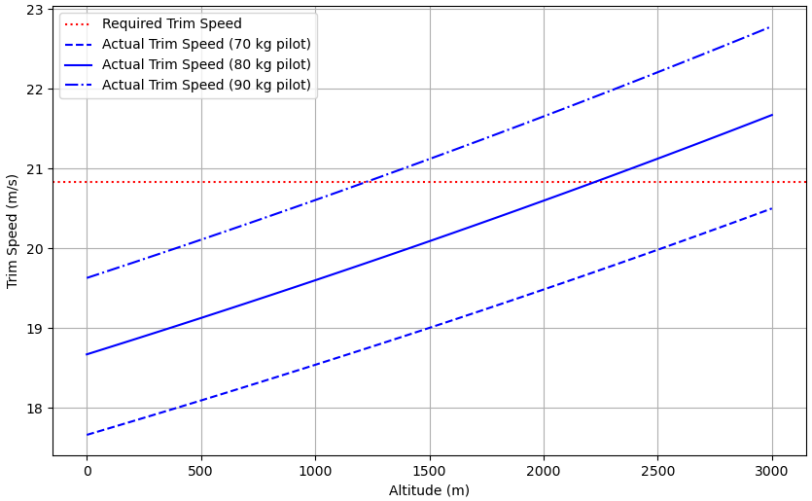


**Figure 3.15:** Trim Speed vs Altitude with Varying Pilot Mass.

**Table 3.6:** Stall Speed with Varying Pilot Mass.

| Pilot Mass | Stall Speed |
|---|---|
| 70 kg | 8.21 m/s |
| 80 kg | 8.68 m/s |
| 90 kg | 9.13 m/s |

By inspecting Figure 3.15, it is clear that the target trim speed is not met for all pilot masses. It is, however, met for the design pilot mass of 80 kg, which is enough to verify the wing design since it is impossible to optimise the wing for every possible pilot mass. For the design pilot mass of 80 kg, the target trim speed is reached at an altitude of approximately 2250 m. Additionally, it is clear from Table 3.6 that the requirements for stall and landing speed are comfortably met even for altered pilot masses.

## 3.9. Analysis of Stability Characteristics Using Numerical Methods

Throughout the PenteFoil design phase, critical attention has been placed on maximizing safety, as per the stakeholder requirements. The dynamic stability of a flying vehicle is crucial to its safety, as it provides a basis for the capabilities of the wing and ensures that the user can remain in control throughout the flight envelope. To adhere to the aforementioned requirements, an analysis of the system's stability must be conducted. Primarily, the longitudinal and lateral stability of the system will be examined through the use of a (decoupled) state-space system to numerically solve for the three-dimensional equations of motion. The five eigenmotions of typical flight will be analysed and conclusions regarding the wing's stability to various state perturbations.

The state-space formulation for the dynamic behaviour of the PenteFoil was derived from literature provided during the TU Delft AE3212-I courses Aerospace Flight Dynamics & Simulation [16]. The system provides a basis to numerically solve decoupled equations of motion for longitudinal and lateral stability. Coupled motion analysis was considered as it would allow for increased accuracy, however was deemed outside the scope of this report. Critically, the subsequent calculations assume that the pilot is instantaneously rigidly attached to the wing, and the C.G. remains in a constant position with respect to the wing.

The coordinate system used throughout the calculations follows the nomenclature provided in the Flight Dynamics course [16]. A visualisation of the coordinate system may be found in Figure 3.16.

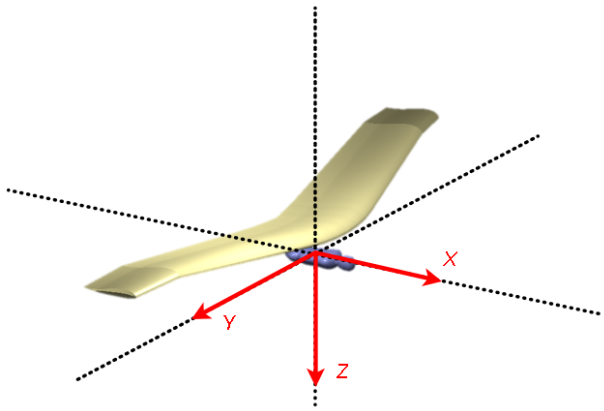


**Figure 3.16:** Coordinate system used for dynamic stability and control analysis.

### 3.9.1. Formulation of Equations of Motion and State-Space

The linearised longitudinal (symmetric) equations of motion are derived using four parameters: the velocity disturbance $\hat{u}$, angle of attack $\alpha$, pitch angle $\theta$, and normalised pitch rate $q\bar{c}/V$. As such, the state-space model solves the 'stick-fixed' longitudinal equations of motion, expressed in Equation 3.2.

$$\begin{bmatrix} C_{X_u} - 2\mu_c D_c & C_{X_\alpha} & C_{Z_0} & 0 \\ C_{Z_u} & C_{Z_a} + (C_{Z_{\dot{a}} - 2\mu_c) D_c} & -C_{X_0} & C_{Z_q} + 2\mu_c \\ 0 & 0 & -D_c & 1 \\ C_{m_u} & C_{m_a} + C_{m_{\dot{a}} D_c} & 0 & C_{m_q} - 2\mu_c K_Y^2 D_c \end{bmatrix} \begin{bmatrix} \hat{u} \\ \alpha \\ \theta \\ \frac{q\bar{c}}{V} \end{bmatrix} = 0 \tag{3.2}$$

For the linearised lateral (asymmetric) equations of motion, four parameters are once again used: sideslip angle $\beta$, roll angle $\phi$, normalised roll rate $pb/2V$ and normalised yaw rate $rb/2V$. Hence, the state-space model solves the 'stick-fixed' lateral equations of motion, expressed in Equation 3.3.

$$\begin{bmatrix} C_{Y_\beta} + (C_{Y_{\dot{\beta}} - 2\mu_b) D_b} & C_L & C_{Y_p} & C_{Y_r} - 4\mu_b \\ 0 & -\frac{1}{2} D_b & 1 & 0 \\ C_{l_\beta} & 0 & C_{l_p} - 4\mu_b K_X^2 D_b & C_{l_r} + 4\mu_b K_{XZ} D_b \\ C_{n_\beta} + C_{n_{\dot{\beta}} D_b} & 0 & C_{n_p} + 4\mu_b K_{XZ} D_b & C_{n_r} - 4\mu_b K_Z^2 D_b \end{bmatrix} \begin{bmatrix} \beta \\ \phi \\ \frac{pb}{2V} \\ \frac{rb}{2V} \end{bmatrix} = 0 \tag{3.3}$$

To derive a continuous dynamic model, these equations of motion are transformed into a linear time-invariant (LTI) system. The exact formulation for this is not described in this report due to functional constraints [17]. As a result, the systems are expressed in the traditional state-space formulation shown in Equation 3.4, with $A$ the state matrix, $B$ the input matrix, $C$ is the output matrix, and $D$ is the feed-through matrix.

$$\begin{aligned} \dot{\overline{x}} &= A\overline{x} + B\overline{u} \\ \overline{y} &= C\overline{x} + D\overline{u} \end{aligned} \tag{3.4}$$

During pure stability analysis, the $B$ matrix and $\overline{u}$ vector are set to zero. Furthermore, the time invariance of the system results in the time-dependent terms $D_c = 0$ and $D_b = 0$ for the longitudinal and lateral systems respectively. As a result, time-variation of environmental parameters is neglected. However, for the time-scale in which the models are used, this assumption causes negligible effects. Furthermore, the linearisation of the system limits the analysis to (relatively) small angles, with the results often diverging at higher orientation angles. Despite these limitations, the models performance is adequate for the scope of this report.

As a result of resource and time constraints, verification and validation of this model is not within the scope of this report. Existing verification and validation has been performed for the used model in the past and can be found through Sachinis et. al [17].

### 3.9.2. Longitudinal Stability Analysis

The symmetric model will analyse the pitching stability of the PenteFoil wing. This will be performed by introducing perturbations to each of the state variables of a system at rest and analysing the system's response. The initial conditions of the system will be set to trim conditions with $V = 20.83$ m/s at an altitude of $h = 2000$ m. This altitude as a reasonable maneuvering altitude for the PenteFoil. Critically while the damping and frequency of the system might change, the overall behaviour of the system will not with changing density altitude. As such, the analysis can be performed at these conditions. XFLR5's Stability Analysis feature was used to extract the longitudinal stability derivatives, shown in Table 3.7. Note that values relating to angle disturbances are presented in *radians*.

**Table 3.7:** PenteFoil Longitudinal Stability Derivatives.

| Coefficient | Value | Coefficient | Value |
|---|---|---|---|
| $C_{x_u}$ | -0.0333 | $C_{m_0}$ | 0.0555 |
| $C_{x_\alpha}$ | 0.2992 | $C_{m_u}$ | 0.0068 |
| $C_{z_u}$ | -0.0034 | $C_{m_\alpha}$ | -0.7312 |
| $C_{z_\alpha}$ | -4.6058 | $C_{m_q}$ | -3.2384 |

Attention has been placed to adjust the stability coefficients between the two systems. XFLR5 uses the methodology as described by Etkin and Reid (1995) [18]. Small changes have been applied to the dimensionless stability derivatives to ensure standardization between the models. Firstly, a $\bar{u} = 0.5$ velocity disturbance will be applied to the model, equating to a velocity of $V_0 = 31.25$ m/s applied to the trim condition. The results of this disturbance are shown in Figure 3.17.

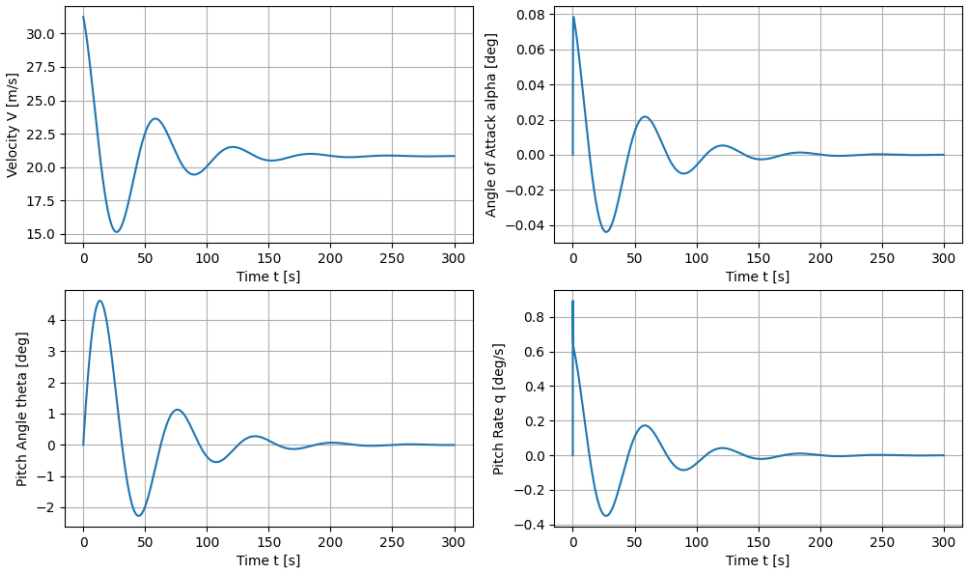


**Figure 3.17:** Dynamic response of the PenteFoil to a $\bar{u} = 0.5$ velocity disturbance.

As expected, the velocity initializes at $V_0 = 31.25$ m/s which causes an instantaneous increase in the pitch rate $q$ and angle of attack $\alpha$. Following this initial rotation, the wing effectively begins climbing and experiences an increase in the pitch angle $\theta$. The (slow) oscillation shown by the velocity disturbance is the phugoid mode, one of the natural modes of aircraft dynamics. Critically, this mode is stable and will not diverge with increasing velocity disturbances. The small $\alpha$ is a point of interest. As a result of the system's small moment of inertia around the Y-axis $I_{yy}$, very little moment is required to cancel a disturbance. As such, small perturbations in the angle of attack are required to maintain stability. The phugoid motion is also shown when a pitch angle $\theta$ disturbance is introduced, shown by Figure 3.18.

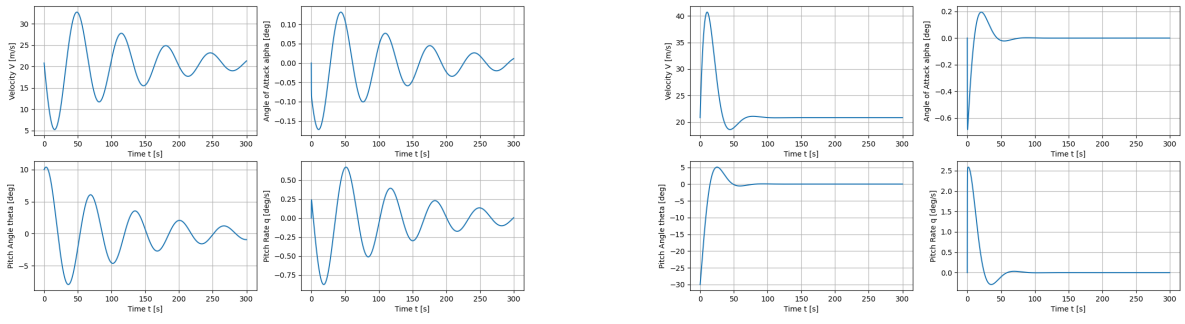

**(a)** $\theta = 10$ degrees.

**(b)** $\theta = -30$ degrees.

**Figure 3.18:** Dynamic response of the PenteFoil to a pitch angle $\theta$ disturbance.

Figure 3.18a shows the response of the system with a positive $\theta = 10°$ disturbance. The system maintains the same oscillatory properties as the previous system, albeit with a higher amplitude. However, the system response varies drastically with a negative $\theta = -30°$ disturbance, with a much faster and more aggressive damping being prevalent. This is beneficial in terms of stability, as the system is more stable to dives and dive recovery. Lastly, an angle of attack $\alpha = 10°$ will be provided to the system, Figure 3.19 (note the smaller time-scale on the x-axis).

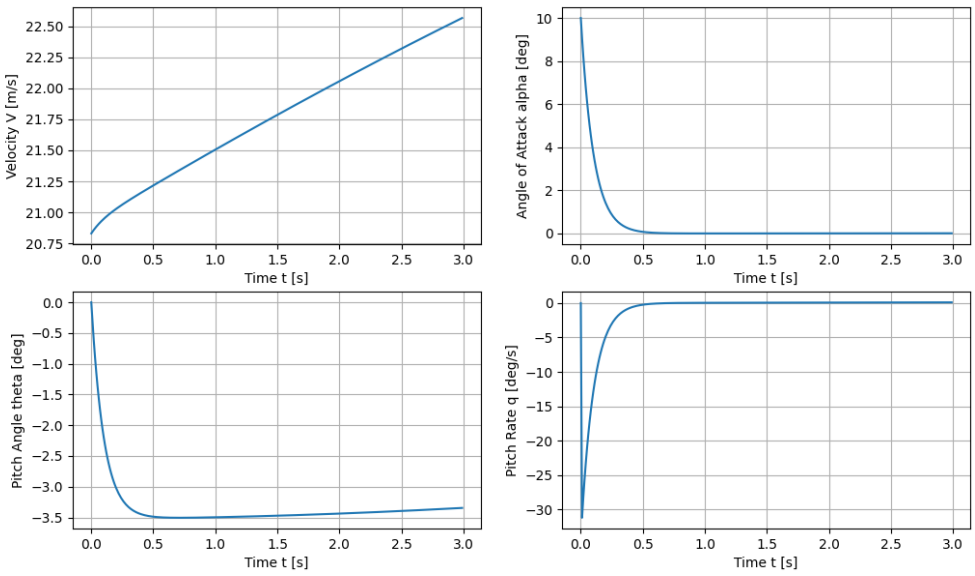


**Figure 3.19:** Dynamic response of the PenteFoil to an $a = 10°$ angle of attack disturbance.

Literature and conventional aircraft dynamics would suggest such a perturbation would lead to the prevalence of the short period motion, a short, quickly damped oscillatory motion. However, no oscillation is present here as a result of the instantaneous $\alpha$ disturbance. This is beneficial in terms of stability, as a reduction in oscillatory motions leads to increased control and predictability of the system. When analysing this system with respect to existing literature, it is critical to consider the effect the position of the C.G. has on the system. In conventional aircraft, the C.G. is vertically positioned closer to the vertical position of the neutral point and center of pressure. However, in the PenteFoil's hang glider-esque configuration, the C.G. lies some considerable distance below the wing. As such, a pendulum effect is created, which adds positively to the stability of the system and increases the damping of aerodynamic oscillations. Thus, the pilot positioning is crucial for the stability of the system, both in the horizontal x-axis and the vertical y-axis. Ultimately however, these results may also highlight potential discrepancies in the system. Potential causes of error will be discussed in Section 3.13.

The longitudinal stability characteristics of the system may also be confirmed by eigenvalues resulting from the state-space representation. The eigenvalues corresponding to the phugoid and short period motions, as well as the period and time to half-amplitude values are shown in Table 3.8.

**Table 3.8:** Eigenvalues of symmetric motion.

| Motion | Eigenvalue | Period $P$ [s] | Half Time $T_{\frac{1}{2}}$ [s] | Time Constant $\tau$ [-] |
|---|---|---|---|---|
| *Phugoid* | $-0.02251 \pm 0.10021j$ | 62.70 | 30.79 | 44.42 |
| *Short Period* | $-9.75784$ | - | 0.07104 | 0.10248 |

## 3.9.3. Lateral Stability Analysis

Following the longitudinal analysis, the asymmetric model will be used to analyse the rolling and yawing stability of the PenteFoil wing. As previously, disturbances will be introduced to the system state variables independently and the dynamic response will be analysed. The initial trim conditions will be kept as previously. The lateral stability derivatives are shown in Table 3.9.

**Table 3.9:** PenteFoil Lateral Stability Derivatives.

| Coefficient | Value | Coefficient | Value | Coefficient | Value |
|---|---|---|---|---|---|
| $C_{Y_b}$ | -0.01523 | $C_{l_\beta}$ | -0.06472 | $C_{n_\beta}$ | 0.00143 |
| $C_{Y_p}$ | -0.02073 | $C_{l_p}$ | -0.50757 | $C_{n_p}$ | -0.07172 |
| $C_{Y_r}$ | 0.01390 | $C_{l_r}$ | 0.12576 | $C_{n_r}$ | -0.21970 |

Similarly to the longitudinal analysis, small adjustments were made to the output derived from XFLR5 to ensure the corrected non-dimensionalisation of the variables. Firstly, a sideslip angle $\beta = 20$ degrees disturbance will be introduced to the model. The results of this perturbation are shown in Figure 3.20.

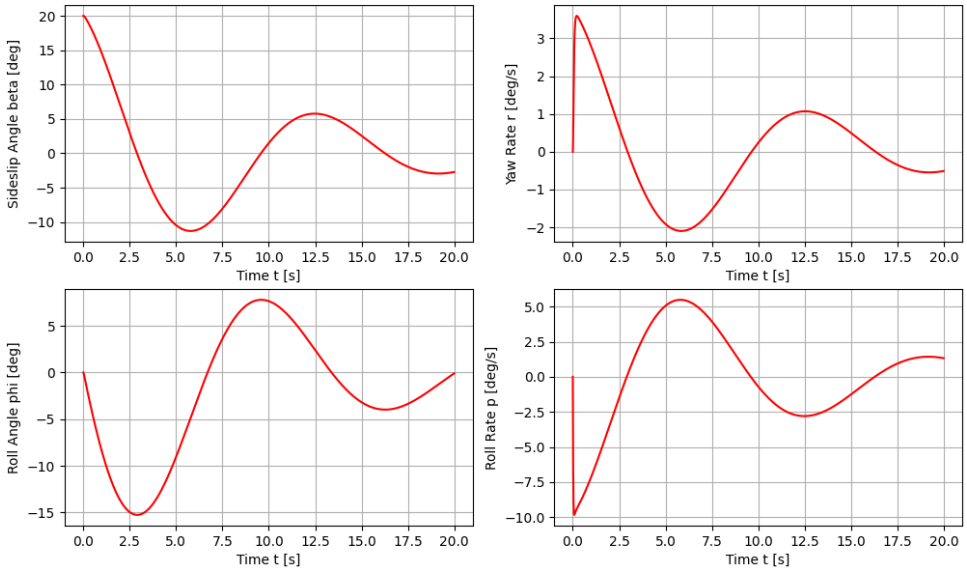


**Figure 3.20:** Dynamic response of the PenteFoil to a $\beta = 20$ degrees sideslip disturbance.

The initial sideslip disturbance leads to an instantaneous yaw rate which begins to reduce the sideslip. Simultaneously, the velocity difference over the two sides of the wing caused by the sideslip leads to a lift differential, which initiates a rolling motion. This damped, oscillatory motion is described as the dutch roll, and is often initiated by a sideslip or yaw perturbations. Critically, this motion is damped, albeit not as well as for most aircraft. This is a result of the lack of a vertical tail, which normally provides the majority of the damping force. In the case of the PenteFoil, the damping is caused by the wing sweep, as well as the low position of the pilot which reduces the amplitude of roll oscillations. For hang gliders and flying wings, the effect of the dutch roll can be reduced by a roll input. Next, a roll rate disturbance of $p = 20$ °/s will be placed on the system, shown in Figure 3.21.

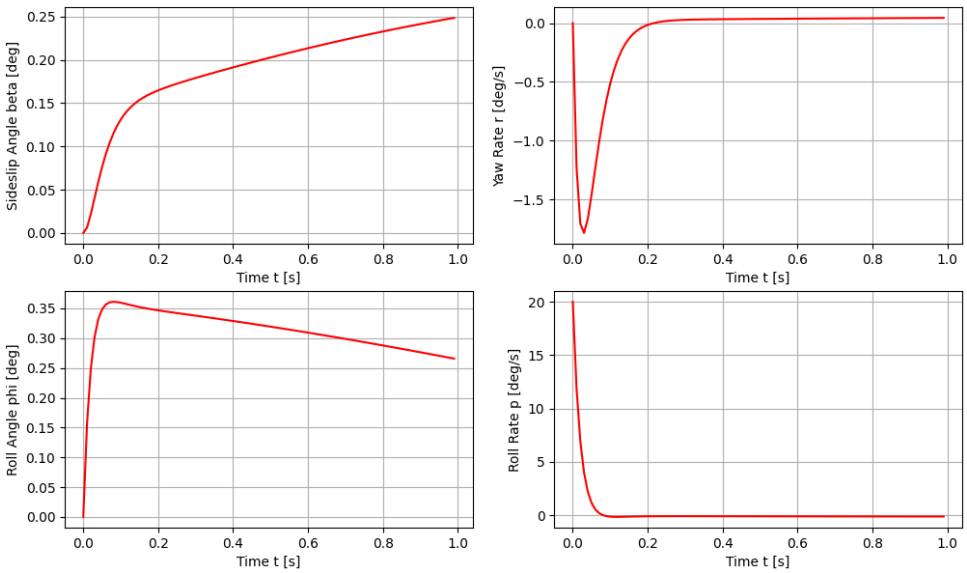


**Figure 3.21:** Dynamic response of the PenteFoil to a $p = 20$ °/s roll rate disturbance.

Critically, the instantaneous rolling motion is very quickly damped and is not oscillatory. This is a result of the roll damping stability derivative $C_{l_p}$, and is vital for the dynamic stability of the wing. This motion is quasi-representative of the aperiodic roll, a motion in which the initial angular acceleration of roll is high, followed by a damping of the motion and a constant roll rate. This will be further explored in Section 3.10, as the true representation of this motion requires a constant roll input. The rolling motion also induces a negative yaw rate due to the presence of adverse yaw, which is further amplified by the lack of a vertical stabiliser. The magnitude of the generated sideslip angle relative to the roll angle must be noted, as this can be the cause of instability with larger perturbations, albeit these cannot be modelled due to the linearity of the system. Following the initial disturbance, the system then enters the dutch roll mode, which is stable. Lastly, the stability of the system to a roll angle $\phi = 20°$ will analysed, Figure 3.22.

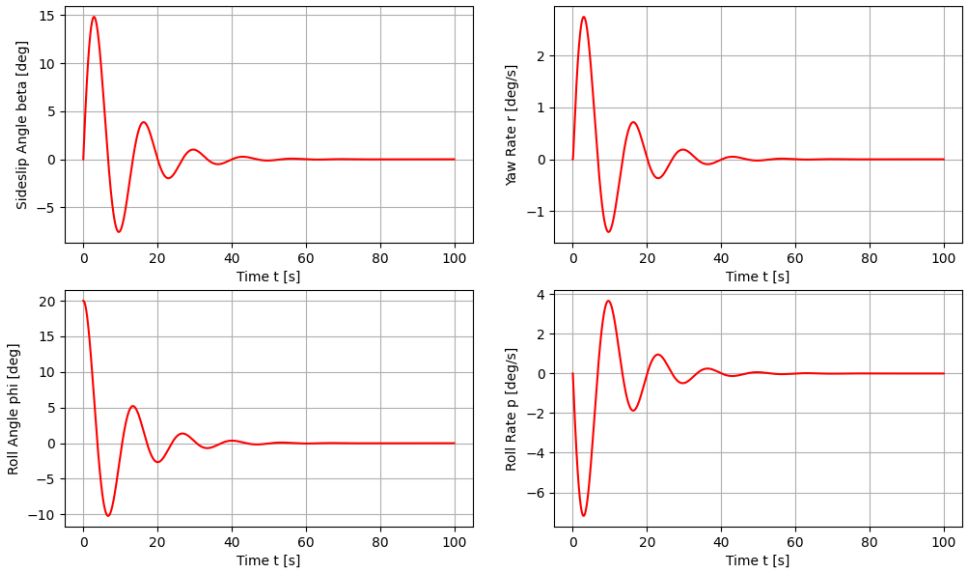


**Figure 3.22:** Dynamic response of the PenteFoil to a $\phi = 20$ degrees roll angle disturbance.

Similarly to the sideslip disturbance, the roll angle disturbance causes a roll rate which tends to stabilise the system. As such, the motion is damped. In traditional aircraft dynamics, a perturbation in the roll angle $\phi$ leads to an unstable motion referred to as the spiral mode. This is accepted in certification and design, as the period of the motion is large (order of magnitude of minutes), providing plenty of margin for correction. In the case of the PenteFoil, the low C.G. with respect to the wing critically adds to the stability of this motion. As a result of the pendulum motion, the displaced C.G. provides a restoring force, resulting in a stable spiral mode. The wing sweep, dihedral, and lack of a vertical tail also aid in the stability of the spiral mode. The oscillation shown in Figure 3.22 is a result of the dutch roll motion, initiated by the adverse yaw as a result of the restoring rolling moment.

The findings of this report regarding the lateral stability of a dynamic system similar to that of a hang glider are corroborated in a paper by Cook and Spottiswoode regarding the flight dynamics of hang gliders [9]. Similarly to the PenteFoil, the aperiodic roll motion is very heavily damped. This is a direct result of the (relatively) large wing span, as well as a potential overestimation of the roll damping derivative as certain non-linear effects of rolling non-stiff structures, such as structure deflection and aerodynamic shape perturbations, are not accounted for. Furthermore, the spiral mode shows a high level of stability, with a short time constant $\tau$.

However, it must be noted that the increased stability of this motion in the system may be caused by the rigid pilot-wing assumption stated previously. In real systems, the pilot is not rigidly attached to the wing and moves significantly with respect to the wing. As such, the stabilizing and non-stabilizing forces acting on the system may. However, the implementation of such a two-body system would lead to a non-linear system, the development of which is outside the scope of this report.

The eigenvalues of the lateral stability state-space system which characterise the behaviour of these modes are shown in Table 3.10.

**Table 3.10:** Eigenvalues of asymmetric motion.

| Motion | Eigenvalue | Period $P$ [s] | Half Time $T_{\frac{1}{2}}$ [s] | Time Constant $\tau$ [-] |
|---|---|---|---|---|
| *Dutch Roll* | $-0.10058 \pm 0.47007j$ | 13.36636 | 6.89141 | 9.94221 |
| *Aperiodic Roll* | $-26.17581$ | - | 0.02648 | 0.03820 |
| *Spiral* | $-47.39596$ | - | 0.01462 | 0.02110 |

## 3.10. Control System Analysis and Effectiveness Estimations

To quantify the true dynamic behaviour of the PenteFoil, the effectiveness of the control options as well as the system's response to control inputs must be quantified. The final control system of the PenteFoil primarily consists of inputs generated by shifting the C.G. of the pilot with respect to the wing. Furthermore, the wing tips may also be folded to provide supplemental roll control. As a result of this unconventional control system, derivation of the required control derivatives poses a significant challenge. The effective two-body system leads to a non-linear system, and a dynamic problem must be solved to calculate all the relevant forces. To simplify the calculations required and the development of the system, a number of assumptions will be made regarding the dynamics of the system:

- **CONT-ASS-1: Quasi-Rigid System -** The pilot and wing are considered rigid at $t = 0$ in order to quantify the effectiveness of the control input.
- **CONT-ASS-2: Constant Pilot Orientation -** The pilot and wing are rigid for the duration of a control input, and their relative orientation does not change. This slightly overestimates the effectiveness of control, as C.G. control inputs tend to become less effective with increasing pitch or roll angle.
- **CONT-ASS-3: Neglecting Wing Motion -** In a two-body system, the movement of the pilot for control would also initiate a rotation in the wing decoupled from the rotation initiated due to the C.G. shift. Due to time constraints, analysis of this rotation is not considered. This underestimates the control effectiveness[9].

A note must be made here about the design concepts being analysed. In contrast to the initial design concept selected at a previous stage of the decision, this control system lacks the implementation of morphing elevons on the trailing edge of the wing. During preliminary calculations, these proved to be too complex to implement with respect to operations and structural constraints, and were deemed redundant. As such, they were omitted from the final design development. Thus, with the critical assumptions in place, the relevant control derivatives can be calculated.

### 3.10.1. Calculation of Control Derivatives and Control Force

Differentiating from the conventional aircraft control derivatives, new control derivatives will need to be derived to quantify the control due to a change in C.G. position, as well as due to the wing tip deflection. As the pilot effectively rotates about a single point directly above on the lower surface of the wing, the C.G. control will be quantified as a result of angular displacements $\theta_g$ and $\xi_g$ for longitudinal and lateral displacement respectively. Coherent with the coordinate system, a positive $\theta_g$ deflection will lead to a pitch down moment, and a positive $\psi_g$ deflection will lead to a rolling moment to the left.

With regards to the folding tips, a deflection $\delta_w$ was defined, with a positive deflection suggesting a downwards deflection of the right wing tip, thus a rolling moment to the right. It is assumed that for pure roll motion, only the wing tip on the side of the desired direction of motion is deflected. The geometric definitions of the deflections as described above are shown in Figure 3.23.

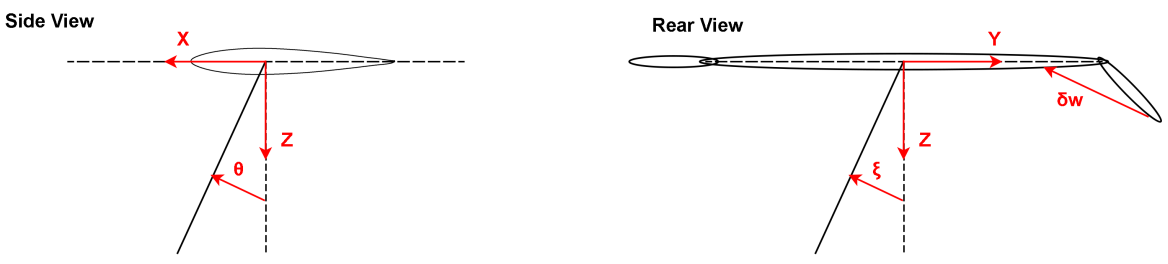


**(a)** Definition of $\theta$.

**(b)** Definition of $\xi$ and $\delta_w$.

**Figure 3.23:** Definition of control angles.

[9] Further development regarding the modelling of this system in hang gliders is further analysed in [19].

Calculating the control derivatives followed a relatively standard methodology. Firstly, force estimations must be made by varying the control displacements. The control derivatives (including the adverse derivatives) can be calculated straight-forwardly through the template equation Equation 3.5, where $C_A$ is the moment coefficient around an axis $A$, and $C_{A_\delta}$ is the respective control derivative with respect to a deflection $\delta$.

$$C_A = C_{A_\delta}\delta \tag{3.5}$$

The aerodynamic forces acting on the wing were calculated using XFLR5, with an analysis as described in Section 3.7. To allow for more complex calculations to be conducted on the extracted data, a custom data loader was created using Python, which allows for direct manipulation of the individual panel elements, and as such allows for the simulation of asymmetric geometries through dataset superposition, as well as for the addition of moving C.G. points, etc. This tool was heavily verified by comparison to the outputs of the XFLR5 calculations. Furthermore, this tool automatically translates the outputs from the XFLR5 coordinate system to the dynamic stability reference system described in Figure 3.16.

Firstly, the longitudinal and lateral C.G. control derivatives were calculated. From pressure force distribution data extracted from XFLR5 at the trim condition, the aerodynamic forces on the wing were calculated at various velocities between $V = [10, 50]$ m/s, with $\rho = 1.225$ kg/m$^3$. This parameterization was necessary, as the effect of a C.G. shift changes with velocity, with the aerodynamic forces becoming larger in magnitude and more dominant at higher velocities. Next, the effect of the pilot was considered by imposing the consequent weight and drag as point forces acting at the C.G. of the pilot. The drag of the pilot was estimated using experimental data and predictions conducted by Kroo for NASA [7]. The lift of the pilot was considered negligible, and is thus not included in this analysis. Furthermore, the derivatives with respect to the sideforce $Y$ are not considered, as the contribution to the sideforce was deemed negligible. Consequently, the two C.G. control derivatives were altered independently at angles between $[-45, 45]$ degrees, and the average slope was obtained for each curve. The results of the relevant control derivatives $C_l$, $C_m$, and $C_n$ are shown in Figure 3.24 and Table 3.11. The values are dimensionless and represent the effectiveness per radian of deflection of the respective angle.

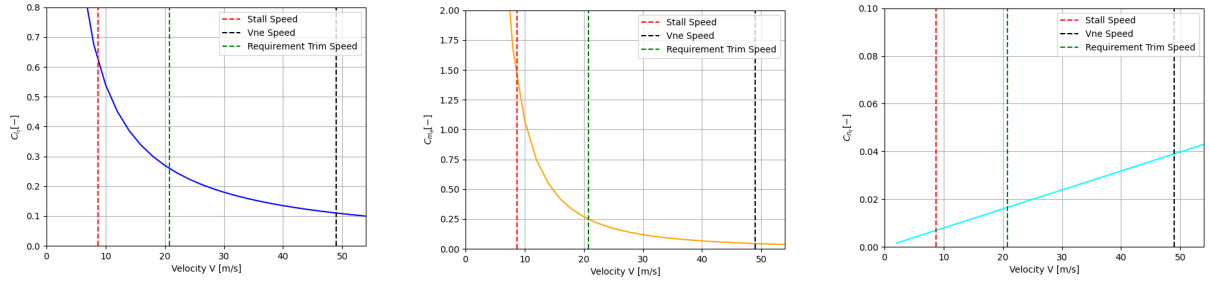


**(a)** $C_{l_\xi}$ **(b)** $C_{m_\theta}$ **(c)** $C_{n_\xi}$

**Figure 3.24:** Results of C.G. control derivative calculations varying with airspeed.

**Table 3.11:** Dimensionless C.G. control derivatives at key velocities.

| **Control Derivative** | **Stall,** $V_s = 8.7$ m/s | **Target Trim,** $V_{trim} = 20.83$ m/s | **Never Exceed,** $V_{ne} = 49$ m/s |
|---|---|---|---|
| $C_{l_\xi}$ | -0.622 | -0.263 | -0.111 |
| $C_{m_\theta}$ | -1.437 | -0.251 | -0.052 |
| $C_{n_\xi}$ | -0.007 | -0.017 | -0.039 |

With regards to the limit of deflection of each of the respective angles, the theoretical limit is a 90° deflection for each. However, practically this cannot be the case due to the relative motion and rotation of the two bodies. Furthermore, at higher C.G. deflection angles the effectiveness of control decreases significantly with increasing deflection. As such, practical limits of 30° for pitch and 45° for roll have been set.

Calculating the control force required for a C.G. shift input was deemed outside the scope of this paper. As previously mentioned, such force derivations require the development of a full two-body dynamic system which could not be fully developed and verified within the time frame of this design project. However, the control method has been proven to be effective and manageable for decades in hang gliders and other sports and continues to remain viable.

For the folding tips, only the lateral control derivatives will be calculated, as the mechanism has negligible contributions to pitch control. An adverse effect to pitch may be generated as a result of the change in the longitudinal position of the center of pressure, however due to the use of a decoupled LTI system, accurately predicting this behaviour is not possible. Nevertheless, this discrepancy does not present a threat to the overall stability of the system as it can easily be accounted for with small pitch control inputs. To correctly place the hinge point for the folding tips, an analysis of their control effectiveness, as well as control force, must be performed at different locations from the tip of the wing. A number of points between $[0.3, 1.5]$ m were selected following discussions regarding aerodynamic and structural considerations. The analysis consisted of generating the different wings at the trim condition for multiple tip deflection angles $\delta_w$, then superimposing half the wing from the ”neutral” position and half from the deflected position (assuming only one side deflects). As such, the subsequent rolling and yawing moment coefficients may be calculated. The results are shown in Figure 3.25.

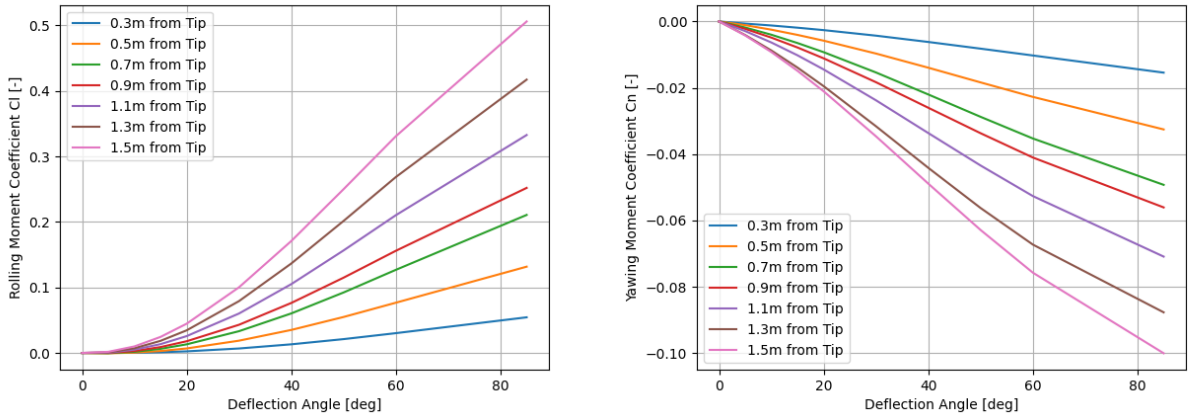


**(a)** $C_l$ **(b)** $C_n$

**Figure 3.25:** Results of folding wing tips moment coefficients varying with tip deflection angle $\delta_w$.

As expected, both the rolling moment and yawing moments increase with deflection angle and tip length, allowing for an easy comparison. The average control derivatives for each tip length are shown in Figure 3.26.

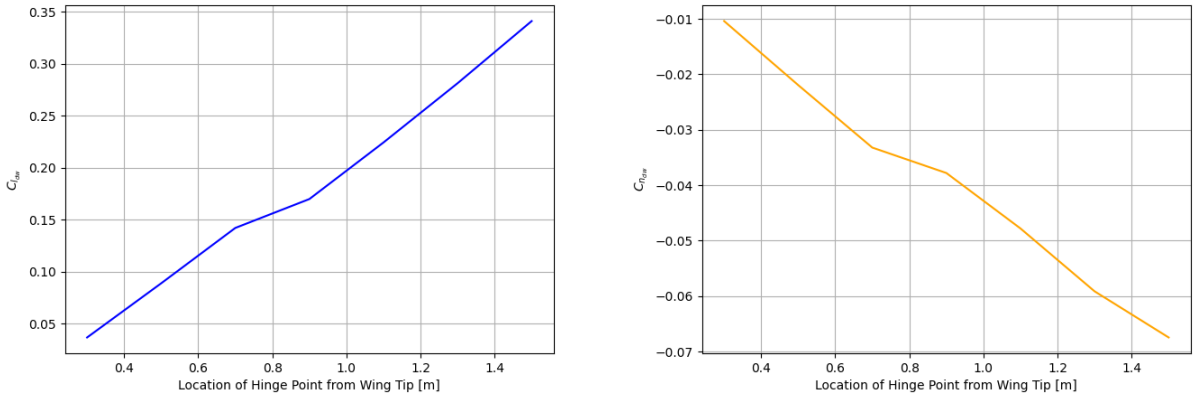


**(a)** $C_{l_{\delta w}}$ **(b)** $C_{n_{\delta w}}$

**Figure 3.26:** Results of folding wing tips control derivatives with position of tip hinge point.

The quasi-linear relationship between the control derivatives and the the location of the folding hinge point is expected, as the effect of taper at the tips is quite small. As such, the resulting ”lift loss” from folding the tips will be almost linear with decreasing surface area. Next, it is critical to analyse the behaviour of the control derivatives with respect to velocity, the results of which are shown in Figure 3.27.

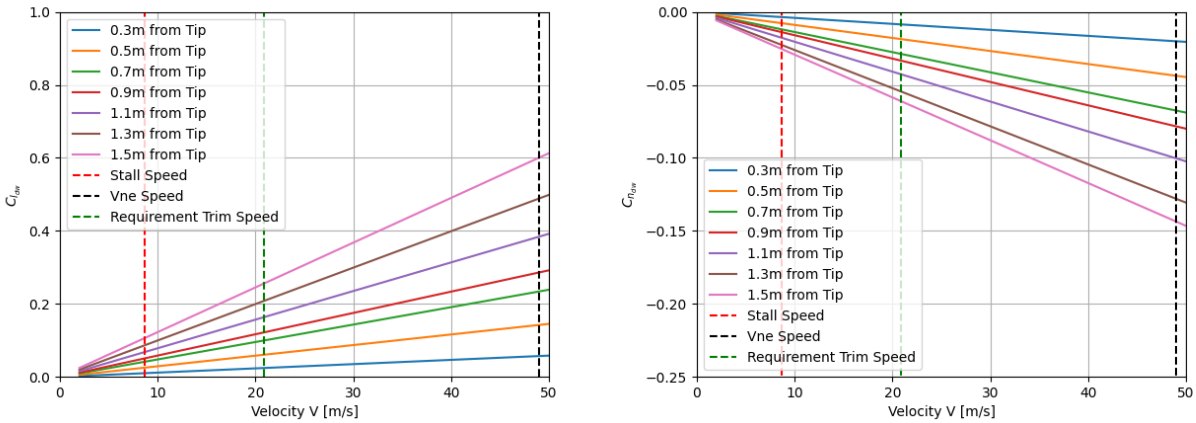


**(a)** $C_{l_{\delta w}}$ **(b)** $C_{n_{\delta w}}$

**Figure 3.27:** Results of folding wing tips control derivatives with velocity.

The derivatives increase linearly with velocity, an outcome of the non-dimensionalization of the derivatives being with respect to $V$ and not $V^2$. As there is no clear maximum, a more practical decision must be made with regards to the final sizing of the folding wing tips. As such, the control force estimation for each tip hinge distance will be generated by deflection and velocity. For this analysis, a straight point load is assumed at the tips centered longitudinally, pointing directly at the C.G. of the pilot. Deviations due to this assumption are negligible. Data for the control force of the folding tips at the trim speed $V_{trim} = 20.83$ m/s and never exceed speed $V_{ne} = 49$ m/s are shown in Figure 3.28, with standard sea level conditions. In addition to the aerodynamic forces a constant structural load of 59 N is applied, representing the force required to buckle the structure against the inflation pressure, as described in Section 4.4.

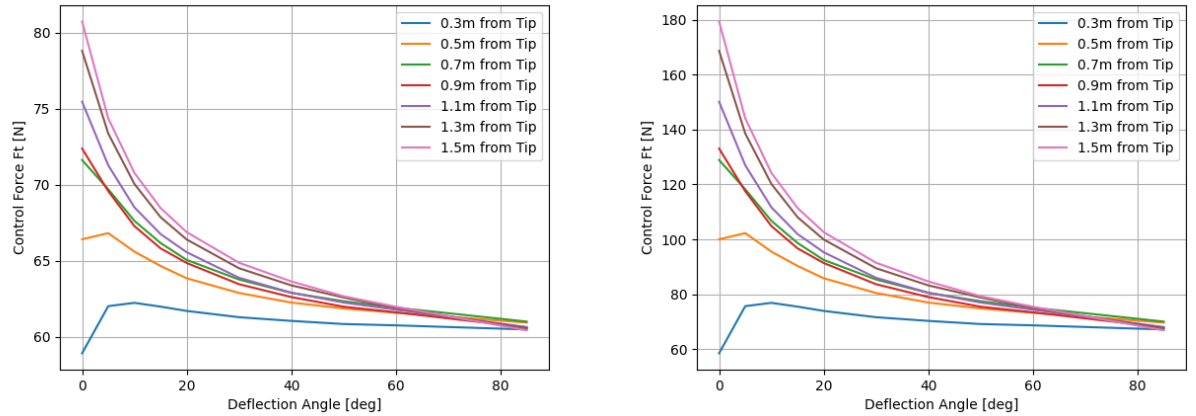


**(a)** $V_{trim} = 20.83$ m/s **(b)** $V_{ne} = 49$ m/s

**Figure 3.28:** Results of folding wing tips control force curves with position of tip hinge point for two velocity cases.

Increasing control force is expected with increasing hinge-tip distance as aerodynamic force scales with area, while the moment arm from the hinge scales linearly by distance. For the given parameters, all configurations provide a control force which is manageable for an average pilot, albeit the difficulty increases considerably when approaching airspeeds near $V_{ne}$. Critical to note however, is the reversal of the control force curves to traditional aircraft. Due to the geometry of the folding wing tips, the force required to maintain the deflection of the wing tip reduces with deflection angle. As such, the control feedback force is reverse, decreasing the accuracy of small corrections and introducing a potential source for instabilities. For this reason, this control method is primarily intended for supplemental use, and not for nominal flight control.

As such, a design choice was made to place the tip hinge point at $d_t = 1$ m from the tip. This decision was made after discussions with structural considerations for the rigidity of the winglet, as well as aerodynamic performance considerations. With this sizing in mind, the lateral control derivatives for the folding wing tips may be quantified, provided in Table 3.12.

**Table 3.12:** Folding tips control derivatives at key velocities.

| **Control Derivative** | **Stall,** $V_s = 8.7$ m/s | **Target Trim,** $V_{trim} = 20.83$ m/s | **Never Exceed,** $V_{ne} = 49$ m/s |
|---|---|---|---|
| $C_{l_{\delta w}}$ | 0.071 | 0.162 | 0.383 |
| $C_{n_{\delta w}}$ | -0.017 | -0.042 | -0.099 |

### 3.10.2. System Response to Control

Following the derivation and quantification of the various control derivatives, estimations of their control performance may be made using the previously derived state-space system. To allow for the implementation of an input vector, the following adjustments will be made to the state equations for the symmetric and asymmetric case, Equation 3.6 and Equation 3.7 respectively.

$$\begin{bmatrix} C_{X_u} - 2\mu_c D_c & C_{X_\alpha} & C_{Z_0} & 0 \\ C_{Z_u} & C_{Z_a} + (C_{Z_{\dot{a}} - 2\mu_c) D_c} & -C_{X_0} & C_{Z_q} + 2\mu_c \\ 0 & 0 & -D_c & 1 \\ C_{m_u} & C_{m_a} + C_{m_{\dot{a}} D_c} & 0 & C_{m_q} - 2\mu_c K_Y^2 D_c \end{bmatrix} \begin{bmatrix} \hat{u} \\ \alpha \\ \theta \\ \frac{q\bar{c}}{V} \end{bmatrix} = \begin{bmatrix} 0 \\ 0 \\ 0 \\ -C_{m_\theta} \end{bmatrix} \begin{bmatrix} \theta \end{bmatrix} \tag{3.6}$$

$$\begin{bmatrix} C_{Y_\beta} + (C_{Y_{\dot{\beta}} - 2\mu_b) D_b} & C_L & C_{Y_p} & C_{Y_r} - 4\mu_b \\ 0 & -\frac{1}{2} D_b & 1 & 0 \\ C_{l_\beta} & 0 & C_{l_p} - 4\mu_b K_X^2 D_b & C_{l_r} + 4\mu_b K_{XZ} D_b \\ C_{n_\beta} + C_{n_{\dot{\beta}} D_b} & 0 & C_{n_p} + 4\mu_b K_{XZ} D_b & C_{n_r} - 4\mu_b K_Z^2 D_b \end{bmatrix} \begin{bmatrix} \beta \\ \phi \\ \frac{pb}{2V} \\ \frac{rb}{2V} \end{bmatrix} = \begin{bmatrix} 0 & 0 \\ 0 & 0 \\ -C_{l_\xi} & -C_{l_{\delta w}} \\ -C_{n_\xi} & -C_{l_{\delta w}} \end{bmatrix} \begin{bmatrix} \xi \\ \delta_w \end{bmatrix} \tag{3.7}$$

A fitting function was used to the previously presented graphs of the various control derivatives to ensure that the control derivatives are correctly scaled with velocity when passed to the state-space. However, only the results for one condition will be presented in this report, as the behaviour varies predictably and linearly with changing velocity and control derivative values.

Similarly to the previous analysis, perturbations will be made to the control inputs and an analysis of the system's response will be performed. The same conditions as the stability analysis will be used, with the trim velocity at sea level. Firstly, the longitudinal pitching behaviour of the C.G. control will be analysed. Negative $\theta = -10°$ and $\theta = -30°$ were analysed, resulting in a pitch up moment around the PenteFoil. The results are shown in Figure 3.29.

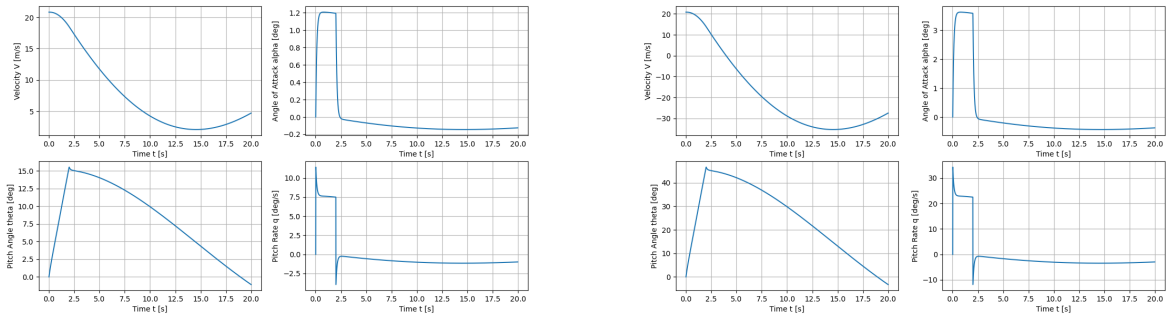


**(a)** $\theta = 10°$ **(b)** $\theta = 30°$

**Figure 3.29:** Dynamic response of PenteFoil system to a negative pitch C.G. $\theta$ deflection.

For both cases, the negative deflection of the C.G. around the $Y$ axis causes a pitch up moment which is quickly damped and a constant angle of attack is maintained as the pitch angle increases. The discrepancies seen primarily in the graph for pitch rate $q$ are a result of discretization error, with a smaller time step reducing their effect. Furthermore, Figure 3.29b shows a pitch rate $q \approx 24$ °/s, confirming requirement **REQ-AERO-09** for pitch rate. It must be noted that the $\theta = 30°$ deflection presented here is not maximal, and the performance of the PenteFoil may be further increased. However, this was not presented as the velocity already increases well below stall, and as such the results would not be of significance. Following the presented motions, the system

enters the stable phugoid mode. The linearity of the system is also clearly demonstrated, with the relevant values between the two cases varying by a factor of three.

Next, the results to positive $\xi = 10°$ and $\xi = 45°$ C.G. roll deflections are shown, Figure 3.30.

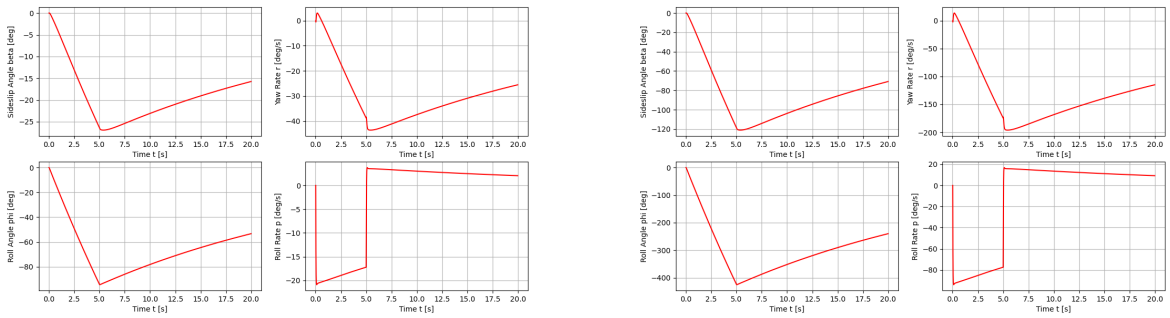


**(a)** $\xi = 10°$ **(b)** $\xi = 45°$

**Figure 3.30:** Dynamic response of PenteFoil system to a positive roll CG $\xi$ deflection.

The motions described above clearly demonstrate the effect of the aperiodic roll, with the maximum roll rate being reached quickly, followed by an almost constant roll rate an increasing roll angle. The significant adverse yaw behaviour is also demonstrated, resulting from the lack of a vertical tail. However, it must be noted that the model does not consider changes in heading, and as such the behaviour of the sideslip angle cannot be resolved too accurately. The general behaviour of the yaw rate with respect to the sideslip angle may be questioned at this point, which may reveal potential error accumulation in the system. This is a well known problem with such linear systems, but part of the compromises made to analyse the general behaviour of the PenteFoil.

By assuming the sideslip angle translates directly to a heading change, a yaw rate of $25$ °/s may be obtained. In turn, this results in a $360°$ turn in a time of 14.4 s, verifying the requirement **REQ-AERO-08**.

Lastly, the results for positive $\delta = 30°$ and $\delta = 60°$ wing tip deflections are shown, Figure 3.31.

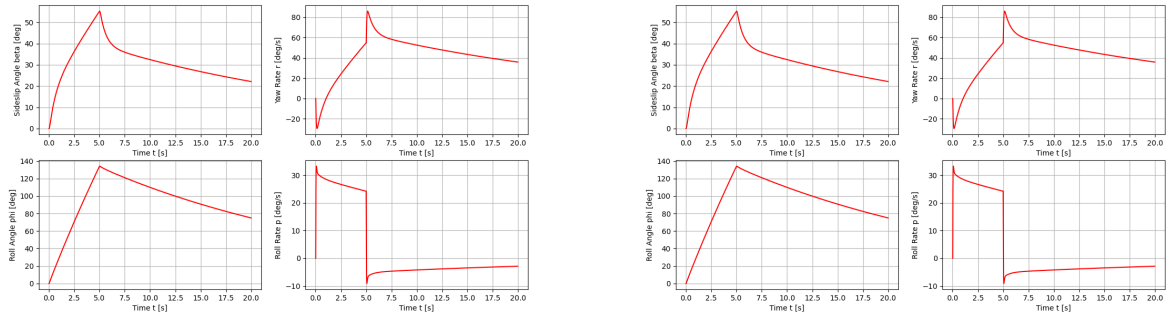


**(a)** $\delta = 30°$ **(b)** $\delta = 60°$

**Figure 3.31:** Dynamic response of PenteFoil system to a positive folding wing tips roll $\delta$ deflection.

Once again, the aperiodic roll coupled with a constant roll rate is shown, as well as the discretization errors shown previously in Figure 3.29. Bearing in mind the coordinate system, a positive deflection of the wing tips results in a positive roll. As such, the two presented rolling control methods show adherence to requirement **REQ-AERO-10** for roll rate, fully quantifying the control performance of the PenteFoil.

## 3.11. Estimation of Effect of Folding Tips on Flight Performance

In addition to the control provided by the ability to asymmetrically deflect the wing tips, aerodynamic performance can also be gained by deflecting them symmetrically. As a result, diving can be accelerated and the trim speed increased. This section very briefly explores this effect.

The final wing configuration was modelled using a similar XFLR5 analysis as in Section 3.6. An analysis was performed for the nominal wing, as well as the fully deflected wing tips ($90°$). The aforementioned data loader

from Python was used to superimpose pressure coefficient data between the wing tips and the main wing body (the deflected wing tips are now effectively at $\alpha = 0°$ with respect to the direction of the flow). The effect of the wing tips experiencing an effective sideslip is not included in this analysis. Figure 3.32 shows the lift and $C_L/C_D$ curves for the nominal and folded wing configuration.

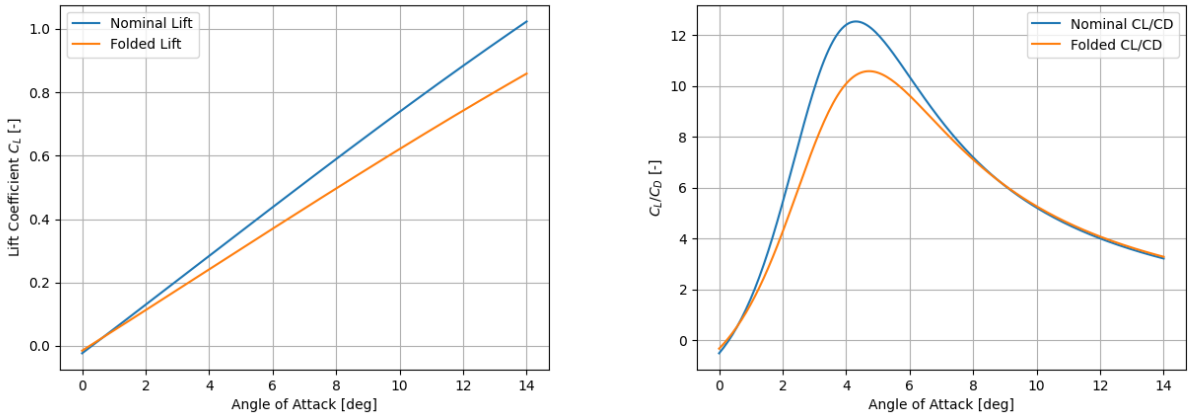


**(a)** $C_L - \alpha$ Curve **(b)** $C_L/-C_D$ Curve

**Figure 3.32:** Effect on lift performance of the folding wing tips, $90°$ deflection.

As a result of the folding wing tips, the effective surface area and local angle of attack reduces significantly. As such, both the lift and drag forces are considerably reduced, with the a $19.5\%$ average reduction in lift coefficient and a $8.35\%$ average reduction in drag coefficient. Consequently, an average of a $10.92\%$ reduction in $C_L/C_D$ is experienced. Assuming a constant angle of attack at the initial trim condition ($\alpha = 6.727°$), the sink rate would increase by $23.4\%$ from $1.67$ m/s to $2.06$ m/s, resulting from a $8.84\%$ increase in the velocity. As such, this mechanism provides some adjustability on the trim speed, as well as some additional performance for diving. To analyse the effect on the stability, Figure 3.33 shows the pitching moment curve of the adjusted configuration.

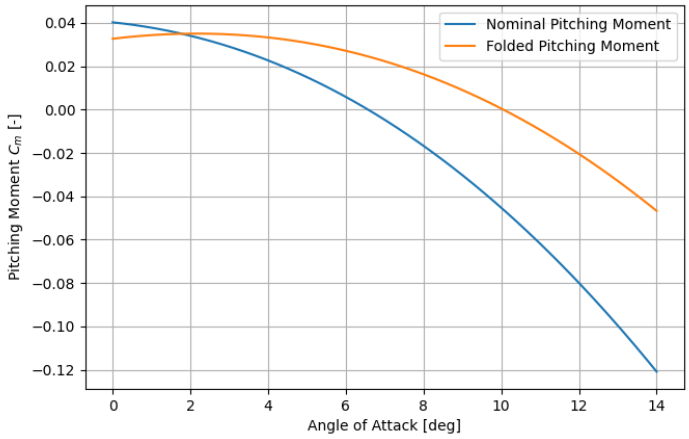


**Figure 3.33:** Effect on pitching moment performance of the folding wing tips, $90°$ deflection.

The folding wing tips effectively remove some of the sweep, resulting in a forward movement of the center of pressure. Hence, a positive pitching moment is generated, resulting in a higher trim angle of attack $\alpha_{t_{new}} = 10.05°$. As shown by Figure 3.32b, the new $C_L/C_D$ resulting from this adjustment is considerably lower than the original trim point, with $L/D = 5.26$. As such, the trim velocity is reduced due to the higher $C_L$. However, the glideslop and sink rate are also considerably increased, making this a favourable maneuver. The calculated values for trim conditions at an altitude $h = 2250$ m are shown in Table 3.13.

**Table 3.13:** Trim values of folded wing showing increased sink rate.

| Parameter | Unit | Nominal Wing | Folded Wing |
|---|---|---|---|
| Trim Velocity $V_t$ | $m/s$ | 20.83 | 19.00 |
| Trim $\alpha$ | ° | 6.727 | 10.050 |
| Lift-to-Drag $L/D$ | - | 12.177 | 5.26 |
| Glideslope Angle $\gamma$ | ° | 4.71 | 10.80 |
| Sink Rate | $m/s$ | 1.67 | 3.56 |

Thus, folding the wing tips provides beneficially aerodynamic performance to the PenteFoil. The reduced lift and drag experienced in the wing would allow for more effective acceleration and velocity control. It must be noted that such maneuvers would require a constant pitch down input (positive $\theta$ deflection) to counteract the resulting pitching moment. However, this pitching moment can easily be applied with the C.G. shift control method analysed previously, and is intuitive as it requires the user to ”dive” forward to pitch down with the wing. The increased trim glideslope as a result of the wing folding may also be used during the landing phase of the flight, to increase the glideslope on approach without significantly increasing the velocity. This would provide a function similar to a sideslip on conventional aircraft.

## 3.12. Final Aerodynamic Performance Characteristics

This section will briefly present the final aerodynamic performance characteristics of the PenteFoil. These are provided in Table 3.14.

**Table 3.14:** PenteFoil Final Aerodynamic Performance Characteristics

| Parameter | Symbol | Value | Unit |
|---|---|---|---|
| *Trim Performance* | | | |
| Angle of Attack | $\alpha_{trim}$ | 6.727 | ° |
| Lift Coefficient | $C_{L_{trim}}$ | 0.509 | - |
| Drag Coefficient | $C_{D_{trim}}$ | 0.0175 | - |
| Lift-to-Drag | $L/D$ | 12.177 | - |
| Gradient of Pitching Moment Coefficient | $C_{m_a}$ | -0.013 | ° |
| Velocity Range (Altitude Dependent) | $V_{trim}$ | 18.69-21.69 | m/s |
| Sink Rate | - | 1.67 | m/s |
| *Stall Performance* | | | |
| Angle of Attack | $\alpha_s$ | 21.50 | ° |
| Lift Coefficient | $C_{L_{max}}$ | 1.6312 | - |
| Drag Coefficient | $C_{D_{stall}}$ | 0.1199 | - |
| Lift-to-Drag | $(L/D)_{stall}$ | 10.71 | - |
| Stall Range | $V_s$ | 8.21-9.13 | m/s |
| *Stability Performance* | | | |
| Phugoid Period | - | 62.70 | s |
| Phugoid Half Time | - | 30.79 | s |
| Dutch Roll Period | - | 13.37 | s |
| Dutch Roll Half Time | - | 6.89 | s |
| *Control Performance (Instantaneous Values)* | | | |
| Maximum Pitch Rate (CG) | - | 23.20 | °/s |
| Maximum Roll Rate (CG) | - | 93.20 | °/s |
| Maximum Roll Rate (Folding Tips) | - | 92.60 | °/s |
| Maximum Control Force (Folding Tips) | - | 75.7 | N |
| Typical Control Force @ Trim (Folding Tips) | - | 170.6 | N |

## 3.13. Future Recommendations

Time and resource restrictions within the scope of this design project limited the analysis which could be performed, and as such, a number of recommendations can be mentioned for future development which would increase the accuracy of the design results and further optimise the design itself. Firstly, pertaining to the airfoil analysis, a geometric optimiser could be drafted which would automatically generate an optimal airfoil shape provided the design targets (such as through particle swarm optimisation). Furthermore, a larger range of existing airfoils could also be analysed to maximise the optimisation process. The CFD process could also be improved by adding more simulations with varying atmospheric parameters, as well as incorporating transient aerodynamic analysis to accurately quantify the stall transition and post-stall behaviour of the airfoil.

During the wing design, a number of improvements could also be made. Firstly, software more accurate than XFLR5 may be used, which would allow for the use of more accurate airfoil data imported from a higher fidelity analysis. Similarly to the airfoil analysis, an optimiser could also be used provided the design targets and airfoil shape to generate a more optimised wing shape. Moreover, three-dimensional CFD simulations may be incorporated to correctly quantify the aerodynamic performance of the wing. This would also allow for simulations to be performed quantifying the flow interference between the pilot and the wing, providing more accurate estima-

tions of performance. Lastly, aero-elastic effects and the performance effects of a non-rigid structure may also be incorporated in a coupled aerodynamic-structural model to provide insight into the behaviour of the static stability of the whole system.

With regards to the stability and control analyses, a number of improvements may be implemented. Firstly, the use of a coupled, non-linear dynamic system may be implemented to estimate the behaviour of the system. Implementing a non-linear system would also lead to the ability to model the system behaviour at higher angles and provided a higher fidelity overview of the extremes of the flight envelope. More accurate methodologies, such as CFD simulations or wind tunnel tests, may also be used to derive the various stability and control derivatives, to further improve the accuracy of the results. Lastly, a full two-body dynamic system may be implemented [19]. This would allow for the correct quantification of the dynamic behaviour of the whole system, as well as provide more accurate estimates of control forces and relative motions between the pilot and wing.

Besides improvements to the applied methodologies, various adjustments and improvements may also be made to the design itself. Primarily, future iterations of the PenteFoil design should attempt to minimise its likeness to a hang glider by increase the pilot's rigidity to the wing, reducing the vertical distance between the pilot and the wing, and incorporating other control methods such as a morphing trailing edge. Furthermore, considerations may be made on the design targets, with potential variants featuring a reduced span and surface area, and increased performance metrics.

# 4 | Structural Design

With the aerodynamic geometry and control method specified, the next step is to translate these into a feasible, manufacturable product through structural design. This chapter outlines the design of the PenteFoil structure, beginning with a review of historical inflatable structure concepts and defining subsystem requirements. The methodology for the design process is presented, followed by a detailed description of the final structural design and structural analysis. The chapter concludes with a sensitivity analysis and recommendations for further design improvements.

## 4.1. Review of Inflatable Aircraft Structural Concepts

This section reviews the historical and modern developments in inflatable aircraft concepts. It highlights significant advancements, from early prototypes to contemporary designs, illustrating the evolution and potential of inflatable structures in aviation.

Inflatable aircraft concepts have a long history, starting in the 1930s. Taylor McDaniel's concept, depicted in Figure 4.1, was a glider made mostly of inflated tubes, with some stiff elements and cables for rigidity. A prototype weighing around 60 kg was built and successfully flight-tested [20].

**Figure 4.1:** McDaniel inflatable glider[10].

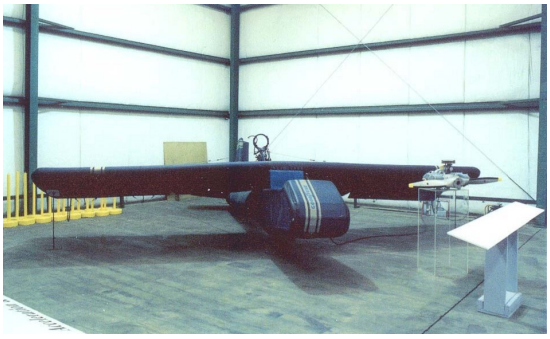

**Figure 4.2:** Goodyear Inflatoplane (GA468)[11].

In the 1950s, Goodyear developed a powered inflatable aircraft with performance comparable to that of a J3 Cub [20]. Shown in Figure 4.2, the aircraft weighed slightly over 100 kg and could be folded into a volume of 1.25 $m^3$. A total of 12 Inflatoplanes were constructed and were flying until the early 1970s.

In the early 2000s, rapid deployment inflatable structures were utilised in military UAVs, as shown in Figure 4.3 [21]. These UAVs, in their folded configuration, could be launched to altitude with a naval gun, enduring loads up to 2800 g. Upon reaching the desired altitude, the wings deployed, enabling a flight duration of up to three hours.

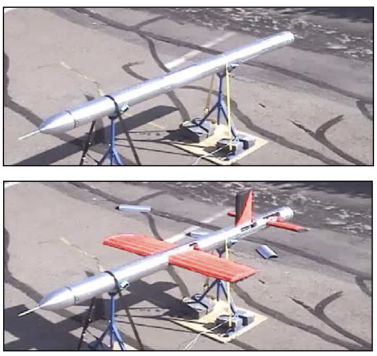

**Figure 4.3:** FASM/QuickLook UAV - Undeployed and Deployed Configurations [21].

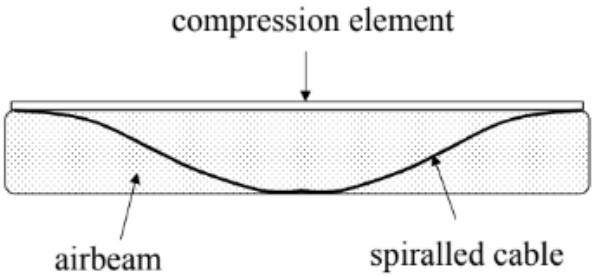


**Figure 4.4:** Basic Tensairity beam [22].

[10] https://www.historynet.com/the-inflatable-rubber-aircraft/, Accessed on 10/06/2024.
[11] https://airandspace.si.edu/collection-objects/goodyear-inflatoplane-ga468/nasm_A19740156000, Accessed on 10/06/2024.

At the beginning of the twenty-first century, the concept of Tensairity was developed [22]. A basic Tensairity beam is composed of three main components: a low-pressure cylindrical airbeam, a compression element tightly connected to it, and a cable spiralling around the airbeam, as depicted in Figure 4.4. The cables are attached to each end of the compression element, completing the force flow. The compressed air pretensions the cables and stabilises the compression element against buckling. In Tensairity, the airbeam primarily stabilises, allowing operation at low air pressure, while the cable and compression element bear the loads. According to Luchsinger et al. (2004), "The main advantages of Tensairity structures are light weight, fast erection and dismantling and small storage and transportation volume" [22].

**Figure 4.5:** Tensairity kite with 11 m² surface area before launch during testing [23].

In 2010, the Tensairity concept was applied to design an ultra-light inflatable kite, shown in Figure 4.5. The use of foldable compressive and tensile elements enabled high strength with lightweight inflatable fabrics at low pressures. The wing weighed just 2.5 kg with an area of 11 $m^2$ and was able to support a mass of 100 kg [23]. The low weight and high transportability led to the implementation of Tensairity as a fundamental structural philosophy of the PenteFoil.

## 4.2. Subsystem Requirements

To constrain and guide the design, a number of subsystem requirements has been defined. This section presents those requirements, starting by introducing definitions of terms used, and then the requirements are grouped in Table 4.1.

Below are the definitions of terms used in formulation of requirements:

**Safety factor** - A margin of safety taken in sizing all components, to provide contingency for unexpected conditions. In the structural design, a safety factor of 1.5 was used for the majority of components. For the ultimate strength of composite components, a safety factor of 3 was used, due to their unpredictable performance.

**Maximum design loads** - The limit wing loading as defined in the gust envelope (see Figure 7.7) multiplied by the **safety factor**. The maximum positive design load factor is $5.3 \cdot 1.5 = 7.95$, and the negative factor is $-2 \cdot 1.5 = -3$.

**Inflation pressure range** - The range of relative pressures of the structure caused by the pressure differential with altitude. From **??** it is designed to be 30000 Pa. This corresponds to a descent from 3000 m to sea level at ISA conditions.

**Seam efficiency** - The ratio of the strength of a fabric at a seam to its nominal strength. From literature, it was found that wave zig-zag stitches in rip-stop nylon fabrics had an SE of 76% [24]. Other fabric types achieved SE values between 75% and 80% when an adequate stitch type was used [24]. During the structure design a seam efficiency of 75% will be used on all fabrics as it is the lowest value.

**Table 4.1:** Structure Subsystem Requirements.

| ID | Requirement |
|---|---|
| **REQ-STR-01-1** | The compressive stress in the compressive elements under the maximum design loads shall be under their ultimate compressive strength. |
| **REQ-STR-01-2** | The tensile stress in the tensile elements under the maximum design loads shall be under their ultimate tensile strength. |
| **REQ-STR-01-3** | The tensile stress in the skin elements under the maximum design loads shall be under their ultimate tensile strength multiplied by the seam efficiency. |
| **REQ-STR-02-1** | The inflation pressure stress in the skin shall be lower than the skin's yield strength multiplied by the seam efficiency, over the entire inflation pressure range. |
| **REQ-STR-02-2** | The inflation pressure stress in the web shall be lower than the web's yield strength multiplied by the seam efficiency, over the entire inflation pressure range. |
| **REQ-STR-02-3** | The inflation pressure stress in the bladder shall be lower than the bladder's yield strength, over the entire inflation pressure range. |
| **REQ-STR-03-1** | The upward wing tip deflection under n=1 shall be less than 3% of the span[12]. |
| **REQ-STR-03-2** | The upward wing tip deflection under the ultimate positive load shall be less than 15% of the span[4]. |
| **REQ-STR-03-3** | The downward wing tip deflection under the ultimate negative load shall be less than 10% of the span[4]. |
| **REQ-STR-03-4** | None of the compression elements shall buckle under the maximum design loads. |
| **REQ-STR-04-1** | The web pre-tension over the entire inflation pressure range shall be higher than the shear loads inside the webs. |
| **REQ-STR-04-2** | The rib skin pre-tension over the entire inflation pressure range shall be higher than the compressive loads. |
| **REQ-STR-05** | The external fabric shall have handling load resistance as good as or better than a paraglider. |
| **REQ-STR-06** | The external fabric shall have UV resistance as good as or better than a paraglider. |
| **REQ-STR-07** | The structure shall weigh less than 10 kg. |
| **REQ-STR-08** | The structure materials, including a 20% contingency margin, shall cost less than €1500. |
| **REQ-STR-09** | All stiff elements of the structure shall have a folded length of less than 1 m. |

The driving requirements were those under ID REQ-STR-01, REQ-STR-02, REQ-STR-03, REQ-STR-04 and REQ-STR-07, as these requirements translated directly to ensuring structural integrity in the whole flight envelope and imposed a maximum for the structure mass, which was crucial for designing a feasible system. The other requirements address fatigue, environmental resistance, costs and foldability of the structure but are not as critical as the project objective can be achieved without satisfying these requirements.

## 4.3. Methodology

This section presents the methodology implemented in designing the structure of the PenteFoil. First, the assumptions are presented. Afterwards, the steps taken to ensure that the structure can carry every type of load over the entire range of design loads. The section ends with a procedure for mass and cost estimation.

### 4.3.1. Main Assumptions

Below is a summary of the assumptions and simplifications made during the structural design process, each accompanied by a justification. These measures were implemented mainly due to resource constraints and to maintain the project scope.

[12] Based on typical deflections of Boeing 787, that are 7% in equilibrium flight and reach up to 10-15% (`https://elib.dlr.de/140326/1/2020_dlrmagazin-166-bending-instead-of-snapping.pdf`, Accessed on 18/06/2024).

**ASM-STR-01** *The lift follows an elliptical distribution.* While the actual lift distribution is not perfectly elliptical, it approximates an elliptical shape due to the wing's taper. This assumption allows for the use of an analytical formula for lift distribution, which simplifies the design process by defining lift as a function of total lift and wingspan, enabling efficient parameter adjustments during iterative design. This formula is shown on Equation 4.1. Once the wing's design has been finalised, an actual lift distribution was implemented and the structural requirements have been verified against the resultant loads.

$$L(y) = \frac{4W}{\pi b}\sqrt{1 - \left(\frac{2y}{b}\right)^2} \tag{4.1}$$

**ASM-STR-02** *The distance between the tension and compression elements in a tensairity structure is an elliptical function of position along the wingspan, being zero at the tip and equal to the web height at the root.* An elliptical function is a simple yet effective approximation of the Tensairity shape and reflects the effect of gravity and boundary conditions on the shape of a tension element. Such height distribution is more representative of reality than the linear distribution assumption taken by Breuer and Luchsinger (2010) in their analysis of web Tensairity kite structures [23].

**ASM-STR-03** *The bending and shear loads are decoupled; bending loads are carried purely by tensile and compressive elements, while shear loads are managed by the webs.* This simplification leverages the properties of tensairity structures, where tensile and compressive elements are designed to efficiently handle bending stresses, and webs are optimised to manage shear stresses. This decoupling allows for a clearer analysis and more straightforward optimisation of each load-carrying component.

**ASM-STR-04** *The load of the cables supporting the pilot is distributed evenly across all webs to which the cables are attached.* This simplification is implemented due to the wing's symmetrical design and the small distances between the webs, which ensure that the forces in the webs are similar in magnitude. This assumption facilitates easier load analysis and design adjustments while maintaining safety margins.

**ASM-STR-05** *Webs carry shear loads proportional to their height.* In other words, it was assumed that the shear flow is the same in every web and it is constant. As the fabric properties were typically documented in terms of forces, the shear flow was integrated over the web height.

**ASM-STR-06** *The distance between the tensile and compressive element in the web stays constant under loads.* As the wing deflects, these elements experience strain, which would typically cause them to press into the web and reduce the distance between them. However, this effect is difficult to model and is assumed to be zero, implying the web has infinite tension and consequantly inflation pressure. This assumption was used by Breuer and Luchsinger (2010) in their analysis of web Tensairity kite structures [23].

### 4.3.2. Internal Loads

The starting point for structural design was to establish the forces acting on a structure and derive internal force diagrams. For straight-and-level, unaccelerated flight (n=1), lift is a distributed force acting upwards. The shear and moment of the lift are relieved by forces created by a wing-harness attachment that are due to the weight of a pilot, and by the weight of a structure itself. The weight of the structure is modelled as follows: the mass of compression and tension elements remain constant along the span, the mass of the fabric creating skin, bladder etc. is proportional to the chord. The load distribution is shown in Figure 4.6.

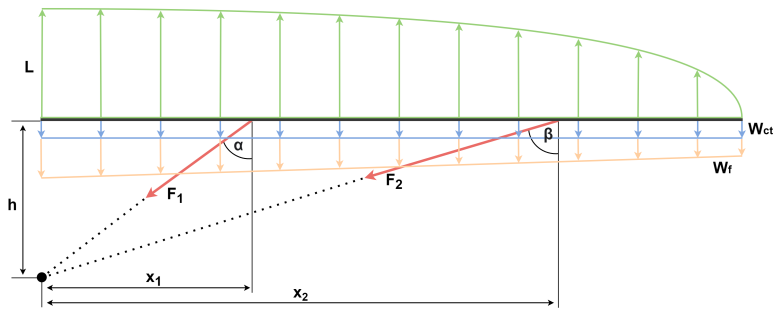


**Figure 4.6:** Free Body Diagram of half of the wing in a straight-and-level, unaccelerated flight. Green colour indicates lift blue is the weight of compression and tension elements and yellow denotes the weight of fabrics.

Once the forces and their magnitudes are defined, the shear diagram can be generated by simply integrating

the vertical forces from the tip, as per Equation 4.2.

$$V(y) = \int_{y}^{\frac{b}{2}} F_z(y)dx \tag{4.2}$$

Next, the shear distribution can be integrated again to obtain the moment distribution via Equation 4.3.

$$M(y) = \int_{y}^{\frac{b}{2}} V(y)dx \tag{4.3}$$

The created shear and moment distributions are used in the following sections to ensure that the structure can bear each load type, in all loading conditions during flight.

### 4.3.3. Design for Shear Loads

As outlined in **ASM-STR-03**, shear forces are carried by the webs. These webs, made from fabric, cannot transfer shear directly because they buckle easily. To carry shear, the fabric must be pre-tensioned with a force greater than the shear force. When the shear force exceeds the pre-tension force, the web will buckle.

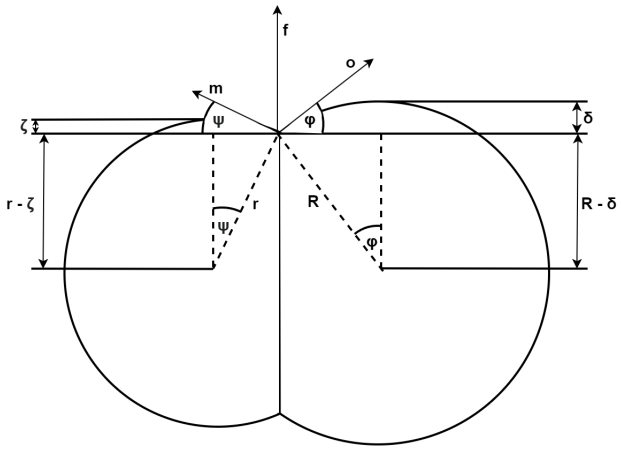


**Figure 4.7:** Pre-Tension in Web Caused by Hoop Stress.

The pre-tension in the web is caused by the hoop stress from two neighboring cells, as shown in Figure 4.7. The pre-tension force $f$ is the sum of the vertical components of the hoop forces $m$ and $n$. The derivation of $f$ is as follows:

$$\cos(\varphi) = \frac{R-\delta}{R} = \frac{R-(R-\frac{h_{web}}{2})}{R} = \frac{h_{web}}{2R} \tag{4.4}$$

Using the Pythagorean trigonometric identity:

$$\sin(\varphi) = \sqrt{1-\frac{h_{web}^2}{4R^2}} \tag{4.5}$$

Given that:

$$o = p \cdot R, \quad m = p \cdot r \tag{4.6}$$

The pre-tension force along the span $f(y)$ can be calculated by:

$$f(y) = p \cdot \left( R(y) \cdot \sqrt{1-\frac{h_{web}^2(y)}{4R^2(y)}} + r(y) \cdot \sqrt{1-\frac{h_{web}^2(y)}{4R^2(y)}} \right) \tag{4.7}$$

Finally, the shear force $V(y)$, previously calculated, is multiplied by the maximum design load and subtracted from the pre-tension force to determine the safety margin. The safety margin must be positive to prevent the web from buckling:

$$SM_{web} = f(y) - V_{ult}(y) \cdot SF \cdot n_{max} \tag{4.8}$$

### 4.3.4. Design for Bending

The structure must be designed to withstand stresses induced by bending loads, and the deflection of the wing must be analysed to ensure that it meets deflection requirements, thereby preventing any significant loss of aerodynamic performance.

The procedure for calculating deflection was adapted from the analysis of a web Tensairity kite [23]. The wing deflection can be determined by integrating the Equation 4.9 twice.

$$\frac{d^2z}{dy^2} = \frac{M(y)}{EI(y)} \tag{4.9}$$

The EI(y) can be calculated using Equations 4.10 and 4.11.

$$EI(y) = EA_{ct} \cdot h(y)^2 \tag{4.10}$$

$$EA_{ct} = \frac{E_c A_c \cdot E_t A_t}{E_c A_c + E_t A_t} \tag{4.11}$$

where subscript c indicates compression element and subscript t indicates tension element. The distance between the tensile and compressive element along the span is denoted by h(y). It is possible to control this distance by sewing the tensile elements into the web. It was decided they will follow an elliptical distribution as mentioned in **ASM-STR-02**. Such a shape maximises the moment of inertia in the highly loaded regions, and allows for easy iteration to optimise the other parts of the structure.


**Figure 4.8:** Web Tensairity cross-section and positioning within the wing's structure.

The area of each element is determined by the choice of the element's cross-sectional dimensions, which is influenced by commercial availability, mass and cost minimisation, and structural requirements.

The stresses in the tensile and compressive elements can be calculated using the following formulas:

$$\sigma(y) = \frac{M(y) \cdot h_{web}(y)}{2I(y)} \tag{4.12}$$

These calculated stresses are then compared against the allowable stress, which is the yield stress of the material divided by a safety factor of 1.5 for tensile elements and 3 for compression elements. This ensures that the stresses remain within safe limits and that the structure can withstand the loads without yielding. It also accounts for the unpredictable behavior of composites used in compression elements.

### 4.3.5. Design for Compression Element Buckling

Structural analysis for buckling of the web Tensairity beam follows the methodology described by Breuer et al. (2007) [25]. While Breuer's work focuses on standard Tensairity beams, the PenteFoil uses a web Tensairity design. An advantage of web Tensairity is its enhanced buckling resistance, as the web provides continuous support for the compression element, unlike a pressurised fabric.

However, there is a lack of analysis or quantification of web Tensairity's buckling performance in the available literature. Wever (2008) [26] mentions in a master's thesis that the introduction of the web increases buckling performance by a factor of 10, but this claim lacks a detailed analysis.

Given this uncertainty, a conservative approach is adopted, designing the beam for buckling as if it were a standard Tensairity. The allowable buckling load for a compression element in Tensairity is calculated using Equation 4.13. As $P$ and $EI$ are known from the bending analysis, Equation 4.13 sets a minimum inflation pressure requirement. During the integration of structural design, buckling requirements were not constraining even when a standard Tensairity structure was assumed, therefore this approach does not make the structure overdesigned.

$$P = 2\sqrt{p \cdot \pi \cdot E \cdot I} \tag{4.13}$$

### 4.3.6. Design for Inflation Pressure

The inflation pressure is beneficial when considering stiffness for buckling resistance, however the structure must also sustain the pressure loads. The pressure directly creates stress in the bladder, which is supported by the outer skin. Figure 4.9 shows the way the pressure loads on bladder and tube were modelled.

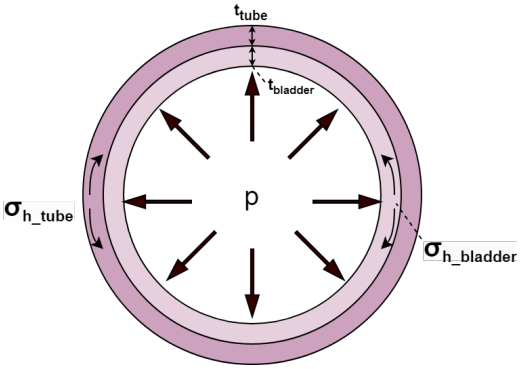


**Figure 4.9:** Modelling the stress due to pressurization on bladder and tube.

As the radius of the bladder R in an inflated beam is typically much larger than the thickness of the bladder or the skin, it can be safely assumed in calculations that the tube and the bladder have an equal radius. The hoop stress due to pressure loads acting on the walls of the bladder and tube $\sigma_h$ is calculated as shown on Equation 4.14.

$$\sigma_h = \frac{pR}{t_{tube} + t_{bladder}} \tag{4.14}$$

For procurement and manufacturing purposes the tube and bladder will have a uniform thickness, and the structure will be uniformly pressurised. From that it can be concluded that the highest hoop stress will occur in a cell that has the largest radius.

The stiffness of the tube-bladder composition was calculated using the rule of mixtures, as indicated in Equation 4.15. With the radius of the bladder and tube equal, thicknesses can be used to find volumetric fractions.

$$E_{tb} = \frac{E_{tube}t_{tube} + E_{bladder}t_{bladder}}{t_{tube} + t_{bladder}} \tag{4.15}$$

As the bladder presses into the tube, the tube and the bladder will have equal deflection, found from Equation 4.16. From this Equation 4.17 is derived.

$$\epsilon_{tb} = \frac{\sigma_{hoop}}{E_{tb}} \tag{4.16}$$

$$\frac{\sigma_{tube}}{E_{tube}} = \epsilon_{tube} = \epsilon_{tb} = \epsilon_{bladder} = \frac{\sigma_{bladder}}{E_{bladder}} \tag{4.17}$$

Thickness t and elastic modulus E depend on a selected material for the tube or bladder, therefore for a given inflation pressure p the maximum circumferential stresses in tube and bladder can be calculated. This stress must be lower than the yield stress of material divided by a safety factor 1.5.

### 4.3.7. Sizing of Ribs

The stiffness of the last 30% of the wing chord will come from spanwise distributed ribs with fabric in between, similar to a surfing kite. Ribs at the rear of the wing do not have Tensairity, so the loads must be supported purely by the rib skin. Since a fabric buckles under compression, the longitudinal pre-tension in the rib skin must be greater than any compressive loads caused by bending moments. This is illustrated in Figure 4.10, where the longitudinal stress $\sigma_l$ is greater than the bending stress $\sigma_b$.

The calculation of $\sigma_b$ is performed as follows: From aerodynamic simulations, it was determined that the last 30% of the wing chord produces 10% of the total lift. The lift at the trailing edge is zero, and it is assumed to vary linearly with chord length. This assumption was verified as a good approximation with CFD simulations. Using this data, the moment along the chord is calculated as described in Subsection 4.3.2. It is assumed that all ribs carry the same bending load. The bending stress $\sigma_b(x)$ in an individual rib along the chord is then computed via Equation 4.18.

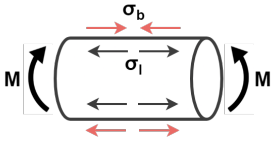


$$\sigma_b(x) = \frac{M(x)R(x)}{I(x)n_{ribs}} \tag{4.18}$$

**Figure 4.10:** Pressure and bending stresses in a rib section.

Finally, the $\sigma_b(x)$ at the maximum design load is subtracted from the longitudinal inflation stress, resulting in a safety margin that must be kept above zero:

$$SM_{rib} = \frac{pR}{t_{tube} + t_{bladder}} - \sigma_b(x) \cdot SF \cdot n_{max} \tag{4.19}$$

It must also be ensured that the fabric can sustain the inflation stresses. The stress in the circumferential direction will always be critical. The longitudinal stress is half of the circumferential stress, and the additional stress from bending will always be lower than the longitudinal stress. Sizing of tubes for inflation pressure was considered in Section 4.3.6.

### 4.3.8. Tip Deflecting Mechanism for PenteFoil

The PenteFoil implements a tip deflecting mechanism. The final 1 meter of the wing will be purely inflatable and will not contain any Tensairity elements. Deflecting the tips downward will be achieved by pulling on a cable attached to a sliding mechanism on the trapezium, which induces buckling in the inflatable structure.

The bending moment required for tip deflection can be calculated using the procedure described in Subsection 4.3.7. The moment will be modeled as a point force $F_d$ acting perpendicularly to the tip. Knowing this force, the required control line tension can be determined. The forces and dimensions for the tip bending mechanism are illustrated in Figure 4.11.

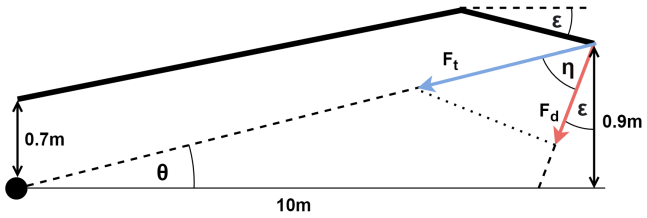


**Figure 4.11:** Tip Bending Mechanism.

From the figure, the equation for the line tension $F_t$ can be derived as follows:

$$F_t = \frac{F_d}{\cos(\eta)} = \frac{F_d}{\cos(90° - \theta - \epsilon)} \approx \frac{F_d}{0.25} \tag{4.20}$$

This equation estimates the control line tension required to buckle the tip. Once the wing starts bending, the required force will drastically reduce.

### 4.3.9. Wing-Harness Attachment Design

One of the critical elements in the structural design is the strategic positioning of the attachment points for the lines supporting the pilot's weight. Properly positioning these points can significantly reduce maximum shear and moment loads in the structure. Additionally, the tension loads in the cables, which create tearing forces on the webs, must be carefully considered. Cables near the root carry most of the vertical load, while cables closer to the tip experience larger tensions due to their inclination relative to the vertical.

Increasing the number of attachment points improves load distribution, enhancing structural performance. However, excessive attachment points complicate the cable system, increasing weight and the risk of entanglement during initialization or flight. To balance these factors and simplify structural analysis, four attachment points per web were chosen (two per symmetry plane). The webs carrying the pilot are selected based on the desired longitudinal position of the pilot.

The cable forces acting on the structure are modelled in the FBD shown in Figure 4.6. To achieve force equilibrium, the sum of vertical components of $F_1$ and $F_2$ must be equal to lift minus the wing's weight. This system is statically indeterminate. To solve it, we can use the compatibility equation derived from the fact that the vertical displacement of both cables will be the same. This is also visualised on Figure 4.12. The magnitude of this deflection can be calculated with Equation 4.21.

For practical reasons all wires will be made of the same material and have the same diameter, therefore Equation 4.21 simplifies to Equation 4.22.

$$\delta_y = \frac{L_1 F_1 cos\alpha}{A_1 E_1} = \frac{L_2 F_2 cos\beta}{A_2 E_2} \tag{4.21}$$

$$L_1 F_1 cos\alpha = L_2 F_2 cos\beta \tag{4.22}$$

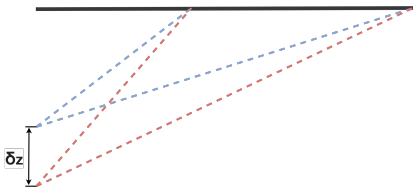


**Figure 4.12:** Sketch visualising compatibility of vertical deflection.

The lengths $L_1$ and $L_2$ can be calculated with the Pythagorean theorem with the knowledge of attachment height h and the lateral position of each attachment point $y_1$ or $y_2$. Using Equation 4.22 and vertical force equilibrium the magnitudes of tensions $F_1$ and $F_2$ are calculated. These values are mainly dependent on attachment points' positions, by varying $x_1$ and $x_2$ we can control the forces that each rope carries. Under **ASM-STR-04**, the load acting on each web due to force in the cable is the tension force divided by the number of pilot-carrying webs.

The primary factor influencing the selection of attachment point locations was the failure mode. The attachment system was designed such that if one attachment point fails, for example due to a tear propagating in a web, the other attachment points can still safely carry the pilot's load, assuming no additional tears in the structure. This design provides the pilot with sufficient time to react to the failure and deploy the emergency parachute, ensuring that the pilot is not placed in a disadvantageous or dangerous position for initiating the emergency protocol.

Additionally, the force acting on each web must remain below the ultimate strength of the chosen web fabric, divided by a safety factor, to ensure no risk of failure when the structure is healthy. The positions of the attachment points were also strategically selected to minimise the maximum shear and moment loads on the structure.

### 4.3.10. Verification & Validation of the Method

To ensure the accuracy and suitability of the calculation model for the PenteFoil, and confirm the validity of the results, several verification and validation procedures were implemented.

The means through which the method has been verified are listed below.

1. The methods and adaptations used in our research were based on established literature concerning Tensairity and inflatable structures. This approach ensured that methodologies were grounded in proven techniques and principles.
2. Peer verification was conducted within the structures department. Each member reviewed and critiqued the approach taken by a single individual for specific problems. Such scrutiny helped identify any potential issues or areas for improvement.
3. The methods implemented were consulted with experts present at TU Delft campus, including Dr. Otto Bergsma and Joep Breuer. These consultations confirmed the correctness of approach and provided valuable insights for enhancing the accuracy and detail of calculations. Their expertise and suggestions were instrumental in refining the used model to suit the project's needs better.

To validate the model, its results were compared with findings from a study by Breuer and Luchsinger (2010) on web-Tensairity beams used in kite applications [23]. Parameters from their study were incorporated into the model. Figure 4.13 illustrates the overlap between our model's predictions and the analytical and experimental results from the cited study.

Firstly, the deflection of web-Tensairity beams was predicted by the model. It was found that the model slightly underestimated deflection compared to experimental results but closely matched analytical predictions from the original study.

Secondly, the model's accuracy was validated by analysing the buckling load of purely inflatable beams. According to this study's structural calculations, these beams buckle at approximately 21 N of force. The deflection graph produced by the model closely mirrored experimental data, where buckling occurred at around 20 N of force.

The implemented procedures enhance confidence in the structural calculation model's outcomes. However, additional validation experiments are required for full validation. The multi-web Tensairity structure of the PenteFoil is significantly more complex than any other structures found in literature with available experimental results, making its performance more uncertain. The only way to fully validate the approach is by producing and testing a high-fidelity PenteFoil prototype.

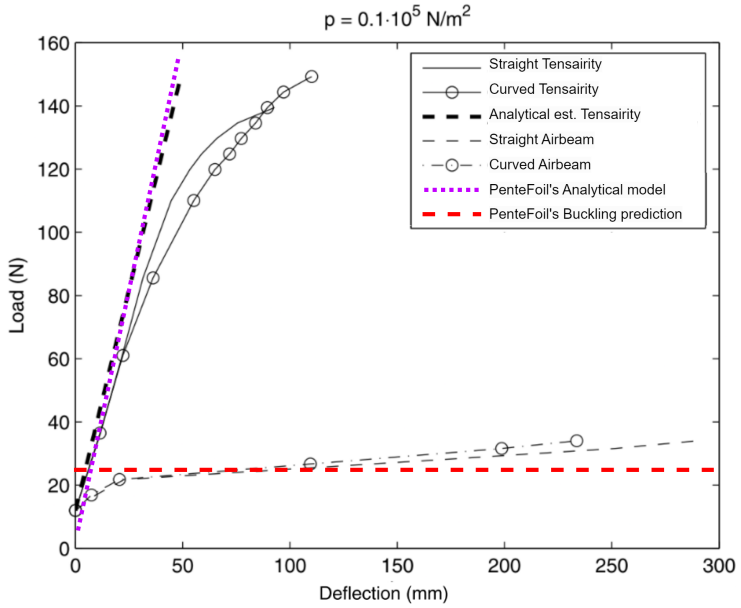


**Figure 4.13:** Comparison of load-deflection behaviour of straight and curved web-Tensairity beams, straight and curved airbeams (no Tensairity) and an analytical estimation for the web-Tensairity beams from literature [23] with the result of the PenteFoil's structural calculation model, for an air pressure of 0.1 × $10^5$ N/$m^2$. Adapted from Breuer and Luchsinger (2010) [23].

## 4.4. Structural Design

In this section, the final structural design is presented. This includes the selected materials, the dimensions of component, their integration into the structure and analysis of mass, cost and performance. The structure has been designed such that its mass and cost is optimised, but it is also manufacturable and uses materials that are commercially available and popular in aerial sport.

### 4.4.1. Material Selection

This part describes the rationale behind material selection for each structural element. Other than for their structural performance, materials were chosen to be commercially available and preferably with a proven track record in flying inflatable structures such as surf kites and parachutes.

The compressive elements are constructed from carbon fibre reinforced polymer (CFRP) circular rods, and the tensile elements are made of Dyneema cables. The exact dimensions of these components are determined in the subsystem description section of this chapter. CFRP rods and Dyneema cables are known for their exceptional performance. Both materials are renowned for their high stiffness and lightweight properties. Furthermore, their effectiveness in Tensairity structures is well-documented in literature [25] [23]. The properties and costs of the carbon rods were sourced from Easy Composites EU[13], while the Dyneema cables were procured from Syntheticropes.eu[14].

The airfoil webs are constructed from a Dyneema fabric. Despite being somewhat costly, Dyneema is exceptionally strong and lightweight, crucial for withstanding point loads from the harness attachment points. Additionally, Dyneema's excellent rip-stopping properties minimise the risk of tears and prevent tear propagation. These Dyneema webs are supplied by extremetextil[15].

The inflatable tubes that maintain the airfoil and rib shapes are made from ripstop nylon, supplied by JWtextec[16]. Ripstop nylon, used in emergency parachutes and kites, offers high tensile strength, and tear resistance, making it ideal for handling impacts and supporting the pressure loads of airtight bladders.

The bladders inside the tubes, essential for airtightness, are made from Thermopolyurethane (TPU). TPU is the most common choice for lightweight, airtight materials in surf kites. This material will be supplied by Jiaxing Inch Eco Materials[17].

The cover skin and trailing edge skin, which primarily provide aerodynamic shape rather than load-carrying functions, will be made from standard nylon fabric supplied by Metropolis Drachen[18]. Although not as strong

[13] https://www.easycomposites.eu/, Accessed on 11/06/2024.
[14] https://syntheticropes.eu/, Accessed on 11/06/2024.
[15] https://www.extremtextil.de/, Accessed on 11/06/2024.
[16] https://www.jwtextec.com/, Accessed on 11/06/2024.
[17] https://yingchengtpu.en.alibaba.com/, Accessed on 11/06/2024.

and slightly heavier, this nylon fabric is very cost-effective, helping reduce the overall cost of the PenteFoil. This material is also commonly used in surf kites, proving its suitability for aerodynamic applications.

### 4.4.2. Structural Design Description

This subsection presents the sizing results of all structural elements. The internal wing structure is shown in Figure 4.14. The first 70% of the wing consists of 10 inflatable cells (yellow) running along the span, with nine shear webs (blue) between them. To reduce the design complexity and weight, the rear 30% of the wing contains 11 inflatable ribs (yellow) in the chord direction, with fabric (red) stretched between them. This configuration results in a trailing edge approximating a Princeton Sailwing, as shown in Figure 4.16. Additional (red) fabric covers the inflatable tubes to improve aerodynamic shape.

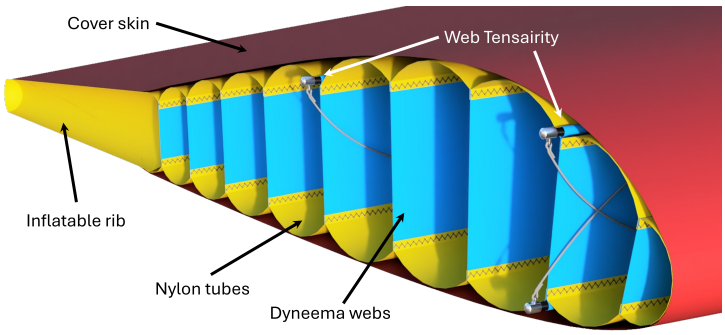


**Figure 4.14:** Visualisation of the internal web Tensairity structure.

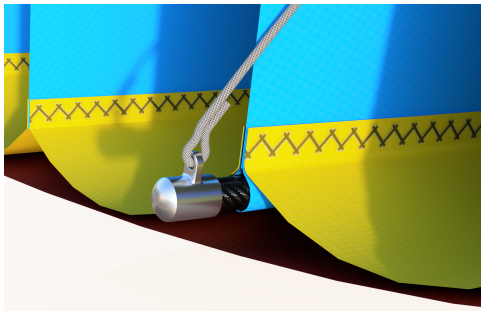

**Figure 4.15:** A close-up view of the web Tensairity attachment.

Two web Tensairity elements were added to selected webs. The compression element sits in a sleeve (blue) sewn into the web, distributing loads evenly along the entire web. The tensile element is tied to an aluminum cap at the end of the CFRP tube. This can be seen in more detail in Figure 4.15. The web Tensairity elements were positioned as follows: the front element between the 2nd and 3rd bubbles at 11% of the chord, and the rear element between the 5th and 6th bubbles at 38% of the chord. This arrangement resembles the front and rear spar configuration of a conventional aircraft, allowing for even load distribution between the two beams.

The web Tensairity structure was designed to accommodate a swept wing shape. While most compression tubes are straight, the tube at the root is curved at a specific angle to achieve the desired sweep. This design is illustrated in Figure 4.17. The desired dihedral is achieved by cutting the web in a specific manner such that it dictates the inclined shape. Figure 4.5 and Figure 4.8 show how the dihedral is achieved in Tensairity structures.

To incorporate a control method, the web Tensairity is truncated one meter from the tip. This design choice creates a section of the wing with lower stiffness, making it easier to deflect. In this truncated section, stiffness is provided solely by inflation pressure and the tension of the control wires.

The front web Tensairity consists of two compression and tension elements positioned symmetrically at opposite ends of the web, effectively resembling a single web Tensairity structure mirrored along the chordline. This configuration enables the beam to carry both positive and negative loads, providing stiffness and strength under negative load factor conditions. The dimensions of the components used for the front web Tensairity structure are summarised in Table 4.2.

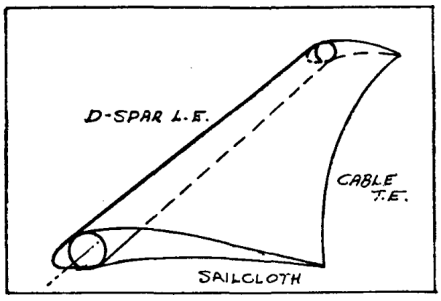


**Figure 4.16:** Princeton sailwing cross-section. [27]

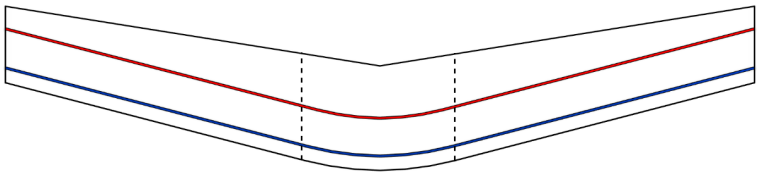

**Figure 4.17:** Curved carbon tube sections (between dashed lines) located at the root to create sweep.

The rear web Tensairity supports the front structure by carrying positive loads and enclosing the cross-section

[18] https://www.metropolis-drachen.de/, Accessed on 11/06/2024.

to counter torsion loads. Since the minimum load factor is much smaller in magnitude than the maximum load factor, the front spar can sustain negative loads on its own, allowing the rear spar to have a standard, unidirectional structure. The rear web Tensairity has dimensions as described in Table 4.3.

**Table 4.2:** Front web Tensairity dimensions.

| Parameter | Value |
|---|---|
| Upper CFRP rod outer x inner diameter | 6x4 [mm] |
| Lower CFRP rod outer x inner diameter | 6x4 [mm] |
| Upper Dyneema cable diameter | 2 [mm] |
| Lower Dyneema cable diameter | 2 [mm] |
| Beam length | 8 [m] |

**Table 4.3:** Rear web Tensairity dimensions.

| Parameter | Value |
|---|---|
| CFRP rod outer x inner diameter | 6x4 [mm] |
| Dyneema cable diameter | 2 [mm] |
| Beam length | 8 [m] |

The design of the airfoil involves sewing pieces of fabric in a specific manner to approximate the desired airfoil shape. This sewing technique creates enclosed ”cells” that vary in radius along the chord. These cells are connected by straight webs, optimised to distribute the load effectively and support the Tensairity design. The material used for making these tubes is N66-30D-B Ripstop[19], which weighs 40 g/m$^2$. Inside these cells, an airtight bladder made from 50 $\mu$m TPU[20], weighing 60 g/m$^2$, ensures air retention.

The cells extend from the leading edge to 70% of the chord length. Beyond this point, the last cell is connected to a trailing edge cable with a straight piece of Spinnaker *M-40* Pro fabric[21], which weighs 44 g/m$^2$. The trailing edge cable ensures the fabric is tightened under load, helping the airfoil maintain its shape. This arrangement provides an optimal balance between aerodynamic performance, structural integrity, and manufacturing feasibility.

To eliminate the circular cell shapes and achieve a smooth outer contour for better aerodynamics, the cells are covered with a smooth piece of fabric made from the same material as the trailing edge. This fabric is sewn to the top of the last cell and attached to the leading edge and the bottom of the last cell with Velcro. This design allows the skin to be ”opened,” providing access to the modular Tensairity tubes, which can be assembled before flight and disassembled and folded afterwards.

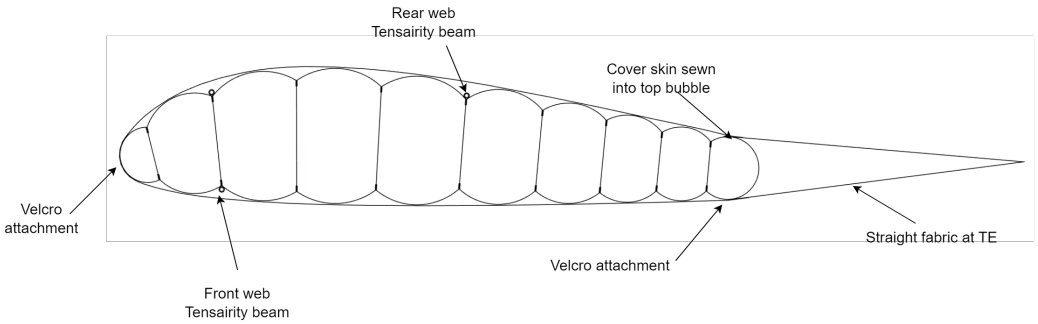


**Figure 4.18:** Internal layout of fabric tubes, tensairity elements and cover skin creating the airfoil shape.

The radii of the cells continuously decrease towards the tip to create a tapered wing, enhancing aerodynamic efficiency. The resultant airfoil shape is illustrated in Figure 4.18. The airfoil shape is maintained throughout the span using tubular ribs extending from the last cell to the trailing edge. The trailing edge fabric is carefully stitched to these tubes to give the trailing edge element its proper shape. The ribs, which are placed every 1 meter, are illustrated in Figure 4.19. These ribs are connected to the last cell, sharing a diameter of 10 cm, and continuously decrease their size to 5 cm diameter at the trailing edge.

[19] https://www.jwtextec.com/index.php?c=content&a=list&catid=289, Accessed on 12/06/2024.

[20] https://yingchengtpu.en.alibaba.com/productgrouplist-801024180/TPU_Film.html?spm=a2700.shop_index.88.24, Accessed on 12/06/2024.

[21] https://www.metropolis-drachen.de/en/Kite-materials/Cloth-Fabric/Spinnaker-fabrics/Spinnaker-M-40-Pro.html, Accessed on 12/06/2024.

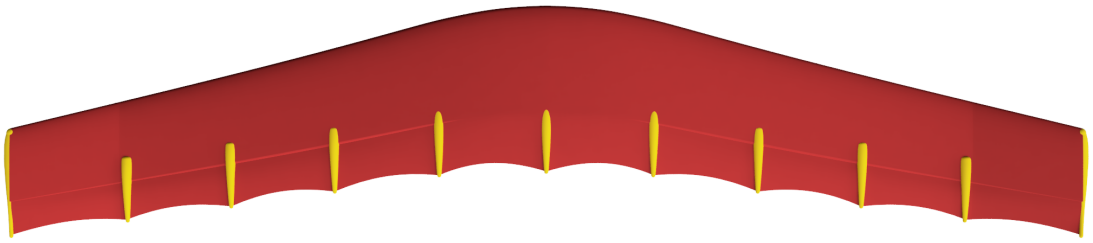

**Figure 4.19:** Arrangement of ribs on the wing.

The webs are made of a Dyneema Composite Fabric CT2E.08[22] that weighs 26 g/m$^2$. The height of each web is summarised in Table 4.4. The webs also house the cables that are part of the pilot attachment system. These cables are sewn into the web with rectangular reinforcement patches to distribute the load evenly along the web's height. This solution is shown graphically in Figure 4.20. The positions of these cables are $y_1 = 1.4$ m and $y_2 = 2.2$ m. These cables are attached at these two points on both left and right side of the wing to the first 6 webs, resulting in a default pilot's C.G. position at $X_{cg} = 0.81$ m. The way the attachment cables are distributed over multiple webs is illustrated on Figure 4.21.

**Table 4.4:** Heights of webs at the root.

| Web # | Height [mm] |
|---|---|
| Web 1 | 97.2 |
| Web 2 | 162.0 |
| Web 3 | 199.8 |
| Web 4 | 185.8 |
| Web 5 | 162.0 |
| Web 6 | 145.8 |
| Web 7 | 130.7 |
| Web 8 | 106.9 |
| Web 9 | 90.7 |

**Figure 4.20:** A photograph presenting the way the harness attachment cable is attached to the structure.

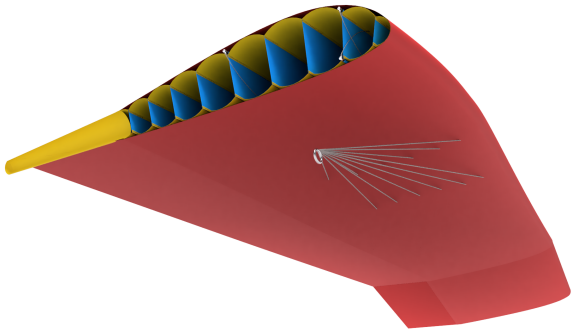

**Figure 4.21:** Distribution of harness attachment cables to the wing's structure.

A final structural element is the steering frame positioned in front of the pilot, rigidly attached to the wing. This frame features a rectangular shape accommodating the control wire handles and enabling pitch control of the wing. Two additional bars on top of the frame run perpendicularly to its plane and are inserted into sleeves sewn onto the bottom of the wing, ensuring a rigid attachment. Due to resource constraints, this structural element was not fully detailed in design. It was qualitatively sized by drawing analogy to the triangular control frame of a hang glider, without undergoing structural analysis, and is recommended for future refinement.

The steering frame is intended to be lightweight and cost-effective rather than excessively strong, leading to the selection of Aluminum 6061T6[23] as it's material. Figure 4.22 shows the model of the control frame.

**Figure 4.22:** Conceptual model of the steering frame.

[22] https://www.extremtextil.de/en/dyneema-composite-fabric-ct2e08-26g-sqm.html, Accessed on 11/06/2024.
[23] https://chassisparts.com/nl-nl/aluminium-tube-3-meter-30x1-5, Accessed 12/06/2024.

### 4.4.3. Structural Analysis

The structural analysis consists of two parts. First, the internal shear and moment diagrams are evaluated. Then, to assess the performance of the structure, all relevant structural parameters are compared to the maximum allowable value derived from requirements and material properties.

Figure 4.23 and Figure 4.24 present the internal shear and moment diagrams for one half of the wing during symmetrical flight at a maximum load factor of n=5.3. This scenario represents the condition where the structure experiences the largest forces. The diagrams show that the strategic positioning of the attachment points effectively reduces the maximum shear force within the structure. Additionally, the placement of these points creates regions of negative shear load, which helps to reduce the maximum moment.

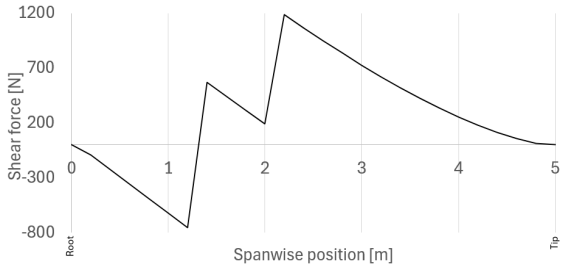


**Figure 4.23:** Internal shear load in half of the wing during symmetrical loading at n=5.3.

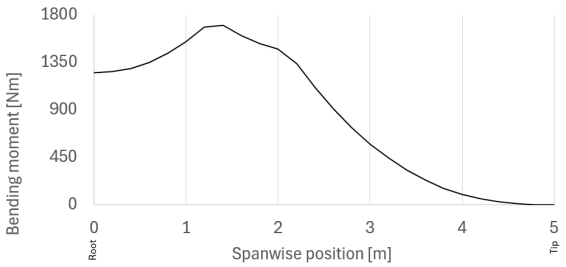


**Figure 4.24:** Internal bending moment in half of the wing during symmetrical loading at n=5.3.

With the completed design and loading curves, a performance analysis of all components was conducted following the procedure described in Section 4.3. For each component, an analysis was performed at the maximum loading conditions, both positive and negative, and over the entire inflation pressure range of 20,000 to 50,000 Pa. From this analysis, the most critical values were found. These values, along with the minimum or maximum allowable values for each parameter, are presented in Table 4.5.

**Table 4.5:** Specifications and Requirements.

| Parameter | Value | Limit | Unit | Related Requirement |
|---|---|---|---|---|
| Tip Deflection n=1 | 0.18 | <0.3 | m | REQ-STR-03-1 |
| Tip Deflection n=5.3 | 0.96 | <1.5 | m | REQ-STR-03-2 |
| Tip Deflection n=-2 | -0.75 | <1 | m | REQ-STR-03-3 |
| $\sigma_{\text{Front Compression}}$ | 117 | <217 | MPa | REQ-STR-01-1 |
| $\sigma_{\text{Rear Compression}}$ | 124 | <217 | MPa | REQ-STR-01-1 |
| $\sigma_{\text{Tension}}$ | 620 | <2000 | MPa | REQ-STR-01-2 |
| $\sigma_{\text{Bladder}}$ | 0.78 | <9 | MPa | REQ-STR-02-3 |
| $\sigma_{\text{Skin}}$ | 61 | <65 | MPa | REQ-STR-01-3, REQ-STR-02-1 |
| $\sigma_{\text{Web}}$ | 51 | <3500 | MPa | REQ-STR-02-2 |
| Min Buckling Pressure Front | 11,500 | <20,000 | Pa | REQ-STR-03-4 |
| Min Buckling Pressure Back | 13,000 | <20,000 | Pa | REQ-STR-03-4 |
| $SM_{web}$ | 34 | >0 | N | REQ-STR-04-1 |
| $SM_{rib}$ | 0.08 | >0 | MPa | REQ-STR-04-2 |
| Total mass | 8.40 | <10 | kg | REQ-STR-07 |
| Total cost | 1009 | <1500 | € | REQ-STR-08 |

### 4.4.4. Mass Estimation

With the size and material chosen for each components, their mass could be estimated. This mass was then used to update the structural weight's effect on the loading, and after a few iterations, the process converged to a fully defined structure.

For estimating the mass of compressive and tensile elements, typically, the mass per meter of a rod was

provided at the manufacturer's website. This value was multiplied by the wingspan to determine the total mass of each element.

The fabrics used in the construction of the PenteFoil include the webs, tubes, covers, ribs, trailing edge foil, and bladders. With the established wing dimensions and airfoil shape, the total fabric surface area required was calculated. The mass per square meter for each chosen fabric was available online at the manufacturer's website. By multiplying the mass per square meter by the total required area for each fabric type, the total mass of the fabrics was determined.

The structure also includes other components, such as connections between tensile and compressive elements, stitches, and inserts sewn into the webs to support the pilot's attachment wires. The detailed design of these elements is beyond the scope of this project. However, their mass effect was estimated to be 5% of the total mass. As a reference, a study on an inflatable wing using the principle of Tensairity [25] reported that the mass of connection elements was 3.8% of the total mass. To be more conservative, this value was increased to 5%.

Table 4.6 presents a breakdown of the estimated mass into each component, along with the fraction of total mass attributed to each component. *Upper compression* refers to the front web Tensairity beam's upper compression element, analogically *lower compression* refers to the lower element. Similarly, *lower tension* refers to the tension element on the bottom of the front beam, which supports the upper compression element, and the logic is reversed when it comes to *upper tension*.

**Table 4.6:** Mass estimation breakdown.

| Element | Value | Fraction |
|---|---|---|
| Tubes | 0.92 kg | 10.9% |
| Webs | 0.31 kg | 3.7% |
| TE Fabric | 0.33 kg | 3.9% |
| Cover Skin | 0.92 kg | 11.0% |
| Upper Compression | 0.22 kg | 2.6% |
| Lower Compression | 0.22 kg | 2.6% |
| Rear Compression | 0.22 kg | 2.6% |
| Lower Tension | 0.04 kg | 0.4% |
| Upper Tension | 0.04 kg | 0.4% |
| Rear Tension | 0.04 kg | 0.4% |
| Bladder | 2.87 kg | 34.1% |
| Ribs | 0.05 kg | 0.6% |
| Tensile | 0.11 kg | 1.3% |
| Compressive | 0.66 kg | 7.9% |
| Fabric | 5.96 kg | 64.2% |
| Control Frame | 1.82 kg | 21.7% |
| Sub Total | 7.98 kg | 95% |
| Connections | 0.42 kg | 5.0% |
| **Total** | **8.40 kg** | 100.0% |

**Table 4.7:** Cost estimation breakdown.

| Element | Value | Fraction |
|---|---|---|
| Tubes | 134.65 € | 13.4% |
| Webs | 276.71 € | 27.4% |
| TE Fabric | 30.00 € | 3.0% |
| Cover Skin | 84.00 € | 8.3% |
| Upper Compression | 67.60 € | 6.7% |
| Lower Compression | 67.60 € | 6.7% |
| Rear Compression | 67.60 € | 6.7% |
| Lower Tension | 3.52 € | 0.3% |
| Upper Tension | 3.52 € | 0.3% |
| Rear Tension | 3.52 € | 0.3% |
| Bladder | 33.99 € | 3.4% |
| Ribs | 6.86 € | 0.7% |
| Tensile | 10.56 € | 1.0% |
| Compressive | 202.80 € | 20.1% |
| Fabric | 566.21 € | 56.1% |
| Control Frame | 27.28 € | 2.7% |
| Sub Total | 806.86 € | 80.0% |
| Losses contingency | 201.71 € | 20.0% |
| **Total** | **1008.57 €** | 100.0% |

### 4.4.5. Cost Estimation

This subsection addresses the cost estimation for the fabrics and structural components used in the design of the PenteFoil. It does not include costs associated with manufacturing, testing, or other operational expenses. The focus is solely on the procurement costs of the materials required for construction.

For the PenteFoil's structure commercially available off-the-shelf fabrics and components were chosen. The prices for these materials were obtained either per meter (for rods and wires) or per square meter (for various fabrics). This approach ensured that the materials used in the design were readily accessible and their costs could be accurately estimated based on market rates.

The cost estimation for each component and fabric was calculated based on the required length or area. The detailed steps are as follows:

1. The total length or area required for each component and fabric was determined based on the structural design parameters. Usually, this was already an output of the mass estimation.
2. The price per meter for rods and wires, and the price per square meter for fabrics, were obtained from commercial suppliers.
3. The basic cost for each material was calculated by multiplying the required dimension by the unit price.
4. To account for potential cutting or manufacturing losses, an additional 20% of each material was included in the cost calculation. This contingency ensures that any unforeseen material wastage or inaccuracies during the manufacturing process do not lead to material shortages.

For example, a fabric required for the wing cover was calculated to be 21 $m^2$ and the price was €4 per square meter, the basic cost would be €84. Including a 20% contingency increases the required area to 25.2 square meters, resulting in a total cost of €100.8. This method was systematically applied to each component and fabric used in the structure.

A detailed breakdown of estimated costs for each component, along with the proportion of total cost allocated to each component, is documented in Table 4.7.

## 4.5. Sensitivity Analysis

During the design process it was noticed that the structural design is very sensitive to the wing's dimensions. To obtain a more detailed insight into this dependence, the dimensions of the wing were varied and their effect on the structure was evaluated. This was achieved through varying wing span and chord length independently.

Firstly the span was varied. It was immediately observed that performance parameters show a large sensitivity to the wing span. The most sensitive were: stresses in compression and tension elements, minimum pressure to avoid buckling and deflection of the tip. Table 4.8 shows the change in values expressed in percentage for different changes in span. Even only a 10% increase of span has increased these parameters by up to 317% increase, and the magnitude of change increased as the span was increased further. However, this does not mean that these parameters decreased with the decrease over span. On the contrary, some parameters increased even more when the span was decreased by 10% than when it was increased by the same amount.

This shows the importance of decreasing the maximum loads in the structure by proper positioning of the attachment points. Furthermore, such behaviour confirms that the structure is highly optimised for the current wing dimensions and for any changes in the wing span the structural optimisation would need to be performed from scratch, starting with reconsidering selected materials. This justifies the use of simplifying analytical functions of span for parameters such as lift distribution as it streamlines the structural design process and allows for easier iterations given the limited time of the project.

**Table 4.8:** Percentage change of a parameter based on change in wing span.

| $\Delta b$ | **-50%** | **-10%** | **+10%** | **+50%** |
|---|---|---|---|---|
| $\sigma_{\text{Compression}}$ | +89% | +163% | +93% | +324% |
| $\sigma_{\text{Tension}}$ | +89% | +179% | +104% | +323% |
| Tip Deflection n=1 | -58% | +53% | +95% | +532% |
| Minimum Buckling Pressure | +257% | +680% | +318% | +1694% |

**Table 4.9:** Percentage change of a parameter based on change in root chord.

| $\Delta c_r$ | **-50%** | **-10%** | **+10%** | **+50%** |
|---|---|---|---|---|
| $\sigma_{\text{Compression}}$ | +98% | +6% | -15% | -41% |
| $\sigma_{\text{Tension}}$ | +110% | +12% | -10% | -38% |
| Tip Deflection n=1 | +321% | +26% | -21% | -58% |
| Minimum Buckling Pressure | +342% | +27% | -19% | -62% |

Another straightforward way to vary the wing shape is by changing its root chord. Adjusting the chord primarily impacts the buckling-related parameters. Increasing the chord reduces the minimum pressure needed to support the compression element, while decreasing the chord has the opposite effect. This behaviour makes sense as a smaller root chord leads to a more slender wing. The stresses and strains in the wing also follow a similar pattern, though with less sensitivity compared to buckling. This is because a smaller airfoil decreases the moment of inertia, which in turn increases stress and strain. The detailed behavior is outlined in Table 4.9.

This analysis shows that the chord length affects structural performance. Increasing the chord enhances the wing's resistance to buckling and bending, however, the root chord is not solely determined by structural considerations. Operational and aerodynamic factors play a crucial role in its design. Therefore, while structural

benefits are gained by increasing the chord, these were carefully weighed against the aerodynamic and practical requirements of the wing.

## 4.6. Future Recommendations

For future development of the PenteFoil's structure, several recommendations have been formulated to increase the accuracy and detail of the design.

1. **Evaluation of CFRP Compression Element Connections:** The CFRP compression elements are constructed from 1-meter long tubes connected similarly to the stiff elements in a tent. The potential weakening effect of these connections should be evaluated and quantified. This includes both the local weakening at the connection points and any cumulative effects that may influence the overall structural integrity. Detailed testing and modelling of these joints will ensure that they meet the required strength and reliability standards. Additionally, the long-term effects of wear from repeated folding and unfolding should be investigated.
2. **Analysis of Seam Weakening:** Seams in the fabric structure introduce potential points of weakness both locally and globally. A comprehensive investigation is necessary to determine how much these seams diminish the load-carrying capacity of the structure. Such procedures may involve tensile tests on sewn samples, stress concentration analysis around seam areas, and development of improved sewing methods or materials that minimise these influences.
3. **Investigation of Tear Propagation Mechanisms:** Dyneema webbing was chosen for its superior ripstopping properties. However, a deeper investigation into tear propagation mechanisms in the web material and other potential fabrics is recommended. Understanding how tears initiate and spread can help in designing more tear-resistant structures or in selecting materials with better performance. This will enhance the overall safety and durability of the wing.
4. **Impact of Bubble Shape and Spanwise Deflection on Aerodynamics:** The structural design should include an analysis of how changes in bubble shapes and spanwise deflection due to forces and internal pressure affect the aerodynamic performance and force distribution of the wing. Computational Fluid Dynamics (CFD) simulations combined with structural analysis can provide insights into these effects, allowing for optimisation of the airfoil shape and bubble design to maintain aerodynamic efficiency under varying conditions.
5. **Evaluation of UV Radiation Effects:** The effects of UV radiation on the materials used in the structure have not been evaluated. Long-term exposure to UV radiation can degrade polymers, affecting their mechanical properties and longevity. Conducting UV resistance tests on the materials and considering UV-protective coatings or additives can help mitigate these effects and prolong the life of the structure.
6. **Consideration of Torsion Effects:** Although torsion was deemed insignificant based on expert advice and the symmetric placement of web Tensairity beams, a more detailed torsional analysis is recommended. This can confirm the assumption and ensure that any minor torsional loads are adequately accounted for, providing a more robust design.
7. **Reducing Simplifications and Complex Analysis:** The current design is based on several simplifying assumptions. To improve accuracy, these simplifications should be reduced, and more complex analysis methods should be employed.
8. **Finite Element Method (FEM) Analysis:** Implementing FEM analysis can significantly enhance the understanding of the structural behavior under various loads and conditions. FEM allows for detailed modeling of complex geometries, material behaviors, and load interactions. This analysis can identify potential failure points, optimise material usage, and improve the overall design robustness.

# Part III - Operations

# 5 | Flight Operations

With the design concluded, this chapter will give a detailed overview of how the PenteFoil should be operated, starting with the operations and logistics concept and equipment description in Section 5.1 and Section 5.2, respectively. Then, the in-flight procedures of controlling the the PenteFoil and possible manoeuvres will be described in Section 5.3. Next, the take-off locations, pre-flight checks, take-off procedure itself and the take-off safety conditions will be discussed in Section 5.4. This chapter ends with the normal and emergency landing procedures described in Section 5.5 and Section 5.6, respectively.

## 5.1. Operations and Logistics Concept Description

This section describes all the operations and logistics involved in the use of the PenteFoil. An overview of the flow between operations and logistics is illustrated in Figure 5.1. The key players for operations and logistics are listed below.

- **Manufacturer:** Manufacturing companies are responsible for the manufacturing compliant with the determined requirements and certification, as well as the transport of the PenteFoil to the retailers.
- **Retailer:** The retailers are responsible for the storage and distribution of the PenteFoils. The retailers have expertise in extreme aerial sports, so they can also act as repair and maintenance shops.
- **User:** The potential users include people who have experience or interest in aerial sports. All potential users should undergo training, at least as extensively as described in Section 6.3. Upon completion of this training, the individual is considered a trained user. This naming convention is used in Chapter 10 for specification of the requirements. People who are interested in flying the PenteFoil, but do not have any experience in aerial sports, need to go through additional training related to operating the parachute and safety procedures of aerial sports before following the nominal training procedure. Once training is completed, the user can purchase or hire a PenteFoil and fly independently. The user collaborates with the retailers during the purchase and maintenance of the PenteFoil, and with trainers during the initiation of their PenteFoiling adventure.
- **Trainer:** The trainer is a trained and experienced user who is responsible for preparing new users for their first and subsequent flights.
- **Flying clubs:** Existing flying clubs can be collaborated with in the initial phase of the PenteFoiling project for purposes of testing, training first users, retailing, and marketing.
- **Recycling:** Once the PenteFoil is damaged beyond repair due to fatigue or an accident, it can be recycled, recovering and reusing as much material as possible.

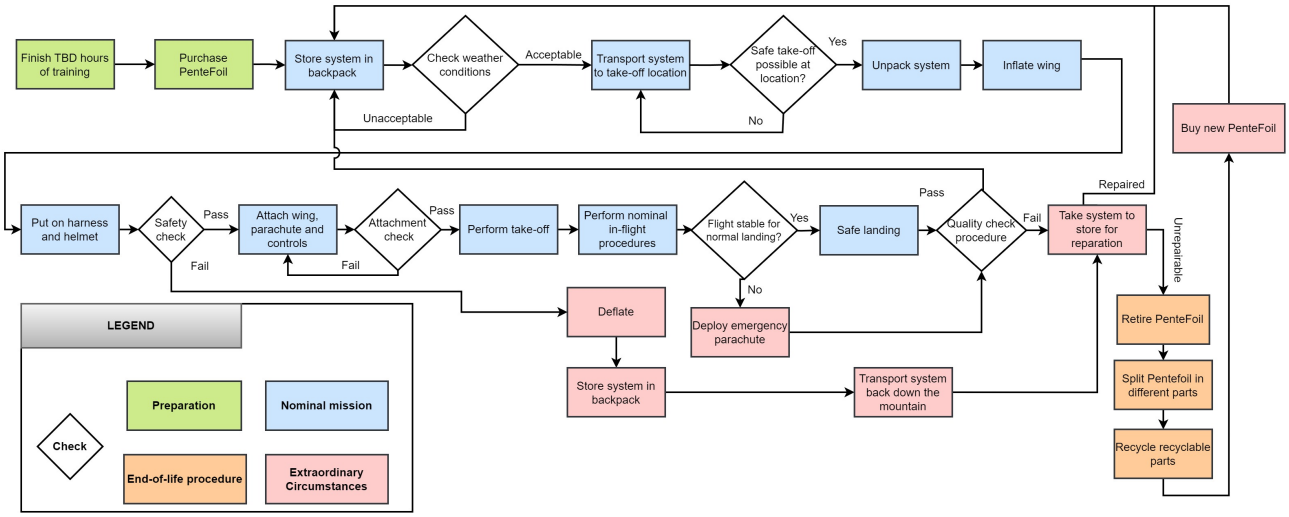


**Figure 5.1:** Operations and logistics concept diagram for the PenteFoil.

## 5.2. Equipment

This section outlines all the essential tools and gear needed to operate the PenteFoil safely and efficiently. The overview of the equipment also provides a basis for all other sections relating to system operation.

### 5.2.1. Harness

Equipping the pilot with an appropriate harness is important. The harness serves as the main connection point between the pilot, the attachment lines and the wing. Harness choice varies with the pilot's skill level, with beginners using training-specific harnesses. Upon completing training, pilots transition to advanced harnesses suitable for challenging manoeuvres.

**Training harness**

A training harness is used for training sessions where pilots take off on foot in a vertical position. These harnesses are commonly used in hang glider training to help the user take off and land in the correct position. The training harness is hooked to the lifeline with a carabiner. The training harness provides little body support, allowing for free movement of the entire body. Furthermore, it is not meant to be used for extended amounts of time and thus prioritises correct position over comfort. An example of the training harness can be seen in Figure 5.2.

**PenteFoil capsule harness**

After completing their training, users shall be ready to utilise the PenteFoil capsule harness. This harness has the highest degree of freedom for aerobatic manoeuvres and offers great comfort for the pilot. The PenteFoil capsule harness integrates features from the hang glider cocoon presented in Figure 5.3. The cocoon harness, favoured by aerobatic hang glider pilots, allows for compact positioning to facilitate extreme dives and manoeuvres. The dive manoeuvre can be seen in Figure 5.4. An additional benefit of this harness is its capability for upright positioning, enabling foot launches and landings. To prevent interference during running, the capsule can be hooked up, keeping the feet unobstructed during take-off and landing.

**PenteFoil skypod harness**

An alternative harness to consider after training is the PenteFoil skypod harness. This harness offers the highest degree of comfort and resembles the style of a hang glider pod harness. As shown in Figure 5.6, a pod harness is designed with a streamlined shape that significantly reduces drag, resulting in better aerodynamic performance. This leads to a higher glide ratio and overall better flight efficiency. Additionally, a pod harness typically offers more support and padding, making long flights more comfortable. Its enclosed design protects the pilot against the wind, keeping them warmer compared to the open-back design of the cocoon harness. However, the manoeuvrability and the ability of achieving a vertical, straight-up body position are compromised compared to the cocoon harness. Moreover, a pod harness is both more complex and heavier than a cocoon harness. The take-off and landing procedures are similar in style. However, the skypod harness has a fully enclosed pod that zips open in the front. Before take-off, the pod hangs behind the pilot, making a running launch possible. Once airborne and stable, the pilot pulls up their legs, slides them into the pod, and zips it closed. This procedure is described in more detail in Section 5.4. All further operational descriptions assume use is made of the skypod harness. A conceptual harness was designed using CAD software Fusion 360 and is presented in Figure 5.5. The design is based on a hang gliding harness commonly used by expert pilots [24].

**Figure 5.2:** Training harness.

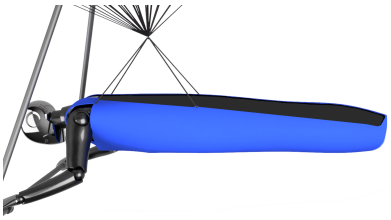

**Figure 5.3:** Example of a cocoon-style harness.

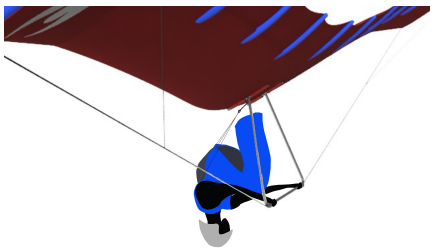

**Figure 5.4:** Dive manoeuvre.

[24] https://www.oregonhanggliding.com/harnessdata.shtml, Accessed on 19/06/2024.

[25] https://greyfitusa.com/collections/hanggliding-harnesses/products/hanggliding-up-straight-training-harness, Accessed on 05/06/2024.

[26] https://www.youtube.com/watch?v=uzRRqxy9OEI, Accessed on 05/06/2024.

[27] https://www.loisirs14.com/pratique-et-avantages-du-deltaplane/, Accessed on 18/06/2024.

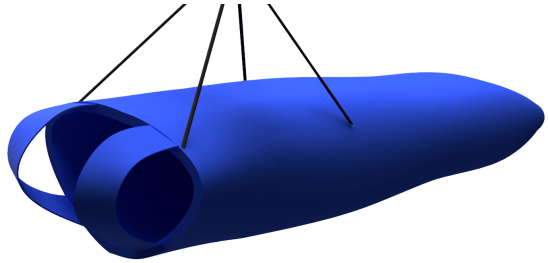

**Figure 5.5:** Harness design.

**Figure 5.6:** A hang glider pod harness[27].

### 5.2.2. Safety Parachute

The information provided in this subsection is based on the guidelines provided by the British Hang Gliding and Paragliding Association (BHPA) [28]. The safety parachute is ultimately a user's choice, as designing the parachute is considered outside the scope of this project, but a recommended parachute of company *Supair*[28] is presented in Figure 5.10. The pilot should choose a parachute conforming to the EN12491 standard, the European standard for emergency parachutes for paragliding and hang gliding. This indicates that the parachute has passed speed opening tests (less than 4 seconds), descent rate tests (maximum of 5.5 m/s), stability tests, and strength tests. Specifically for the strength test, manufacturers have the choice to test for two speeds. Successfully certified parachutes are provided with a certification label: 'not suitable for speeds over 32 m/s (115 km/h)' or 'not suitable for speeds over 49 m/s (176 km/h)'. The PenteFoil can reach speeds of up to 49 m/s within its flight envelope, providing the pilot with the necessary information to select an appropriately certified parachute. The pilot must also check the available sizes of the parachute to accommodate for the total take-off weight. This weight equals the pilot's total weight plus the total weight of the PenteFoil system. The maximum take-off weight for the PenteFoil is set to 105 kg, providing the pilot with the necessary information to decide on a suitable parachute.

**Maintenance and repacking**

The pilot should learn to repack their parachute and should become familiar with the entire system. This can be achieved through parachute-repacking events organised by aerial sports clubs, where a licensed packer should be present to supervise. Alternatively, a pilot can directly approach a licensed packer for instruction. The parachute should be repacked, vented and inspected every six months. This contributes to proper parachute deployments and avoids unintentional deployments.

**Pre-flight parachute checks**

The manufacturer of the parachute provides an extensive checklist detailing all necessary checks to be performed before each use. The following list outlines essential checks applicable in all cases:

- Check that the parachute container is properly closed and closure pins are secure and free to release.
- Check that the deployment handle is within reach and accessible.
- Check that no slack loop of the riser is outside of the parachute container.

**Using the emergency parachute**

Practising the use of the rescue parachute is crucial for understanding its deployment. The emergency parachute manual should include manufacturer instructions for real deployment and ground practice. Some hang gliding and paragliding clubs have constructed suspended systems that allow pilots to attach their harnesses and practice deployment during disorienting movements. The steps of properly deploying the rescue parachute are discussed in Section 5.6.

### 5.2.3. Helmet

The safety regulations for aerial sports differ from those for other extreme sports, such as mountain biking. Aerial sports helmets (EN966 certified) undergo safety certification tests, but the rigorousness of their safety standards is among the lowest in the helmet market. Consequently, it is common to observe aerial sports pilots opting for downhill mountain bike helmets (ASTM F1952 certified) or e-bike helmets (NTA-8776 certified) due to their higher safety ratings[28]. For comparison, both are shown in Figure 5.7 and Figure 5.8 respectively. For the PenteFoil, pilots should consider using downhill mountain bike helmets or e-bike helmets. These helmets offer optimal protection against operational and external hazards. While the necessary information is provided to help pilots make an informed decision, the choice of helmet ultimately rests with the individual pilot.

[28] https://supair.com/en/produit/parachute-supair-shine/, Accessed on 18/06/2024.
[29] https://www.hangglidingflightschool.com/equipment.php, Accessed on 04/06/2024.

**Figure 5.7:** Mountain biking helmet[30].

**Figure 5.8:** Paragliding helmet[31].

### 5.2.4. Hook Knife

The hook knife is an essential safety element designed to cut away the attachment when the wing needs to be detached from the user due to safety hazards. This is an essential tool used in kitesurfing for the same reason. Potential use cases include emergency water landing or crashing into trees. Using the knife is a measure used only during an emergency to free an overly restrictive line or harness or to ensure the emergency parachute deploys correctly. The purchase of an appropriate hook knife is the choice and responsibility of the user. For the hook knife to be effective and safe, the attachment system should connect the four lines into one before reaching the carabiner, allowing the user to cut away safely with a single cut. The hook knife is also neglected in the cost, mass, and volume estimations due to its low price and small size.

### 5.2.5. Hand Pump

A hand pump is an essential element of the PenteFoil operations. For the purpose of mass and volume estimations a standard multi-purpose pump was found in a local sports supply store[32]. The pump is very similar to pumps used for kitesurfing or camping, weighs 1.4 kg and can provide 4.7 litres of air volume in each pumping cycle. An example picture of the pump is shown in Figure 5.9.

**Figure 5.9:** *Decathlon* inflation pump[31].

**Figure 5.10:** *Supair* emergency parachute[30].

The structure needs 1900 L of air in order to be inflated at the required pressure, which requires 400 pump cycles. The pump was tested in the shop by conducting 20 pump cycles which have taken on average 22.1 $\pm$ 1.2 seconds over 5 tries. Interpolation of these numbers shows that the structure can be inflated within around 7.5 minutes, which with a contingency margin of 2.5 minutes or 33% still yields possible inflation under 10 minutes.

[30] https://www.mantel.com/fox-racing-rampage-2022-mtb-helm?, Accessed on 04/06/2024.
[31] https://paraglidingguide.com/gear-guides/choosing-the-right-paragliding-helmet/, Accessed on 04/06/2024.
[32] https://www.decathlon.nl/p/handpomp-voor-kamperen-ultim-comfort-10-psi-aanbevolen-voor-opblaasbare-tent/_/R-p-327638?channable=02893b736b756964003431303839363337a&mc=8601387&utm_source=google, Accessed on 14/06/2024.
[33] https://www.parashop.co.za/product-category/reserves/, Accessed on 19/06/2024.

## 5.3. Flight Procedure

This section describes the procedures necessary to fly the PenteFoil once the take-off procedure is completed. It will discuss the possible manoeuvres and the required control inputs to achieve them. The mechanisms behind the controls and the control system effectiveness have already been described in Section 3.10. Thus this section will focus on the control system input mechanisms, starting with describing the essential control manoeuvres, pitch, roll and turning, which are needed for all PenteFoil operations. It will then provide an overview of four advanced control techniques, utilisation of which is reserved for more experienced PenteFoil users, to show possibilities of advancement in the sport and satisfy **REQ-STK-02-2** 'The system shall provide an enjoyable experience according to potential users.' Every described control manoeuvre is achieved with the use of C.G. shifting.

### 5.3.1. Pitch Control

Pitch control is performed by the C.G. shifting mechanism of the PenteFoil. The user can adjust the pitch of the wing using the front control bar. To pitch up, the user pushes on the rod, shifting their C.G. backwards relative to the wing and causing a positive pitching moment. To pitch down, the user pulls on the control rod bringing their C.G. forward relative to the wing, causing a negative pitching moment. The pitch control mechanism to a great extent mimics the control system of a hang glider, thus it can be considered a user verified control method. It is also very intuitive for the user, the greater the desired pitch angle, the greater the force required to achieve it, as well as the deflection of the user's body. The C.G. shift range for pitch is ultimately limited by the user's strength and arm length.

### 5.3.2. Roll Control

The user can also control the roll motion of the PenteFoil by utilising the C.G. shift. To control the roll the user shall shift their C.G. left or right. This can be done by using the control bars by pulling the body to the desired side respectively. The placement of hands on the bar is not predefined as it is decided upon by the user based on their comfort. If the user pulls to move themselves to the left underneath the wing, the wing will roll to the left as their C.G. shifts left. To roll to the right, the user must pull themselves to the right, thereby shifting their C.G. to the right. The roll control system is intuitive for the user as the roll deflection is dependent on the force used by the user to shift their C.G. Just like the pitch control, the C.G. shift range for roll is limited by the user's strength and arm length.

### 5.3.3. Turning

To make a turn with the PenteFoil, the pitch and roll have to be combined due to the lack of inherent yaw control. To induce a turn, roll and pitching-up movements must be conducted simultaneously. First, the user rolls in the direction of the desired turn using C.G. shift, causing the wing to bank. Then, the user can pitch up to turn into this direction, by shifting their C.G. backwards.

In order to make a right turn, the C.G. is first shifted to the right, which causes a rolling moment to the right. The user can control the bank angle based on the desired turn radius - the higher the bank angle, the smaller turn radius that can be achieved.

To exit the turn, the user should steadily move beyond the equilibrium position to initiate a roll in the opposite direction. Once in the desired symmetric position, the user should stop the rolling motion by returning to the equilibrium condition. Turning left follows the same procedure but in the opposite directions.

### 5.3.4. Wing Tip Folding

The wing tip folding can be achieved with the use of the control handles attached to the control bar. The control handles are able to slide on the bar with the use of linear bearings attached to the inner side of the handle[34]. The movement of the control handles is ultimately limited by the geometry of the bottom stiff control rod. To maintain the desired position of the wingtips in flight, the handle can be securely attached to one spot on the control bar using a simple tube clamp. This clamp functions by tightening around the bar, similar to those used on bicycle seats. The clamp has been customized for easy clamping and unclamping and requires significantly less clamping force due to counteracting loads, approximately ten times lower in magnitude. The tip folding control handle is presented in Figure 5.11.

The user shall unfold the wing tips simultaneously to prevent inducing roll. This skill can be developed during the PenteFoil training procedure, where the user learns to apply force on the handles based on various factors such as position on the PenteFoil, wind conditions, and other elements that could differentiate the lift, thus the required folding force, across the wingtips. The wing tips will move back to their equilibrium, extended position on their own due to the lift produced by the airfoil at the wing tips. Moreover, a symmetrical control system can

[34] https://www.123kogellager.nl/kogellager-behuizing/lineaire-transmissie/lineaire-lager/kh2540-pp?gad_source=1, Accessed on 14/06/2024.

be developed for training purposes. However, this falls outside of the scope of the report, and the goal for the in-flight control is to achieve independently folding wingtips.

Other handle designs might be possible, as this part is highly customisable and dependent on the preference of the user. Possible modifications include improvement of the handle ergonomics, or different clamping system. Comfort of using such a handle can be tested during the prototyping phase of the PenteFoil.

**Figure 5.11:** Tip folding control handle.

**Figure 5.12:** Folded wing tip.

### 5.3.5. Thermal Winds

Rolling manoeuvres momentarily increase the sink rate of the PenteFoil, resulting in a loss of altitude. Altitude can be regained by utilising thermal winds. More experienced users can take advantage of these winds to extend their flight time and/or increase the number of manoeuvres they can perform in a single flight. The thermal winds are commonly utilised in hang- and paragliding[35]. This subsection presents a brief description of how to utilise thermal winds in PenteFoiling. The use of thermal winds is generally a complex procedure and is utilisable by more experienced users, such as users with paragliding or glider flying experience.

Thermal winds are mostly present during low atmospheric pressure days, especially near mountain ridges[36]. Users can use a variometer of their choice for an indication of entering and leaving a thermal zone.

Once a thermal zone is located, the user should stay within the zone by circling in the column of air. The user shall maintain a steady bank angle and speed to maximize lift from the thermals. Advanced users might be able to identify visual cues and patterns in the landscape to find the thermals, even without the use of a variometer.

### 5.3.6. Diving

The user can achieve high dive angles and speeds by combining 2 control methods - shifting the C.G. forwards to decrease the pitch and furthermore, they can fold the wing tips to reduce the lift and increase the speed up to the $V_{ne}$ of 49 m/s. Aggressive diving procedures shall be utilised only by experienced users with good timing and flight recovery skills attempting this procedure shall fall within the individual assessment of the user. Diving allows users to achieve high accelerations and speeds on the flight envelope limits and perform aerobatic manoeuvres.

### 5.3.7. Deep Spiral

Deep spiral is another method for decreasing altitude rapidly. It is essentially a prolonged turn to one side - the wing is constantly turning and due to the decrease lift it has a high sink rate and enters a spiral. The spiral can be considered another aerobatic manoeuvre of the PenteFoil, since it allows the user to obtain high centripetal accelerations and enjoyable feeling.

Before entering a spiral the pilot should assess the available altitude and determine potential sources of collision, such as other pilots or landscape. The spiral should be attempted in the same procedure as inducing a turn, however, the turn is not recovered for a prolonged time.

During the deep spiral, high and prolonged accelerations might be possible. Pilots should attempt this procedure on their own responsibility and based on their own assessment of the acceleration that they can sustain. Furthermore, higher wing loading will cause higher control force required. The pilot should be aware of their own strength and capabilities and during training the accelerations in the spiral shall be increased gradually.

[35] `https://rvhpa.org/weather/`, Accessed on 14/06/2024.
[36] `https://www.ushpa.org/page/thermals-part-three-thermalling-technique`, Accessed on 14/06/2024.

The spiral can be recovered from by pushing up in the direction opposite to the ground in order to start a roll out of the spiral, until the wing is back in its symmetric equilibrium position.

## 5.4. Take-Off Procedure

This section outlines the step-by-step take-off procedure for the PenteFoil and is intended to provide a comprehensive guide and understanding of launching the PenteFoil safely and effectively. It first discusses some possible locations and provides an overview and analysis of weather conditions in these locations, and then the procedure itself.

### 5.4.1. Take-Off Locations

The PenteFoil is designed to provide a more exhilarating alternative to paragliders, and as such, it is intended to take off from the same locations paragliders typically use. A preferred take-off scenario involves a gentle downslope at the mountain peak with a light headwind. This setup allows users to run into the headwind, gaining speed and achieving lift-off.

An analysis of suitable take-off locations reveals that wind direction significantly influences the viability of a location for take-off, as depicted in Figure 5.13. On the windward side of the mountain (left side in the illustration), there are smoother airflow patterns, conducive to a stable take-off. In contrast, the leeward side (right side) experiences more turbulent air due to the mountain's obstruction, making it less favorable for take-off.

Therefore, it is crucial for PenteFoil users to initiate take-offs from the windward side of the mountain. This choice minimises the risk of encountering the more turbulent air during the critical phase of take-off, ensuring a safer and more reliable launch experience.


**Figure 5.13:** The wind over a mountain[37].

A further analysis was done with the use of Windninja, a tool designed to, e.g. help firefighters predict wind direction, and thus the direction of wildfire spreading[38]. These winds are calculated at 10 meters above ground level. In this software, the wind speeds are shown by vectors where the colour and length show the wind speed. The strength of the wind speeds is shown by red being the strongest (23.06 - 29.14 m/s), then orange (17.35 - 23.05 m/s), then yellow (11.57 - 17.34 m/s), then green (5.79 - 11.56 m/s) and then blue being the weakest winds (0 - 5.78 m/s).

First, an analysis of a paragliding hot spot Chamonix-Mont Blanc in France was conducted. The location was chosen based on its high popularity within the paragliding and wingsuiting community. The results of this first simulation can be seen in Figure 5.14. In this analysis, the phenomenon of windward and leeward winds can also be seen. Where the windward side has a stronger flow up the mountain. The leeward side has a lot weaker winds shown by the blue arrows.

Another, more extensive analysis was conducted on the valley at Lago di Garda to examine the influence of wind direction on flight conditions. This location was selected based on a collective decision by members of DSE Group 11, as it featured in an earlier phase of the DSE project within one of the concept renders. This location is only an example and the PenteFoil is able to be flown in many different locations. Four simulations were performed, each with a different wind direction: from behind the mountain, from the front, and from the right and left sides, which are defined in Figures 5.15-5.18.

In the first simulation, the wind was coming from behind the mountain, as depicted in Figure 5.15. The results indicate that wind speeds at the top of the mountain are high, as shown by the orange and red arrows. However, on the leeward side of the mountain, wind speeds are significantly reduced, as indicated by the blue arrows.

[37] https://www.weather.gov/source/zhu/ZHU_Training_Page/winds/Wx_Terms/Flight_Environment.htm, Accessed 18/06/2024.
[38] https://www.firelab.org/project/windninja, Accessed 18/06/2024.

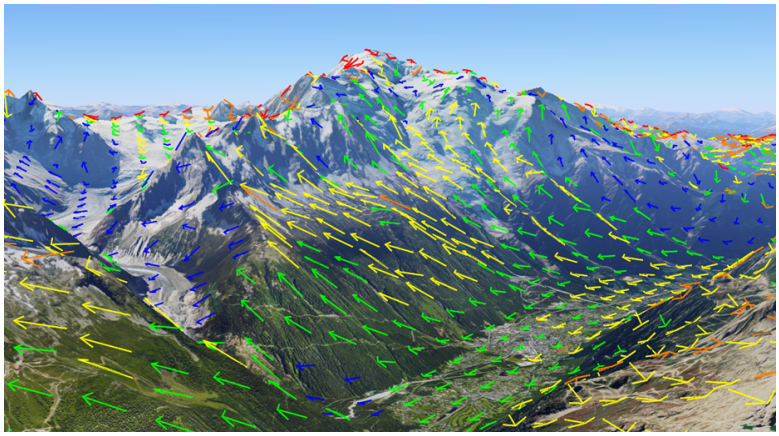

**Figure 5.14:** Simulation of the winds on the mountain in Chamonix, France.

In the second simulation, the wind was chosen to come from the front of the mountain. This simulation is shown in Figure 5.16. The first thing that stands out is that the winds in the valley of Lago di Garda are relatively low. However, the wind at the top of the mountain is much stronger and less turbulent on the windward side with this wind direction.

For the third and the fourth simulations shown in Figure 5.17 and Figure 5.18 respectively, the wind is coming from the side of the mountain. These simulations showed an increase in wind strength within the valley, as the wind is less disturbed by the surrounding mountains compared to winf from the fornt or the back. However, the winds on the sides of the mountain became quite gusty. This is indicated by the more variable wind speeds on the side of the mountain, with small areas of higher and lower wind speeds, suggesting that the wind is less constant and more turbulent compared to the first two simulations.

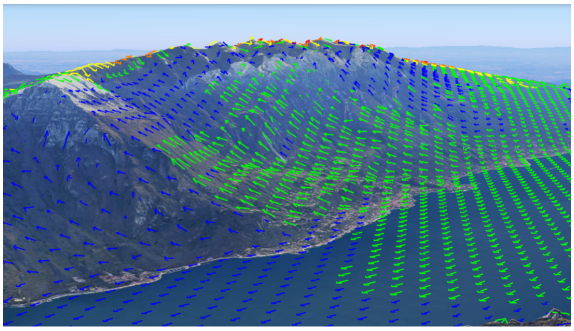

**Figure 5.15:** Simulation of the wind coming from behind the mountain.

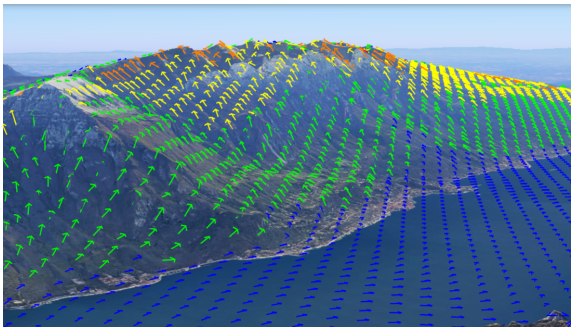

**Figure 5.16:** Simulation with the wind coming from the front of the mountain.

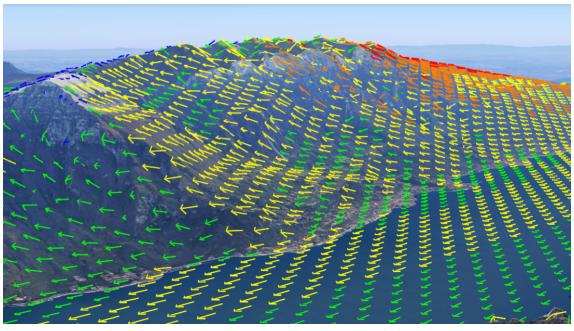

**Figure 5.17:** Simulation with the wind coming from the right side of the mountain.

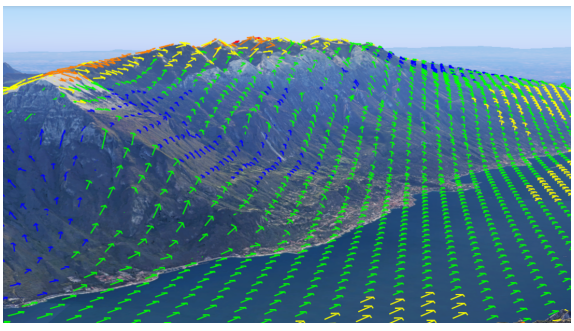

**Figure 5.18:** Simulation with the wind coming from the left side of the mountain.

For paragliders, there is an effective tool available to assist users in choosing a suitable takeoff location called the ”Paragliding Map”[39]. This map provides many popular takeoff sites and indicates which locations are viable based on current weather information. It evaluates conditions by checking for factors such as rain, gusts, and wind direction, helping users make informed decisions about their flight. It can be utilised in the same way for the operations of the PenteFoil.

[39] `https://www.paraglidingmap.com/app/`, Accessed on 19/06/2024.

This analysis shows the significant impact of wind direction on the viability of a location for safe takeoff. Therefore, selecting an appropriate takeoff site must be based on a thorough safety assessment and the skill level of the user. Before takeoff, it is crucial to verify the wind direction and gusts to ensure that conditions allow for a safe launch. In conclusion, this section served as a blueprint for wind analysis which should be performed by each pilot before their take-off to assess the safety, and furthermore it outlined two exemplar locations suitable for PenteFoiling experience.

### 5.4.2. Pre-flight checks

To ensure the PenteFoil is in proper condition before take-off, the following pre-flight checks should be carried out. These checks are designed to detect any defects before the PenteFoil is airborne. Performing these checks carefully and routinely before each take-off significantly enhances the safety of flying the PenteFoil. If any of the pre-flight checks show signs of structural deficiencies the user should abort the take-off and consult a certified professional. Several of the following flight checks include equipment checks. Chosen equipment, description, and its justification was presented in detail in Section 5.2.

1. **Check last inspection date of the PenteFoil.** To safely use The PenteFoil, it should be checked every 30 flights or every 6 months by a certified professional according to FAA regulations for parachutes[40], which handle similar loads and use a similar material to the PenteFoil. Certification of the PenteFoil's maintenance shops is outside of the scope of this report and is provided by relevant authorities. Moreover, the PenteFoil undergoes a user check before every flight.
2. **Check last inspection date of the emergency parachute.** The emergency parachute should be unfolded, vented, inspected, and repacked every 6 months by a certified rigger.
3. **Inspect the structure of the PenteFoil for visible damage.** Apart from the professional inspection every 6 months, the PenteFoil should be checked by the user before every take-off. During initialisation, the carbon tubes should be checked for any cracks before assembly and inflation. Once inflated, the inflatable structure should be checked for leakage. A pressure gauge is installed at the inflation point. The take-off should be aborted if the lost pressure exceeds a threshold that would cause the PenteFoil's pressure to drop below 20 kPa during the planned flight time and descent height, including a safety factor of 2 to account for a possible increase in leakage rate during the flight. Furthermore, the inflatable beams should be checked on the outside for any tears or major scratches. This is conducted both visually and by feeling for scratches manually.
4. **Check the condition of connection points and lines.** User attachment and control system connection points should be manually checked for malfunctions and visually for damage. The connection points such as carabiners should be pulled and shaken by the user with moderate force to check if they are properly secured and locked. All lines should be checked for damage by visual inspection of outer weaving.
5. **Inspect the PenteFoil harness.** The cocoon/pod harness should be visually checked for damage such as tears. The harness is usable even with the presence of minor scratches, however, it is advised that they are repaired or patched by the user before the flight.
6. **Inspect the parachute harness.** Parachute harnesses should be inspected according to the guidelines provided by the manufacturer.
7. **Inspect the helmet, hook knife, and other safety equipment.** Finally, the helmet and other equipment should be checked. The helmet should fit properly and should not be able to be removed without undoing the clips. The hook knife should be checked for breaks. Any other equipment chosen by the user should be examined based on the guidelines provided by the manufacturer. Once everything is properly examined the user can prepare for take-off by putting on the harness.

Apart from the structural and safety checks, the weather conditions should be assessed by the user. The following list provides a guideline for weather assessment for the user, however, this assessment is in the end fully dependent on the user.

1. **Check the wind and gust speed.** Wind above 20 kts can be dangerous by limiting the control effectiveness of the PenteFoil and greatly increasing the risk of collision when flying in mountainous regions.
2. **Check the outdoor temperature and sun radiation.** Since PenteFoiling is a sport, connected with elevated heart rate and some physical exhaustion, it shall not be conducted in extreme temperature conditions and extreme sun radiation due to the possibility of fainting during flight, nausea, decreased decision-making skills, and other consequences. These weather conditions shall be individually assessed by the user.
3. **Check the precipitation.** Precipitation such as rain may decrease the flight performance, increase the PenteFoil's weight, decrease visibility, or increase the risk of slipping during take-off and landing. Thus, flying in rain is not advised, however, it is assessed individually by the user on their own responsibility.

[40] `https://www.uspa.org/first-time-student-skydivers/skydiving-equipment`, Accessed on 14/06/2024.

In the end, the take-off decision falls within the individual assessment of the user. All of the presented checks provide a guideline for preventing the potential sources of risk during operation. User is free to conduct more extensive checks based on their own assessment, however the assessment procedure presented in this report should always be taken into consideration.

### 5.4.3. Preparations

After completing all pre-flight checks, the pilot can begin preparing for the flight. The pilot should adjust and secure all buckles and straps on the chosen harness to ensure a well-positioned and secure fit. The body weight must be distributed evenly across all harness contact points. The main harness is attached to the wing by connecting the four harness lines to the main carabiner connecting all the attachment lines. The harness was described in detail in Section 5.2.

### 5.4.4. Take-Off

The following list provides the model take-off procedure, designed based on the take-of procedure followed by hang gliders. The specific take-off procedure for a pod harness is shown in Figure 5.19. The take-off procedure can be slightly modified by the user on their own responsibility, however, the one presented below is designed for maximum safety and recommended to be applied by all users.

1. After assembly, position at the launch site facing into the wind.
2. Put on the PenteFoil harness as specified in the user guide.
3. Hold the control frame with a relaxed grip.
4. Position the PenteFoil wing above your head at a slightly positive angle of attack relative to the incoming wind, depending on the wind speed and the slope of the launch terrain. The pilot should be able to feel which angle of attack provides highest lift-to-drag ratio, this angle of attack should be maintained.
5. Start running with small and controlled steps down the hill while maintaining the correct wing position as described in step 4.
6. Increase the ground speed while maintaining a central body position relative to the control frame.
7. Continue running to gain additional airspeed as the PenteFoil begins to lift.
8. Maintain a forward-leaning posture to ensure a clean launch.
9. Bring your legs toward your chest, keeping movements smooth and steady to maintain stability.
10. Gently slide their legs one by one into the skypod harness pocket, ensuring both legs are securely and comfortably positioned inside the pocket.
11. Zip up the skypod using the line attached to the skypod.
12. Continuously monitor your surroundings and control the PenteFoil by shifting their centre of gravity during steps 9 through 12.
13. Once smoothly transitioned into the PenteFoil skypod harness, relax and enjoy the flight while remaining vigilant about weather changes and maintaining control of the PenteFoil.

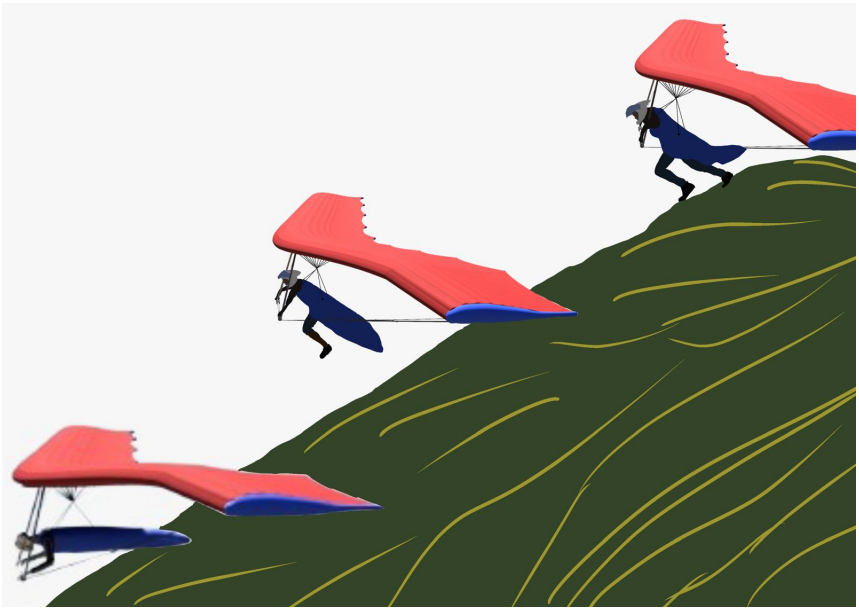

**Figure 5.19:** Running take-off procedure for a PenteFoil skypod harness showing three take-off stages.

### 5.4.5. Safety Conditions

The pilot shall not attempt the launch if any of the following situations occurs:

- Wing is not inflated to the correct pressure described in Section 4.4 with a deviation of more than 5%.
- The wind causes a negative ground speed. This limits the pilot's control over the chosen landing zone.
- Another pilot launches/flies within 200 m of the take-off location.
- The pilot suspects structural damage or any other issues with the system.

In the end, safety assessment is the responsibility of the user. While these guidelines provide a framework for best practices and potential hazards, it is crucial for individuals to exercise their own judgment and due diligence. Each situation is unique, and users must remain vigilant, adapting their approach based on their own risk assessment. The user should always prioritize personal and collective safety and consult professionals if uncertain about specific circumstances.

## 5.5. Landing Procedure

The following section will describe the landing procedure step by step. Similarly to the take-off procedure, it has been designed to ensure maximum safety and it is recommended to follow this procedure for all users. The landing procedure has been designed based on the landing procedures followed by hang gliders due to the high similarity of the procedure, defined by a FAA certified hang glider pilot and instructor[41]. The following list provides a short overview of the whole procedure, however each element shall be described and trained in detail during the user training.

1. Locate the landing sight. The landing sight should be flat, free of any obstacles, and provide sufficient space for landing. The user is fully responsible for the assessment of landing safety.
2. Approach landing sight, while descending slowly and steadily.
3. Once in the vicinity of the landing sight start trimming the aircraft for landing.
4. Unzip the skypod and remove the legs one by one out of the PenteFoil skypod harness while keeping the movements smooth and steady to maintain stability.
5. Once the PenteFoil is trimmed, get into a vertical position at a height that is considered safe by the user. Typically, this height is around 10 metres above ground for hang gliders, thus this height is also recommended for the PenteFoil. However, the landing height falls into individual assessment by the user.
6. Descend further while getting on the trajectory to land in a straight line with the headwind.
7. Slowly start the flare of the wing in a relaxed manner with a firm grip, once at roughly 5 meters above the ground. To do that, the wing should be pitched up by pushing on the control rod, while at the same time moving the hands up the control bar to allow more pitch.
8. Descend further until at roughly 1 meter above the ground where the wing shall be fully flared up until the stall limit. The flare manoeuvre involves pitching the wing up to a high angle of attack, which significantly increases both lift and induced drag, in effect decreasing the forward speed and sink rate, allowing for a smooth and controlled landing. The flare performed by a hang glider pilot is presented in Figure 5.20.
9. Stall the wing when the feet reach the ground by pushing the control frame and fully extending their arms. In the ideal scenario, the pilot lands vertically without the need to run. However, it is possible to touchdown while running, where the pilot shall further stall the wing.
10. Touchdown and quickly get away from the landing sight to accommodate other aerial sport flyers to land safely by unhooking the harness from the wing carabiner connection and carrying the wing above head.

## 5.6. Emergency Landing Procedures

The PenteFoil might become temporarily or permanently uncontrollable, which is highly undesirable and can potentially lead to hazardous outcomes. This section provides the user with proper instructions on handling such situations and the use of the emergency parachute.

The possible scenarios include collision with another user, a bird, or natural terrain, structural failure, unstable and uncontrollable flight, fainting or feeling unwell, and many others.

Proper safety training equips a user with the knowledge to assess the severity of the situation and attempt recovery. Recovery attempt is preferable to deploying the emergency parachute with sufficient altitude. However, if the altitude is below the minimum safe deployment height, the emergency parachute should be deployed immediately to maximise the chances of a safe landing.

[41] `https://www.youtube.com/watch?v=Lur7cp7O7PQ&ab_channel=IanBrubaker`, Accessed 18/06/2024.

**Figure 5.20:** A flared landing performed by a hang gliding pilot [58].

Uncontrollable flight below the minimum parachute deployment altitude is an extremely unsafe situation. Parachute deployment altitude is specified for each user chosen parachute by the manufacturer. In this case, the emergency parachute cannot be deployed safely anymore, however, it can be used to mitigate consequences of a crash landing thus it shall always be deployed. Otherwise, the pilot should always attempt recovery or attempt minimising the descent rate.

1. **Decide to throw the emergency parachute.** The first step is deciding to deploy the emergency parachute. The pilot should deploy the rescue parachute in two scenarios: first, when the wing becomes uncontrollable and recovery is impossible; second, when the pilot descends below the critical height, requiring parachute deployment for a safe emergency landing due to a non-functional wing. The pilot shall attempt recovery of the flight until they reach minimum parachuting altitude.
2. **Locate the deployment bag handle.** The deployment bag is the storage location of the rescue parachute located on the front of the PenteFoil's capsule harness. Locating the bag handle before the flight helps avoid pulling the wrong strap.
3. **Get the parachute out by pulling the emergency parachute handle.** Once the pilot has decided to pull the emergency parachute. The pilot shall pull the emergency parachute handle to take the emergency parachute out of the container. It is essential that this is in an easy-to-reach position and the pilot could even do it with their eyes closed. A spiral can be very disorientating and every second count in an emergency. Furthermore, it is important to have practised the pulling of the emergency parachute while being suspended, which could influence the ease of pulling it. In an ideal situation, if the pilot has the time and is not disorientated, the pilot shall decide the safest direction to throw the emergency parachute.
4. **Throw the parachute.** Immediately, in one continuous motion after pulling the parachute out of its container, the pilot shall throw it towards the selected location. A powerful throw is necessary to minimise the risk of improper deployment or tangling before the parachute is opened.
5. **Check that the deployment is correct.** The pilot should check whether the emergency parachute has correctly opened. In case of parachute entanglement, the pilot shall try to untangle the line for proper deployment. It is of high importance to continuously check the condition of the parachute.
6. **Position your legs underneath you for landing.** Once the pilot gets close to the ground, they shall make sure to put their legs underneath them to break the fall. This has to be done while the emergency parachute in most cases does not provide enough lift for a comfortable landing. To further break the fall, PLF (Parachute landing fall) is a method that can be practised to reduce injuries from an emergency parachute landing. This method is a common practice and will be further discussed in the training.

# 6 | Ground Operations

After the flight operations have been discussed, this chapter outlines the ground operations that are necessary for a safe PenteFoil flight. This is done first by looking at the folding of the system in Section 6.1. Subsection 6.1.1 and Subsection 6.1.2 explain the estimations of folded volume of the system and initialisation time. The transportation of the system to the take-off location and from the landing location will be discussed in Section 6.2. The training for users that want to fly the PenteFoil will be discussed in Section 6.3 and a sensitivity analysis was performed in Section 6.4 to investigate the influence of operations on the design of the system. All operations performance metrics have been summarised in Section 6.5.

## 6.1. Folding

One of the main advantages of the inflatable structure of the PenteFoil is its foldability. **REQ-SYS-02-3-2** and **REQ-SYS-02-3-3** specify the maximum volume of the folded structure of 75 litres, with dimensions not exceeding 1 metre in any direction. So far, the assembled structure has been presented, thus the following section will detail the process of folding the system.

The primary challenge in folding up the structure is the compression elements. These consist of tubes that span the whole wing. The compression elements were split into 1 m sections, which yielded 30 CFRP tube pieces. Since it is preferable to have the maximum possible length of the segments to reduce the negative influence of joints on the structural strength of compression elements and quicker assembly time, the maximum folded length that complies with **REQ-SYS-02-3-3** was chosen. Carbon fibre sleeves, shown in grey colour in Table 6.1, were used to allow the insertion of tubes into each other. The carbon sleeves have the same skin thickness as the inner tube, with an inner diameter of 6 mm and an outer diameter of 8 mm, which allows for a snug fit into the sleeve. The carbon sleeve is attached using an E1 epoxy adhesive to the end of all but one carbon tube. The sleeve is sufficiently strong due to the same material and skin thickness as the compression element. Through the insides of the tubes, an elastic string is inserted to prevent losing the sections during transportation. An overview of this description is presented in Table 6.1. Once the compression rods are assembled, they can be inserted into place, snugly fitting the fabric sleeves.

As established in Chapter 4, during gusts causing negative wing loading the compression rods on top will be loaded in tension. However, since the PenteFoil structure uses compression elements on both the top and the bottom, carbon rods do not have to act as tensile elements during loading opposite to their location. They have to, however, be able to sustain possible deflections of the wing - meaning that they should not slide out of their metal sleeves in operation. Thus, the fabric limits its span-wise movement due to its high elastic modulus. In Chapter 4 it has been estimated that the strain of the skin will not exceed 0.5%, thus the minimum length of the sleeves should be 10 mm, however, there is a possibility of sliding off the tubes during assembly before putting them into the wing sleeve, thus sleeves with a length of 100 mm are used. The folded carbon tube sections shall then be wrapped and secured by a single velcro strap for storage. They can be attached to the outside of the backpack for easy transportation, similar to how kitesurfing boards are transported.

### 6.1.1. Volume Estimation

The folded-up volume has been estimated based on the volume of materials used. This estimation, however, assumed 100% folding efficiency of the fabrics and tubes, therefore the folding efficiency was estimated and incorporated into the volume results. The volume of the folded tubes is around 1.1 litre assuming packing efficiency of 78% for 30 elements assuming a hexagonal (most optimal) distribution of circular elements [42]. The bladder and fabric have a fabric volume of 2.4 and 2.3 litres respectively. However, this assumes the volume of the raw material, not the fabric. The volume of the fabric is estimated to be 91% greater due to the packing of the fibers in the fabric, based on the difference in density between extruded nylon (1.15 kg/dm³) and nylon fabric (0.67 kg/dm³)[43]. Furthermore, the fabric packing efficiency was established at 50% based on team members' experience with nylon kite folding, an estimate with high uncertainty due to little available research on the estimation of fabric folding efficiency. This estimation, however, can be easily verified and refined at the stage of prototyping and measuring the folded-up volume directly.

The harness should be perfectly foldable into 3 litre volume, thus including the efficiency factor this gives 5.7 litres[44]. The volume of the recommended pump is 10 litres according to the manufacturer[45], however this piece

[42] http://datagenetics.com/blog/june32014/index.html, Accessed on 18/06/2024.

[43] https://www.matweb.com/search/DataSheet.aspx?MatGUID=fb48404b7e04433bb3ee3d2a0af922ff, Accessed on 18/06/2024.

[44] https://www.rotorharness.com/produtos-cocoon.asp, Accessed on 18/06/2024.

[45] https://www.decathlon.nl/p/handpomp-voor-kamperen-ultim-comfort-10-psi-aanbevolen-voor-opblaasbare-tent/_/R-p-327638?channable=02893b736b756964003431303839366337a&mc=8601387&utm_source=google, Accessed on 18/06/2024.

of equipment is chosen by the user and it may vary. The maximum volume of the folded parachute is found from manufacturer specifications at 3.8 litres[46].

To reduce the folded volume of the whole structure, the user may utilise the inflating pump and vacuum bags, which can be assumed of negligible volume and taken by the user's preference. Lastly, the user-chosen helmet is considered of negligible volume. As the helmet can be attached to the backpack or transported on the user's head, thus it is not accounted for in the estimations. The overview of estimated folded up structure volume is presented in Table 6.1.

**Table 6.1:** Volume fractions of PenteFoil equipment.

| Element | Volume [litre] | Fraction |
|---|---|---|
| Tubes | 1.1 | 2.2% |
| Bladder | 9.1 | 18.0% |
| Fabric | 8.8 | 17.3% |
| Harness | 5.7 | 11.3% |
| Pump | 10 | 19.6% |
| Parachute | 3.8 | 7.4% |
| Stiff Frame | 3.1 | 6.1% |
| Tensile Elements | 3.0 | 5.9% |
| Attachments | 5.0 | 9.8% |
| Handles | 1.2 | 2.3% |
| Vacuum Bag | Negligible | Negligible |
| Helmet | Negligible | Negligible |
| **Total** | **50.8** | **100.0%** |

**Figure 6.1:** CFRP rods folding system.

The material folds up similarly to kitesurfing kites. It is first deflated and then folded up. Starting from the tip chord, the material should be folded towards the root chord, with the folds laying at the spanwise locations of the inflatable ribs - which are spaced around 1 metre apart. Once folded up, the PenteFoil should be once again folded at the root chord, folded into 3, and then folded into 3 once again, however perpendicular to the span and then in half for the last time in the same axis. This should give the approximate folded dimensions at 0.25 m, 0.33 m, and 0.22 m, which corresponds to the combined volume of bladder and fabric at 17.9 litres. The total volume of the folded-up PenteFoil has been estimated at 50.8 litres.

### 6.1.2. Initialisation and Termination Time

A rough estimation was made for the time to initialise the system. The unpacking and unfolding of the structure is assumed to take 5 minutes, which includes unpacking and unfolding the system and properly aligning the lines and attachments. After that 4 minutes are necessary to assemble the compression elements and fit them into the wing sleeve. After that inflation is assumed to take 10 minutes which will be further explained in Subsection 5.2.5. The steering frame must then be put together which is assumed to take 2 minutes after which 1 more minute is used to put it into its sleeves. After the steering frame is in place the lines that allow folding the wing tips must be attached which is assumed to take 2 minutes. Finally, the harness and cocoon should be properly secured to the wing by attaching it to the which is assumed to take another three minutes. The full initialisation is therefore roughly estimated to be 27 minutes. This satisfies **REQ-STK-02-4-1**, which states that the PenteFoil "shall be initialised within 30 minutes by trained users". However, this is an estimate and should be tested once a prototype is produced.

The estimated time of the structure folding is around 3 minutes based on the folding experiment performed on a kitesurfing kite. Adding folding the tubes of the compression elements and steering frame on top of that, estimated at 5 minutes, based on tent folding procedure which utilises similar tubes[47]. The deflation is estimated at 4 minutes. The folding up of lines and attachments is estimated at 5 minutes, this gives a total time of 17 minutes for termination of the PenteFoil. This would satisfy **REQ-STK-02-4-3** which states "shall be easily terminated within 30 minutes by trained users". These estimations are conservative, and this time could be reduced with proper training and experience.

[46] `https://supair.com/en/produit/parachute-supair-shine/`, Accessed on 24/06/2024.

[47] `https://www.youtube.com/watch?v=VOGOZ3zxe70&ab_channel=videocamper`, Accessed on 14/06/2024.

## 6.2. Transportation

As it was established that the PenteFoil structure fits within 50.8 litres, an appropriate storing device should be used. Kitesurfing commonly uses backpacks to store and transport the inflatable kites, which gave inspiration to a similar method being used in the PenteFoil design. The folded PenteFoil might cause air gaps once inserted into the backpack, moreover, the volume estimation assumes efficient folding, and thus the backpack has to be of a larger volume. The choice of the backpack falls within the user's chosen equipment, with a volume constraint of at least 50.8 litres, a commonly seen size used for sports backpacks is 60 litres. The backpack shall be lightweight so that it can be put inside the cocoon with the user during flight so that it can be brought down together with the whole system. Another option for the backpack would be to make the harness multi-functional such that it can be used as a backpack as well. During the development of the harness, this should be investigated further, as this would improve the transportability of the system.

## 6.3. Training

The training of users will be an essential step to ensure a safe flight. Therefore, this training is designed to make users feel and act safe while flying the PenteFoil. As different potential users will have different level of experience with aerial sports, the training is designed such that even people with no experience can fly the PenteFoil safely after the training is completed. This section will outline the training of users to ensure safe use of the PenteFoil. The training of potential users shall start after the PenteFoil has passed certification.

### 6.3.1. Safety Training

Safety training consists of theoretical training and physical training to ensure that the user can properly handle safety risks. This is done in an indoor facility with users wearing the PenteFoil harness to familiarise themselves with flight equipment. The training aims to provide a clear explanation of common use cases of the emergency parachute and the operation of the parachute.

The safety training will give an in-depth view of how to regain control and when to use the emergency parachute. Using videos and proper descriptions of possible circumstances, the trainees will learn how to assess the situation and what steps should be taken to make the situation as safe as possible. The concept of throwing height will also be discussed, which means that the trainees learn when they should try to regain control and when the emergency parachute is the best option.

Throwing the emergency parachute is important to ensure proper opening. Grabbing the handle of the emergency parachute in a stressful and possibly disorienting emergency is an important step that can be practiced in a training environment. Furthermore, the throw of the emergency parachute will decide how well and how quickly the parachute will open. For proper opening of the emergency parachute, the throw should be powerful which can also be practiced.

When the emergency parachute is properly deployed, the PenteFoil should not influence the emergency parachute. If this were to happen it could lead to entanglement or other unwanted scenarios. Therefore the user should know how to cut the PenteFoil to ensure it does not influence the emergency parachute. A landing with an emergency parachute will be harder than a normal landing and could still lead to injuries. Luckily the impact can be reduced by landing according to the parachute landing fall (PLF) method. During the safety training, the PLF method will be explained and practiced[48].

### 6.3.2. VR Training

Another method of training can be VR training. New and experienced users can experience flying the PenteFoil in virtual reality. The VR setup allows practice without risk of injuries or fatal accidents. By simulating real flight conditions, the VR experience helps users get comfortable with the controls and handling before moving on to actual PenteFoil flights. VR training can also be used as safety training by simulating emergencies. In this way, recoveries and the use of the emergency parachute could be practised.

MYRTUS XR is an example of a VR hang gliding game that can be run on QUEST 2 from META[49]. The software can be adjusted to match the mechanics of the PenteFoil by adjusting the graphic design and control system. The conceptual training set-up is shown in Figure 6.2 shows how the setup would look like, the user is hanging in a harness with a control stick in both his hands and VR goggles on his head. Finally, a fan is put in front of the user to make the experience even more realistic and varying the airspeed based on the airspeed in the simulator. A visualisation of the training setup is shown in Figure 6.2.

[48] https://www.paraglidingsanfrancisco.com/parachute-landing-fall/, Accessed on 19/06/2024.
[49] https://myrtusxr.tilda.ws/, Accessed on 19/06/2024.

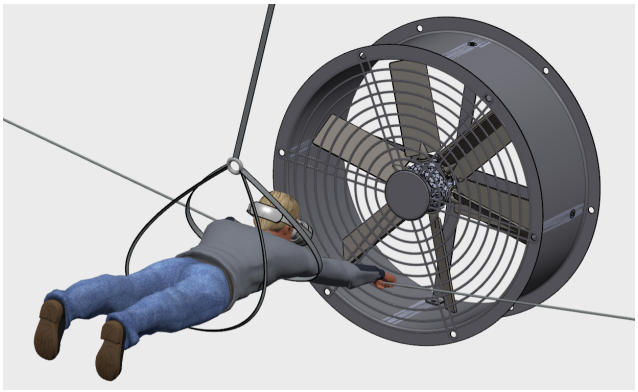

**Figure 6.2:** Set-up of VR training equipment.

**Figure 6.3:** Parasailing [1].

### 6.3.3. ParaFoiling Training

Parasailing is a recreational activity where a person is towed behind a boat while attached to a specially designed parachute, known as a parasail. The parasail is connected to the boat by a long rope, and as the boat speeds up, the parasail lifts the attached person providing a thrilling experience of flying. In parasailing, the takeoff begins with the person harnessed to the parasail on a platform at the back of the boat deck. As the boat accelerates, the parasail inflates and begins producing lift, causing the rope to tighten and lift the person off the deck. The boat continues to accelerate, allowing the rope to become fully deployed and letting the user achieve a stable flight. The parasailing flight is presented in Figure 6.3 for visualisation purposes.

The same procedure can be used in PenteFoil training, with 2 modifications. First of all, the PenteFoil should be attached to the participating person. Second of all, the parasail should be of a smaller size, since now the lift is also generated by the PenteFoil. The size of the parasail depends on the users experience - more experienced users will be able to fully discard the parasail and fly at a higher speed with the PenteFoil itself. For PenteFoiling operations, this procedure has been named ”ParaFoiling” compared to ”parasailing”.

The advantage of ParaFoiling compared to a real flight is that the consequences of a crash in case of losing control are mitigated by crashing into the water. However, an additional risk is drowning. Drowning can be avoided by wearing a life vest during the ParaFoiling. The user can release the boat line by incorporating commonly used quick release sailing carabiners. Besides that, as the PenteFoil is inflated, it will float and the boat crew can easily recover the user from the water in case of losing control of the wing.

ParaFoiling also presents the possibility of attaching an extra parachute to the PenteFoil which is already deployed. This parachute creates lift which keeps the PenteFoil in the air at lower speeds, allowing the user to learn the controls at lower speeds. When the user loses control the user will fall in the water with the parachute deployed, which decreases the impact. Different sizes of parachutes will be used for users with different skill levels to practice until they can fly the PenteFoil without the parachute.

This training procedure is used again for the purpose of testing described in a latter Verification & Validation chapter in Subsection 9.2.1.

## 6.4. Sensitivity Analysis

The design of the PenteFoil was primarily influenced by key operational factors such as take-off, landing, and safety. This sensitivity analysis will explore how changes in these operational factors could have impacted the design.

Starting with the take-off procedure, the system is designed to function for a running take-off. However, another option would be to use towing to get into the air. This would alter the structure of the system since there would be an additional load on the PenteFoil during the towing to propel the PenteFoil. This would mean that the structure has to be able to repeatedly handle this force. Furthermore, there is also an option to use only base jumping as a take-off method. If this was the case the attachment to the system could be changed to be completely rigid since no running is needed for the take-off.

Now looking at landing, the wing was highly designed for landing with the stall speed being low enough to allow for a stand-up landing. That is why the stall speed requirement was set at 11.5 m/s. If the landing procedure was changed This maximum stall speed could be increased as the stall speed is no longer necessary for landing.

The transportability of the system has also highly influenced the design. Everything must be as light and as

[50] `https://www.checkyeti.com/nl/water-sports/griekenland/greece/parasailing`, Accessed on 14/06/2024.

compact as possible to make the system transportable. As stated in the requirements it should fold to 75 liters and a maximum of 25 kg. If this was not a requirement there would be more options for the structure of the system. The system could then be a rigid structure that is not inflatable. This would mean that it would probably look like a hang glider which is 20 to 40 kg and their folded-up volume is upwards of 80 litres. While because of these requirements our design is only 15 kg and 75 litres. In addition to this hang gliders are folded up with a length of 2 metres and our design can be folded up to a length of 1 metre.

Last but not least the safety of the system was also an important factor in the design. Because of this the stability and the controllability of the system were very important in the design. If the system was allowed to be less safe. The systems speed and agility can be increased to cause a more thrilling flying experience. For this, the aerodynamic design would be changed such that a 360° turn can be performed faster than 14.4 seconds, which is the time needed for our design to perform a 360° turn.

## 6.5. Operations Parameters Summary

Table 6.2 provides an overview of all the performance metrics defined in this chapter.

**Table 6.2:** Operations parameters summary table.

| Design Parameter | Value |
|---|---|
| Total volume | 50.8 l |
| Recommended backpack volume | 60 l |
| Folded wing dimensions | 0.25 x 0.33 x 0.22 m |
| Assembly time | 27 min |
| Inflation time | 10 min |
| Disassembly time | 17 min |

# 7 | Design and Performance Summary

This chapter serves as a general summary of all major design aspects that are characteristic to the PenteFoil. First, a summary of the final design is given in Section 7.1. The main performance metrics are then given in Section 7.3. During the design, many design decisions led to a design that resembles that of a hang glider. Section 7.4 serves as a comparison between these concepts.

## 7.1. Final Design

The goal of this section is to provide a concise summary of the final design and highlight its key features, offering readers a comprehensive overview of the unique aspects that distinguish the PenteFoil. Figures 7.1-7.6 present different views of the final design's 3D model.

**Figure 7.1:** Isometric view of the PenteFoil with tips unfolded.

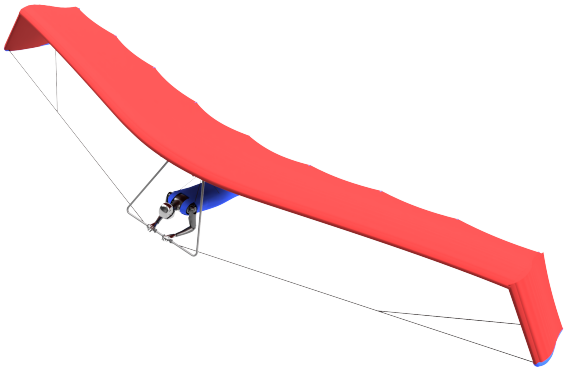

**Figure 7.2:** Isometric view of the PenteFoil with tips folded.

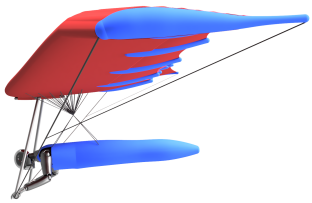

**Figure 7.3:** Side view of the PenteFoil tips unfolded.

**Figure 7.4:** Front view of the PenteFoil tips unfolded.

**Figure 7.5:** Top view of the PenteFoil tips unfolded.

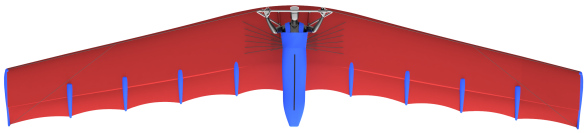

**Figure 7.6:** Bottom view of the PenteFoil tips unfolded.

The above visualisations mainly highlight the wing shape (in red) and the stiffening ribs (in blue), the user attachment (in blue under the wing) and the steering features consisting of the stiff frame and tip-folding handles.

The PenteFoil features a sporty wing design, with a higher aspect ratio than a typical hang glider, resulting in a surface area of 12.41 $m^2$ and a span of 10 m. The design stands outs thanks to the naturally occurring curvatures creating sweep and dihedral and between the ribs, which is the result of implemented structural solutions. The ribs and majority of the platform is inflated, which is well visible in the visualisations.

The system operates similarly to a hang glider in terms of take-off, flight and landing operations. The PenteFoil's primary advantage over hang gliders lies in its inflatable wing design, minimising the need for stiff elements. This feature allows the wing to be folded down to a compact size, fitting neatly into a regular-sized backpack for easy transport. While the inflatability simplifies the initialisation process, it does require carrying a hand pump as part of the system. Another significant advantage is its ability to fold the wingtips during flight, enabling the PenteFoil to achieve higher speeds when desired.

## 7.2. Flight & Gust Envelope

The flight and gust envelopes are tools in the design and analysis of aircraft to ensure their structural integrity and safety under various operational conditions. The flight envelope defines the limits of airspeed, operation altitude and load factor within which the aircraft can safely operate. It encompasses all permissible flight maneuvers and conditions, ensuring the aircraft can withstand the associated aerodynamic forces. The gust envelope, on the other hand, accounts for the additional loads that arise from atmospheric turbulence and sudden changes in wind speed, known as gusts. By considering these envelopes during the design phase, it can be insured that the structure is robust enough to handle both steady-state and dynamic loads, preventing structural failure and enhancing overall flight safety.

**Flight Envelope**

The flight envelope is established based on the requirements and certification specified in the CS23 regulations by the FAA. The limiting loading factors, $n_{max}$ and $n_{min}$, are defined in Table 7.1 according to these regulations[51]. Using these load factors, the flight envelope can be established.

For positive load factors, the flight regime is bounded by a parabolic curve between $0 \leq n \leq n_{max}$, rising with speed as described by Equation 7.1. Subsequently, the load factor decreases linearly from $n_{max}$ at the manoeuvring speed to $n_{max}$ at the dive speed.

For negative load factors, the flight envelope is bounded by a parabolic curve between $n_{min} \geq n \geq 0$, also following Equation 7.1. A horizontal line is then drawn connecting $V_s$ and $V_m$ at $n = -1$. Following this, the load factor increases linearly up to $V$. Finally, the red line closes the flight envelope, connecting the positive and negative load boundaries at the design limit speed.

The entire flight envelope is indicated in blue in Figure 7.7. The speed parameters $V_s$, $V_m$, and $V_D$ are derived from the flight diagram, which are crucial for the design. The stall speed, $V_s$, is the speed at which a positive load of 1 is created. The manoeuvring speed, $V_m$, is the speed at which the positive load factor reaches its maximum of 5.3 g. Finally, the dive speed, $V_D$, was established as the limiting speed set by the team. The maximum recorded speed for hang gliders is 41 m/s[52], the dive speed for PenteFoiling is set at 49 m/s. This represents a 20% increase compared to hang gliders, aiming to enhance the thrilling experience.

To complete the flight envelope, the operational altitude is defined. To comply with **REQ-STK-02-5** altitudes up to 3,500 m are considered as the maximum height rope ways reach in Europe[53]. Furthermore, the temperature and density at higher altitudes drop to such levels that they cannot be sustained comfortably by pilots for an extended amount of time. Landing sites in mountainous regions are usually situated above 500 meters, as the valleys themselves are elevated compared to sea level. This height difference results in a design criteria that the PenteFoil structure should withstand pressure differences of 30,000 Pa corresponding to 3,000 m height difference at this level.

$$n = \frac{C_L \frac{1}{2} \rho V^2 S}{W} \tag{7.1}$$

**Table 7.1:** Important parameters in the flight envelope.

| Parameter | Value | Unit |
|---|---|---|
| $V_s$ | 11.5 | m/s |
| $V_m$ | 27.0 | m/s |
| $V_D$ | 49.0 | m/s |
| $n_{max}$ $(@V_m)$ | 5.3 | - |
| $n_{max}$ $(@V_D)$ | 4.3 | - |
| $n_{min}$ $(@V_m)$ | -1.0 | - |
| $n_{min}$ $(@V_D)$ | -0.2 | - |

[51] https://www.faa.gov/documentLibrary/media/Advisory_Circular/AC_23-19A.pdf, Accessed on 18.06.2024.

[52] https://www.quora.com/What-is-the-highest-speed-to-which-a-glider-has-ever-been-aerotowed-to, Accessed on 19.06.2024.

[53] https://aplinsinthealps.com/matterhorn-glacier-paradise-the-highest-cable-car-station-in-europe/, Accessed on 19.06.2024.

### Gust Envelope

The gust envelope was established by first looking at the gust strengths defined by the airworthiness authority in the applicable airworthiness standards. It was found that the gusts for the gust envelope are most commonly defined as 50 ft/sec (15.24 m/s) at cruise speed and 25 ft/sec (7.62 m/s) at design speed limit [29]. For our design, the cruise speed is 75 km/h (20.83 m/s) and the design speed limit is 49 m/s. Knowing this Equation 7.2 can be used to calculate the corresponding load factor [29].

$$n = 1 + \frac{K_g \rho_0 U_{de} V_E a}{2(W/S)} \tag{7.2}$$

In Equation 7.2, $K_g$ is the gust alleviation factor, $U_{de}$ is the maximum gust velocity, $a$ is $\partial Cl/\partial\alpha$, W is weight in kgf [29].

The gust alleviation factor can be determined using Equation 7.3 [29].

$$K_g = \frac{0.88\mu_g}{5.3 + \mu_g} \tag{7.3}$$

For Equation 7.3, variable $\mu_g$ (the aeroplane mass ratio) has to be calculated first which can be done by Equation 7.4 [29].

$$\mu_g = \frac{2(W/S)}{\rho_0 \overline{C} a g} \tag{7.4}$$

These equations were then used in Python to calculate the load factor for the PenteFoil. From these calculations, the following values were found:

- $n_{max}(@V_C) = 3.55$
- $n_{min}(@V_C) = -1.55$
- $n_{max}(@V_D) = 4.00$
- $n_{min}(@V_D) = -2.00$

After that, the gust loads are extrapolated between these points and the resulting graph is shown in yellow together with the flight envelope in blue in Figure 7.7.

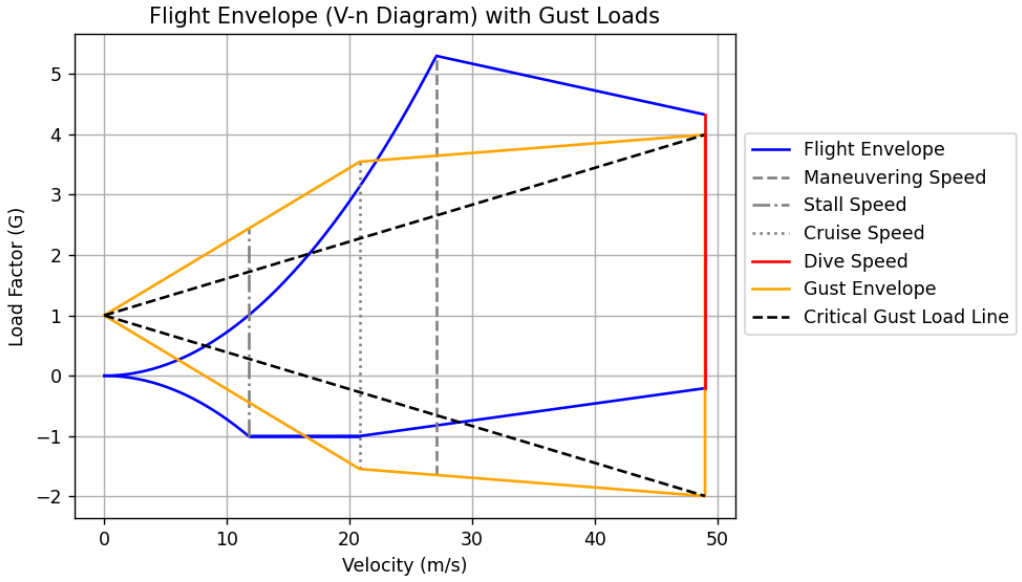


**Figure 7.7:** PenteFoil flight & gust envelope.

## 7.3. Performance

This section provides a brief overview of the performance metrics of the PenteFoil. These parameters are essential for potential users, as they provide insights into the operational limits and handling characteristics. Furthermore, a performance summary can help potential users assess the suitability of the PenteFoil for their

**Table 7.2:** PenteFoil Performance Parameters.

| Parameter | Value | Unit |
|---|---|---|
| Take-off airspeed | 11.0 | m/s |
| Landing airspeed | 8.7 | m/s |
| Stall speed | 8.7 | m/s |
| Trim speed | 20.83 | m/s |
| Never exceed speed | 49 | m/s |
| Trim sink rate | 1.71 | m/s |
| Parachute sink rate | 5.42 | m/s |
| Trim L/D | 12.17 | - |
| Maximum C_L | 1.63 | - |
| Trim C_L | 0.51 | - |
| Maximum tip deflection | 0.96 | m |
| Operational inflation pressure range | 20,000-50,000 | Pa |
| Folded Volume | 55 | L |
| Total system mass | 15 | kg |
| Nominal user mass | 80 | kg |
| Maximum user mass | 90 | kg |

specific needs, whether for recreational flying or sports competitions. Table 7.2 summarises the numerical performance parameters and is followed by a brief discussion of PenteFoil's performance.

The inflation pressure ranges specified can be translated to altitude ranges, though the exact width of this interval varies depending many factors such as altitude, atmospheric pressure and temperature. For instance, using the ISA as a reference, if landing at sea level is planned, the PenteFoil can take off from up to 3000 meters altitude. However, if the flight begins from a higher altitude, such as 4500 meters, the aircraft can safely descend to 1000 meters. As the pilot is likely unable to be aware of exact altitude during flight, it is recommended to plan the flights such that the differential of 3000 meters is not exceeded.

The wing of the PenteFoil is designed to ensure both longitudinal and lateral stability, encompassing both static and dynamic stability characteristics. This provides pilots with a safe, predictable and manageable flying experience across various flight phases.

Finally, the nominal user mass represents the optimised mass for which the system is designed. The PenteFoil is engineered to ensure safe flight a system mass of 105 kg, which corresponds to a maximum user mass of 90 kg. Compared to the nominal user mass of 80 kg, that requires larger inflation pressures and decreases the suitable altitude range. The exact ranges depending on the mass were not specified in this project and are left as a recommendation for the future.

## 7.4. Comparison to Hang Gliders

This section will highlight the key differences between hang gliders and the PenteFoil. It shows how the latter outperforms the former in various aspects and can dominate the aerial sports market. Table 7.3 summarises the main features in which the designs differ from each other and is elaborated on below.

The structure of a traditional hang glider consists mostly of tubes, sails, and cords. The airfoil shape is primarily dictated by the stiff tubes, which add significant weight, resulting in a wing mass of 20-40 kg. In contrast, the PenteFoil uses web Tensairity, where the airfoil shape is maintained by inflatable tubes, providing an aerodynamic shape with a much lower weight of 8.4 kg. Additionally, the PenteFoil can be folded into a backpack and transported by a single person, unlike a hang glider which requires a car for transport. This portability increases the number of possible take-off locations and makes the sport more accessible, eliminating the need for designated drivers who transport the hang glider without being able to fly.

[54] https://www.ushpa.org/page/what-is-hang-gliding-and-paragliding, Accessed on 18/06/2024.
[55] https://dynamicflight.com.au/hang-gliding/hang-gliding-faq/, Accessed on 18/06/2024.

**Table 7.3:** Differences between a typical hang glider and the PenteFoil.

| Design Characteristic | Hang Glider | PenteFoil |
|---|---|---|
| Structure | Stiff; Tubes, Sails and Cords | Inflatable; Web Tensairity |
| Control Method | C.G. Shift | C.G. Shift, Folding Tips |
| Wing Mass | 20-40 kg[54] | 8.4 kg |
| $L/D_{trim}$ | 10 [15] | 12 |
| Transport to flight location | Only by Car | On Foot, or with Ski Lift |
| Suspension Distance | 1.50 m | 0.55 m |
| Initialisation time | 4 minutes[55] | 27 minutes |

The largely inflated wing of the PenteFoil improves the aerodynamic shape. This results in a slightly higher $L/D_{trim}$, when compared to a Talon 2 hang glider. The PenteFoil outperforms the hang glider in other aerodynamic characteristics as well, this was described in more detail in Section 3.7.

The PenteFoil offers a reduced suspension distance, approximately one-half that of traditional hang gliders. This closer suspension enhances the pilot's connection to the wing, increasing the perceived thrill and improving comfort and stability by reducing sway caused by flow disturbances.

Moreover, the folding tips control method provides a significant advantage in flight experience. This innovative method, not used in any current air sports, combined with shifting the C.G., offers high pitch and turn performance, making it ideal for experienced users.

However, the PenteFoil takes longer to set up, requiring almost a half hour for initialisation due to the need for inflation and attaching the Tensairity system. In contrast, an experienced pilot can set up a hang glider in approximately 4 minutes[54]. Despite this longer setup time, the benefits in performance and portability make the PenteFoil a strong contender in the aerial sports market.

# 8 | Manufacturing

This chapter describes the manufacturing plan for the PenteFoil. It is divided into two parts. Section 8.1 outlines the process of manufacturing the initial functional prototypes of the PenteFoil. Section 8.2 part details the large-scale manufacturing process of the final product.

The goal of the prototype phase is to create an accurate aerodynamic shape capable of performing flight tests with a real human or a robot/mechanical system of equivalent mass, as quickly and cost-effectively as possible. This prototype will also be used for design iteration.

The second part focuses on the manufacturing of the final, iterated product. This design will be used for final validation of the concept, certification, and eventual sale to customers. At this stage, it is crucial that the production process is easily scalable to accommodate growing sales.

## 8.1. Prototype Manufacturing

This section describes the manufacturing process for the PenteFoil prototype. The prototype does not need to comply with the final design specifications exactly. It does not have to be foldable or meet weight requirements. Instead, it will use different materials, prioritizing speed and cost-efficiency. Multiple designs will likely be created to iterate the concept.

The structure of the PenteFoil is very similar to wingfoils or surfing kites, so a similar manufacturing approach can be taken. Many online tutorials exist on how to make wingfoils[56] and surfing kites[57,58]. These tutorials will guide the prototype manufacturing approach and can be used as a reference in the future.

### 8.1.1. Material Selection and Cutting

All fabric elements will be made of Spinnaker 60D[59] fabric, chosen for its low cost and accessibility. It is significantly heavier than the materials used in the final design, but can be used as weight is not critical for the prototype. The additional thickness ensures adequate strength, despite the lower performance compared to the fabrics used in the final design.

The bladder will be made from 0.1 mm LDPE[60], which is heavier and weaker than the final design's TPU. However, the additional thickness provides enough strength to the bladder and makes the material easier to work with. Unlike TPU, LDPE is widely accessible in online stores withing the EU.

Using the existing 3D models, flat patterns for cutting will be created with ExactFlat[61] software. Full-scale patterns will be printed on paper and transferred to the fabric with a marker. The fabrics can then be cut using a soldering iron[62], shown in Figure 8.1, which prevents frayed edges.

### 8.1.2. Stitching and Welding

**Figure 8.1:** Velleman VTSS4N 48Watt Soldering Station[64].


**Figure 8.2:** Singer Promise F1412 - Sewing machine[65].

The fabric elements will be stitched together using a Singer F1412 sewing machine[57], see Figure 8.2. This model can create various stitching patterns. The different patterns can be tested and the one with the highest

[56] https://www.youtube.com/watch?app=desktop&v=T5P0ObTBHEk, Accessed on 17/06/2024.
[57] https://shane.engineer/blog/diy-kiteboard-kite, Accessed on 17/06/2024.
[58] https://www.youtube.com/watch?v=qmE7jIoHlW0, Accessed on 17/06/2024.
[59] https://www.metropolis-drachen.de/Baumaterial/Tuch/Spinnakertuecher/Spinnaker-60D.html, Accessed on 17/06/2024.
[60] https://jipsnel.nl/ldpe-folie-150cm-x-100mt-100-micron, Accessed on 17/06/2024
[61] https://www.exactflat.com/, Accessed on 17/06/2024.

seam efficiency selected.

As can be seen in Figure 4.14 each inflatable tube will be stitched to a web on the top and bottom. One of the stitches can be easily made with the fabrics open, but the second stitch is not accessible. Therefore, half of the stitches will be made on the outside of the tube. The top and bottom stitches are shown in red in Figure 8.3.

Nylon fabrics are very slippery which can make stitching very difficult. To avoid misalignment the fabric will be taped in place. One final consideration for stitching is the web's fibre direction. The webs need to transfer shear, and properties of fabrics are largely dependent on the fibre direction. Placing fibres diagonally, as shown in Figure 8.4, will prevent the fibres from slipping with respect to each other.

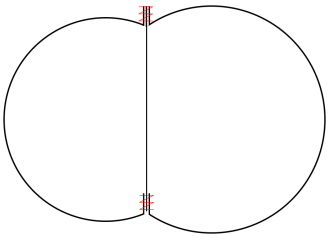

**Figure 8.3:** Stitching of the shear web and tubes, internal stitch (bottom) and external stitch (top).

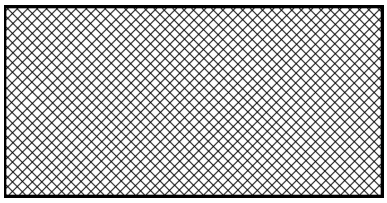

**Figure 8.4:** Fibre orientation in the shear web fabric.

Welding of the bladder is much simpler. Long straight seams can be made with an impulse sealer[64], see Figure 8.6. For more precise connections (in corners etc.) a soldering iron[62], set to a low temperature, can be used.

### 8.1.3. Structural Elements

For compressive elements GRP tubes were selected, which are significantly cheaper than CFRP used in the final design. To account for the lower material properties 10x6.35 mm tubes[65] will be used, as opposed to 6x4 mm in the final design. For ease of manufacturing 2 m tubes can be bought, minimising the necessary number of connections.

The tensile elements will be made with 2 mm Dyneema lines, same as the final design. They will be stitched into the webs, and attached to the ends of compressive tubes. This is shown in Figure 4.15. All control and attachment lines will also use 2mm Dyneema for simplicity.

The trapezium will be made from aluminum tubing. As the prototype does not need to be foldable, tubes longer than 1m can be used. This will minimise the amount of cutting and necessary connections. The tubes will be connected using bolted fittings[66], shown in Figure 8.5.

**Figure 8.5:** Customised aluminum tube fittings[38].

**Figure 8.6:** 30cm impluse sealing machine[36].

The manufacturing of structural elements does not require any specialised tooling or equipment. Cutting and finishing can be done with hand tools. The use of fittings removes the need for welding aluminium.

[62] https://www.soldeerbout-shop.nl/soldeerstations/7-velleman-vtss4n-48watt-soldeerstation-5410329442477.html, Accessed on 17/06/2024.

[63] https://www.bol.com/nl/nl/p/singer-promise-f1412-naaimachine/9200000040273087/, Accessed on 17/06/2024.

[64] https://www.bol.com/nl/nl/p/seal-apparaat-30cm-sealmachine-folie-lasser/9200000103115440/, Accessed on 17/06/2024.

[65] https://carbonfibreprofiles.com/products/2m-grp-tubes?variant=40367673147428, Accessed on 18/06/2024.

[66] https://www.chinabalustrade.com/products/Pipe-Fitting-Customized-Aluminum-Welded-Tube-Connectors-in-3-ways.html, Accessed on 18/06/2024.

### 8.1.4. Additional Equipment

For the pilot attachment, a hang glider pod harness will be utilised. Some modifications may be needed as the human is closer to the wing than in a typical hang glider. This can be explored in more detail once a specific pod is selected.

The required safety equipment will be largely dependant on the types of tests the prototype will be used for. All of the equipment will be bought off the shelf, and does not need in house manufacturing.

### 8.1.5. System Integration

With all the individual elements manufactured, the full system has to be assembled. Firstly, sleeves will be made for the aluminium frame to slide into and stitched to the tubes, this is shown in Figure 8.7.

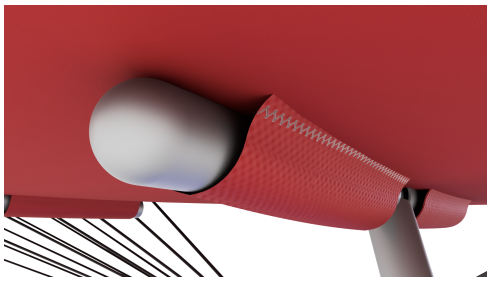

**Figure 8.7:** Sleeve attachment of the aluminum frame to the wing structure.

**Figure 8.8:** PenteFoil side-view, showing pod attachment and tip folding lines.

Secondly, the pod attachment and tip folding ropes (see Figure 8.8) have to be integrated into the webs. The connection method is shown in Figure 4.20. Stitching of the attachment points needs high precision and will be done by hand. Finally, the trailing edge cable needs to be sewn into the fabric, making use of the sewing machine, and properly tensioned.

### 8.1.6. Cost and Time Estimation

This subsection provides an initial estimate of the cost and time required to produce the first PenteFoil prototype. Given the lack of prior experience in manufacturing a structure like this, these estimates are preliminary. More accurate estimates, for design iterations, will be possible after constructing the first prototype.

**Table 8.1:** Initial Prototyping Material Costs.

| Item | Tot. Required for One Prototype | Mistake Allowance | Order Size | Price per piece/meter | Total Cost | Fraction |
|---|---|---|---|---|---|---|
| LDPE 150cmx100m | 47.77 $m^2$ | 3x | 1 | € 177.91 | € 177.91 | 9.0% |
| Spinnaker ”60D” 150cm | 64.42 $m^2$ | 3x | 130 m | € 4.90/m | € 637.00 | 32.1% |
| 10x6.35 2m GRP | 24.00 m | 1.5x | 18 | € 6.92 | € 124.56 | 6.3% |
| 2mm Dyneema Rope | 60.00 m | 2x | 120 m | € 0.44/m | € 52.80 | 2.7% |
| Paragliding Pod | 1 | - | 1 | € 250.00 | € 250.00 | 12.6% |
| 30x27 3m Al6060T6 tubes | 5.00 m | 1.5x | 3 | € 16.37 | € 147.33 | 7.4% |
| Miscellaneous | - | - | - | - | € 595.54 | 30.0% |
| **Total** | - | - | - | - | **€ 1,985.14** | **100.0%** |

The initial prototype is expected to be challenging to build, particularly due to the precision required for stitching. To account for potential mistakes, extra material will be purchased. For fabrics and bladders, a 3x allowance is included as these are the most difficult to work with. Dyneema rope will have a 2x allowance due to the need

for multiple attachment and control line versions. For aluminum and GRP tubes, a 1.5x allowance is used, as these elements only need to be connected together, reducing the likelihood of mistakes.

A pre-owned hang gliding Pod will be purchased to save money. Based on review of current offers on eBay[67], a preliminary budget of €250 was assigned to it. Additionally, 30% of the total material cost is added for miscellaneous items, including valves, stitching thread, fittings, connectors, etc. The costs for all materials are summed up in Table 8.1.

Table 8.2 shows the estimated tool costs for the prototype. Prices were sourced from the footnotes included in the previous subsection at the time of writing. An additional budget of €250 was included for hand tools and other items not considered in the manufacturing plan.

The total estimated cost for the first prototype is €2,425, which is very reasonable for such a complex system.

**Table 8.2:** Initial Prototyping Tool Costs.

| Tool | Price |
|---|---|
| Soldering Iron | € 20.00 |
| Sewing Machine | € 144.95 |
| Impulse Sealer | € 24.95 |
| Hand tools & Miscellaneous | € 250.00 |
| **Total** | **€ 439.90** |

Given the lack of prior experience in manufacturing these types of structures, time estimates are not highly accurate. Therefore, expert advice was used. Joep Breuer was consulted regarding his experience manufacturing an 11 $m^2$ Tensairity kite, as mentioned in Section 4.1. Creating the kite prototype took him 12 weeks. The PenteFoil structure is significantly more complex, but four people can work on it instead of one. Because of this, it is estimated to take between 8 and 12 weeks.

## 8.2. Full-scale Production

The production of the final product will not be done in house. A manufacturer with relevant experience will be selected. Because of the many similarities of the design hang glider or kite surfing manufacturers should be considered. The manufacturers should have experience and facilities for working with all types of materials used in the PenteFoil, in particular composites and Dyneema which can be challenging to work with.

One a specific manufacturer is selected, suppliers for all parts and materials should be reevaluated. Finding suppliers close to the production facility can significantly reduce lead times, cost, and environmental impact. Ordering materials in large quantities can further reduce costs.

Once suppliers and manufacturers are chosen, detailed production plans and technical drawings will be developed and provided to them. These plans are yet to be created and will be essential for the final iteration of the design.

[67] `https://www.ebay.com/`, Accessed on 18/06/2024.

# 9 | Verification & Validation

To make sure that the system complies with the requirements and can properly fulfill its intended mission the verification & validation plan was created. The verification & validation shall begin with subsystem and preflight tests, in Section 9.1 these tests are further described. After the preflight tests, the flight tests can be started, which is detailed in Section 9.2. As this project unfortunately only focuses on the design of the PenteFoil the verification and validation will need to be performed later in the design process.

## 9.1. Preflight Verification & Validation

Preflight all the subsystems and the complete system should be tested individually first. This is done to find inaccuracies in the subsystems and integration and improve them before the first flight tests. Furthermore, preflight testing will focus more on the subsystem so that the subsystems can be tested in more detail. This section will describe the proposed preflight tests that should be used to ensure the system is thoroughly tested before the first flight test. With a literature study, Inspection testing, Computer model testing, Wind tunnel testing, structure testing, environmental testing and potential user testing the subsystems and the integration of the subsystem will be properly tested for their compliance with the requirements before the first flight tests of the integrated system will be performed.

### 9.1.1. Literature Study

First of all, a small literature study has to be conducted. This will be done by asking questions to people working at test facilities and gathering information from the internet. With this literature study requirements like: 'Can be manufactured with currently available techniques' and 'Can be manufactured with currently available materials' and other requirements that need analysis of a subsystem without needing a model for calculations (like the cost of a single product) will be verified.

### 9.1.2. Inspection Testing

The verification and validation also make use of an inspection test. An inspection test is to verify that the requirement is met by looking at the system. For instance, looking at whether the volume of the system folded up is below 75 litres. In this way, a few requirements like the volume of the folded-up system, the weight and the connection method to the wing can be tested. Since specific requirements were set on the volume, weight and connection method of the system.

### 9.1.3. Computer Model Testing

For model testing, a computer model is created and simulations are run to estimate aerodynamic performance and analyse stability and controllability of the wing. It is crucial to first verify and validate the model before using it to ensure accurate results. To do this, unit tests should be conducted first to check each part of the code individually. Then, test the integrated model with known inputs and outputs to confirm it produces the expected results. Extreme value tests can further validate the model. Once verified and validated, the model produces accurate and useful results that will then be used for testing the aerodynamic performance of the PenteFoil. Tests with different speeds and angles of attack will show the aerodynamic performance of the PenteFoil and ensure compliance with the requirements set on performance. The costs associated with running these simulations are negligible, as the software utilised (*XFLR5*) is open-source. Furthermore, the software is relatively straightforward to comprehend and execute, and it is readily accessible as long as you have an operational computer or laptop. This simulation provides a first-order estimate and is not perfectly accurate. However, since the costs are low it is perfect to use it for the preliminary design of the model. More accurate results will be obtained from a wind tunnel test.

### 9.1.4. Wind Tunnel testing

Wind tunnel testing will continue on the back of computer model testing looking at the aerodynamic performance of the PenteFoil. The wind tunnel test will provide accurate results on aerodynamic performance like lift, drag and aerodynamic coefficients. However, it can also give a better indication of the pressures along the wing and stall properties of the wing. Furthermore, tests can be done to see the influence of the folding wingtips on the aerodynamic performance. The wind tunnel test will be important to ensure the stability and controllability of the PenteFoil, making sure that the wing is agile while being safe at the same time.

### 9.1.5. Structure Testing
A structure test will verify the strength and durability of the structure. The Tensairity tubes will be put into a test bench to test for their ultimate strength, by applying an increasing load to the structure until the structure fails. This will demonstrate what loads the structure can handle and what manoeuvres can be performed without exceeding this ultimate limit. The Tensairity tubes must also be tested on whether they are durable enough. A fatigue test. To do this the Tensairity tubes should be put into another test bench where the structure is loaded and unloaded with expected flight loads gotten from the computer model or wind tunnel test. This will be done until the structure fails. With that, an indication can be made for how many flight cycles or flight hours the Tensairity tubes can sustain without maintenance. It is important to know how many flights the PenteFoil can fly before the structure should be checked for maintenance to ensure structural safety.

### 9.1.6. Environmental Testing
The structure and skin should also be tested on whether they can withstand the different types of environmental exposure the PenteFoil will encounter. First of all, the system performance should be tested in different conditions to make sure the material can perform in both hot and cold temperatures and that the structure does not fail because of quick changing temperatures. Furthermore, the wing should be tested to withstand UV exposure which causes degradation over time and could influence performance. The wing should also be tested for abrasion, due to the outdoor nature of operating the PenteFoil, it could be susceptible to abrasion. It should be tested that the structure of the PenteFoil remains strong enough even with some wear and tear.

### 9.1.7. Potential User Testing
Finally, for the subsystem tests, there will be a test to check the comfortability of the harness and the ease of controlling the PenteFoil. For This test, potential users will provide feedback on the comfortability of the harness and the ease of the controls. To do this, potential users will be put into the harness to rate their comfort. The ease of controllability will also be tested in this harness by recreating the controls in this test setup so that the user can get a feel for the controls. In this way the potential users get an idea of what the system is going to be like and valuable feedback will be gotten on controllability and comfortability.

## 9.2. Flight Verification & Validation
After the preflight verification and validation are complete, the full integrated flight tests can begin. This is done to find any issues resulting from the integration of the subsystems during flight. This section will describe the flight tests that need to be done before the PenteFoil can be sold on the international market. With parafoiling testing, take-off and landing testing and finally certification testing.

### 9.2.1. ParaFoiling Testing
The flight testing procedure for the PenteFoil also involves a method inspired by the sport of parasailing. For this test, a Cherokee 30 boat equipped with a deck will be rented for €700,- per day (excl. propellant)[68]. The test pilot will securely attach the PenteFoil to themselves using a harness as described in Section 5.2. A rope, connected to a winch system on the boat, will also be attached to the pilot's harness. For take-off, the boat accelerates to build up speed. As the PenteFoil begins to generate lift, the winch gradually releases the rope, allowing the PenteFoil to ascend smoothly and gain altitude.

The testing method offers a valuable opportunity to observe the PenteFoil's responsiveness to user inputs. By equipping the user with an accelerometer on their chest and integrating force gauges into the control lines, data can be collected on the position and acceleration responses of the PenteFoil due to forces exerted. The IAM-20680 from TDK will be used as an accelerometer, which is a high-performance 6-axis MotionTracking device that combines a 3-axis gyroscope and a 3-axis accelerometer. For the strain gauges the Tractel Handifor will be placed in between each control line to measure the real-time forces applied on the control lines by the user. The specifications of the measurement hardware is given in Table 9.1 and Table 9.2.

**Table 9.1:** Specifications TDK IAM-20680[69].

| | **TDK IAM-20680** | |
|---|---|---|
| Weight | 0.14 | g |
| Price | 20.41 | € |
| Measuring accuracy | $\pm 2$ | % |

**Table 9.2:** Specifications Tractel Handifor[70].

| | **Tractel Handifor** | |
|---|---|---|
| Weight | 500 | g |
| Price | 248.05 | € |
| Measuring accuracy | $\pm 0.5$ | % |

[68] https://www.commercialtowables.com/product/592/products-watersports-boats-parasailing-boats-cherokee-30-, Accessed on 04/06/2024.

This setup collects real-time data of the response of the PenteFoil in user input. The data is used to calculate the stability and aerodynamic coefficients of the PenteFoil like $C_l, C_d, C_{m_\alpha}$. These coefficients can be used to verify the accuracy of the computer simulations and verify if the PenteFoil complies with the requirements specified in Section 3.1.

### 9.2.2. Take-off and Landing Testing

The 'parafoil' tests cannot accurately simulate the take-off and landing procedures, necessitating real flight tests. For these tests, experienced pilots equipped with additional joint safety gear will run down a hill to take off and land in a controlled way. Dunes are the preferred testing environment because they minimise the potential damage from a fall, ensuring a safer landing. A testing site could be 'The Big Daddy' dune in Sossusvlei, Namibia. In this area, wind speeds of 30 km/h are common[71], allowing for initial tests at a ground speed of 45 km/h in trim condition. With a height of 325 meters, the dune enables the test pilot to perform low-altitude flights with a sand landing area, which makes landings softer in case of a hard touchdown.

### 9.2.3. Certification Testing

When these full system flight tests are performed the system can also be certified by showing its compliance with all the regulations set for the PenteFoil. This is the last step before the PenteFoil can be sold to users. So it is important to safely show that the PenteFoil can fulfill its mission and meet the set requirements for aerial sports by performing the certification tests.

After all this extensive testing is passed, great confidence can be had in the system. And finally, the real first flight can be performed.

### 9.2.4. Red Bull Flugtag

The Red Bull Flugtag offers an ideal platform to test the PenteFoil prototype in a real-world scenario. In this event, participants pilot homemade, human-powered flying machines from an elevated platform into water, allowing for practical evaluation of flight performance. The event will reveal the prototype's strengths and weaknesses, enabling necessary refinements.

**Figure 9.1:** Red Bull Flugtag event where participants design, build, and pilot homemade, human-powered flying machines off a platform into a body of water[72].

Moreover, the Red Bull Flugtag is a widely recognised event with significant media coverage and large audiences. Showcasing the PenteFoil at this event can enhance brand image by associating it with creativity and innovation. Successful participation can validate the PenteFoil, potentially attracting investors and early adopters.

The audience and judges expect ready-to-fly machines. Starting with a deflated wing and inflating it on the platform can surprise and engage the audience, demonstrating the wing's quick deployment—a key selling point. This approach can increase social media visibility, providing viral marketing opportunities. The live

[69] https://docs.rs-online.com/f36c/A700000007834651.pdf, Accessed on 05/06/2024

[70] https://www.tractel.com/en/product/handifor-digital-weigher/5811, Accessed on 05/06/2024

[71] https://www.meteoblue.com/en/weather/historyclimate/climatemodelled/sossusvlei_namibia_3353011, Accessed on 04/06/2024.

[72] https://kickstartsidehustle.com/red-bull-flugtag-how-red-bull-went-from-0-to-200k-attendees-on-an-event-nobody-heard-of/ ,accessedon19.06.2024.

demonstration highlights the wing's practicality, ease of transportation, rapid deployment, and versatility, setting the PenteFoil apart from traditional fixed-wing designs.

# 10 | Requirements Compliance & Feasibility

This chapter aims to look back at the requirements established in the baseline phase, and evaluate whether these have been met or not. If any requirements have not been met, the reasons for this, or the necessary modifications to fulfill the requirements, are discussed in the feasibility analysis.

## 10.1. Stakeholder Requirements

**Table 10.1:** Stakeholder Requirements.

| Identifier | Requirement | Method | Status |
|---|---|---|---|
| **REQ-STK-01** | The project shall be completed with the available resources. | Inspection | ✓ |
| **REQ-STK-02-1** | The system shall have safety on par with parapente. | Analysis | Pending |
| **REQ-STK-02-2** | The system shall provide an enjoyable experience according to potential users. | Test | Pending |
| REQ-STK-02-2-1 | The user shall have a direct feeling of connection to the product. | Test | Pending |
| REQ-STK-02-2-3 | The system shall be cool according to at least 80% of potential users. | Test | Pending |
| REQ-STK-02-2-4 | Using the product shall not cause excessive discomfort according to at least 99% of potential users. | Test | Pending |
| **REQ-STK-02-3** | The cost of a single product excluding maintenance and operations shall be below 10K euros. | Analysis | ✓ |
| **REQ-STK-02-4** | The system shall be easy to use according to at least 80% of potential users. | Test | Pending |
| REQ-STK-02-4-1 | The product shall be initialised within 30 minutes on average by trained users. | Demonstration | Pending |
| REQ-STK-02-4-2 | The product shall be easily terminated within 30 minutes on average by trained users. | Demonstration | Pending |
| REQ-STK-02-4-3 | The product shall be easy to learn within 20 hours of training on average for potential users. | Test | Pending |
| REQ-STK-02-4-4 | The product shall be easily controllable according to at least 90% of trained users. | Test | Pending |
| REQ-STK-02-4-5 | The product shall be able to operate in mountainous environments. | Analysis, Test | Pending |
| **REQ-STK-02-5** | The system shall be easily transportable for potential users. | Test | Pending |
| REQ-STK-02-5-1 | The system shall be easily transportable for at least 80% of potential users when walking up a mountain. | Test | Pending |
| REQ-STK-02-5-2 | The system shall fit in ski lifts together with a person. | Demonstration | Pending |

**see next page**

**Table 10.1 – Continued**

| Identifier | Requirement | Method | Status |
|---|---|---|---|
| **REQ-STK-02-6** | The system shall be able to carry the user's weight during flight. | Analysis, Test | Shown by analysis |
| **REQ-STK-03** | The system shall be made sustainably according to the sustainability officer. | Analysis | ✓ |
| **REQ-STK-04** | The system shall be manufacturable. | Analysis | ✓ |
| **REQ-STK-05** | The product shall be compliant with the relevant EASA and FAA safety regulations. | Analysis | Pending |

## 10.2. Mission Requirements

**Table 10.2:** Mission Requirements.

| Identifier | Requirement | Method | Status |
|---|---|---|---|
| **REQ-MIS-01-1** | The system shall allow for a safe landing at least 99.9% of the time. | Testing | Pending |
| REQ-MIS-01-1-1 | The system shall be able to provide a sink rate of no more than 5 m/s for the landing procedure. | Analysis | ✓ |
| REQ-MIS-01-1-2 | The system shall be able to provide a horizontal speed of no more than 8.5 m/s for the landing procedure. | Analysis | ✓ |
| REQ-MIS-01-1-3 | The system shall not harm the user during landing in at least 99.9% of the attempts. | Analysis | Pending |
| **REQ-MIS-01-2** | The system shall have stability and controllability during flight on par with paragliders. | Analysis | ✓ |
| REQ-MIS-01-2-1 | The system shall have longitudinal static stability. | Analysis | ✓ |
| REQ-MIS-01-2-2 | The system shall provide yaw control on par with paragliders. | Analysis | No yaw control |
| REQ-MIS-01-2-3 | The system shall provide roll control on par with paragliders. | Analysis | ✓ |
| REQ-MIS-01-2-4 | The system shall provide pitch control on par with paragliders. | Analysis | ✓ |
| **REQ-MIS-01-3** | The system shall include an adequate emergency response procedure according to at least 99.9% of potential users. | Test | Pending |
| REQ-MIS-01-3-1 | The system shall allow for the engagement of an emergency parachute within 5 seconds. | Demonstration | Pending |
| REQ-MIS-01-3-2 | The emergency system shall allow the user to descend to the ground uninjured in at least 99.9% of the attempts. | Analysis | Pending |
| **REQ-MIS-01-4** | The system shall have safety in case of unfavourable weather conditions on par with paragliders. | Analysis | Pending |
| REQ-MIS-01-4-1 | The system shall be able to sustain gusts of at least 30 km/h without catastrophic failure. | Test | Pending |
| REQ-MIS-01-4-2 | The emergency landing procedure shall be able to be initiated in case of a sudden change in weather conditions in at least 99.9% of the attempts. | Test | Pending |
| **REQ-MIS-01-5** | The system shall be able to carry the weight of at least 80% of potential users during flight. | Analysis | Pending |

**see next page**

**Table 10.2** – Continued

| Identifier | Requirement | Method | Status |
|---|---|---|---|
| REQ-MIS-01-5-1 | The system shall produce enough lift to balance the weight of at least 80% of potential users. | Test | Pending |
| REQ-MIS-01-5-2 | The system shall support the weight of at least 80% of users without deflecting more than 10% of the wingspan at the wing tips. | Test | Pending |
| **REQ-MIS-02-1** | The system shall provide satisfying velocity performance according to at least 80% of potential users. | Test | Pending |
| REQ-MIS-02-1-1 | The system shall be able to reach an acceleration of 5 $m/s^2$. | Demonstration | Pending |
| REQ-MIS-02-1-2 | The system shall have a sink rate of maximum 1.5 m/s at trim conditions. | Demonstration | Shown by analysis |
| REQ-MIS-02-1-3 | The system shall have a trim speed of 75 km/h below 3000 m. | Demonstration | Pending |
| REQ-MIS-02-1-4 | The system shall have a top speed of at least 120 km/h below 3000 m. | Demonstration | Pending |
| **REQ-MIS-02-2** | The system shall have adequate agility according to at least 80% of trained users. | Test | Pending |
| REQ-MIS-02-2-1 | The system shall have a roll rate of at least 1 rad/s. | Demonstration | Pending |
| REQ-MIS-02-2-2 | The system shall provide a turn rate of 20 seconds to complete a 360-degree turn. | Demonstration | Pending |
| **REQ-MIS-02-3** | The system shall provide a comfortable experience according to at least 95% of potential users. | Test | Pending |
| REQ-MIS-02-3-1 | A typical flight shall not cause excessive muscle strain according to at least 95% of potential users. | Test | Pending |
| REQ-MIS-02-3-2 | The attachment of the system to the user shall not cause excessive discomfort according to at least 95% of potential users. | Test | Pending |
| **REQ-MIS-02-4** | The system shall give a feeling of direct connection to the wing according to at least 85% of trained users. | Test | Not satisfied |
| REQ-MIS-02-4-1 | The user shall be directly connected to the structure. | Inspection | 0.55 m suspended |
| REQ-MIS-02-4-2 | The user shall not be suspended on wires. | Inspection | 0.55 m suspended |
| **REQ-MIS-03-1** | The system shall be simple according to at least 85% of potential users. | Test | Pending |
| REQ-MIS-03-1-1 | The mechanism shall be understandable within 20 hours by at least 90% of potential users. | Test | Pending |
| REQ-MIS-03-1-2 | Operating the system shall not require specialised technical knowledge. | Test | Pending |
| **REQ-MIS-03-2** | The system shall be transportable to the flight locations by at least 75% of potential users. | Demonstration | Pending |
| REQ-MIS-03-2-1 | The product shall have a maximum weight of 25 kg. | Inspection | Shown by analysis |
| REQ-MIS-03-2-2 | The folded-up system shall have a maximum volume of 75 litres. | Inspection | Pending |
| REQ-MIS-03-2-3 | The folded-up system shall be able to be carried on the back of at least 75% of potential users. | Test | Pending |
| **REQ-MIS-03-3** | The system shall be easily initialised by trained users. | Test | Pending |
| REQ-MIS-03-3-1 | The system shall not take more than 30 minutes to initialise in 80% of attempts by trained users. | Test | Pending |

**see next page**

**Table 10.2** – Continued

| Identifier | Requirement | Method | Status |
|---|---|---|---|
| REQ-MIS-03-3-2 | The initialisation of the system shall not require any mechanical joints. | Analysis | ✓ |
| REQ-MIS-03-3-3 | The system shall not take more than 20 minutes to terminate in 80% of attempts by trained users. | Test | Pending |
| **REQ-MIS-03-4** | The system shall have intuitive controls. | Test | ✓ |
| REQ-MIS-03-4-1 | The system control system shall give direct feedback to the user. | Demonstration | ✓ |
| REQ-MIS-03-4-2 | The system shall be controllable with the movement of the user's body. | Demonstration | ✓ |
| **REQ-MIS-03-5** | The system shall be able to take off in various take-off environments. | Demonstration | Pending |
| REQ-MIS-03-5-1 | The system shall be capable of taking off by running down from a dune. | Demonstration | Pending |
| REQ-MIS-03-5-2 | The system shall be capable of taking off by jumping from a mountain. | Demonstration | Pending |
| **REQ-MIS-04-1** | The preliminary design shall be created with the available resources. | Inspection | ✓ |
| REQ-MIS-04-1-1 | The design shall be performed using facilities available at the TU Delft. | Inspection | ✓ |
| REQ-MIS-04-1-2 | The preliminary design shall be created within the time of DSE. | Inspection | ✓ |
| **REQ-MIS-04-2** | The system shall be manufacturable. | Analysis | ✓ |
| REQ-MIS-04-2-1 | The system shall be manufacturable with currently available materials. | Analysis | ✓ |
| REQ-MIS-04-2-2 | The system shall be manufacturable with currently available techniques. | Analysis | ✓ |
| **REQ-MIS-04-3** | The system shall be sustainable. | Test | Pending |
| REQ-MIS-04-3-1 | The system shall be made of at least 60% recyclable materials by mass. | Analysis | ✓ |
| REQ-MIS-04-3-2 | The system shall be made of at least 20% recycled materials by mass. | Analysis | Pending |
| REQ-MIS-04-3-3 | The system shall be sustainable according to 80% of the group members. | Test | ✓ |
| **REQ-MIS-04-4** | The product shall be compliant with the relevant EASA and FAA safety regulations. | Analysis | Pending |
| **REQ-MIS-04-5** | The cost of a single product excluding maintenance and operations shall be below 10K euros. | Analysis | ✓ |

## 10.3. Subsystem Requirements

**Table 10.3:** Subsystem Requirements.

| Identifier | Requirement | Method | Status |
|---|---|---|---|
| **REQ-SYS-01-1-1** | The system shall provide lift sufficient for stable flight at the trim speed. | Analysis | ✓ |

**see next page**

**Table 10.3** – Continued

| Identifier | Requirement | Method | Status |
|---|---|---|---|
| REQ-SYS-01-1-1-1 | The system shall have a L/D of 7 or more at trim conditions. | Analysis | ✓ |
| REQ-SYS-01-1-1-2 | The lift provided by the system shall be equal to or higher than the weight of the system. | Analysis | ✓ |
| **REQ-SYS-01-1-2** | The system shall provide satisfying velocity performance according to at least 80% of trained users. | Test | Pending |
| REQ-SYS-01-1-2-1 | The system shall have a maximum sink rate of 1.5 m/s at trim conditions. | Demonstration | Shown by analysis |
| REQ-SYS-01-1-2-2 | The system shall have a trim speed of 75 km/h below 3000 m. | Demonstration | Pending |
| REQ-SYS-01-1-2-3 | The system shall have a top speed of at least 120 km/h below 3000 m. | Demonstration | Pending |
| **REQ-SYS-01-1-3** | The system shall have high agility according to at least 80% of users. | Test | Pending |
| REQ-SYS-01-1-3-1 | The system shall provide a turn rate of 20 seconds to complete a 360-degree turn. | Demonstration | Pending |
| REQ-SYS-01-1-3-2 | The system shall have a roll rate of at least 1 rad/s. | Demonstration | Pending |
| **REQ-SYS-01-2-1** | The system shall be controllable. | Demonstration | Pending |
| REQ-SYS-01-2-1-1 | The system shall provide the possibility of changing yaw with the input of the user. | Demonstration | No yaw control |
| REQ-SYS-01-2-1-2 | The system shall provide the possibility of changing roll with the input of the user. | Demonstration | Shown by analysis |
| REQ-SYS-01-2-1-3 | The system shall provide the possibility of changing pitch with the input of the user. | Demonstration | Shown by analysis |
| REQ-SYS-01-2-1-4 | The control mechanisms should be simple enough to be learned within 20 hours by 90% of potential users. | Test | Pending |
| REQ-SYS-01-2-1-5 | The control mechanisms should be understandable without prior technical knowledge by at least 90% of potential users. | Test | Pending |
| REQ-SYS-01-2-1-6 | The system control system shall give force feedback to the user. | Demonstration | Shown by analysis |
| REQ-SYS-01-2-1-7 | The system shall be controllable with the movement of the user's body. | Demonstration | Shown by analysis |
| **REQ-SYS-01-2-2** | The system shall have stability on par with paragliders. | Analysis | Pending |
| REQ-SYS-01-2-2-1 | The system shall exhibit stable pitching behaviour, returning to its trimmed angle of attack after disturbances ($C_{m_\alpha} < 0$). | Analysis | ✓ |
| REQ-SYS-01-2-2-2 | The system shall remain stable while experiencing gust speeds of up to 7.5 m/s at the trim speed. | Analysis | Pending |
| **REQ-SYS-01-3** | The system shall include an emergency landing protocol. | Inspection | |
| REQ-SYS-01-3-1 | The system shall allow for the engagement of an emergency parachute within 5 seconds of a decision to engage it. | Demonstration | Pending |

**see next page**

**Table 10.3** – Continued

| Identifier | Requirement | Method | Status |
|---|---|---|---|
| REQ-SYS-01-3-2 | The emergency system shall allow the user to get to the ground safely in at least 99% of the deployments. | Analysis | Pending |
| REQ-SYS-01-3-3 | The system shall have safety on par with paragliders in case of unfavourable weather conditions. | Analysis | Pending |
| REQ-SYS-01-3-4 | The system shall include a helmet. | Inspection | ✓ |
| **REQ-SYS-01-4-1** | The structure shall transfer operational loads. | Analysis | ✓ |
| REQ-SYS-01-4-1-1 | The structure shall transfer lifting loads without catastrophic failure. | Analysis | ✓ |
| REQ-SYS-01-4-1-2 | The structure shall transfer control loads without catastrophic failure. | Analysis | ✓ |
| **REQ-SYS-01-4-2** | The structure shall provide sufficient strength and stiffness. | Analysis | ✓ |
| REQ-SYS-01-4-2-1 | The structure shall deflect less than 10 % of the wingspan length during flight. | Analysis | ✓ |
| REQ-SYS-01-4-2-2 | The structure shall survive the user load during operation without catastrophic failure. | Analysis | ✓ |
| REQ-SYS-01-4-2-3 | The structure shall survive gust loads during flight without failing. | Analysis | ✓ |
| **REQ-SYS-01-4-3** | The structure shall be connected to the user. | Inspection | ✓ |
| REQ-SYS-01-4-3-1 | The structure shall provide a direct attachment of the user to the wing. | Inspection | 0.55 m suspended |
| REQ-SYS-01-4-3-2 | The structure shall attach to the users torso. | Inspection | ✓ |
| REQ-SYS-01-4-3-3 | The attachment system of the structure shall not cause discomfort according to at least 95% of potential users. | Test | Pending |
| **REQ-SYS-01-5-1** | The system shall be able to take off from the flight location. | Demonstration | Pending |
| REQ-SYS-01-5-1-1 | The system shall be able to take off at an airspeed of at most 13 m/s. | Demonstration | Shown by analysis |
| REQ-SYS-01-5-1-2 | The system shall be capable of taking off by running down from a dune. | Demonstration | Pending |
| REQ-SYS-01-5-1-3 | The system shall be capable of taking off by jumping from a mountain. | Demonstration | Pending |
| REQ-SYS-01-5-2 | The system shall be able to be landed safely in at least 99.9% of attempts. | Analysis | Pending |
| REQ-SYS-01-5-2-1 | The sink rate during landing shall be at most 5 m/s. | Analysis | Pending |
| REQ-SYS-01-5-2-2 | The horizontal speed during landing shall be at most 8.5 m/s. | Demonstration | Pending |
| REQ-SYS-01-5-2-3 | The airspeed during landing shall be at most 11.5 m/s. | Demonstration | Pending |
| **REQ-SYS-01-5-3** | The system shall be able to be initialised by trained users. | Test | Pending |
| REQ-SYS-01-5-3-1 | The system initialisation shall not require any tools other than those included in the system. | Demonstration | ✓ |

**see next page**

**Table 10.3** – Continued

| Identifier | Requirement | Method | Status |
|---|---|---|---|
| REQ-SYS-01-5-3-2 | The system initialisation shall be completed with one person. | Test | Pending |
| REQ-SYS-01-5-3-3 | The system initialisation shall be completed in 30 minutes on average by trained users. | Test | Pending |
| **REQ-SYS-01-5-4** | The system shall be able to be terminated by trained users. | Test | Pending |
| REQ-SYS-01-5-4-1 | The system termination shall not require any tools other than those included in the system. | Demonstration | ✓ |
| REQ-SYS-01-5-4-2 | The system termination shall be completed with one person. | Test | Pending |
| REQ-SYS-01-5-4-3 | The system termination shall be completed in 20 minutes on average by trained users. | Test | Pending |
| **REQ-SYS-02-1** | The system shall be created with the available resources. | Analysis | ✓ |
| REQ-SYS-02-1-1 | The preliminary system design shall be completed in 50 working days. | Inspection | ✓ |
| REQ-SYS-02-1-2 | The preliminary system design shall be completed by 10 students. | Inspection | ✓ |
| REQ-SYS-02-1-3 | The preliminary system design shall be created using TU Delft facilities. | Inspection | ✓ |
| **REQ-SYS-02-2** | The system shall be manufacturable. | Analysis | ✓ |
| REQ-SYS-02-2-1 | The system shall be manufacturable with currently available materials. | Analysis | ✓ |
| REQ-SYS-02-2-2 | The system shall be manufacturable with currently available techniques. | Analysis | ✓ |
| **REQ-SYS-02-3** | The system shall be human-transportable by trained users. | Test | Pending |
| REQ-SYS-02-3-1 | The total system, including helmet and parachute shall weigh at most 25 kg. | Inspection | ✓ |
| REQ-SYS-02-3-2 | The folded-up system, including the parachute shall have a volume of at most 75 litres. | Inspection | Pending |
| REQ-SYS-02-3-3 | The folded-up system shall not be longer than 1 m in any dimension. | Inspection | Pending |
| **REQ-SYS-02-4** | The system shall be sustainable. | Test | |
| REQ-SYS-02-4-1 | The system shall be made of at least 60% recyclable materials by mass. | Analysis | ✓ |
| REQ-SYS-02-4-2 | The system shall be made of at least 20% recycled materials by mass. | Analysis | Pending |
| REQ-SYS-02-4-3 | The entire manufacturing process of the system shall generate greenhouse gases equivalent to at most 400 kg of CO2. | Analysis | Pending |
| REQ-SYS-02-4-4 | The system shall be compliant with relevant EU environmental regulations. | Analysis | Pending |
| REQ-SYS-02-4-5 | The system shall be sustainable according to at least 80% of the group members. | Test | ✓ |
| **REQ-SYS-02-5** | The system shall be compliant with relevant regulations. | Analysis | Pending |

**see next page**

**Table 10.3** – Continued

| Identifier | Requirement | Method | Status |
|---|---|---|---|
| REQ-SYS-02-5-1 | The system shall be compliant with the applicable sections of EASA CS-22 regulations. | Analysis | Pending |
| REQ-SYS-02-5-2 | The system shall be compliant with the applicable sections of FAA AC 23-19A regulations. | Analysis | Pending |
| REQ-SYS-02-5-3 | The system shall be compliant with applicable sections of EN 926-1 equipment standard regulations. | Analysis | Pending |
| REQ-SYS-02-5-4 | The system shall be compliant with applicable sections of EN 1651 regulations. | Analysis | Pending |
| **REQ-SYS-02-6** | The cost of a single product excluding maintenance and operations shall be below 10K euros. | Analysis | ✓ |

## 10.4. Feasibility Analysis

As can be seen in the requirement compliance matrices, not all requirements are met. Fortunately, however, most of these have an acceptable effect on the system performance. In this section, an explanation is given for why the design does not meet the specific requirement, or which modifications would be required in order to meet it.

Some requirements are marked as 'pending'. This means that, since no testing has taken place yet, these requirements should be verified at a later stage of design or during testing. Taking a look at the requirement compliance matrices, some requirements are marked as 'shown by analysis'. This essentially means that the verification (in the form of demonstration or testing) is still pending, but that analyses in this stage of the design have verified the requirement's feasibility.

From the mission requirements in Section 10.2, it can be seen that the yaw requirement (**REQ-MIS-01-2-2**) is not complied with. This, however, is not a design flaw, but rather due to an inherent quality of the system. As roll and yaw are coupled, no separate yaw control mechanism is required. Turns are realised purely by means of roll control. The same reasoning holds for **REQ-SYS-01-2-1** in Section 10.3.

Another group of requirements that has not been achieved contain **REQ-MIS-02-4** (**REQ-MIS-02-4-1** and **REQ-MIS-02-4-2**) in Section 10.2 and **REQ-SYS-01-4-3-1** in Section 10.3. These requirements state that the user shall be directly attached to the wing, and not by means of wires. As discussed in Section 7.4, landing without performing a C.G. shift was deemed infeasible earlier in the design process. This eliminated the option of direct attachment to the wing, as this would cause major complications for attachment and the landing procedure. This is a disadvantage to users, as it eliminates some of the feeling of a direct connection to the wing. A measure taken to minimise the effect it has on the flying experience is to suspend the pilot on a distance considerably shorter than conventional hang gliders. This distance is set at $0.55\,\mathrm{m}$, which is the required offset to perform a safe landing and realise control.

With this in mind, further research might investigate other possible landing methods to make a rigid wing-pilot attachment possible. Initially, a solution was proposed with which the pilot released a strap for landing, ending in a straight position. This was deemed infeasible due to the large sway and C.G. movement this would cause, resulting in a pitch up motion. During this motion, controlling the system would also be too challenging to realise. Therefore, for the user to be attached to the wing, a landing procedure would need to be designed with minimal sway and with the possibility of maintaining sufficient control over the system. Since the design is almost reaching its end, researching new landing methods is left as a recommendation for further research.

# 11 | Resource Allocations

This chapter reflects the team's approach towards resource allocation and provides contingencies where appropriate. It summarises the project by describing how time was allocated to different activities and presents the mass breakdown of the system. This chapter does not contain the volume and cost breakdown structure as the volume analysis was performed in Section 6.1, and the cost analysis was done with more detail and is documented separately in Chapter 14.

## 11.1. Time

Table 11.1 presents the breakdown and comparison of the initially allocated man-hours to each project phase and the actual realised work, expressed in man-hours. It shows that the effort for Conceptual Design was underestimated, taking up 8.3 percentage points more of the total time than planned. The team's restructuring and planning for the Detailed Design phase is reflected by the increase in project planning effort. This resulted in less time to complete the Detailed Design and close out the project, as the project time was limited to 3760 man-hours, equivalent to 10 people working 8-hour shifts for 47 workdays. Despite this, some project work was also done outside the scheduled sessions, bringing the total effort to 3800 man-hours.

**Table 11.1:** Target and Actual Time Allocation.

| Activity | Target [man-hours] | Target Fraction | Actual [man-hours] | Actual Fraction |
|---|---|---|---|---|
| Project Planning | 400 | 10.6% | 450 | 11.8% |
| Project Definition | 480 | 12.8% | 480 | 12.6% |
| Conceptual Design | 720 | 19.1% | 1040 | 27.4% |
| **Detailed Design** | **1820** | **48.4%** | **1590** | **41.8%** |
| Wing Design | 728 | 19.4% | 660 | 17.4% |
| Structural Design | 364 | 9.7% | 280 | 7.3% |
| Operations Design | 728 | 19.4% | 650 | 17.1% |
| Project Close-Out | 340 | 9.0% | 240 | 6.3% |
| **Total** | **3760** | **100.0%** | **3800** | **100.0%** |

## 11.2. Mass

The main limitation on the total mass budget is derived from requirement REQ-MIS-03-2-1, which states that the product's maximum mass is 25 kg. With this being an upper bound of the system's mass, during the Project Definition phase an approach of optimising allocation of well under 25 kg was implemented, with the sum of after-contingency values converging to the maximum mass.

The past approach for the mass budget allocation was as follows: The literature was studied for subsystems of functions and requirements similar to this project's, such as kites, inflatable wings, hang gliders and wingsuits. The values found in the study were used as a first estimate and were translated into the values more applicable to this project, based on factors like dimensions, materials as well as other requirements for the project. Furthermore, the level of uncertainty of subsystem detail specification and maturity of technologies was investigated, and based on this analysis the contingency margins were defined.

At the current stage of design there is enough detail known to accurately define the mass of each subsystem such that no contingency margin is required. The mass breakdown was updated and is compared to the initial plan in Table 11.2.

The main wing's mass was described in Subsection 4.4.4 and is estimated to be 8.40 kg. This includes everything that makes up the main wing, including the fabrics, stiff components, steering frame. It does not include the mass of cables with which the user is attached, as that is considered part of the attachment subsystem

The attachment subsystem consists of cocoon and attachment cables. The commercially available cocoons

weigh 3 kg, and the total length of the attachment cables made out of 2mm Dyneema is roughly 43 m, which translates to mass 0.2 kg. The attachment has a total mass of 3.4 kg.

The safety system consists of an emergency parachute, a helmet and the hook knife. Using commercially available Supair Shine parachute[73], we find its mass to be 1.25 kg. As it was described in Subsection 5.2.3, the mountain bike helmets are suitable for the PenteFoil. These, on average weigh 834 g [74] The hook knife's mass vary depending on the model, but is generally very small - for example the AirDesign Paragliding hook knife has a mass of 53 g[75].

The only supporting accessory that is to be taken into account in mass analysis is a hand pump to inflate the wing. The pump used for inflation proposed in Subsection 5.2.5 weighs 1.4 kg.

Analysing Table 11.2 reveals that the initial mass budget was accurate, with the total mass overestimated by only 0.87 kg. The final masses of the wing, attachments, and supporting accessories are all within their respective contingency margins. Incorporating high-tech commercially available safety elements enabled a nearly two-fold reduction in their mass.

**Table 11.2:** System Mass Breakdown.

| Subsystem | Target Mass [kg] | Contingency | Target Fraction | Actual Mass [kg] | Actual Fraction |
|---|---|---|---|---|---|
| Main Wing | 8 | 30% | 50.00% | 8.4 | 55.52% |
| Attachment | 2.5 | 30% | 15.63% | 3.2 | 21.15% |
| Safety | 4 | 10% | 25.00% | 2.13 | 14.08% |
| Supporting Accesories | 1.5 | 10% | 9.38% | 1.4 | 9.25% |
| **Total** | **16** | **-** | **100.00%** | **15.13** | **100.00%** |

[73] https://supair.com/en/produit/parachute-supair-shine/, Accessed on 18/06/2024.
[74] https://enduro-mtb.com/en/lightweight-and-convertible-full-face-helmets-review/, Accessed on 18/06/2024.
[75] https://ad-gliders.com/produkt/hook-knife/?lang=en, Accessed on 18/06/2024.

# Part IV - Risk and Financial Analysis

# 12 | Technical Risk Management

Based on the design concept established in the midterm report [14], several technical risks were identified. The severity of the risks were quantified in a risk map. Furthermore, a risk management plan was constructed to implement in the design and the relevant risks are assessed through a risk map once more.

## 12.1. Technical Risks

The technical risks are identified based on the different aspects of the mission and are shown below. For reference, the following abbreviations are used: OPS - operations, ENV - environment, STR - structures.

- **TR-OPS-1** The hand pump fails during initialisation.
- **TR-OPS-2** The parachute fails to deploy in an emergency.
- **TR-OPS-3** Pilot fails to run hard enough for take-off.
- **TR-OPS-4** Pilot errors.
- **TR-OPS-5** The trailing edge of the wing touches the ground during landing or take-off.
- **TR-OPS-6** Ropes used to fold wing tips tear apart.
- **TR-OPS-7** Ropes used to fold wing tips get stuck in certain positions.
- **TR-ENV-1** Hit a sharp flying object.
- **TR-ENV-2** Extreme unexpected weather leads to uncontrollable situations.
- **TR-ENV-3** Pilot blackout.
- **TR-ENV-4** Helmet detaches.
- **TR-STR-1** Non-critical leak in the inflated structure.
- **TR-STR-2** Critical leak in the inflated structure.
- **TR-STR-3** Part of the harness tears apart.
- **TR-STR-4** Attachment between wing and harness fails.
- **TR-STR-5** Wear and tear of the foil.
- **TR-STR-6** UV degradation of the foil.
- **TR-STR-7** Part of the wing structure plastically deforms due to bending stress.
- **TR-STR-8** Part of the wing structure buckles due to shear.
- **TR-STR-9** The bladder tears due to a high pressure difference.
- **TR-STR-10** Control bar plastically deforms due to fatigue.
- **TR-STR-11** The rear of the wing buckles, which has no tensairity, due to bending stress.

The severity of the risks was assessed with their likelihood and impact in Table 12.1, where the risk is the likelihood multiplied by the impact. The likelihood scale can be found in Table 12.2. The impact quantifies the magnitude of the consequences following from the risk, on a scale from one to five. This scale can be translated to negligible, low, moderate, significant and catastrophic. The relevant impact from 1 to 5 is defined as:

- **Negligible (1):** The risk, if realised, would have minimal consequences on the project's timeline, budget, stakeholders, or objectives. Minor setbacks or inconveniences could occur but are unlikely to significantly affect the overall success of the PenteFoil.
- **Low (2):** This level of impact is categorised as low given they could potentially end up disrupting the project or cause delays. This effect on the project's objectives or stakeholders is expected to be manageable. The risk may require attention and mitigation efforts but are not expected to significantly threat the success of the project.
- **Moderate (3):** When these risks are materialised they would have a noticeable impact on the objectives, timeline, budget, or stakeholders of the project. The risks could lead to moderate disruptions, delays, or additional costs that will require more extensive strategies to mitigate or contingency plans to manage effectively. Project may still proceed but the risks may need significant efforts to address and mitigate their effects to prevent larger consequences.

- **Significant (4):** The realization of these risks would have substantial consequences on the timeline, budget, objectives or stakeholders of the project. These risks result in considerable threats to the success of the project and may result in significant delays, disruptions, or cost overruns which would affect the projects viability or long term outcomes. Managing these risk would need proactive measures, resource allocation, and potentially revisiting strategies or project plans to mitigate them effectively.
- **Catastrophic (5):** If this risk is realised it would have severe irreversible, or catastrophic consequences on the project's objective, stakeholders, or the organization as a whole. These risks pose an existential threat to the success or the organization's viability of the project, resulting in extensive damage, loss, or harm that has long-lasting implications. The risks require comprehensive and immediate attention, with emergency response measures, crisis management protocols, and potentially reevaluating the feasibility or strategic direction included. This to mitigate the devastating effects.

Furthermore, the likelihood is defined as follows:

- **Highly Unlikely (1):** Possibility of occurrence is <1%.
- **Unlikely (2):** Possibility of occurrence is 1-30%.
- **Possible (3):** Possibility of occurrence is 30-50%.
- **Probable (4):** Possibility of occurrence is 50-70%.
- **Highly Probable (5):** Possibility of occurrence is >70%.

**Table 12.1:** Risk assessment of the severity of each risk with their respective likelihood and impact.

| ID | Likelihood | Impact | Risk | Physical Impact |
|---|---|---|---|---|
| TR-OPS-1 | 1 | 2 | 2 | Initialisation fails |
| TR-OPS-2 | 1 | 5 | 5 | Emergency landing can not be performed |
| TR-OPS-3 | 2 | 4 | 8 | Take-off can not be performed |
| TR-OPS-4 | 3 | 4 | 15 | Flight can be affected or landing ends badly |
| TR-OPS-5 | 3 | 4 | 12 | The wing gets damaged making it less stable and controllable or the pilot falls and gets injured |
| TR-OPS-6 | 2 | 3 | 6 | Wing tips can not be folded anymore, disabling the dive mechanism |
| TR-OPS-7 | 3 | 4 | 12 | Wing tips are constantly folded or unfolded making the system less stable and hard to control |
| TR-ENV-1 | 2 | 4 | 8 | Aerodynamics influenced negatively, not enough lift |
| TR-ENV-2 | 3 | 4 | 12 | Uncontrollable situations |
| TR-ENV-3 | 2 | 5 | 10 | No control of system anymore |
| TR-ENV-4 | 2 | 3 | 3 | Head is not protected in case of an emergency |
| TR-STR-1 | 4 | 3 | 12 | Possibly less stable and risk of bigger leak |
| TR-STR-2 | 2 | 4 | 8 | Not enough lift provided anymore |
| TR-STR-3 | 3 | 4 | 12 | Pilot has issues holding on to the structure |
| TR-STR-4 | 2 | 5 | 10 | Pilot falls out of the sky |
| TR-STR-5 | 2 | 3 | 6 | The material performs worse and can cause failure |
| TR-STR-6 | 2 | 3 | 6 | The material performs worse and can cause failure |
| TR-STR-7 | 3 | 5 | 15 | Part of the wing deforms and attached person is pulled in an uncomfortable position causing an uncontrollable system |
| TR-STR-8 | 3 | 4 | 12 | Part of the wing deforms negatively affecting the aerodynamic performance |
| TR-STR-9 | 3 | 5 | 15 | Wing structure deflates and lift goes down dramatically |
| TR-STR-10 | 2 | 5 | 10 | Uncontrollable system |
| TR-STR-11 | 3 | 3 | 9 | Aerodynamics performance is negatively affected |

**Table 12.2:** Initial risk map showing the impact and likelihood of all risks.

| | | | | | |
|---|---|---|---|---|---|
| **5 (Catastrophic)** | TR-OPS-2 | TR-ENV-3, TR-STR-4, TR-STR-10 | TR-STR-7, TR-STR-9 | | |
| **4 (Significant)** | | TR-OPS-3, TR-STR-2, TR-ENV-1 | TR-ENV-2, TR-STR-3, TR-OPS-4, TR-OPS-5, TR-OPS-7 TR-STR-8 | | |
| **3 (Moderate)** | | TR-ENV-4, TR-OPS-6 | TR-STR-11 | TR-STR-1 | |
| **2 (Low)** | TR-OPS-1 | | | | |
| **1 (Negligible)** | | | | | TR-STR-6 |
| Impact / Likelihood | **1 (<1%)** | **2 (>1%, <30%)** | **3 (>30%, <50%)** | **4 (>50%, <70%)** | **5 (>70%)** |

The risk is a combination of likelihood and impact. Red indicates the risk has a value higher than 13; these are the most severe risks. Orange risks have values between 7 and 13. Yellow risks have a risk level of 5 or 6, and green indicates a low risk level below 5.

## 12.2. Risk Management Plan

In this section, a risk mitigation plan will be presented for each risk. The goal is to reduce the overall risk by reducing either the impact or the likelihood of each problem. Table 12.3 shows what mitigation strategy was implemented to reduce the severity of the risks. In Table 12.4 the new risk map after mitigation can be seen. It should be noted that not all risks have been implemented yet due to time limitations.

**Table 12.3:** Risk mitigation action overview, with the likelihood, impact, and new risk level after mitigation actions.

| ID | Mitigation Action | Likelihood | Impact | New Risk | Responsible member |
|---|---|---|---|---|---|
| TR-OPS-1 | Provide backup inflation mechanism | $1 \rightarrow 1$ | $2 \rightarrow 1$ | $2 \rightarrow 1$ | Bram |
| TR-OPS-2 | Monthly check quality parachute | $1 \rightarrow 1$ | $5 \rightarrow 5$ | $5 \rightarrow 5$ | Pilot |
| TR-OPS-3 | Training procedure has to be completed before pilots are allowed to fly | $2 \rightarrow 1$ | $4 \rightarrow 4$ | $8 \rightarrow 4$ | Bram |
| TR-OPS-4 | System as controllable as possible and only pilots that completed the training procedure are allowed to fly | $3 \rightarrow 1$ | $4 \rightarrow 4$ | $12 \rightarrow 8$ | Bram |
| TR-OPS-5 | The chordwise length of the wing will be smaller than 2.5 meters | $3 \rightarrow 1$ | $4 \rightarrow 4$ | $12 \rightarrow 4$ | Vito |
| TR-OPS-6 | Design strong control ropes with safety factor | $2 \rightarrow 1$ | $3 \rightarrow 3$ | $6 \rightarrow 3$ | Dimitri |
| TR-OPS-7 | Design so that wing tips automatically go back to original position | $3 \rightarrow 1$ | $4 \rightarrow 4$ | $12 \rightarrow 4$ | Dimitri |
| TR-ENV-1 | Fly in safe airspace as taught in training procedure | $2 \rightarrow 1$ | $4 \rightarrow 4$ | $8 \rightarrow 4$ | Bram |
| TR-ENV-2 | Fly only when good weather is expected from multiple weather forecasts | $3 \rightarrow 1$ | $4 \rightarrow 4$ | $12 \rightarrow 4$ | Pilot |
| TR-ENV-3 | Medical check before flight | $2 \rightarrow 1$ | $5 \rightarrow 5$ | $10 \rightarrow 5$ | Bram |
| TR-ENV-4 | Check if helmet is attached properly before flight | $2 \rightarrow 1$ | $3 \rightarrow 3$ | $6 \rightarrow 3$ | Pilot |
| TR-STR-1 | Strengthen critical stress locations in foil with thicker material | $4 \rightarrow 2$ | $3 \rightarrow 3$ | $12 \rightarrow 6$ | Jakub |
| TR-STR-2 | Monthly check quality of material foil | $2 \rightarrow 1$ | $4 \rightarrow 4$ | $8 \rightarrow 4$ | Pilot |
| TR-STR-3 | Monthly check harness for any degradation | $3 \rightarrow 1$ | $4 \rightarrow 4$ | $12 \rightarrow 4$ | Pilot |

**Table 12.3:** Risk mitigation action overview, with the likelihood, impact, and new risk level after mitigation actions.

| ID | Mitigation Action | Likelihood | Impact | New Risk | Responsible member |
|---|---|---|---|---|---|
| TR-STR-4 | Attach emergency parachute separately and attach extra safety attachment | 2 → 2 | 5 → 1 | 10 → 2 | Bram |
| TR-STR-5 | Material with good degradation performance and monthly checks | 2 → 1 | 3 → 3 | 6 → 3 | Szymon |
| TR-STR-6 | Choose material that does not degrade from UV that much or apply a coating | 2 → 1 | 3 → 3 | 5 → 1 | Szymon |
| TR-STR-7 | Apply safety margin to tension and compression and design the failure mode such that the failing part of the structure detaches from the attachment | 3 → 1 | 5 → 4 | 15 → 4 | Jakub |
| TR-STR-8 | Apply pre-tension with a safety factor | 3 → 1 | 4 → 4 | 12 → 4 | Szymon |
| TR-STR-9 | Apply safety factor to design bladder and allowed pressure | 3 → 1 | 5 → 5 | 15 → 5 | Jakub |
| TR-STR-10 | Design control bar with safety factors | 2 → 1 | 5 → 5 | 10 → 5 | Szymon |
| TR-STR-11 | Pre-tension the rib skin with a safety factor | 3 → 1 | 3 → 3 | 9 → 3 | Szymon |

**Table 12.4:** Post-mitigation risk map showing the impact and likelihood of all risks after mitigation actions.

| | | | | | |
|---|---|---|---|---|---|
| **5 (Catastrophic)** | TR-OPS-2, TR-ENV-3, TR-STR-9, TR-STR-10 | | | | |
| **4 (Significant)** | TR-STR-2, TR-ENV-1, TR-ENV-2, TR-OPS-3, TR-OPS-4, TR-OPS-5, TR-OPS-7, TR-STR-3, TR-STR-7, TR-STR-8 | | | | |
| **3 (Moderate)** | TR-ENV-4, TR-STR-11, TR-OPS-6, TR-STR-5, TR-STR-6 | TR-STR-1 | | | |
| **2 (Low)** | | | | | |
| **1 (Negligible)** | TR-OPS-1 | TR-STR-4 | | | |
| Impact / Likelihood | **1 (<1%)** | **2 (>1%, <30%)** | **3 (>30%, <50%)** | **4 (>50%, <70%)** | **5 (>70%)** |

Table 12.4 shows that the severity of the risks has been reduced for every risk and therefore all risks have been mitigated. As not every risk is fully prevented, a contingency plan for every risk is made and shown in Table 12.5. The risks that were still in the yellow part in Table 12.4, were marked yellow in Table 12.5 as well.

**Table 12.5:** Proposed contingency plan for all the identified risks.

| ID | Contingency plan |
|---|---|
| TR-OPS-1 | Pilot walks back down the mountain to repair or buy new inflation mechanism. |
| TR-OPS-2 | Pilot tries to land as good as possible to reduce damage. |
| TR-OPS-3 | Pilot aborts take-off. |
| TR-OPS-4 | Pilot tries to correct mistake or use the emergency landing parachute to land. |
| TR-OPS-5 | Pilot aborts take-off. |
| TR-OPS-6 | Pilot starts landing procedure. |
| TR-OPS-7 | Pilot starts landing procedure and uses emergency parachute if necessary. |
| TR-ENV-1 | Pilot uses emergency parachute to land if damage is critical. |
| TR-ENV-2 | Pilot tries to fly out of extreme weather and land. |
| TR-ENV-3 | Not possible. |
| TR-ENV-4 | Pilot starts landing procedure. |
| TR-STR-1 | Pilot starts landing procedure to prevent the leak from becoming critical. |
| TR-STR-2 | Pilot uses emergency parachute for landing. |
| TR-STR-3 | Pilot starts landing procedure as soon as possible. |
| TR-STR-4 | Pilot uses emergency parachute to land. |
| TR-STR-5 | Replace product when wear becomes too severe. |
| TR-STR-6 | Replace product when degradation becomes too severe. |
| TR-STR-7 | Pilot uses emergency parachute to land when aerodynamics is affected too much. |
| TR-STR-8 | Pilot starts landing procedure if still possible or uses emergency parachute. |
| TR-STR-9 | Pilot uses emergency parachute for landing. |
| TR-STR-10 | Pilot uses emergency parachute for landing. |
| TR-STR-11 | When aerodynamics is affected too much, pilot uses emergency parachute for landing. |

# 13 | RAMS Analysis

The Reliability, Availability, Maintainability, and Safety (RAMS) analysis is made to ensure the system's performance meets the highest standards of safety and dependability. This chapter evaluates the PenteFoil's design and operational parameters, assessing its ability to consistently perform under various conditions while minimising the likelihood of failures and ensuring user safety.

## 13.1. Reliability Analysis

Reliability is defined as the probability that a product, system, or service will perform its intended function adequately for a specified time period, or will operate in a defined environment without failure[76]. In the case of the PenteFoil, the environment is defined as in flight and the intended function is providing lift. The reliability for this critical requirement should be equal to 100%. This means that the PenteFoil wing structure should not leak or break and the skin cover should not tear apart for 100% of the time. This is assuming that the PenteFoil is properly checked on leaks and tears according to the manual before take-off. Because the inflatable structure of the PenteFoil is so essential there is no room for it to fail. Therefore, proper maintenance and safety are crucial to ensure the reliability of the PenteFoil. The inflatable structure of the PenteFoil is absolutely critical, leaving no room for failure. Therefore, diligent maintenance and proper safety measures are essential to ensure the PenteFoil's reliability.

## 13.2. Availability Analysis

The objective of the availability analysis is to ensure that the PenteFoil system is operational and ready for use when needed, with minimal downtime. To achieve this, the Mean Time Between Failures (MTBF) and the Mean Time to Repair (MTTR) for all subsystems will be estimated. The MTTR indicates the time necessary to execute repairs, assuming that all subsystems can be repaired locally, thus excluding shipping time.

However, when the PenteFoil is used in remote locations, local repairs might not be possible. In such cases, the damaged subsystem must be shipped, which decreases overall availability. An overview of the estimated hours for each subsystem and the overall availability is provided in Table 13.1. The availability of each subsystem is calculated using the formula shown in Equation 13.1.

For a safe flight, all subsystems must be operational, meaning the PenteFoil cannot take off if any subsystem is unavailable. To improve availability, spare parts can be brought along. For example, extra control lines and an extra helmet can be easily replaced in case of a failure. For the Helmet and the handpump, the MTTR of the subsystem is indicated as 0, suggesting it is advisable to buy a new one instead of repairing it. The overall availability is determined by multiplying the availability of all subsystems, leading to the total availability of the PenteFoil of 94.86%. Having a spare part for each subsystem can effectively ensure 100% availability, but it also doubles the hardware costs. It is up to the user to decide which spare subsystems to purchase.

$$Availability = \frac{MTBF}{MTBF + MTTR} \cdot 100\% \tag{13.1}$$

**Table 13.1:** Availability results of the subsystems in the PenteFoil (hours).

| Sub-system | MTBF | MTTR | Availability |
|---|---|---|---|
| Control lines | 400 | 2 | 99.5% |
| Tensairity structure | 300 | 4 | 98.68% |
| Harness | 400 | 2 | 99.50% |
| Helmet | 750 | 0 | 100% |
| Parachute[77] | 200 | 6 | 97.09% |
| Handpump | 750 | 0 | 100% |
| **Total** | | | 94.86% |

[76] `https://asq.org/quality-resources/reliability#`, Accessed on 10/06/2024.

## 13.3. Maintainability Analysis

To mitigate and manage issues with the PenteFoil, an effective maintenance and inspection schedule is required. The inspection should be done after initializing and before terminating the PenteFoil. Additionally, scheduled maintenance is required to avoid accidents due to failure. The following outlines and explains the inspection and maintenance tasks required.

- Pre-Flight Inspection
    1. Check for visible signs of wear, punctures, or seam damage before each use.
    2. Ensure all attachment points and inflation mechanisms are secure and undamaged.
- Post-Flight Inspection
    1. Inspect the PenteFoil thoroughly after each flight, focusing on areas prone to damage.
    2. Clean and dry the PenteFoil before storing it to prevent mold and material degradation.
- Regular Maintenance
    1. Conduct a detailed inspection and maintenance session at a certified shop every 30 flight hours or every 6 months, whichever comes first.
    2. Repair any minor leaks or damage immediately to prevent them from worsening.
- Annual Overhaul
    1. Perform a comprehensive inspection and maintenance session annually.
    2. Replace any components showing significant wear or damage, even if they are not currently leaking.

The frequency of leakage in the inflatable structure for the PenteFoil project can be managed effectively through high-quality materials, precise manufacturing, and rigorous maintenance practices. Additionally a pressure sensor can be placed in the tensairity tubes that starts to squeak in case of a leak. While minor leaks might occur approximately every 100-200 hours of use, proactive inspection and maintenance can significantly reduce the occurrence and impact of such leaks, ensuring the PenteFoil remains reliable and safe for use[78].

## 13.4. Safety Analysis

The primary goal of the PenteFoil is to offer users a thrilling aerial sport experience while ensuring their safety. Achieving this requires a careful balance between agility and stability, ensuring the PenteFoil operates in a safe and reliable manner. To ensure it is not susceptible to the same types of accidents as other aerial sports, an analysis was performed on accidents in paragliding and hang gliding. Fatality reports from the United States Hang Gliding and Paragliding Association were utilised for this purpose. The reasons for fatal incidents in both paragliding and hang gliding were examined, and the accidents were categorised accordingly. All incidents were classified under the following causes.

- Gusts: An unexpected gust causes the wing to be pushed into an obstacle or ground.
- Wing collapse: A wing collapse causes a loss of control
- Collision: A collision with obstacles like powerlines, trees or other gliders led to the accident.
- Pilot error: Pilot error can include many things, from a poorly performed manoeuvre to flying in bad conditions or not following the safety instructions properly which led to the accident. Every accident where the system functioned properly but the pilot made a clear mistake.
- stall: The full wing or part of the wing stalled, causing a loss of control and resulting in the accident.
- Glider failure: Something structural from the glider broke and caused the accident.
- Pilot medical issue: There was an accident reported of a pilot becoming unresponsive mid-air likely due to a medical issue.
- Entangled in lines: The pilot gets entangled in the lines which led to the fatality.
- Unknown: Unfortunately, there are also unresolved accidents and their causes are unknown or are still under investigation.

[77] https://www.quora.com/How-many-times-can-you-use-the-same-parachute-before-it-is-retired-from-use-in-skydiving, Accessed on 24/06/2024.

[78] https://www.kitemana.com/info/blog/how-to-check-your-kite-gear-1275, Accessed on 11/06/2024.

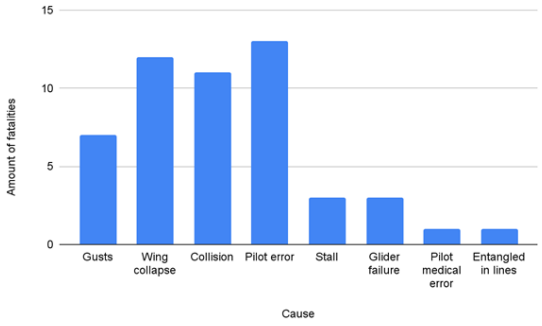


**Figure 13.1:** Amount of fatalities over the years 2013 to 2022 per cause.

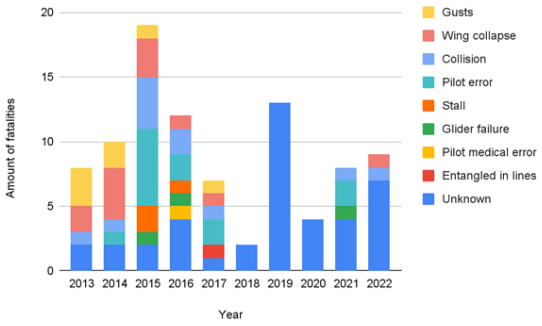


**Figure 13.2:** Amount of fatalities per year.

From Figure 13.1 and Figure 13.2, we can see that the main causes of fatal accidents are wing collapses, collisions, pilot errors and gusts.

### Wing collapse

Starting with wing collapses, wing collapses happen a lot in paragliding because of thermals or turbulent air. However, since our wing is an inflated stiff structure it should not collapse like paragliders do. In addition to that the wing is designed to withstand a load factor of 7.95 as explained in Section 4.2.

### Gusts

The PenteFoil has a much lighter wing compared to a hang glider. As a result, it could be more susceptible to gusts from thermals and turbulent air. To overcome this the wing is designed to be stable as explained in Section 3.7. Therefore the wing should return to controllable flight conditions even with a hands-up response. Such that even when the user does not correct the motion it should return to stable flying conditions. However, at lower altitudes, the emergency parachute might need to be thrown as the wing will have to little time to recover.

### Pilot Errors

Pilot errors are also a huge contributor to fatal accidents, from not properly following the safety instructions to performing manoeuvres improperly. A very striking incident was of an experienced pilot who had been flying for 17 years and was a tandem instructor. In 2015 he had neglected to fasten his leg straps and fell out of the harness during a tandem flight. Indicating the necessity to stick to the safety procedures even for very experienced pilots. Therefore proper instruction and training are crucial for the PenteFoil. Trainees should be taught in a safe environment and should be made aware of the risks for themselves and others.

### Colission

Collisions were also a major cause of accidents. Most of the collisions were due to misjudgement by the pilot, such as hitting a tree, powerline or other obstacle resulting in a fatal crash. These accidents can be avoided by training the users on how to properly plan their flight path. Another reason for some collisions is insufficient line of sight. Thus making sure that users only fly in suitable flying conditions is important to be able to spot hazards and take avoiding action in time.

Apart from the causes of accidents in hang gliding and paragliding, an overview of other risks affecting the PenteFoil specifically is provided in Chapter 12. Some of these risks pose direct threats to the user. Therefore this section also lists these threats, explains the actions taken during the design phase to mitigate these risks, and outlines steps that can be taken if such incidents occur.

### Control System Failure

The control system of the PenteFoil has been explained in Section 5.3. The controls of the PenteFoil consist of a bar that enables the user to control their C.G. and with that the pitch and roll and two wires attached to the wing tips that allow wing tip folding.

In the event of a malfunction in the control wires, users can still manage roll control by shifting their centre of gravity left or right, enabling a safe landing. If the control bar becomes unusable, both pitch and roll control are lost. However, the PenteFoil's design ensures static stability, allowing for a safe glide descent with a vertical sink rate of 3 m/s. Should the glide path lead towards a tree or sharp stones, the user must deploy the emergency parachute. This procedure, detailed in Subsection 5.2.2, restores flight path control, allowing the user to navigate to a safe landing spot.

**Structural Failure**

Structural failures, depending on their location and type, can potentially lead to catastrophic consequences for the PenteFoil. Severe loss of lift due to such failures may prevent the PenteFoil from maintaining flight. This risk is particularly dangerous at low altitudes, where deploying the emergency parachute is not feasible. To minimise the likelihood of such events, the design process has incorporated redundancy and safety margins. Additionally, preventive and regular inspections play a crucial role in detecting and addressing potential structural issues before they lead to failure. The complete collapse of the wing structure is unlikely because the attachment points would likely tear away from the web before such a collapse could occur. Unlike hang gliders, which are assembled from two separate parts at the middle, the wing in this case is a single, large structure. This design significantly increases stiffness and structural integrity.

**Dangerous Weather**

Harsh weather could create threats for the PenteFoil. Encountering gusts in flight could excessively stress the structure or damage it. As can be seen in the flight envelope in Figure 7.7, the PenteFoil is designed to cope with a load factor for gusts up to 5.3, anything beyond this value risks damaging the PenteFoil. A second weather phenomenon that poses danger to PenteFoil users is fog/clouds near the ground, as it might force PenteFoil users to land without vision. To avoid this situation it is of uttermost importance to check the weather forecast thoroughly as described in the pre-flight check in Subsection 5.4.2.

**Stall**

Stall is a phenomenon where the flow of air separates from the wing due to a high angle of attack, resulting in a sudden decrease in lift. Stall can lead to hazardous conditions, potentially causing an unrecoverable freefall. However, the PenteFoil airfoil is desgned with a negative $C_{m_\alpha}$, which automatically reduces pitch and subsequently increases velocity when nearing stall conditions, enhancing safety.

# 14 | Cost Breakdown Structure

This chapter presents the CBS of the PenteFoil. A cost breakdown structure is essential in engineering projects as it provides a detailed financial overview, breaking down the project costs into manageable sections. A CBS ensures detailed project management and improves risk mitigation by identifying financial hot-spots. It also promotes transparency and better communication among stakeholders, facilitating informed decision-making and performance measurement. Ultimately, a CBS is crucial for effective financial planning, documentation, and securing necessary funding, ensuring the project's success within the allocated budget[79].

The CBS includes three essential types of costs: labor, material and overhead. Labor costs cover the money spent on the workforce, categorised by service or manufacturing, and are directly tied to the project's production. Material costs encompass expenses for raw materials, parts, components, insurance, and freight, distinguishing between direct and indirect materials. Lastly, overhead costs include ongoing business expenses such as office space, utilities, and taxes, which, while not directly contributing to profits, are vital for the project's overall execution. All costs indicated below include tax.

The production costs are indicated for the production of 380 PenteFoils (one batch) in one year. The batch size is determined by the capacity of the already existing factory's in Sri Lanka. Chapter 15 elaborates on why Sri Lanka was chosen as production country.

**Material Costs**

The material costs of the PenteFoil are estimated in Subsection 4.4.5. The materials are bought in batches for 380 PenteFoils. The advantage of large batches is that spare materials can be easily included without significant costs, and the freight costs to Sri Lanka are negligible. The materials for a batch of 380 PenteFoils cost €383,356.60 , with a detailed breakdown provided in Table 4.7.

**Production Costs**

Once the necessary materials are available, production of the PenteFoil can commence. The manufacturing will take place in Sri Lanka, a location chosen for its expertise and facilities in producing kites from similar materials[80]. The factory cost for producing each PenteFoil is about €1,700.00. Additionally, a team of five engineers will be hired to oversee quality assurance, ensuring that each PenteFoil meets top standards before being shipped to Rotterdam for sale. Besides the employees in Sri lanka, there will be a warehouse administrator in Delft who manages all packages coming in and out. The warehouse administrator receives an salary of €38.000 a year[81]. Additionally, the four PenteFoil business owners will do the marketing and execute the overall strategy of the company, they are paid €44.000 gross[82] a year.

**Overhead Costs**

To establish the warehouse, a 150 m² plot of land will be leased in Delft at an annual cost of €38,000[83]. In addition to this, there will be a one-time expense of €32,000 to construct the warehouse on the leased land[84]. Furthermore, a budget of €10,000 will be set aside for essential office supplies, such as printer cartridges and coffee for employees, ensuring that the workplace is well-equipped and comfortable for daily operations[85]. This comprehensive approach not only secures the necessary space and infrastructure but also addresses the ongoing needs of the staff, contributing to a more efficient and pleasant working environment.

Figure 14.1 provides an overview of the costs for one year when producing a single batch of 380 PenteFoils. Additionally, a 15% contingency is applied to the total cost for unexpected expensiveness and loss of materials during manufacturing, resulting in final expenses of €1,740,000 for the first year[86].

As the popularity of the PenteFoil grows, the company can scale up its operations to produce multiple batches per year. This expansion will lead to a reduction in overhead costs and allow for more favorable deals with the production company in Sri Lanka and material suppliers. The increased efficiency and cost savings from scaling up will enable the business owners to allocate more funds towards their salaries or bonuses. This

[79] https://www.projectmanager.com/blog/cost-breakdown-structure, Accessed on 18/06/2024.
[80] https://www.duotonesports.com/en, Accessed on 10/06/2024.
[81] https://lokaleregelgeving.overheid.nl/CVDR711489/1, Accessed on 18/06/2024.
[82] https://www.nationalevacaturebank.nl/carriere/salaris/salaris-berekenen/modaal-inkomen?, Accessed on 18/06/2024.
[83] https://delft.notubiz.nl/document/14038611/1/Grondprijzenbeleid+2024-2028+def_5814983, Accessed 10.06.2024.
[84] https://www.buildingsguide.com/costs/what-does-it-cost-to-build-a-warehouse/, Accessed on 10/06/2024.
[85] https://smallbusiness.chron.com/average-cost-per-month-office-supplies-12771.html, Accessed on 18/06/2024.
[86] https://multiproject.org/learningcentre/contingency-funds-what-are-they-and-how-much-should-you-set-aside/, Accessed on 10/06/2024.

strategic growth not only boosts production capacity but also enhances profitability, ensuring sustainable financial rewards for the business owners. Insurance and taxes for the PenteFoil project, which are necessary to cover liabilities, employee benefits, and compliance with legal requirements, should also be taken into account. However, due to time constraints, these aspects have not been further detailed in this report beyond the taxes related to gross salary numbers and material costs.

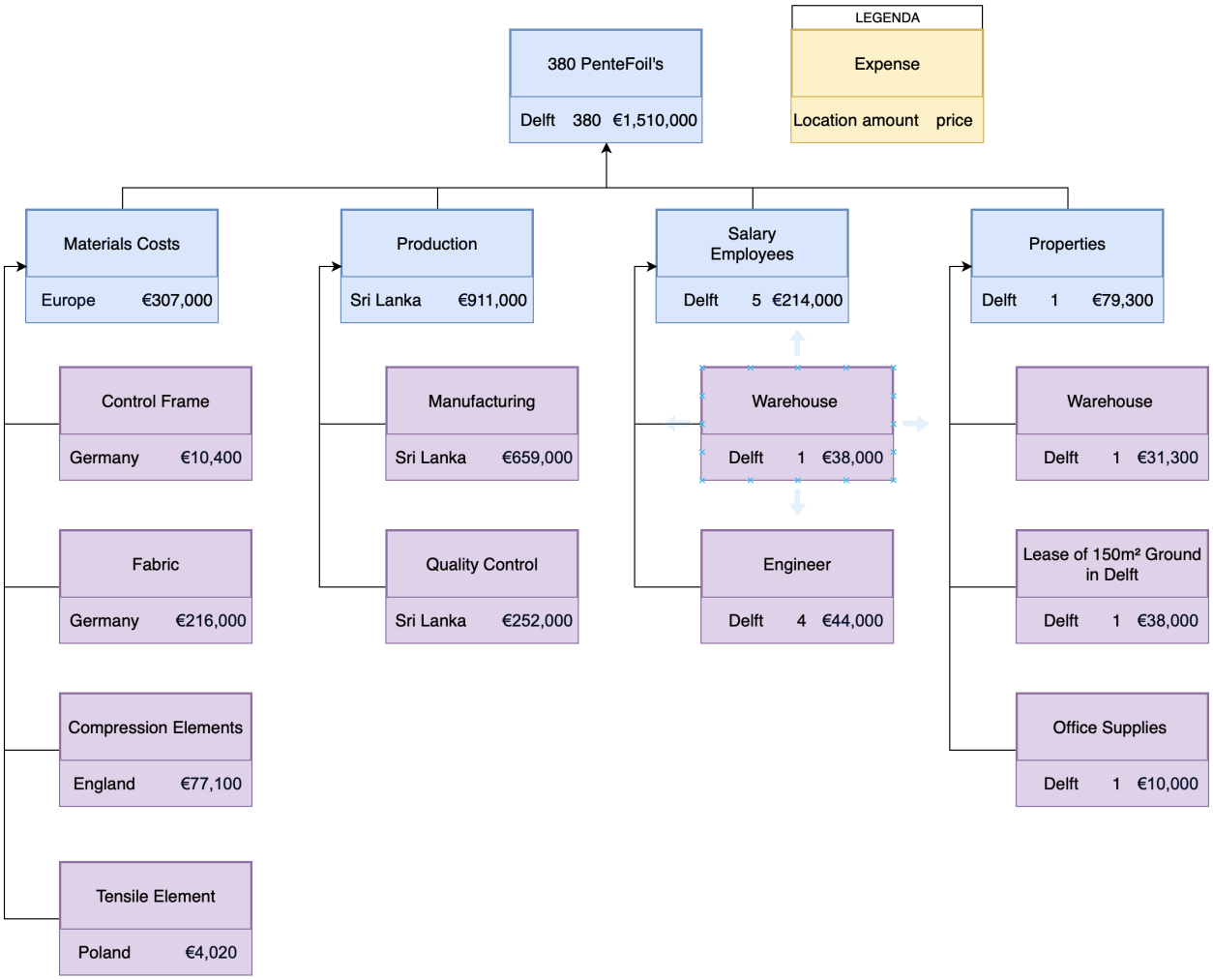


**Figure 14.1:** Cost breakdown structure for the first year of the PenteFoil company.

# 15 | Return On Investment (ROI) & Operating Profit Overview

This chapter presents an overview of the Return on investment (ROI) and operational profit analysis for the PenteFoil project. The purpose of examining the financial aspects of the project is to provide stakeholders, potential investors, and project team members with valuable insights into the economic viability and sustainability of the project. Subsequent sections will explore the costs associated with product development, operations, and marketing, as well as revenue projections and profitability metrics.

## 15.1. Product Development Cost Estimation

**Funding:** To demonstrate the potential of the PenteFoil project, a pre-seed crowdfunding campaign will be launched on platforms such as Indiegogo, Kickstarter, or SeedInvest. This campaign aims to generate buzz, validate the concept, and attract supporters and early adopters. During this phase, backers will contribute small amounts of money in exchange for early access to the PenteFoil.

Following the pre-seed crowdfunding campaign, the first seed round will commence, indicating demand and excitement for the PenteFoil project. At this early stage, the primary objective is to validate the concept and develop a prototype or proof of concept showcasing the feasibility of the PenteFoil. The funding goal of €50,000 will be presented to early-stage venture capitalists, angel investors, friends, and family who share the vision.

An additional funding option involves applying for the Graduate Entrepreneur program, which offers pre-seed tickets of €75,000[87]. Upon successfully proving the concept and demonstrating potential for growth, the startup will seek additional funding in a second seed round. This investment will be utilised for further development, team expansion, and marketing efforts. Subsequent funding rounds, such as Series A, Series B, and beyond, will be pursued to scale the business, expand into new markets, and achieve profitability.

**Research and Development (R&D) Costs:** The conceptual design of the PenteFoil is completed by 10 students from the Faculty of Aerospace Engineering as part of their design synthesis project. Instead of receiving monetary compensation, the students are awarded 15 European study credits for their 400 hours of work. Since no significant prototyping and testing are conducted during this conceptual design stage, the total costs are negligible.

The PenteFoil project is developing an innovative product that typically requires 27 months to complete [30]. The average startup has four employees at the birth of the company[88]. The four employees who continue their efforts to develop PenteFoil will be the company's co-founders. They will pay themselves according to the minimum income level designed to ensure that individuals and families have enough financial resources to meet their basic needs, which is €2,070 per month in the Netherlands, according to UWV[89]. For the PenteFoil project, this would amount to a total personnel cost of €297,980 for the three years of development. These three years include 6 months of contingency time on top of 27 months of development.

The average development timeline for mechanical invention prototypes is 4-8 weeks, while for sewing prototypes, it is 4 weeks[90]. Combining the 27 months to develop the PenteFoil with the 4-8 week timeline of a single iteration, it would be possible to make at least 3 prototypes before reaching a finalised design ready for sale. The first prototype is assumed to take 12 weeks to complete. This would result in producing one prototype per year, which takes 2-3 months to create, leaving the remainder of the year for testing and iterating on the model. The manufacturing and assembly of the prototypes will incur no additional costs on top of the material costs, which amount to €1,009, as it will be carried out in-house by four employees.

The PenteFoil must be tested in a wind tunnel, which costs approximately €36,800 for 45 hours of usage at an hourly rate of €792[91]. This time is allocated per prototype, resulting in a total of 135 hours of wind tunnel testing over the first three years of the project. After wind tunnel testing, the next step is flight testing the PenteFoil, which is estimated to cost around €4,016 for a 5-day testing setup as described in Chapter 9. This must be repeated for each of the three different prototypes. To comprehend the structural limits of the PenteFoil, various structural tests are conducted, as outlined in Chapter 9. These tests encompass multiple bench tests

[87] https://www.graduate.nl/funding, Accessed on 10/06/2024.

[88] https://www.bls.gov/spotlight/2022/business-employment-dynamics-by-age-and-size/home.htm, Accessed on 10/06/2024.

[89] https://www.uwv.nl/particulieren/bedragen/detail/sociaal-minimum, Accessed on 17/06/2024.

[90] https://lanpdt.com/rapid-prototyping-company/, Accessed on 17/06/2024.

[91] https://www.aa.washington.edu/AERL/KWT/rateguide, Accessed on 10/06/2024.

and fatigue testing, with an estimated total cost of €8,000 per prototype. The environmental testing can be conducted using a device known as the UV Accelerated Weathering Tester, which assesses conditions such as sunlight, rain, humidity, and dew. The cost of this equipment ranges between €2,275 and €3,640 [92]. The PenteFoil must undergo certification testing to demonstrate compliance with safety and regulatory standards in the countries where it will be sold. The certification costs for a single prototypes is estimated to be €296 per prototype[93]. The estimated accumulated costs for the PenteFoil up to the finalised design with three prototypes made and tested is shown in Table 15.1.

**Table 15.1:** Estimated R&D Costs for Three Prototypes.

| **Item Description** | **Total Cost (€)** |
|---|---|
| Material Cost | 6,000 |
| Wind Tunnel Testing | 106,812 |
| Flight Testing | 12,048 |
| Structural Testing | 24,000 |
| Certification | 888 |
| 1 x Environmental Test Machine | 3,640 |
| Three Years Salary (4 co-founders) | 297,979.2 |
| **Total R&D Cost** | **451,367.2** |

After finalizing the design, the PenteFoil will be manufactured, the optimal batch quantity that should be produced at any time, originates from the economic batch quantity shown in Equation 15.1 [31].

$$Q = \sqrt{\frac{2cdr}{h(r-d)}} \tag{15.1}$$

Where Q is the quantity to be purchased or manufactured, c is the cost of processing an order for delivery, d is the demand in the period for that stock item, h is the cost of holding a unit of stock, and r is the rate of production. This calculation is not feasible at this stage, but it should be performed in later stages to find an accurate and optimal batch quantity.

**Production Costs:**The PenteFoil wing is comparable to a kite wing but it has more complicated panel lay outs and more inflatable parts, making it more expensive to produce. Sri Lanka has favorable production conditions and a skilled workforce, which is why major kiteboarding companies like Duotone produce their kites there[94]. According to Maramenides, a professional kiteboarder and owner of Epic Kites Kiteboarding[95], "So in few words a 12 meter EPIC kite comes out to be around $595 for kite only without the bar and lines, and that is our cost for orders of 380 kites a month"[96]. Estimating the increased cost owing to the PenteFoil's complexity suggests a greater investment in labor. Furthermore, considering the quotation dates back to 2013, one must factor in cost escalation due to inflation, input price fluctuations, technological advancements, and regulatory mandates. This inflationary effect can be addressed using Equation 15.2, where $C_n$ is the cost of producing the product after $n$ years, $C_0$ is the initial cost of producing the product, $r_i$ is the inflation rate in year $i$, $n$ is the number of years.

$$C_n = C_0 \times \prod_{i=1}^{n}(1 + r_i) \tag{15.2}$$

A projection from 2013 to the anticipated production year of 2026, employing the global inflation rate from 2000 to 2022 (with forecasts extended until 2028)[97], indicates a price increase of around double the cost

[92] https://www.liyi-tech.com/sale-8781153-uv-accelerated-weathering-tester-environmental-uv-light-testing-equipment.html, Accessed on 11/06/2024.

[93] https://zoek.officielebekendmakingen.nl/stcrt-2023-32008.html#:~:text=De%20kosten%20voor%20een%20speciaal,de%20kosten%20%E2%82%AC%20120%20bedragen., Accessed on 10/06/2024.

[94] https://www.duotonesports.com/en, Accessed on 10/06/2024.

[95] https://www.epickiteskiteboarding.com/, Accessed on 10/06/2024.

[96] https://kiteforum.com/viewtopic.php?t=2382855&start=50, Accessed on 10/06/2024.

[97] https://www.statista.com/statistics/256598/global-inflation-rate-compared-to-previous-year/, Accessed on 10/06/2024.

($1,078) per kite from the initial cost of $595. Considering the PenteFoil's increased complexity, with 10 tenserity tubes similar to the inflatable leading edge of a kite, it is reasonable to anticipate a conservative threefold increase in cost per unit due to the added production time, which could increase by up to three times. This number can change based on future estimations based on prototype manufacuring time, cost and complexity. Nonetheless, the technological advancements over the last decade have enhanced sewing efficiency, improved user experience and reduced complexity [32]. Therefore, a total cost increase factor of 1.5 is assumed due to complexity. Hence, the estimated cost per PenteFoil wing, excluding compressive elements in the tensairity tubes or the frame used for support, is projected to be $1,617, equivalent to €1,504 when producing 380 units monthly.

After producing the wing, the cost of the compressive elements, amounting to €203, needs to be added. Additionally, the cost of the frame is included, which is €27[98] .

The entire system undergoes quality control, safety testing, and certification before being packaged and shipped to distribution centers for consumer orders. The quality assurance team will be in charge of this and consist of at least 5-6 members These employees should have an aerospace engineering background, with an average monthly pay of €4,132, with five employees totaling €20,656 per month. The quality assurance team will also act as support staff and sales representatives.

Logistics costs are also considered and estimated. Shipping a 20 ft container from Sri Lanka to the Netherlands costs between €5,658 and €6,253. The container has a volume of 33 cubic meters and can hold 542 units of 50.8 liters each plus an extra 10 liters added for packaging and protection for shipping[99]. The remaining space can be shared with other kite companies to reduce shipping costs and share the risk, given there will be only 380 units shipped at one time. The shipping takes approximately 28 days, which provides a reasonable inventory restocking timeline[100]. A warehouse of 111.48 $m^2$ costs around €31,248 to build[101]. The warehouse will be built in the vicinity of the port of Rotterdam in Delft which has a leasing cost of €38,000 for 150 $m^2$ of land[102]. There will be a warehouse worker active which costs around €3810.75 per month[103].

Contingency funds, estimated at 5-15% of the total cost per unit, are intended to cover any unexpected expenses[104]. The contingency margin will be applied to the total cost for each batch produced and shipped.

The total R&D + Setup costs is €475,641 which is the sum of:

- Total personnel cost for the conceptual design = €0.
- Total R&D Costs including salary, prototyping and testing, up to the finalised design with three prototypes = €444,393
- Warehouse setup cost = €31,248.

The total cost per PenteFoil unit is €2,046.193 which is the sum of:

- Total cost of the compressive elements and the control frame = €230.
- Manufacturing cost per unit = €1,504.
- Logistics cost per unit = €16.
- Certification costs per unit = €296.

The total operational cost per month after the first year is €35,911 which is the sum of the monthly expenses of:

- Cost of the warehouse worker = €3,811.
- Total cost of the five quality assurance team members which act as support staff and sales representatives for the month there is no active production = €20,656.
- Total cost of the four co-founders = €8,277.
- Total cost for leasing the land for the warehouse = €3,167.

The total R&D + Setup costs of first three years of €617,000 is the sum of:

- Total personnel cost for the conceptual design = €0.
- Cost of materials for three prototypes = €6,000.

[98] https://flybubble.com/connectors/karabiners., Accessed on 10/06/2024.

[99] https://www.movehub.com/lk/international-shipping/the-netherlands/amsterdam-from-colombo/, Accessed on 10/06/2024.

[100] https://www.fluentcargo.com/routes/sri-lanka/netherlands, Accessed on 10/06/2024.

[101] https://www.buildingsguide.com/costs/what-does-it-cost-to-build-a-warehouse/, Accessed on 10/06/2024.

[102] https://lokaleregelgeving.overheid.nl/CVDR711489/1, Accessed on 10/06/2024.

[103] https://www.salaryexpert.com/salary/job/warehouse-worker/netherlands/amsterdam, Accessed on 10/06/2024.

[104] https://multiproject.org/learningcentre/contingency-funds-what-are-they-and-how-much-should-you-set-aside/, Accessed on 10/06/2024.

- Windtunnel testing costs = €106,812.
- Flight testing costs = €12,048.
- Structural testing costs = €24,000.
- certification costs = €888.
- Environmental test machine = €3,640.
- Total personnel cost for three years of R&D = €297,979.
- Warehouse setup cost (building) = €31,248.
- Nine months of marketing = €142,000

A detailed overview of the estimated costs of the R&D and setup costs together with the cost estimation of the production of a batch of 380 PenteFoils can be seen in Table 15.2.

**Table 15.2:** Estimated R&D and setup costs plus a cost estimation of producing a single batch of 380 PenteFoil units.

| Category | Description | Estimated Cost |
|---|---|---|
| R&D + Setup Costs | Conceptual Design, Prototyping, Testing, Research Personnel, warehouse Setup | €475,640.91 |
| Batch (380 Units) Cost | Raw Materials, Manufacturing Processes, Logistics, certification | €777,553.34 |
| Operational Cost (per month) | Leasing, Salary: (Warehouse Worker, Co-founders, Quality Assurance Team) | €35,910.45 |
| Contingency | Unexpected Expenses Per Batch (15%) | €116,633.00 |
| Batch Cost + 15% Contingency Margin | | €894,186.34 |

### 15.1.1. Revenue Projections

**Pricing Strategy:** Determining the price point of the PenteFoil is crucial to the successful launch of the business. The market's leading hang gliders include models that cost up to €15,344.[105,106,107,108]. The performance of the PenteFoil will be on par with these high-performance hang glider models. Additionally, the PenteFoil has the unique feature of being foldable into a volume of 50.8 liters, making it the most portable hang glider on the market. Innovation requires time for consumers to adapt and build trust in its potential. The unique selling point of the PenteFoil, combined with its aggressively positioned price point of €10,000, will drive future pilots towards gradual acceptance and groundbreaking achievements. However, the price point of the PenteFoil may change in the future, adapting to and following market demand and trends. This could potentially increase/decrease the amount of units that can be sold on average.

**Market:** The declining numbers of schools, manufacturers, and new pilots obtaining ratings suggest a declining interest in hang gliding. In contrast, paragliding, the primary competitor of hang gliding, has witnessed increased popularity attributed to its portability and perceived safety advantages[109]. This situation presents PenteFoil with an opportunity to target the younger demographic by offering an exhilarating alternative to paragliding, while maintaining comparable portability. By introducing innovative control methods, PenteFoil can position itself as a fresh and exciting option, distinct from both hang gliders and paragliders.

Additionally, there is potential to gain traction with the PenteFoil project by producing a small batch within the first three years, which will be distributed to flying schools and clubs around Europe. This strategy can generate early interest in the PenteFoil and provide valuable feedback from experienced and new users, as well as instructors. This method helps promote the product to its target audience and allows the company to start out by producing a smaller batch in the first year of production, which could be beneficial in terms of cost and marketing effort. However, it is difficult to estimate the effect this will have on sales. Therefore, it has not yet been included in the ROI and cost breakdown chapters, but will be kept in mind as an option for later implementation.

**Revenue Streams:** The potential revenue streams for the PenteFoil include direct-to-consumer (B2C) sales, business-to-business (B2B) wholesale transactions, leasing arrangements, and licensing agreements with established distributors serving the hang glider and aerial sport sectors. Nevertheless, the primary focus will be on establishing the PenteFoil and the overarching company as an exciting new brand that captivates consumers' interest and entices them to experience it firsthand.

[105] https://www.a-i-r-usa.com/products, Accessed on 06/06/2024.
[106] https://humanbirdwings.net/best-hang-glider/, Accessed on 06/06/2024.
[107] http://www.northwing.com/gliderprices.aspx, Accessed on 06/06/2024.
[108] https://instinct.pro/collections/willswing, Accessed on 06/06/2024.
[109] https://www.smithsonianmag.com/air-space-magazine/rise-and-fall-of-hang-gliding-180972601/, accessed on 06.06.2024

Marketing and sales expenses are estimated to be around 2-5% of total revenue for business-to-business (B2B) and 5-10% of total revenue for business-to-consumer (B2C). For the initial year of production, the marketing and sales are estimated to cost approximately €15,833 per month[110].

**Five-Year Financial Forecast:** The plan outlines annual costs and phases for the company's initial five years of operation. The first three years prioritises establishing infrastructure for smooth manufacturing and logistics, alongside a 27-month R&D phase, with an additional focus on nine months of marketing activities. The cost of the co-founders' salary is included as the primary operational expense for the first three years. In the fourth year, production will commence with one batch of 380 PenteFoils planned for sale within the first month. However, a 5% contingency is included in the manufacturing and shipping costs per batch to account for the probability of units being broken or rendered unusable for flight due to errors in shipping or manufacturing. Operational costs and marketing will span the entire year. By the fifth year, the plan forecasts an expanded market presence, allowing for the production and sale of two batches annually. In this year, marketing expenditures will double as the revenue from selling two batches in one year increases. A detailed overview of the annual financial projection of costs and revenue can be seen in Table 15.3.

**Table 15.3:** Financial projections for the PenteFoil project.

| Year | Expected Costs (€) | Expected Revenue (€) |
|---|---|---|
| 1-3 | 617,000 | 0 |
| 4 | 1,515,111.70 | 3,420,000 |
| 5 | 2,599,298.04 | 6,840,000 |

## 15.2. ROI Calculation

To justify the initial expenditure of the PenteFoil project, a financial performance evaluation includes an ROI calculation to determine whether the investment is yielding returns.

**Initial Investment:** is the sum of all initial costs, including R&D, manufacturing setup, marketing launch, and initial operational costs which is €617,000 in the first three year, €1,515,111.70 in the second year and €2,599,298.04 in the third year.

**Operating Profit:** The expected operating profit is calculated by subtracting total costs from total revenue which is €0 -€617,000 = -€617,000 for the first three years, €3,420,000 - €1,515,111.70 = €1,904,888.3 in year four and €6,840,000 - €2,599,298.04 = €4,240,701.96 for year five.

**Return on Investment (ROI)** The ROI is calculated as the ratio of operating profit to initial investment, expressed as a percentage. The ROI of the PenteFoil project can be computed using Equation 15.3.

$$\text{ROI} = \left( \frac{\text{Operating Profit}}{\text{Initial Investment}} \right) \times 100 \tag{15.3}$$

Using Equation 15.3 to calculate the projected profits for the fourth year results in an ROI of 125.58%. The ROI for the fifth year is 163.15%. In the first three years there are only R&D activities resulting in an ROI of -100%.

## 15.3. Operational Profit Overview

To gain deeper insights into the cash flow and liquidity of the project during its initial five years, refer to the comprehensive monthly/annual profit and loss (P&L) statement in Table 15.4. The statement projects monthly and annual revenues, costs, and operating profit. Unit sales are anticipated to increase exponentially. After the production of the first batch, the company needs to sell a total of 284 units to generate sufficient liquidity for producing an additional batch. Analysis indicates that from the third year onward, the company is expected to maintain adequate liquidity to support sustainable growth in production rates. To clarify, the total revenue for years four and five must include a 5% contingency to account for potential losses in units during manufacturing and shipping, which is not currently included in Table 15.4. Therefore, the total revenue, gross profit, and operational profit will be lower than indicated.

[110] https://www.bdc.ca/en/articles-tools/marketing-sales-export/marketing/what-average-marketing-budget-for-small-business, Accessed on 06/06/2024.

**Table 15.4:** Five-Year Profit and Loss Statement.

| Year/Month | Revenue (€) | Cost of Goods Sold (€) | Gross Profit (€) | Operating Expenses (€) | Operating Profit (€) |
|---|---|---|---|---|---|
| **Years 1-3 Total** | 0 | 0 | 0 | 617,000 | -617,000 |
| **Year 4** | | | | | |
| January | 0 | 0 | 0 | 51,743.78 | -51,743.78 |
| February | 20,000 | 4,093.86 | 15,906.14 | 51,743.78 | -35,837.64 |
| March | 20,000 | 4,093.86 | 15,906.14 | 51,743.78 | -35,837.64 |
| April | 40,000 | 8,187.72 | 31,812.28 | 51,743.78 | -19,931.50 |
| May | 80,000 | 16,375.44 | 63,624.56 | 51,743.78 | 11,880.78 |
| June | 160,000 | 32,750.88 | 127,249.12 | 51,743.78 | 75,505.34 |
| July | 300,000 | 61,407.93 | 238,592.07 | 51,743.78 | 186,848.29 |
| August | 490,000 | 100,389.12 | 389,610.88 | 51,743.78 | 337,867.10 |
| September | 610,000 | 124,837.59 | 485,162.41 | 51,743.78 | 433,418.63 |
| October | 670,000 | 137,221.38 | 532,778.62 | 51,743.78 | 480,034.84 |
| November | 580,000 | 118,871.90 | 461,128.10 | 51,743.78 | 409,384.32 |
| December | 870,000 | 178,300.06 | 691,699.94 | 51,743.78 | 639,956.16 |
| **Year 4 Total** | **3,800,000** | **894,186.34** | **2,905,813.66** | **583,731.36** | **2,322,082.30** |
| **Year 5** | | | | | |
| January | 0 | 0 | 0 | 67,577.13 | -67,577.13 |
| February | 40,000 | 8,184.77 | 31,815.23 | 67,577.13 | -35,761.90 |
| March | 50,000 | 10,230.97 | 605,769.03 | 67,577.13 | 538,191.90 |
| April | 90,000 | 18,415.74 | 652,584.26 | 67,577.13 | 585,007.13 |
| May | 170,000 | 34,886.26 | 735,113.74 | 67,577.13 | 667,536.61 |
| June | 320,000 | 65,549.38 | 830,450.62 | 67,577.13 | 762,873.49 |
| July | 590,000 | 120,789.99 | 869,210.01 | 67,577.13 | 801,633.88 |
| August | 970,000 | 198,684.62 | 771,315.38 | 67,577.13 | 703,739.25 |
| September | 1,200,000 | 245,543.16 | 954,456.83 | 67,577.13 | 886,879.70 |
| October | 1,320,000 | 268,097.84 | 1,051,902.16 | 67,577.13 | 984,325.03 |
| November | 1,140,000 | 233,478.82 | 906,521.18 | 67,577.13 | 838,944.05 |
| December | 1,710,000 | 350,646.00 | 1,359,354.00 | 67,577.13 | 1,291,776.87 |
| **Year 5 Total** | **7,600,000** | **1,788,372.68** | **5,811,627.32** | **810,925.56** | **5,000,701.76** |

# Part V - Future Development

# 16 | Further Development

This chapter describes the further development of the PenteFoiling project after the completion of the DSE. First, the most important next steps for the project are outlined in Section 16.1. Based on these steps a Project Design and Development Logic was created, described in Section 16.2. Finally, the steps were summarised and allocated in time using a Gantt chart, which can be found in Section 16.3.

## 16.1. Overview of Next Steps

This section outlines the most important next steps after the end of the DSE. Following this procedure will help move PenteFoil from a preliminary design concept to a commercially viable product.

All design tasks completed until now were purely theoretical. This approach allows for rapid development and doesn't require a lot of resources but has many limitations. The performed calculations relied on many assumptions that only approximate real-world phenomena. To address this, the most important step at this stage of design is creating a functioning prototype of the PenteFoil. This can help validate the design and serve as a proof of concept for potential investors, aiding in fundraising needed to launch full-scale production. Details regarding the prototype manufacturing and costs are outlined in Section 8.1.

In addition to creating the prototype, it is crucial further develop the safety and training procedures of the PenteFoil. This involves researching existing regulations and standards related to training to verify compliance and identify any gaps. Ensuring adequate training can reduce risks and improve the overall safety and reliability. Furthermore, additional safety research is essential, with special attention given to understanding the effects of gusts and methods to prevent wing collapse, major safety concerns identified in Section 13.4. Performing tests with the prototype can provide valuable insights into the safety of the PenteFoil.

Once the prototype has been thoroughly tested and iterated upon, full-scale production can begin. Establishing contact with manufacturers and suppliers to obtain detailed information on costs and feasibility of production is necessary. These partnerships will play an important role in ensuring a smooth transition from prototyping to production.

Parallel to this, extensive marketing efforts should be launched to generate interest and secure market position. Further market research should be conducted, including engaging with the hang gliding community and obtaining letters of intent. It is also recommended to collaborate with flying schools in the Netherlands, which could offer PenteFoil flying to their customers. Building strong relationships with stakeholders will help create buzz and attract potential buyers.

## 16.2. Project Design and Development Logic

The Project Design and Development Logic diagram presents all practical activities required to fully design and develop the PenteFoil. It emphasises activities that would need to be performed once the DSE ends, such as prototyping, production and sales & marketing. As the realisation of such a system is an iterative process, multiple iteration loops have been integrated into the diagram. The process starts with the design, after which prototyping is performed. Once the prototype demonstrates a successful functioning of the system, sales, marketing and production can take place in parallel. A manufacturing plan and sales strategy can be set up at the same time. A key decision in the production process is whether to manage production in-house or to outsource it. Once the developed products have been tested and the logistics have been worked out, production can take place on a larger scale. Client satisfaction and the amount of sales can then be used as a measure of success of the project.

## 16.3. Further Development Gantt Chart

The last diagram of this chapter is the Project Gantt Chart. It presents the post-DSE activities in the Gantt chart format. The Project Gantt Chart flows logically from the Project Design and Development Logic diagram, but gives yet another unique perspective of the project. It does this by giving an indication of the start and end times of different post-DSE activities and their planned duration. It serves as an initial estimate for the schedule for the post-DSE activities and may be subject to change. For simplicity and clarity, iteration loops have not been included and the option for outsourcing the production process has not been shown.

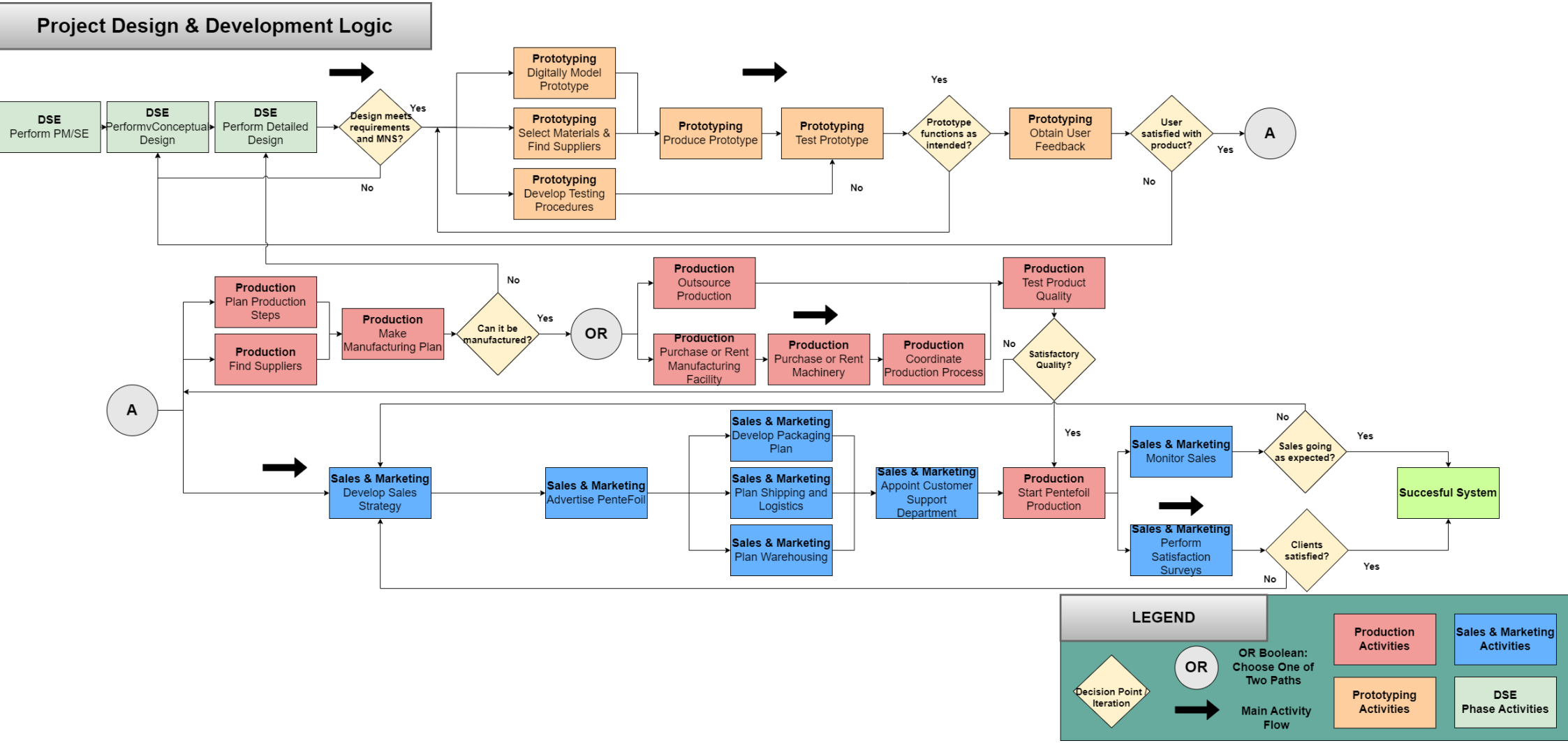
Project Design & Development Logic
DSE
Perform PM/SE
DSE
PerformvConceptua
Design
DSE
Perform Detailed
Design
Design meets requirements and MNS?
Yes
No
Prototyping
Digitally Model
Prototype
Prototyping
Select Materials &
Find Suppliers
Prototyping
Develop Testing
Procedures
Prototyping
Produce Prototype
Prototyping
Test Prototype
Prototype functions as intended?
Yes
No
Prototyping
Obtain User
Feedback
User satisfied with product?
Yes
No
A
Production
Plan Production
Steps
Production
Find Suppliers
Production
Make
Manufacturing Plan
Can it be manufactured?
Yes
No
OR
Production
Outsource
Production
Production
Purchase or Rent
Manufacturing
Facility
Production
Purchase or Rent
Machinery
Production
Coordinate
Production Process
Production
Test Product
Quality
Satisfactory Quality?
No
A
Sales & Marketing
Develop Sales
Strategy
Sales & Marketing
Advertise PenteFoil
Sales & Marketing
Develop Packaging
Plan
Sales & Marketing
Plan Shipping and
Logistics
Sales & Marketing
Plan Warehousing
Sales & Marketing
Appoint Customer
Support
Department
Production
Start Pentefoil
Production
Yes
Sales & Marketing
Monitor Sales
Sales & Marketing
Perform
Satisfaction
Surveys
Sales going as expected?
No
Yes
Clients satisfied?
No
Yes
Succesful System
LEGEND
Decision Point / Iteration
OR
OR Boolean: Choose One of Two Paths
Main Activity Flow
Production Activities
Sales & Marketing Activities
Prototyping Activities
DSE Phase Activities

| ID | WBS | Task Name | Duration |
|---|---|---|---|
| 0 | **0** | **PenteFoiling Project - Post DSE** | **30 mons** |
| 1 | **1** | **Prototyping Phase** | **14 mons** |
| 2 | 1.1 | Digitally Model Prototype | 2 mons |
| 3 | 1.2 | Select Materials & Find Suppliers | 2 mons |
| 4 | 1.3 | Develop Testing Procedures | 4 mons |
| 5 | 1.4 | Produce Prototypes and Iterate | 6 mons |
| 6 | 1.5 | Test Prototype | 4 mons |
| 7 | 1.6 | Obtain User Feedback | 2 mons |
| 8 | **2** | **Production Phase** | **14 mons** |
| 9 | 2.1 | Plan Production Steps | 3 mons |
| 10 | 2.2 | Find Suppliers | 3 mons |
| 11 | 2.3 | Make Manufacturing Plan | 2 mons |
| 12 | 2.4 | Purchase or Rent Manufacturing Facility | 1 mon |
| 13 | 2.5 | Purchase or Rent Machinery | 1 mon |
| 14 | 2.6 | Coordinate Production Process | 2 mons |
| 15 | 2.7 | Test Product Quality | 3 mons |
| 16 | 2.8 | Start PenteFoil Production | 1 mon |
| 17 | **3** | **Sales & Marketing Phase** | **16 mons** |
| 18 | 3.1 | Develop Sales Strategy | 3 mons |
| 19 | 3.2 | Advertise PenteFoil | 5 mons |
| 20 | 3.3 | Develop Packaging Plan | 2 mons |
| 22 | 3.5 | Plan Warehousing | 2 mons |
| 21 | 3.4 | Plan Shipping and Logistics | 3 mons |
| 23 | 3.6 | Appoint Customer Support Department | 1 mon |
| 24 | 3.7 | Monitor Sales | 2 mons |
| 25 | 3.8 | Perform Satisfaction Surveys | 2 mons |

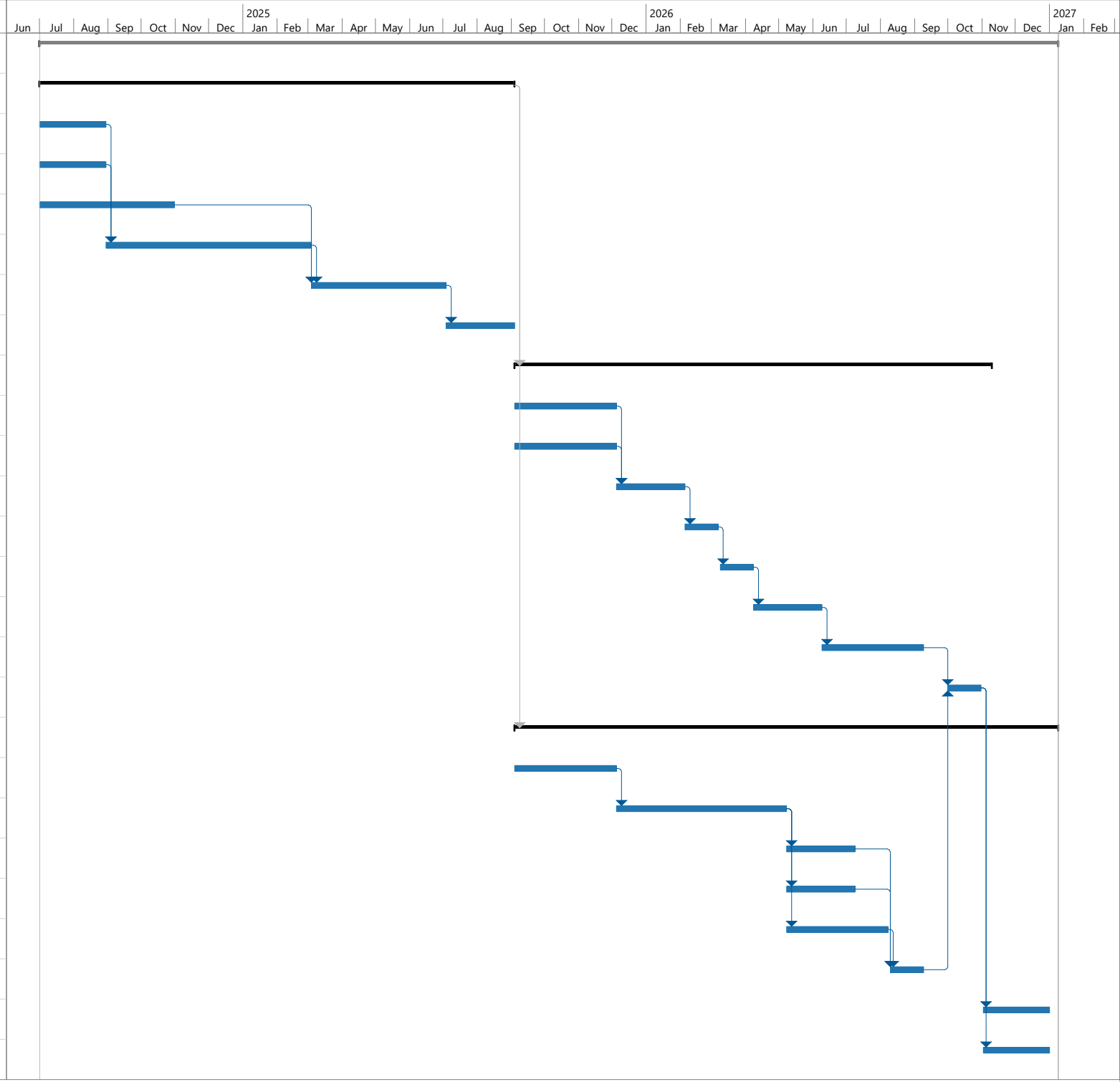


Project: PenteFoiling Project - Post DSE
Date: Mon 24-6-24

Task Summary Project Summary

# 17 | Sustainable Development Strategy

As climate change is one of the biggest concerns of this era, sustainable development is crucial for a greener future. Therefore the PenteFoil will be designed with sustainability in mind. First, sustainable development strategies in the design are discussed, after which the actions implemented by the group are elaborated upon.

## 17.1. Sustainable Development Strategies in the Design

The PenteFoil is an unpowered system, eliminating carbon emissions during flight. In order to develop a sustainable system, material choice and production methods will have the biggest impact on the sustainability of the design. Some sustainable development strategies have been established and are shown below.

1. **Circular Design Approach:** A circular design approach is incorporated where the focus is to reduce waste as much as possible. Firstly, 87% of the mass of the materials are recyclable. At the end-of-life, the design of the PenteFoil will allow the product to be separated into different parts and sent to different companies for recycling. The non-recyclable modular CFRP tubes can be reused for example in the camping tent structures, and the Dyneema cables can be applied to fishing rods production. Furthermore no recycled materials have been incorporated in the design yet, however nylon and aluminium tubes are easily recycled from old canopies or tents and aluminum cans respectively. For further development companies that recycle these materials can be contacted to include more circularity in the manufacturing process.
2. **Sustainable Manufacturing Processes (Fair Trade):** Waste generation will be reduced by deploying sustainable manufacturing practices. This can be assessed by the relative weight of waste in the production of the final product. Furthermore, collaborating with manufacturing companies in Sri Lanka it is aimed to implement Fair Trade practices. One of the goals is to ensure that all workers involved in the production of the PenteFoil receive fair wages that meet or exceed the local living wage standards. This commitment will help improve the quality of life for workers and their families. In addition to fair wages, safe and healthy working conditions will be ensured, aligning with international labor standards. To demonstrate the commitment to Fair Trade principles, a Fair Trade certification for PenteFoiling manufacturing operations in Sri Lanka will be sought. This certification will provide assurance to customers that the PenteFoil is produced under ethical conditions. Transparency in the supply chain will be maintained by regularly publishing reports on labor practices, environmental impact, and community engagement efforts. Finally, producing the PenteFoil in Sri Lanka significantly reduces CO2 emissions, as the necessary facilities are already in place and do not need to be constructed. This is based on the assumption that the same manufacturing facility will be used as Epic Kites.
3. **Minimalist Design Approach:** By simplifying the design to include only the essential components needed for the mission, we can reduce the amount of materials used and processed. For example, all Tensairity wires and rods have the same dimensions, so the components can be ordered in bulk and used for different purposes. This approach leads to lower emissions and less waste production.
4. **Modular Design for Repair:** A modular design allows for easier maintenance. It will be possible to repair or replace parts that are damaged more easily. This increases the lifespan of the PenteFoil and thereby makes it more sustainable.
5. **Durable Materials:** By using materials with a long lifetime in the environment they will have to perform, the PenteFoil will be more durable and therefore more sustainable. This has not been incorporated yet, for further development the material of the foil should been chosen so that UV degradation will be reduced as much as possible to increase its lifetime.
6. **Life Cycle Assessment:** Apart from these design approaches, a life cycle assessment will be performed upon further development. This assessment evaluates the environmental impact in terms of waste and emissions for the process, from the raw material extraction to the end-of-life disposal. This assessment will be used to optimise a sustainable development.

It should be noted that the manufacturing of the PenteFoil does not fit within the scope of the DSE, so the development strategies made for manufacturing companies and the logistics behind this will not be implemented but are given as a strategy for future development.

## 17.2. Sustainable Strategies Implemented by the Team

In addition to the sustainable strategies for the system itself. There are some sustainable development strategies that can be implemented by the team itself in order to promote a sustainable process.

1. **Designated Sustainability Officer:** One of the team members has been appointed to be the sustainability officer. The sustainability officer is responsible for the sustainability of the design. The main task for the sustainability officer is to create sustainability goals and to check throughout the design project whether the group is on the right track to reach the sustainability goals.
2. **Cross-Functional Team Collaboration:** The team consists of 10 members who have experience in various fields. These disciplines comprise of engineering, business administration, computer science, robotics, management, value sensitive innovation, climate change impact adaptation & mitigation, project management, finance, and designing sustainable transitions. This diverse team provides different perspectives and expertise to address the sustainability challenges.
3. **Incorporate Sustainability Criteria into Decision-Making Processes:** Sustainability criteria are integrated into decision-making processes at every stage of the project, from design and concept development to operations and manufacturing. Design alternatives and strategic decisions are evaluated considered with environmental, social and economic factors in mind.

## 17.3. Recycling Plan

One of the key sustainable practices implemented in the design was the use of recycled and/or recyclable materials for the structure. This aspect was briefly mentioned in Section 17.1. Still, to provide the reader with more awareness of how exactly these materials align with the sustainable approach, this section proposes possible sources of recycled materials and ways to recycle the materials at the end of life.

Below are the materials of the PenteFoil that can be sourced from other applications to be reused in the system of this project:

- **Ripstop nylon:** Can be recycled from used parachutes, old tents, and outdoor gear like backpacks and jackets. Ripstop nylon is widely used in outdoor and sporting goods due to its resistance to tearing and lightweight nature.
- **TPU:** Can be recycled from inflatable products like air mattresses, inflatable boats, and some sports equipment.
- **Dyneema cables:** Can be recycled from fishing nets, climbing ropes, and high-performance sailing ropes.
- **Aluminium:** Can be recycled from beverage cans, old aircraft, automotive parts, and construction materials. Aluminum is one of the most recyclable materials, with a well-established recycling industry.

The materials that cannot be recycled to use in the PenteFoil are Dyneema webs, Velcro straps and CFRP tubes. The Dyneema webs are the most critically loaded structural component, and to avoid the unexpected loss of strength due to fatigue it is recommended to implement brand new fibres in the PenteFoil product. While CFRP are technically recyclable, the recycling processes for CFRP are more complex and energy-intensive, and it is more sustainable to buy new tubes. The use of recycled Velcro is also limited, as Velcro may loose its fastening properties over time of active use.

Below are the proposed applications for recycling PenteFoil's materials at the end of life:

- **Ripstop nylon:** Can be recycled into new outdoor gear such as tents, backpacks, and jackets. Recycled ripstop nylon can also be used in the production of tarps, lightweight covers, and kites.
- **TPU:** Can be recycled into new inflatable products like air mattresses, inflatable boats, and sporting goods. TPU can also be repurposed for making flexible hoses, seals, and industrial coatings.
- **Dyneema cables and fibres:** Can be recycled into new climbing ropes, marine ropes, and high-strength industrial cords.
- **Aluminium:** Can be recycled into new beverage cans, automotive parts, aircraft components, and construction materials. Aluminum can be continuously recycled into the same types of products without losing its properties.
- **CFRP:** Can be recycled into reinforced plastic components for automotive and aerospace industries, new sporting goods like bicycle frames and golf clubs. Recycled carbon fiber can also be used in construction materials and other high-strength, lightweight applications.
- **Velcro:** Can be recycled into new hook-and-loop fasteners for clothing, footwear, and various consumer products. Depending on the recycling process, Velcro can also be repurposed into industrial fastening solutions or components for medical devices.

This analysis shows that the majority of the materials can both be recycled and is recyclable, proving the implementation of sustainability of the design.

# Part VI - Recommendations and Conclusion

# 18 | Conclusion & Recommendations

## 18.1. Conclusion

The purpose of this report was to present the outcome of the work by a group of 10 students in the past 10 weeks on design of the PenteFoil, an inflatable wing attached directly to the user filling the gap between wingsuit flying, paragliding and hang gliding. The report covers in detail all aspects of developing a new product that adresses the market gap of the aerial sports: market analysis, design, associated operations, management of risk and resources and business analysis.

The idea of the PenteFoil originated from humankind's long-lasting dream of achieving flight using only the modified human body, inspired by flying animals. Today, aerial sports such as paragliding, hang gliding, skydiving, and wingsuit flying continue to pursue this dream. Wingsuit flying, in particular, offers a thrilling high-speed experience but poses significant risks due to limited control methods and the potential for catastrophic consequences from minor miscalculations or unexpected conditions.

To enhance the safety of wingsuit flying, inspiration can be drawn from paragliding, which boasts a lower mortality rate due to its inherently stable, large inflatable wing and suspension lines that ensure stability and dynamic control. However, paragliding's slower speeds, sitting position and passive flying experience may not appeal to thrill-seekers or those looking for a more natural flight experience. This led to the development of PenteFoiling, an activity that merges the advantages of both sports together.

The PenteFoil features a wing design that is innovative, elegant, and sporty, attracting all thrill-seekers, visualised in Figure 18.1 and Figure 18.2. A reflexed airfoil was deemed necessary for stability, leading to the selection of a modified MH-81 airfoil with a 5-degree upward deflection of the trailing edge. The final wing design boasts a span of 10 m, a root chord of 1.37 m, and a tip chord of 1 m. A smooth curvature achieves a dihedral of 5° and a sweep of 12° at the quarter-chord. The wing is by default trimmed at 75 km/h at a $C_L$ of 0.5, and it was designed to be both longitudinally and laterally stable.

**Figure 18.1:** The PenteFoil with tips unfolded.

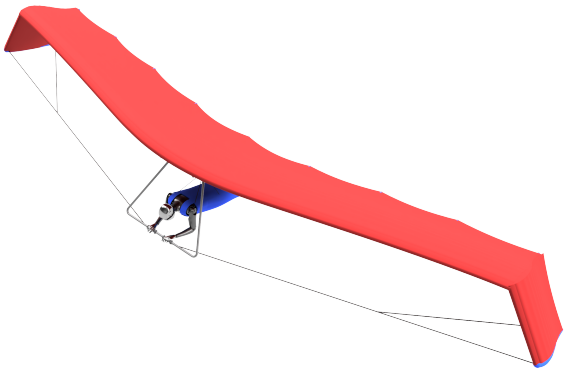

**Figure 18.2:** The PenteFoil with tips folded.

The PenteFoil's wing structure was meticulously designed to balance mass, cost, operatability and manufacturability. The wing comprises a series of 10 enclosed cells formed by sewing fabric pieces to approximate the desired airfoil shape. These cells have varying radii and are connected with straight webs to optimise load distribution. The cells extend from the leading edge to 70% of the chord, transitioning to a straight elements that converge at a trailing edge cable to maintain tension and shape under load. Tubular ribs placed every 1 meter extend from the last cell to the trailing edge, ensuring the airfoil shape is consistent across the span. The ripstop nylon tubes houses an airtight TPU bladder inside each cell. The wing features a smooth outer fabric layer for better aerodynamics, attached with Velcro for ease of assembly. The strength and stiffness are mainly provided by web Tensairity beams, whose structural elements include CFRP compression elements and tension elements and webbing made out of Dyneema. Additionally, an aluminium steering frame in front of the pilot provides control, though this element was not designed in detail. 87% of materials making up the structure are recyclable, and, if arranged with the appropriate suppliers in the future, a significant portion of them can be made from recycled items. Figure 18.3 presents a cross-sectional view of the PenteFoil wing, highlighting the airfoil shape and the most important structural elements.

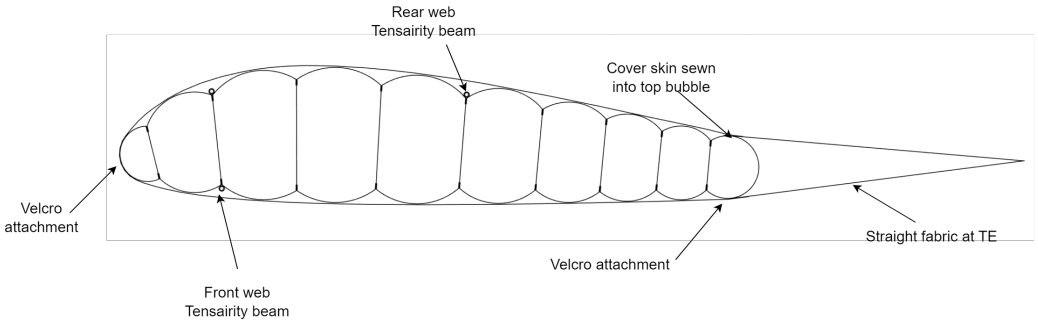


**Figure 18.3:** The cross-section view visualising the airfoil shape and structural elements.

The operations of the PenteFoil resemble those of an advanced hang glider but with the advantage of compactness, transportability and wingtip folding. The PenteFoil can be folded into a backpack, making it easy to transport to the take-off location by hiking up a mountain or using a ski lift. It is capable of operating at an altitude differential of at least 3 km, depending on the launch altitude. The wing must be inflated to the specified pressure using a hand pump before take-off. During take-off, the wing is held above the body using the steering frame. After running against the wind to achieve lift-off, the skypod can be zipped up to align the pilot with the wing. In flight, the PenteFoil is controlled by bracing against the steering frame and shifting the body's C.G. The wing also allows achieving higher speeds by folding the wing tips to dive. To land, the skypod should be unzipped, and the wing slowly flared up, stalling roughly 1 meter above the ground to touch down gently.

The PenteFoil includes an emergency landing procedure using an emergency parachute, enhancing safety. Additionally, wearing a helmet is mandatory, and a hook knife is included to cut off the wing if it interferes with the parachute deployment. These safety measures ensure that pilots can handle unexpected situations and land safely.

Furthermore, the report reviewed various critical aspects of the PenteFoil project. It includes an examination of safety protocols, manufacturing processes, and testing procedures. A plan for post-DSE development is provided, outlining the steps needed to further refine and commercialise the PenteFoil. Additionally, an analysis of the business aspects involved in bringing the PenteFoil to market is presented, covering everything from cost estimation and mass production strategies to marketing and distribution plans. This approach ensures that all factors necessary for successfully realising the PenteFoil are thoroughly considered and addressed.

## 18.2. Recommendations

This section presents recommendations aimed at improving the design concept of the PenteFoil. These are additional to the future steps taken in developing the project outlined in Chapter 16. They are intended to further enhance performance, user experience, and market acceptance, beyond the level considered in this report.

1. **Ergonomics Testing**
    - Conduct ergonomics testing with experienced hang glider pilots to ensure the design meets user expectations and is comfortable and intuitive to control.
2. **Stakeholder Involvement**
    - Consult with various stakeholders, form backgrounds different than engineering, about the current design, to refine and improve the product based on more diverse perspectives.
3. **Material Exploration**
    - Explore alternative materials that offer better performance, durability, or lower environmental impact.
4. **Initialisation and Folding Mechanisms**
    - Design more efficient initialisation and folding procedures to speed up user operations. Simplify the current method, to help avoid user error, improving safety.
5. **Aerodynamic Improvements**
    - Conduct CFD or wind tunnel tests to analyse post-stall behavior for landing.
    - Investigate the impact of imperfect airfoil shapes (caused by the inflatable structure) on lift and drag.
    - Analyse flow interference effects of the pilot and wing on lift and drag using CFD.
    - Study ground effect phenomena during landing through CFD or wind tunnel testing.
6. **Training Program Development**

- Improve the training program so that provides a realistic flying experience. This could also be used to gather data for further design improvements.

7. **Model Variations**
   - Design different models or configurations tailored to specific target groups such as beginners, performance-oriented users, acrobats, children, and various body types.
8. **Partnerships**
   - Approach companies like Red Bull known for their involvement in extreme sports, to contribute resources and expertise to the project.
9. **Durability Testing**
   - Conduct long-term durability testing to evaluate the effects of aerodynamic and handling loads over time, as well as environmental impacts such as UV exposure and humidity.
10. **Safety Research**
    - Explore different training and user education methods, which can minimise the likelihood and severity of user errors.
    - Perform additional safety research, focusing on the effects of gusts and methods to prevent wing collapse.

These recommendations are designed to advance the PenteFoil project by addressing current limitations and identifying opportunities for improvement. They aim to guide on enhancing the design concept rather than outlining the immediate next steps in the development process. Implementing these strategies will help develop a user-friendly, and market-competitive product.

# References


[1] F. Zöllner. *Leonardo da Vinci: The Complete Paintings and Drawings*. Köln: Taschen, 2016, p. 644.

[2] P. Bouchat and E. Brymer. “BASE Jumping Fatalities Between 2007 and 2017: Main Causes of Fatal Events and Recommendations for Safety”. In: *Wilderness & Environmental Medicine* 30.4 (2019). PMID: 31704133, pp. 407–411. DOI: 10.1016/j.wem.2019.07.001. URL: https://doi.org/10.1016/j.wem.2019.07.001.

[3] O. Mei-Dan et al. “Fatalities in Wingsuit BASE Jumping”. In: *Wilderness & Environmental Medicine* 24.4 (2013), pp. 321–327. DOI: 10.1016/j.wem.2013.06.010. URL: https://doi.org/10.1016/j.wem.2013.06.010.

[4] F. Feletti et al. “Incidents and Injuries in Foot-Launched Flying Extreme Sports”. In: *Aerospace Medicine and Human Performance* 88.11 (2017), pp. 1016–1023. DOI: https://doi.org/10.3357/AMHP.4745.2017.

[5] U. Canbek et al. “Characteristics of injuries caused by paragliding accidents: A cross-sectional study”. In: *World Journal of Emergency Medicine* 6.3 (2015), pp. 221–224. DOI: 10.5847/wjem.j.1920-8642.2015.03.011.

[6] M. Wilkes, G. Long, and M. Tipton. “Quantifying Risk in Air Sports: Flying Activity and Incident Rates in Paragliding”. In: *Wilderness and Environmental Medicine* 33 (1 2022).

[7] I. Kroo. *Aerodynamics, Aeroelasticity, and Stability of Hang Gliders - Experimental Results*. Tech. rep. NASA Ames Research Center, 1981.

[8] E. Kilkenny. “An Experimental Study of the Longitudinal Aerodynamic and Static Stability Characteristics of Hang Gliders”. PhD thesis. Cranfield Institute of Technology, 1986.

[9] M. Cook and M. Spottiswoode. “Modelling the flight dynamics of the hang glider”. In: *The Aeronautical Journal* 109.1102 (2005). DOI: 10.1017/S0001924000001007.

[10] R. Langtry and F. Menter. “Correlation-Based Transition Modeling for Unstructured Parallelized Computational Fluid Dynamics Codes”. In: *AIAA Journal* 47 (2009). DOI: https://doi.org/10.2514/1.42362. URL: https://arc.aiaa.org/doi/10.2514/1.42362.

[11] S. Lu, J. Liu, and R. Hekkenberg. “Mesh Properties for RANS Simulations of Airfoil-Shaped Profiles: A Case Study of Rudder Hydrodynamics”. In: *Journal of Marine Science and Engineering* (2021). DOI: https://doi.org/10.3390/jmse9101062. URL: https://www.mdpi.com/2077-1312/9/10/1062.

[12] T. Majid and B. Jo. “Comparative Aerodynamic Performance Analysis of Camber Morphing and Conventional Airfoils”. In: *Applied Sciences* (2021). DOI: https://doi.org/10.3390/app112210663. URL: https://www.mdpi.com/2076-3417/11/22/10663.

[13] E. Kilkenny. *Full Scale Wind Tunnel Tests on Hang Glider Pilots*. Tech. rep. Delft University of Technology, 1984.

[14] T. van Holten et al. *PenteFoiling Midterm Report*. Tech. rep. Delft University of Technology, 2024.

[15] P. Dees. “Hang Glider Design and Performance”. In: *10th AIAA Aviation Technology, Integration, and Operations (ATIO) Conference*. 2010.

[16] J. Mulder et al. *Flight Dynamics: Lecture Notes*. AE3212-I Flight Dynamics course, TU Delft. 2013.

[17] P. Sachinis et al. *Flight Dynamics Report*. Tech. rep. TU Delft, 2024.

[18] E. Reid and R. Loyd Duff. *Dynamics of Flight - Stability and Control*. John Wiley & Sons, INC., 1995.

[19] Y. Ochi. “PILOT’S CG LOCATION AND ATTITUDE CONTROL FOR LATERAL MANEUVER OF A HANG GLIDER”. In: *Congress of the International Council of Aeronautical Sciences* (2016).

[20] T. Mcdaniel. *Flying machine*. US Patent 1,905,298. Apr. 1933.

[21] T. Smith et al. “Ballute and Parachute Decelerators for FASM/Quicklook UAV”. In: *17th AIAA Aerodynamic Decelerator Systems Technology Conference and Seminar*. DOI: 10.2514/6.2003-2142. eprint: https://arc.aiaa.org/doi/pdf/10.2514/6.2003-2142. URL: https://arc.aiaa.org/doi/abs/10.2514/6.2003-2142.

[22] R. Luchsinger et al. “The new structural concept Tensairity: Basic principles”. In: *Progress in structural engineering, mechanics and computation* (2004), pp. 323–328.

[23] J. Breuer and R. Luchsinger. “Inflatable kites using the concept of Tensairity”. In: *Aerospace Science and Technology* 14.8 (2010), pp. 557–563.

[24] D. Raj and M. Devi. “Performance analysis of the mechanical behaviour of seams with various sewing parameters for nylon canopy fabrics”. In: *International Journal of Clothing Science and Technology* 29.4 (2017), pp. 470–482.

[25] J. Breuer, W. Ockels, and R. Luchsinger. “An inflatable wing using the principle of Tensairity”. In: *48th AIAA Structures, Structural Dynamics and Materials Conference* (2007). URL: http://resolver.tudelft.nl/uuid:306785d0-f75b-4378-a145-75905c83efa7.

[26] T. Wever. “Tensairity: The effect of internal stiffeners on the buckling behaviour of an inflatable column: An experimental study”. Master’s thesis. Delft, Netherlands: Delft University of Technology, Faculty of Civil Engineering and Geosciences, Structural Design Lab, Oct. 2008.

[27] T. Sweeney and W. Nixon. “An introduction to the Princeton sailwing windmill”. In: *WIND ENERGY CONVERSION SYSTEMS* (1973), p. 70.

[28] British Hang Gliding and Paragliding Association. *Parachute Advice*. https://www.bhpa.co.uk/pdf/Parachute_Advice.pdf. Accessed: 2024-06-04. n.d.

[29] European Union Aviation Safety Agency. *CS-23 Amendment 2 (corrigendum)*. 2020. URL: https://www.easa.europa.eu/sites/default/files/dfu/CS-23%20Amendment%202%20(corrigendum).pdf.

[30] A. Spaulding. “New Product Development Practices Of The U.S. Confectionery Manufacturers: 2006 Survey Preliminary Findings”. In: *American Agricultural Economics Association (New Name 2008: Agricultural and Applied Economics Association), 2006 Annual meeting, July 23-26, Long Beach, CA* (2006).

[31] J. Law and G. Owen. *A Dictionary of Accounting*. 3rd ed. Oxford University Press, 2005. ISBN: 0192806270, 9780192806277.

[32] L. Li et al. “Computer Modeling of Sewing Machine Pedal Mechanism Based on Information Technology”. In: *Advances in Transdisciplinary Engineering*. Advances in Transdisciplinary Engineering 33 (2022), pp. 343–348. DOI: 10.3233/ATDE221185.

# A | Functional Analysis

In this chapter, the tasks and activities to be performed in the lifetime of the PenteFoil are outlined. The diagrams in this chapter have been used as guidelines throughout the project, providing clarity in the functions the system needs to accomplish. In Section A.1 the Functional Breakdown Structure is discussed, and in Section A.2 the Functional Flow Diagram is discussed.

## A.1. Functional Breakdown Structure

This diagram shows the Functional Breakdown Structure (FBS) of the functions that need to be performed by the design team and the functions that our design should comply with. The project has been divided into five main functions; *Design the PenteFoil System*, *Produce the PenteFoil System*, *Distribute the PenteFoil System*, *Operate the PenteFoil System* and *Retire the PenteFoil System*. Since this project focuses mostly on the design of the PenteFoil system, the design and operational functions of the PenteFoil system have been expanded with sub-functions.

The Functional Breakdown Structure diagram visually represents the hierarchy of functions required to create and operate the PenteFoil system. It provides a summary of the essential functions necessary for both design and operation. On the following page, the FBS diagram illustrates the top-level functions, as well as lower-level design and operational functions, offering a comprehensive understanding of how these functions interrelate. This hierarchical breakdown clarifies the specific capabilities the system must possess.

## A.2. Functional Flow Diagram

This chapter includes two Functional Flow Diagrams (FFD) to illustrate the functional progression of the PenteFoil system. The first diagram covers the entire lifecycle of the PenteFoil, while the second focuses on its operational functions. The first Functional Flow Diagram shows the tasks and functions spanning the PenteFoil's lifecycle, from initial market analysis and system design to operation and eventual retirement of the system. This diagram highlights the relationships between various functions and provides a clear roadmap to achieve a successful system.

The second diagram details the functions specific to the operation of the PenteFoil. It begins with transportation and setup, followed by flight procedures, including emergency landing protocols, and concludes with packing up the system. This cycle can be repeated for each operation. When the PenteFoil's final flight is completed, the system should be sustainably retired. This diagram indicates all the functions that the system will have to perform to complete a flight and therefore is a handy tool when designing the system to check whether the system can comply with all the functions during operating conditions.

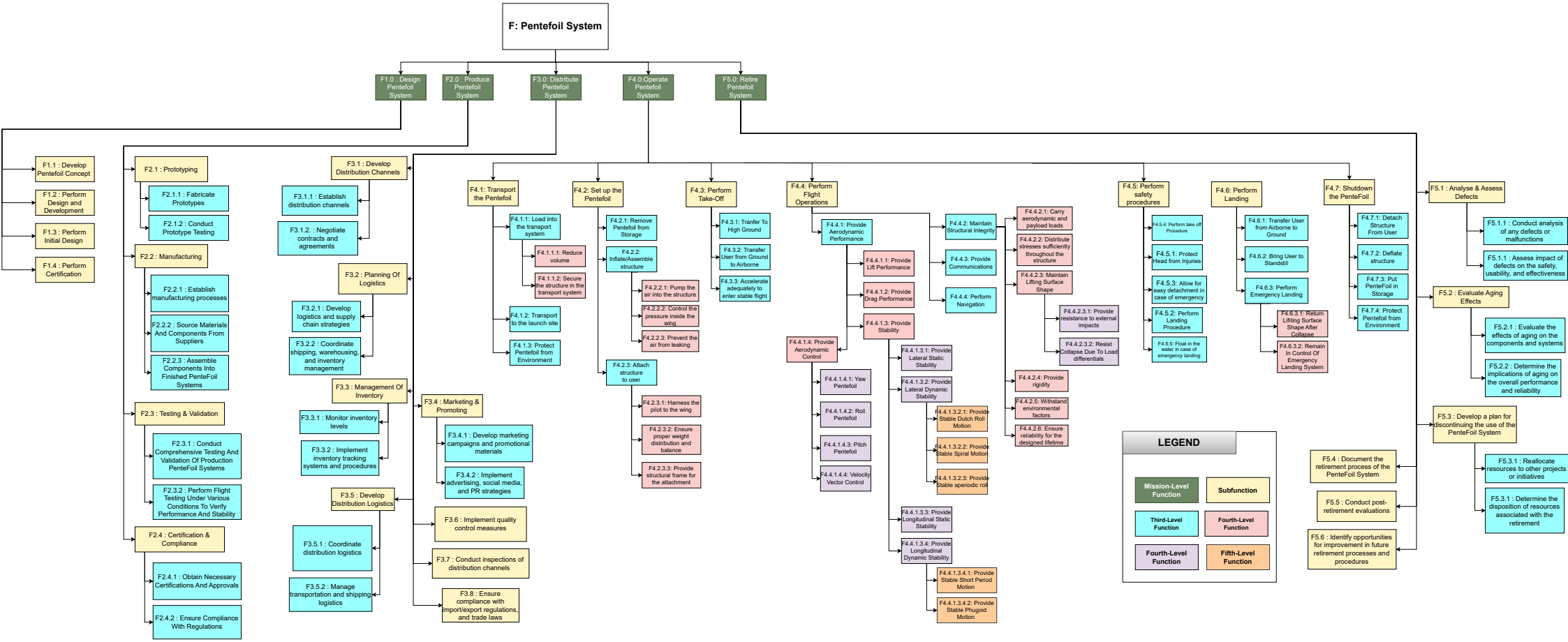
F: Pentefoil System
F1.0 : Design Pentefoil System
F2.0 : Produce Pentefoil System
F3.0: Distribute Pentefoil System
F4.0:Operate Pentefoil System
F5.0: Retire Pentefoil System
F1.1 : Develop Pentefoil Concept
F1.2 : Perform Design and Development
F1.3 : Perform Initial Design
F1.4 : Perform Certification
F2.1 : Prototyping
F2.1.1 : Fabricate Prototypes
F2.1.2 : Conduct Prototype Testing
F2.2 : Manufacturing
F2.2.1 : Establish manufacturing processes
F2.2.2 : Source Materials And Components From Suppliers
F2.2.3 : Assemble Components Into Finished PenteFoil Systems
F2.3 : Testing & Validation
F2.3.1 : Conduct Comprehensive Testing And Validation Of Production PenteFoil Systems
F2.3.2 : Perform Flight Testing Under Various Conditions To Verify Performance And Stability
F2.4 : Certification & Compliance
F2.4.1 : Obtain Necessary Certifications And Approvals
F2.4.2 : Ensure Compliance With Regulations
F3.1 : Develop Distribution Channels
F3.1.1 : Establish distribution channels
F3.1.2. : Negotiate contracts and agreements
F3.2 : Planning Of Logistics
F3.2.1 : Develop logistics and supply chain strategies
F3.2.2 : Coordinate shipping, warehousing, and inventory management
F3.3 : Management Of Inventory
F3.3.1 : Monitor inventory levels
F3.3.2 : Implement inventory tracking systems and procedures
F3.4 : Marketing & Promoting
F3.4.1 : Develop marketing campaigns and promotional materials
F3.4.2 : Implement advertising, social media, and PR strategies
F3.5 : Develop Distribution Logistics
F3.5.1 : Coordinate distribution logistics
F3.5.2 : Manage transportation and shipping logistics
F3.6 : Implement quality control measures
F3.7 : Conduct inspections of distribution channels
F3.8 : Ensure compliance with import/export regulations, and trade laws
F4.1: Transport the Pentefoil
F4.1.1: Load into the transport system
F4.1.1.1: Reduce volume
F4.1.1.2: Secure the structure in the transport system
F4.1.2: Transport to the launch site
F4.1.3: Protect Pentefoil from Environment
F4.2: Set up the Pentefoil
F4.2.1: Remove Pentefoil from Storage
F4.2.2: Inflate/Assemble structure
F4.2.2.1: Pump the air into the structure
F4.2.2.2: Control the pressure inside the wing
F4.2.2.3: Prevent the air from leaking
F4.2.3: Attach structure to user
F4.2.3.1: Harness the pilot to the wing
F4.2.3.2: Ensure proper weight distribution and balance
F4.2.3.3: Provide structural frame for the attachment
F4.3: Perform Take-Off
F4.3.1: Tranfer To High Ground
F4.3.2: Transfer User from Ground to Airborne
F4.3.3: Accelerate adequately to enter stable flight
F4.4: Perform Flight Operations
F4.4.1: Provide Aerodynamic Performance
F4.4.1.1: Provide Lift Performance
F4.4.1.2: Provide Drag Performance
F4.4.1.3: Provide Stability
F4.4.1.3.1: Provide Lateral Static Stability
F4.4.1.3.2: Provide Lateral Dynamic Stability
F4.4.1.3.2.1: Provide Stable Dutch Roll Motion
F4.4.1.3.2.2: Provide Stable Spiral Motion
F4.4.1.3.2.3: Provide Stable aperiodic roll
F4.4.1.3.3: Provide Longitudinal Static Stability
F4.4.1.3.4: Provide Longitudinal Dynamic Stability
F4.4.1.3.4.1: Provide Stable Short Period Motion
F4.4.1.3.4.2: Provide Stable Phugoid Motion
F4.4.1.4: Provide Aerodynamic Control
F4.4.1.4.1: Yaw Pentefoil
F4.4.1.4.2: Roll Pentefoil
F4.4.1.4.3: Pitch Pentefoil
F4.4.1.4.4: Velocity Vector Control
F4.4.2: Maintain Structural Integrity
F4.4.2.1: Carry aerodynamic and payload loads
F4.4.2.2: Distribute stresses sufficiently throughout the structure
F4.4.2.3: Maintain Lifting Surface Shape
F4.4.2.3.1: Provide resistance to external impacts
F4.4.2.3.2: Resist Collapse Due To Load differentials
F4.4.2.4: Provide rigidity
F4.4.2.5: Withstand environmental factors
F4.4.2.6: Ensure reliability for the designed lifetime
F4.4.3: Provide Communications
F4.4.4: Perform Navigation
F4.5: Perform safety procedures
F4.5.4: Perform take off Procedure
F4.5.1: Protect Head from Injuries
F4.5.3: Allow for easy detachment in case of emergency
F4.5.2: Perform Landing Procedure
F4.5.5: Float in the water in case of emergency landing
F4.6: Perform Landing
F4.6.1: Transfer User from Airborne to Ground
F4.6.2: Bring User to Standstill
F4.6.3: Perform Emergency Landing
F4.6.3.1: Return Lifting Surface Shape After Collapse
F4.6.3.2: Remain In Control Of Emergency Landing System
F4.7: Shutdown the PenteFoil
F4.7.1: Detach Structure From User
F4.7.2: Deflate structure
F4.7.3: Put PenteFoil in Storage
F4.7.4: Protect Pentefoil from Environment
F5.1 : Analyse & Assess Defects
F5.1.1 : Conduct analysis of any defects or malfunctions
F5.1.1 : Assess impact of defects on the safety, usability, and effectiveness
F5.2 : Evaluate Aging Effects
F5.2.1 : Evaluate the effects of aging on the components and systems
F5.2.2 : Determine the implications of aging on the overall performance and reliability
F5.3 : Develop a plan for discontinuing the use of the PenteFoil System
F5.3.1 : Reallocate resources to other projects or initiatives
F5.3.1 : Determine the disposition of resources associated with the retirement
F5.4 : Document the retirement process of the PenteFoil System
F5.5 : Conduct post-retirement evaluations
F5.6 : Identify opportunities for improvement in future retirement processes and procedures
LEGEND
Mission-Level Function
Subfunction
Third-Level Function
Fourth-Level Function
Fourth-Level Function
Fifth-Level Function

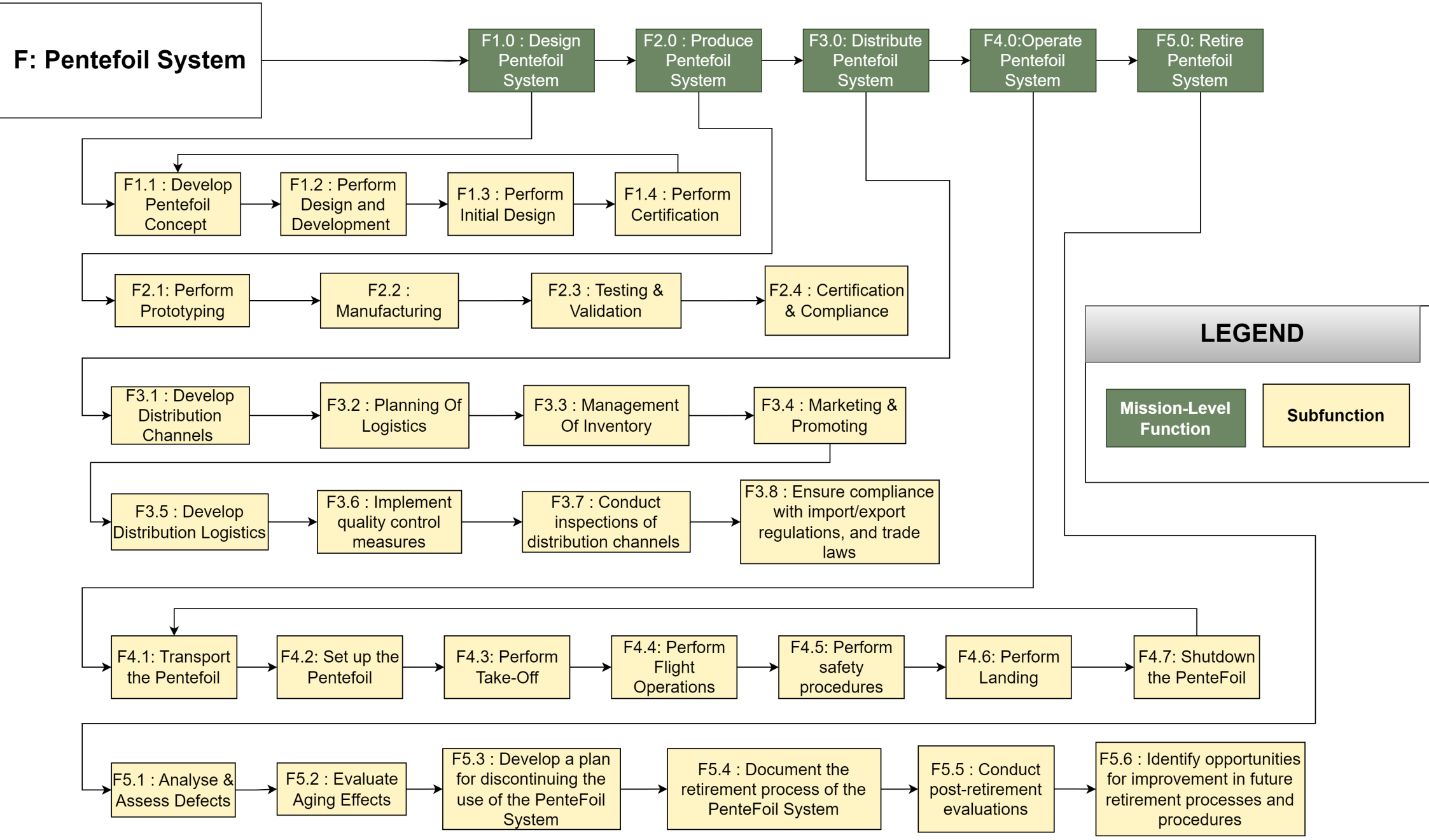
F: Pentefoil System
F1.0 : Design Pentefoil System
F2.0 : Produce Pentefoil System
F3.0: Distribute Pentefoil System
F4.0:Operate Pentefoil System
F5.0: Retire Pentefoil System
F1.1 : Develop Pentefoil Concept
F1.2 : Perform Design and Development
F1.3 : Perform Initial Design
F1.4 : Perform Certification
F2.1: Perform Prototyping
F2.2 : Manufacturing
F2.3 : Testing & Validation
F2.4 : Certification & Compliance
F3.1 : Develop Distribution Channels
F3.2 : Planning Of Logistics
F3.3 : Management Of Inventory
F3.4 : Marketing & Promoting
F3.5 : Develop Distribution Logistics
F3.6 : Implement quality control measures
F3.7 : Conduct inspections of distribution channels
F3.8 : Ensure compliance with import/export regulations, and trade laws
F4.1: Transport the Pentefoil
F4.2: Set up the Pentefoil
F4.3: Perform Take-Off
F4.4: Perform Flight Operations
F4.5: Perform safety procedures
F4.6: Perform Landing
F4.7: Shutdown the PenteFoil
F5.1 : Analyse & Assess Defects
F5.2 : Evaluate Aging Effects
F5.3 : Develop a plan for discontinuing the use of the PenteFoil System
F5.4 : Document the retirement process of the PenteFoil System
F5.5 : Conduct post-retirement evaluations
F5.6 : Identify opportunities for improvement in future retirement processes and procedures
LEGEND
Mission-Level Function
Subfunction

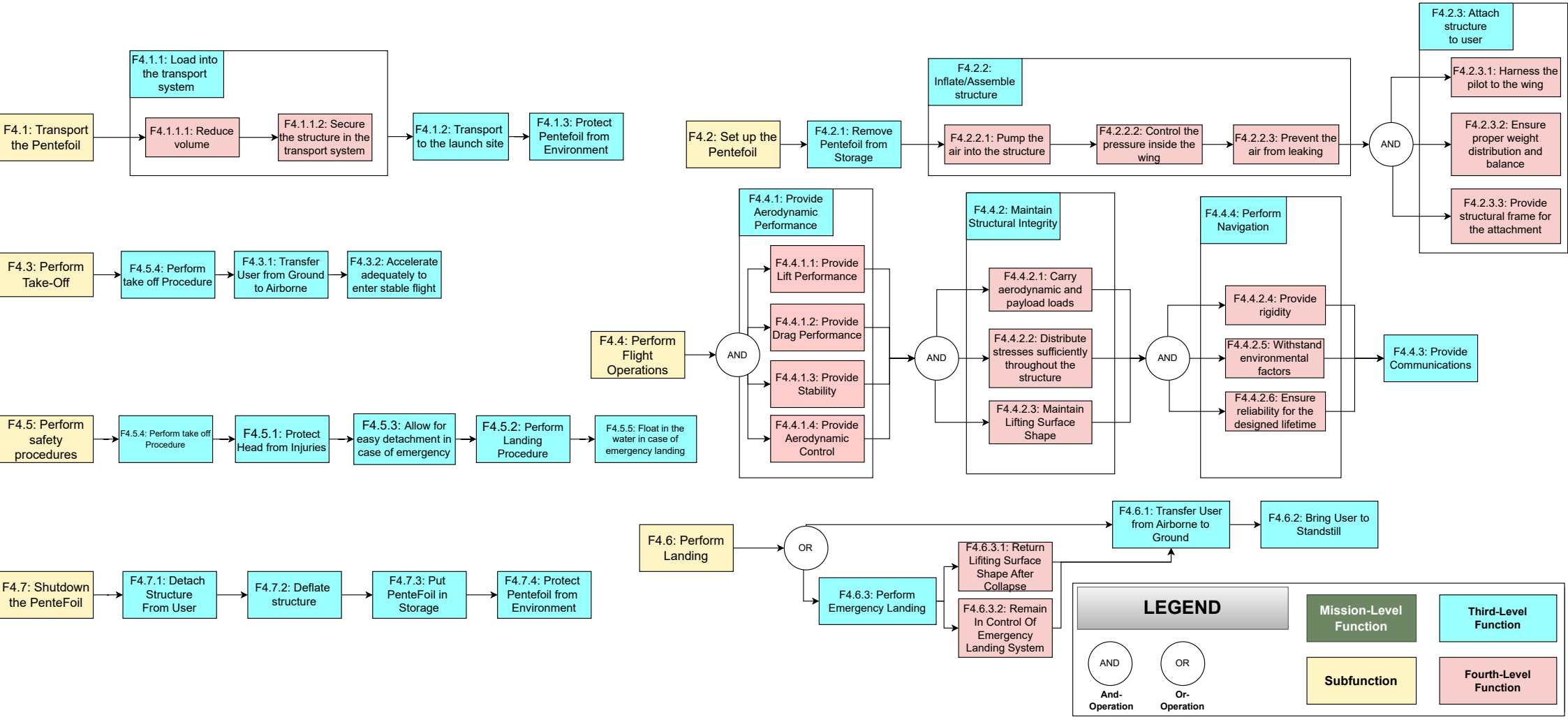
F4.1: Transport the Pentefoil
F4.1.1: Load into the transport system
F4.1.1.1: Reduce volume
F4.1.1.2: Secure the structure in the transport system
F4.1.2: Transport to the launch site
F4.1.3: Protect Pentefoil from Environment
F4.2: Set up the Pentefoil
F4.2.1: Remove Pentefoil from Storage
F4.2.2: Inflate/Assemble structure
F4.2.2.1: Pump the air into the structure
F4.2.2.2: Control the pressure inside the wing
F4.2.2.3: Prevent the air from leaking
AND
F4.2.3: Attach structure to user
F4.2.3.1: Harness the pilot to the wing
F4.2.3.2: Ensure proper weight distribution and balance
F4.2.3.3: Provide structural frame for the attachment
F4.3: Perform Take-Off
F4.5.4: Perform take off Procedure
F4.3.1: Transfer User from Ground to Airborne
F4.3.2: Accelerate adequately to enter stable flight
F4.4: Perform Flight Operations
AND
F4.4.1: Provide Aerodynamic Performance
F4.4.1.1: Provide Lift Performance
F4.4.1.2: Provide Drag Performance
F4.4.1.3: Provide Stability
F4.4.1.4: Provide Aerodynamic Control
AND
F4.4.2: Maintain Structural Integrity
F4.4.2.1: Carry aerodynamic and payload loads
F4.4.2.2: Distribute stresses sufficiently throughout the structure
F4.4.2.3: Maintain Lifting Surface Shape
AND
F4.4.4: Perform Navigation
F4.4.2.4: Provide rigidity
F4.4.2.5: Withstand environmental factors
F4.4.2.6: Ensure reliability for the designed lifetime
F4.4.3: Provide Communications
F4.5: Perform safety procedures
F4.5.4: Perform take off Procedure
F4.5.1: Protect Head from Injuries
F4.5.3: Allow for easy detachment in case of emergency
F4.5.2: Perform Landing Procedure
F4.5.5: Float in the water in case of emergency landing
F4.6: Perform Landing
OR
F4.6.1: Transfer User from Airborne to Ground
F4.6.2: Bring User to Standstill
F4.6.3: Perform Emergency Landing
F4.6.3.1: Return Lifiting Surface Shape After Collapse
F4.6.3.2: Remain In Control Of Emergency Landing System
F4.7: Shutdown the PenteFoil
F4.7.1: Detach Structure From User
F4.7.2: Deflate structure
F4.7.3: Put PenteFoil in Storage
F4.7.4: Protect Pentefoil from Environment
LEGEND
Mission-Level Function
Third-Level Function
Subfunction
Fourth-Level Function
AND
And-Operation
OR
Or-Operation